

**RELIABILITY ANALYSIS AND
RELIABILITY-BASED OPTIMISATION
DESIGN OF SWATH SHIPS**

by

Yongchang PU, MSc

Thesis submitted for the Degree of Doctor of Philosophy



**Department of Naval Architecture and Ocean Engineering
University of Glasgow**

June 1995

© Yongchang Pu 1995

ProQuest Number: 13832116

All rights reserved

INFORMATION TO ALL USERS

The quality of this reproduction is dependent upon the quality of the copy submitted.

In the unlikely event that the author did not send a complete manuscript and there are missing pages, these will be noted. Also, if material had to be removed, a note will indicate the deletion.



ProQuest 13832116

Published by ProQuest LLC (2019). Copyright of the Dissertation is held by the Author.

All rights reserved.

This work is protected against unauthorized copying under Title 17, United States Code
Microform Edition © ProQuest LLC.

ProQuest LLC.
789 East Eisenhower Parkway
P.O. Box 1346
Ann Arbor, MI 48106 – 1346

Thesis
10297
Copy 1



To
My wife, son, parents, parents-in-law
and all my family members

DECLARATION

Except where reference is made to the work of others,
this thesis is believed to be original

ACKNOWLEDGEMENTS

I am whole-heartedly grateful to Professor Douglas Faulkner, the Head of Department, and Dr. P.K. Das for their expertised guidance, advice and encouragement throughout the duration of my study.

I sincerely thank Dr. H.S. Chan, Professor Y. Murotsu, Professor K. Schittkowski, and Mr. C.C. Fang for their generous help at various levels of my research.

Gratitude is further acknowledged to Lord Y.G. Bao, British Council, Chinese government and colleagues in Shanghai Jiao Tong university for offering me Sino-British Friendship Scholarship Scheme which enable my study in Scotland.

Thanks are also given to Mrs Isobel Faulkner for editing the draft of my thesis.

Finally, I would like to express my gratitude to my wife and all my family members, especially to my parents-in-law for looking after my son in the last three and half years. This thesis is dedicated to them.

SUMMARY

The primary objective of the current research presented in this thesis was to develop a rationally-based structural design procedure for SWATH type vessels by applying reliability analysis and reliability-based optimisation techniques.

Firstly, the primary loads for PATRIA, a built SWATH ship, were calculated by a theoretical method developed by Chan (1990,1991). The response amplitude operators of loads in regular waves were calculated by a three-dimensional oscillating source distribution method in association with linearised potential theory. A program, SPEC, was developed to carry out spectral analysis and to calculate extreme design values as well as instantaneous pressure distribution in the submerged parts of the vessel. Furthermore several factors, such as load combination and longitudinal side force distribution, which are important in structural analysis, were discussed.

Having determined the primary loads acting on PATRIA, a series of finite element analyses was carried out aimed at increasing the understanding of the structural behaviour of the ship, and establishing a simplified model for system reliability analysis and multiple criteria optimisation.

At the component level the existing ultimate strength formulations for plate panels and stiffened plates were discussed and calibrated by using a considerable amount of experimental and numerical data. A new algorithm for stiffened plates was proposed. The reliability of plating and stiffened plates was then evaluated by using AFOSM, SORM and Monte Carlo simulation methods to investigate the accuracy of these methods for these types of limit states equations. It is found that Guedes Soares' formulae and Faulkner's method are the best for plate panels and stiffened plates respectively. The results for failure probability from SORM are much better than those from AFOSM. In these cases the AFOSM always underestimates the failure probability. The largest relative errors of failure probability and reliability index reach -45.1% and 7.4% respectively. Considering the nominal nature of reliability index the difference between the two methods is so small that the values obtained from AFOSM are acceptable in practice.

At the system level the conventional β -unzipping method was extended by introducing a discarding process in searching for significant failure modes of the

structural system. The extension could save computational time when the combined load effects are considered in the analysis. The method was then used to analyse a typical frame in PATRIA. In the analysis the combined load effect including buckling was considered. It is found that the most critical part is in the haunch area, and all the critical sections in the identified significant failure modes are in the haunch area. Hence it may be said that more attention should be paid to the haunch area. The buckling has a moderate effect on system reliability in this particular case, and should be considered in the analysis.

Finally, the reliability-based optimisation techniques were used to achieve an efficient design. Various reliability-based optimisation formulations and their associated problems were first discussed. An algorithm, in which the component and system reliability indices could be balanced, was proposed. The proposed strategy was then applied to optimise the one-dimensional model for the transverse cross-deck frame in PATRIA. It is found that:

- The algorithm works very well. Computational time in the analysis is not a problem because the system reliability calculation is only applied to the optimum structure.
- The original design is quite close to the optimal one, so the margin for optimisation is small. It is of interest to note that the system reliability index for the original structure is only 3.756, while it is 4.712 for the optimum structure, at the same time the optimum one is 13% lighter than the original one.
- The haunch area is confirmed as the critical part. From the values of design variables of the optimum structure, it is observed that increasing the thickness of the side shell is the most efficient way to improve the safety in this area. Because the dimensions of the flange were fixed during optimisation, their effect on the safety is not investigated in this study. The dimensions of the flange might be an important factor influencing the safety because increasing of the area of the flange would shift the neutral axis toward the flange so that the maximum stress in the flange would decrease.

NOMENCLATURE

CHAPTER 1 and CHAPTER 2

P_f	= Failure probability
P_{fmon}	= Failure probability predicted by Monte Carlo simulation
P_{f1}	= First order approximation of the failure probability
P_{f2}	= Second order approximation of the failure probability
$f(x_1, \dots, x_n)$	= The joint probability density function of the random variables
$F(x_1, \dots, x_n)$	= The distribution function of the random variables
n	= The number of the random variables
M (or Z)	= Safety margin equation
$\mathbf{X} = \{x_1, \dots, x_n\}$	= The vector of the random variables
\mathbf{X}^*	= The design point in original space
$\mathbf{U} = \{u_1, \dots, u_n\}$	= The vector of the random variables in standard normalised space
\mathbf{U}^*	= The design point in standard normalised space
$P(\bullet)$	= The probability of an event
$\Phi(\bullet)$	= The standard normal distribution function
β	= Reliability index
m_i (or μ_i)	= The means of the basic random variables x_i
σ_i	= The standard deviation of the basic random variables x_i
k_i	= The main curvatures of the failure surface
e_1, e_2	= The relative errors of first and second order methods respectively
FP_k	= Linearised plasticity condition at the k th failure element
R_k	= The resistance of the k th failure element
w_k	= The plastic section modulus of the k th failure element
A_k	= The cross-sectional area of the k th failure element
σ_y	= The yield stress
σ_{yi}	= The yield stress of the i th section
σ_{ei}	= The buckling stress of the i th section
d	= The factor to consider the effect of buckling
F_{xi}, F_{yi}	= The nodal forces of the i th section in x and y direction respectively
M_{zi}	= The bending moment of the i th section
\mathbf{x}_i	= The vector of nodal forces
δ_i	= The vector of nodal displacements in local co-ordinate system
δ	= The vector of nodal displacements in global co-ordinate system
δ_i^e	= The vector of elastic nodal displacements in local co-ordinate system

δ_t^p	= The vector of plastic nodal displacements in local co-ordinate system
K_t	= The stiffness matrix of an element
K	= The total stiffness matrix
$K_t^{(r)}$	= The reduced stiffness matrix of an element
$x_t^{(r)}$	= The equivalent nodal forces vector with opposite sign
L	= The external loads vector
$R^{(r)}$	= The fictitious loads vector in global co-ordinate system
$K^{(p)}$	= The total stiffness matrix at pth failure stage
$K^{(0)}$	= The total stiffness matrix of the original structure
$ K^{(0)} $	= The determinant of the original total stiffness matrix
F_i	= The failure event corresponding to $M_i \leq 0$
$P(F_i \cap F_j)$	= The failure probability of the intersection of F_i and F_j
$\Phi_n(\bullet)$	= n-dimensional normal distribution function
β	= Reliability index vector
ρ	= The correlation vector among the variables x_i
b	= Rosenblatt transformation matrix
P_{fp}	= Failure probability of a parallel system
β_p	= Reliability index of a parallel system
M^e	= Equivalent safety margin
β^e	= Reliability index of the equivalent safety margin
α^e	= Sensitivity factor vector of the equivalent safety margin
$\Delta\beta^{(i)}$	= increment of reliability index at the ith stage
β_s	= Reliability index of the structural system
P_{fu}	= The upper bound of the failure probability
P_{fl}	= The lower bound of the failure probability

CHAPTER 3

$F_i (i=1,\dots,6)$	= The six components of primary loads defined in Fig. 3.1
M	= The ship's mass
\bar{y}_G	= The transverse distance of the centre of gravity of one hull to the ship's centreline
$i_{kl}=i_{lk}$	
i_{45}	= The product moment of inertia of one hull about the longitudinal and vertical ship centrelines
i_{56}	= The product moment of inertia of one hull about the vertical ship centreline and the neutral axis of the cross-deck

$\xi_j (j=1, \dots, 6)$	= Motion amplitudes for each direction
$\ddot{\xi}_j$	= The acceleration of body motion in the jth direction
ε_j	= Phase angles for each direction
F_{jp}, F_{js}	= Fluid forces on port and starboard hulls due to quasi-hydrostatic and hydrodynamic pressure in the jth direction
ω	= Frequency
$S(\omega)$	= The wave spectral density function
$S_r(\omega)$	= The response spectral density function
RAO	= The response amplitude operator
m_j	= The jth order moment of response spectrum
g	= Gravity acceleration
U	= The characteristic wind speed at 19.5 metres above sea level
N	= The number of observations
ε	= The bandwidth parameter
T	= duration of specified sea in hours
m_0	= area under response spectrum
m_2, m_4	= 2nd and 4th moment of response spectrum respectively
α	= risk parameter
k	= number of encounters with a specified sea in ship's lifetime
$\bar{\gamma}_n$	= The most probable extreme value
γ_n	= The design extreme value
a_v	= The vertical acceleration
a_L	= The lateral acceleration

CHAPTER 4

σ_c	= Critical buckling stress of a plate
σ_0 (or σ_{0p})	= Yield stress of the plate material
σ_{0s}	= Yield stress of the stiffener material
σ_{0e}	= The effective yield stress of the stiffened plate
σ_p	= Proportional limit stress
E	= Young's modulus
E_t	= Structural tangent modulus in compression
ν	= Poison ratio
σ_r (or σ_{rp})	= Residual stress of the plate
σ'_r	= Non-dimensional residual stress, $\sigma'_r = \frac{\sigma_r}{\sigma_0}$
σ_{rs}	= Residual stress in the stiffener
η	= As-welded residual stress factor defining width = ηt of yield

	tension zone in plate elements each side of weld
δ_0	= Central deflection of the plate
δ'_0	= Non-dimensional central deflection of the plate, $\delta'_0 = \delta_0/t$
δ_{0s}	= Initial stiffener deflection
$\delta_{0s1}, \delta_{0s2}$	= Initial stiffener deflections in adjacent stiffeners respectively
e	= Load eccentricity
b	= The width of the plate
t	= The thickness of the plate
a	= The length of the column
h_w	= The height of the web
t_w	= The thickness of the web
A_s	= Area of the stiffener
A_t	= Area of the cross section
A_w	= Area of the web
A_f	= Area of the top flange
A_e	= Effective area of the stiffened plate
z_p	= The distance from the neutral axis to the plate
z_s	= The distance from the neutral axis to the stiffener
H	= The distance from neutral axis of box to mid-thickness of the plate
β	= Plate slenderness
β_e	= Effective plate slenderness
λ	= Stiffener slenderness
ϕ_c	= Ultimate strength of clamped plate
ϕ_s	= Ultimate strength of simply supported plate
σ_x	= Compressive stress in x-direction
σ_{xu}	= Ultimate compressive stress in x-direction
σ_y	= Compressive stress in y-direction
σ_{yu}	= Ultimate compressive stress in y-direction
σ_m	= Compressive strength of the plate
ϕ_b	= The strength of an unwelded plate
$\Delta\phi_b$	= Strength reduction due to residual stress
ϕ_F	= Ultimate strength of a plate predicted by Faulkner's method
ϕ_{ca}	= Ultimate strength of a plate predicted by Carlsen's method
ϕ_G	= Ultimate strength of a plate predicted by Guedes Soares' method
b_{em}	= The maximum effective width
b_{emR}	= The maximum effective width with residual stress
b_e	= Effective width
b_{e0}	= The effective width at strain equal to zero
b_{e0R}	= The effective width at strain equal to zero with residual stress

b_{e2R}	= The effective width at strain equal to two with residual stress
$b_{e\infty}$	= The effective width at large strain
σ_e	= Compressive stress at the edges
σ_u	= Ultimate stress of a stiffened plate
σ_E	= Pinned Euler stress of a column
r_{ce}	= Effective radius of gyration for column collapse
r	= Radius of gyration for column collapse
I'_e	= Effective moment of inertia
b'_e	= The tangent effective width of the plate
R_r	= The factor considering the residual stress effect on the plate
R_y	= The factor considering the biaxial compression effect on the plate
R_τ	= The factor considering the shear stress effect on the plate
M	= Safety margin equation
X_m	= Model uncertainty factor
σ_s	= External loads effect
P_f	= Failure probability
P_{fmon}	= Failure probability predicted by Monte Carlo simulation
P_{f1}	= First order approximation of the failure probability
P_{f2}	= Second order approximation of the failure probability
e_1, e_2	= The relative errors of first and second order methods respectively
β_r	= Reliability index

CHAPTER 5

K_t	= Torsional constant
I_{yy}	= Second area moment about y-axis
I_{zz}	= Second area moment about z-axis
A	= Cross-sectional area
S_{ay}	= Effective shear area in y-direction
S_{az}	= Effective shear area in z-direction
σ_{max}	= The maximum transverse stress in the deck
σ_{nom}	= The average transverse stress in the deck
b, b_e	= The hull breadth and effective breadth at transverse section
L	= Spacing of the frames
u, v	= Deformations in x- and y-direction
R_i	= Resistance of a section
β_s	= Reliability index of the structural system
P_{fu}	= The upper bound of the failure probability
P_{fl}	= The lower bound of the failure probability

CHAPTER 6

$C(\mathbf{d}, \mathbf{X})$	= The objective function referring to cost or weight
$\mathbf{d}=(d_1, \dots, d_n)$	= Design variable vector
$\mathbf{X}=(x_1, \dots, x_{nr})$	= Random variable vector
β	= Reliability index
β_{ci}	= Reliability index of the i th critical section
β_{cia}	= Allowable reliability index of i th critical section
β_s	= System reliability index
β_{sa}	= Allowable system reliability index
$\beta_{R,s}$	= Residual system reliability index
$\beta_{R,sa}$	= Allowable residual system reliability index
d_i	= The i th design variable
d_i^L, d_i^u	= The lower and upper bounds of the i th design variable
nc	= The number of constraints in the optimisation
n	= The number of design variables
M_p	= The number of the failure modes
ml	= The number of external loads
M	= The safety margin equation
\mathbf{u}^*	= The design point in standard normalised space
ρ	= Density of the material
σ_{yi}	= The yield stress of the i th section
σ_{ei}	= Buckling stress of the i th section
R_i	= The resistance of the i th failure element
w_i	= The plastic section modulus of the i th failure element
A_i	= The cross-sectional area of the i th failure element
F_{xi}, F_{yi}	= The nodal forces of the i th section in x and y direction respectively
M_{zi}	= The bending moment of the i th section
\mathbf{x}_t	= The vector of nodal forces
γ	= Factor to considering the effect of buckling
a_{ij}	= nodal force at the i th section in x direction caused by unit load of the j th external load
c_{ij}	= nodal force at the i th section in y direction caused by unit load of the j th external load
b_{ij}	= Moment at the i th section in z direction caused by unit load of the j th external load

CONTENTS

DECLARATION	ii
ACKNOWLEDGEMENTS	iii
SUMMARY	iv
NOMENCLATURE	vi
CONTENTS	xii
CHAPTER 1 INTRODUCTION	1
1.1 General	1
1.2 The State-of-the-Art of Reliability Methods	1
1.2.1 Component Reliability Methods	2
1.2.2 Structural System Reliability Methods	7
1.3 The State-of-the-art in SWATH Structural Design	12
1.4 The Aims and Scope of the Thesis	17
CHAPTER 2 RELIABILITY METHODS	21
2.1 Introduction	21
2.2 Component Reliability Methods	21
2.2.1 First-Order Second Moment Method	22
2.2.2 Second-Order Method	25
2.2.3 Simulation Method	29
2.2.4 Application to a Few of Cases	30
2.3 System Reliability Methods	32
2.3.1 Basic Assumptions	32
2.3.2 Automatic Generation of Safety Margins	33
2.3.3 The Extended β -Unzipping Method	42
2.3.4 Multi-normal Integration	43
2.3.5 Equivalent Safety Margin	49
2.3.6 Evaluation of Structural System Reliability	51
2.3.7 Application to a Frame Structure	52
2.4 Discussions	55

CHAPTER 3	PRIMARY LOADS ON SWATH SHIPS	59
3.1	Introduction	59
3.2	Primary Loads	60
3.2.1	Components of Primary Loads	60
3.2.2	Available Methods For Determination of Primary Loads	61
3.2.3	Extreme Value and Spectral Analysis	64
3.2.4	Hydrodynamic Instantaneous Pressure Distribution	68
3.3	Results of PATRIA	68
3.3.1	Seakeeping	69
3.3.2	Loads	71
3.3.3	Accelerations	73
3.3.4	Instantaneous Pressure Distribution	76
3.4	Discussions	79
CHAPTER 4	ULTIMATE STRENGTH AND RELIABILITY	
	ANALYSIS OF STIFFENED PLATES	105
4.1	Introduction	105
4.2	Behaviour of Unstiffened Plates	106
4.2.1	The Parameters which Influence the strength	106
4.2.2	Available Strength Formulae	112
4.2.2.1	Faulkner's Method	112
4.2.2.2	Carlsen's Method	114
4.2.2.3	Guedes Soares' Method	115
4.2.2.4	Vilnay's Method	116
4.2.2.5	Imperial College's Method	117
4.2.3	Calibration and Comparison of the Existing Methods	119
4.3	Behaviour of the Stiffened Plates	122
4.3.1	The Parameters Influencing the Strength	122
4.3.2	Existing Methods	127
4.3.2.1	Faulkner's Method	127
4.3.2.2	Carlsen's Method	129
4.3.2.3	Imperial College's Method	132
4.3.2.4	Proposed Method	134
4.3.3	Calibration and Comparison of the Methods	136
4.4	Reliability Analysis of Stiffened Plates	141
4.4.1	Reliability Analysis of Unstiffened Plates	141
4.4.2	Reliability Analysis of Stiffened Plates	147
4.5	Discussions	151

CHAPTER 5	STRUCTURAL ANALYSIS AND SYSTEM RELIABILITY ANALYSIS OF A SWATH	179
5.1	Introduction	179
5.2	Modelling of a Typical Frame Section of PATRIA	180
5.2.1	Ship Particulars	180
5.2.2	Materials	180
5.2.3	Three-Dimensional Model	181
5.2.4	Two-Dimensional Model	184
5.2.5	One-Dimensional Model	186
5.3	Loads	187
5.4	System Reliability Analysis of the 1D-Model	188
5.4	Conclusions	190
CHAPTER 6	STRUCTURAL SYSTEM RELIABILITY-BASED OPTIMISATION OF SWATH SHIPS	240
6.1	Introduction	240
6.2	Optimisation Based on Elemental Reliability Index	241
6.3	Optimisation Based on the System Reliability Index	242
6.4	Proposed Algorithm for System Reliability-Based Optimisation	245
6.5	Target Reliability in the Optimisation	247
6.6	Application to a SWATH Ship	248
6.7	Conclusions	254
CHAPTER 7	CONCLUSIONS AND RECOMMENDATIONS	260
7.1	General	260
7.2	Prediction of Primary Loads	261
7.3	Ultimate Strength and Reliability Analysis of Plate Panels and Stiffened Plates	262
7.4	Structural Analysis and System Reliability Analysis of PATRIA	263
7.5	Reliability-Based Optimisation	264
7.6	Recommendations for Future Study	265
7.7	Closing Remarks	266
REFERENCES		268

CHAPTER 1 INTRODUCTION

1.1 GENERAL

SWATH (Small Waterplane Area Twin Hull) is a novel concept. Its geometric features, comparing to other types of vessels, are shown in Fig. 1.1. Because of its good seakeeping performance, large deck area, large transverse stability, high sustained speed at most headings to ocean wave, and the low vertical motion and acceleration amplitudes, which are important for deck operations, it is widely used in a variety of fields such as naval, ferry, strategic positioning, surveillance, oceanographic and hydrographic survey, personnel transport, offshore patrol, offshore range support, mine warfare, towing and vertically deployed aircraft platform etc. On the other hand, SWATH has some disadvantages, namely, extreme weight sensitivity (structural weight reaches about 40% of the displacement), large draught and freeboard (to avoid heavy slamming in the wet-deck), potential for upper hull and lower deck impact, unusually large beam ratio, relatively slow speed in calm water, high construction cost. SWATH concept is weight critical, which means that the structural design can not be too conservative.

Since the introduction of reliability method in ship and offshore engineering in the early 70's, it is widely recognised as a powerful tool to develop a rational design procedure, especially for an innovative structure.

The thesis aims at developing some general tools for reliability analysis, including component and system reliability methods, and reliability-based optimum design. The developed methods are then applied to SWATH ships to identify the critical parts and to approach a rational design.

1.2 THE STATE-OF-THE-ART OF RELIABILITY METHODS

Reliability analysis techniques have been rapidly developed in past decades. Reliability methods may be classified as reliability at component level and reliability at structural system level. If only one failure surface is involved in analysis, it is

defined as component level. If more than one failure surface are involved, it is defined as system level.

1.2.1 Component Reliability Methods

Reliability analysis was developed first for structural components. At present most of the codes are developed based on component reliability, although some of them tried to take system reliability effect into account. The component reliability methods have been maturing for the past decades in the sense that arbitrary accuracy could be achieved by existing methods (combining FORM, SORM and Monte-Carlo simulation).

It is well known that for time-independent problems of reliability analysis, the probability of structural failure may be defined as:

$$P_f = \int_F f(x_1, \dots, x_n) dx_1 \dots dx_n \quad (1.1)$$

where $f(x_1, \dots, x_n)$ is the joint probability density function of the basic variables $\mathbf{X} = \{x_1, \dots, x_n\}$. F is the failure domain. Due to the complexity of the joint probability density function and the failure domain, the above integral is hardly obtained for most of the practical cases. Therefore, approximate methods have been sought.

Existing methods could be divided into the following categories according to the way the failure surface is represented.

- (1) The First Order and Second Moment method
- (2) The Second Order method
- (3) Simulation-based Method.

Some researchers think that the FORM/SORM and simulation-based methods are competitive and tried to figure out which is better. In fact, these two methods have their own advantages and disadvantages. In the situation where the failure surface is smooth and is not too strongly non-linear, the FORM/SORM is better. In other cases, where the number of variables is large (e.g. greater than 20) or the failure surface equation is so irregular that the FORM/SORM can not be successfully

applied, the simulation-based method is superior to FORM/SORM. Therefore, FORM/SORM are complimentary.

The First Order and Second Moment Method (FORM)

The first order and second moment method was introduced by Lind and Hasofar and extended to more general situations by Fiessler and Rackwitz (it is also called Advanced First Order and Second Moment Method -AFOSM).

The basic idea of the method is to transform the variables $\mathbf{X} = \{x_1, \dots, x_n\}$ to the standard normalised space $\mathbf{U} = \{u_1, \dots, u_n\}$ first. Then in the space \mathbf{U} , the failure surface is linearized at the so-called design point \mathbf{U}^* . So,

$$\begin{aligned}
 P_{f1} &= P(M \leq 0) = \int_{\mathbb{F}} f(x_1, \dots, x_n) dx_1 \dots dx_n \\
 &= P(\boldsymbol{\alpha}^T (\mathbf{U} - \mathbf{U}^*) \leq 0) = P(\boldsymbol{\alpha}^T \mathbf{U} + \beta \leq 0) \\
 &= \Phi(-\beta)
 \end{aligned} \tag{1.2}$$

where $\beta = \boldsymbol{\alpha}^T \mathbf{U}^*$ is the shortest distance from the failure surface to the origin in standard normalised space, and is called reliability index. P_f is failure probability. M is safety margin equation.

The advantages of FORM are:

- (1) The computing time is short
- (2) The design point specifies the region which contribute most to the total probability
- (3) For a linear limit surface and normal basic variables, the method is exact.

The disadvantages of the method are:

- (1) As in general optimisation procedures, it may quite often be questionable whether or not the obtained solution is actually the minimum (reference is made to the typical problem of the global minimum of optimisation procedure)
- (2) It is not possible to estimate the error of approximation
- (3) There is a drastic increase in error with increasing dimension of the problem

- (4) For some "algorithms", as discussed in Dolinski, (1983), the results even depend on the ordering (numbering) of the random variables for the case of mutual dependence (of course, if general non-linear constraint programming is used, the ordering should not affect the solution).

As to the above disadvantages, in order to diminish the errors in FORM, one needs to investigate various orders of basic variables and various initial points for optimisation procedure.

In principle, the β can be obtained by any general non-linear optimisation method, but their accuracy and efficiency are quite different in some cases. Liu and Kiureghian (1991) have investigated the performances of most optimisation algorithms for reliability calculation. It is found that the Fiessler and Rackwitz algorithm and a Sequential Quadratic Programming method show good accuracy and efficiency.

Chen and Lind (1983) proposed a method for more accurately calculating reliability index by probability integration using a three-parameter normal tail approximation to a non-normal distribution for each random variable. It is claimed that the method is faster and more accurate than Rackwitz-Fiessler's algorithm.

Another algorithm was derived by Wu and Wirsching (1987). A weighting function is chosen to get an optimum equivalent normal distribution and a least-squares method is used to fit a high quality three-parameter normal cumulative distribution function to a non-normal distribution function.

Mebarki et al (1990) presented a so-called 'new level-2 method' in which the failure domain is replaced by a hypercone, and the bounds of failure probability can be obtained. But the procedure to find the parameters of the hypercone is difficult and the evaluated bounds are not narrow.

Second Order Method (SORM)

As summarised above, the FORM is accurate only when the failure surface is flat. If the failure surface is non-linear or the basic variables are not all normally distributed, the approximation from FORM may not be acceptable. In these cases, the second-order reliability analysis should be used. In the second-order method, the failure surface is represented by a second-order surface at design point, usually a

paraboloid or a sphere. Several methods for this purpose have been derived (Breitung, 1984; Fiessler, et al, 1979; Tvedt, 1984 and 1985; etc.).

In all these methods the paraboloid is fitted either to the principal or the main curvatures of the failure surface at the design point. They are defined by the eigenvalues of the matrix of second-order derivatives of the surface. Calculation of the second-order derivative matrix is time-consuming and 'noise' may be introduced to the limit-state surface.

Kiureghian et al (1987) presented an alternative paraboloid fitting procedure by using point-fitting techniques. Although this method sounds less accurate than others, due to the omission of the off-diagonal elements in second order derivative matrix from the theoretical point of view, the advantages of the method could be summarised as follows:

- (1) It is easy to implement and requires less computation for large number of variables
- (2) It is insensitive to noise in the failure surface
- (3) It coincidentally takes account of the effect of higher order terms of the limit state surface along the co-ordinate system
- (4) It facilitates the use of Tvedt's formula
- (5) The error is stable and reasonably small.

Because there are singularities in the formulae of Breitung (1984) and Tvedt (1984) an exact integral algorithm was derived by Tvedt (1988). Combined with saddle point integration technique, the method can obtain exact failure probability in the numerical sense.

A more efficient algorithm was proposed by Kiureghian et al (1991), in which the principal curvatures of the limit state surface at design point are determined by an iterative scheme without computing the second-order derivative matrix or solving the eigenvalue problem. The curvatures are calculated in the decreasing order of their magnitudes, which is also the order of their importance in reliability analysis.

Cai and Elishakoff (1994) presented a new analytical approximation for the second-order method which is presumably applicable to most cases. The singularity problem mentioned above can be overcome in this method.

The AFOSM and SORM are applied not only to single failure surface but also to series or parallel systems. Various first-order approximations for series and parallel systems can be seen in Baker and Thoft-Christensen (1982) and Hohenbichler and Rackwitz (1983).

Madsen (1985) incorporated the second-order formula, derived by Tvedt (1984), into Ditlevsen's bounds formulae to achieve a narrower bounds for a series system. The joint failure probability in any two modes is evaluated at a joint β -point instead of at local β -point. Bennett (1987) reported some favourable experiences to this method.

Hohenbichler et al (1986) employed the joint β -point idea to derive an asymptotic second-order approximation for a parallel system. This formula is very efficient and accurate. Later this method was extended to the multi-normal integration by Gollwitzer and Rackwitz (1988).

Simulation-based Method

As discussed in the foregoing sections, FORM/SORM are now widely used in many practical situations. If the distribution function of \mathbf{X} in Eq. (1.1) is not differentiable and/or the failure domain cannot be represented by linear or quadratic form, FORM/SORM concepts are no more suitable for computing the integrals as Eq. (1.1). In some cases FORM/SORM can not give satisfactory results. One of the most attractive alternatives, no doubt, is by applying importance sampling techniques first proposed by Shinozuka (1983).

Importance sampling is an extension of Monte Carlo simulation. The idea of Monte-Carlo simulation is quite straightforward. Due to lack of theoretical attraction and being computationally costly, this method has not been extensively studied by structural engineers until the 1980's.

At present there are more than forty different papers, such as Schueller and Stix (1987), Harbitz (1985), Hohenbichler and Rackwitz (1988), Verma et al (1989), Bucher (1988), Karamchandani et al (1989), Melchers (1990), Ibrahim (1991), Karamchandani and Cornell (1991), Schueller et al (1989), Yasuhiro and Ellingwood (1993), and many others, on importance sampling techniques covering about ten

different schemes, some of which differ only in details and implementation. A good review can be seen in Melchers (1990).

Engelund and Rackwitz (1993) carried out a benchmark study on importance sampling techniques in structural reliability. The existing methods are classified into four groups:

- * Direct method (Shinozuka, 1983; Ibrahim, 1991; Fu and Moses, 1987; Schueller and Stix, 1987; Melchers, 1989; Harbitz, 1985);
- * Updating method (Hohenbichler and Rackwitz, 1988; Schall et al, 1988);
- * Adaptive method (Bucher, 1988; Melchers, 1990; Karamchandani et al, 1989; Wu, 1992; Ang et al, 1991)
- * Spherical sampling (Ditlevsen et al, 1990; Bjerager, 1988).

It is concluded that it is not possible to identify one of the methods as being the best under all circumstances. In practical applications the selection of an importance sampling method should be based on the available knowledge about the specific problem.

1.2.2 Structural System Reliability Methods

It has been recognised for many years that a fully satisfactory estimate of the reliability of a structure must be based on a structural system reliability analysis because most real structures possess redundant strength. The failure of one component (element) usually does not cause the collapse of the whole structure. Only in the cases of statically determinant structures, where the failure of any single component will give rise to the loss of the total structure, it is sufficient and reasonable to evaluate the reliability of the structure system by a component method.

Structural engineers are always concerned about :

- 1) What is the reliability level of the system? How much difference between system reliability and the reliability of each element?
- 2) What is the relationship between the system reliability and the redundancy of the structure?

- 3) Which element has the highest probability to fail first? Which element will follow the failure after the occurrence of first failure?
- 4) How sensitive is the system reliability when the main variables change?

System reliability methods are useful tools for solving the problems mentioned above.

Structural system reliability methods may be classified as analytical methods and approximate methods. The analytical methods consist of Numerical Integration, Simulation-based Methods, Reduced Space Approach and Response Surface Based Approach. All the analytical methods can only be applied to relatively simple cases such as classic frames. For complicated structures only the approximate methods are applicable to. Approximate methods are composed of Failure Path Approach, Survival-Set Approach and Plasticity-Based Approach. The Failure Path Approach can be divided into Incremental Load Method, β -Unzipping Method as well as Branch-and-Bound method, which are the most widely used methods in practice. Discussions in this study will focus on the Failure Path Approach.

Structural system reliability analysis has three main steps:

- 1) Modelling the structure and defining the random variables;
- 2) Searching the failure modes of structure;
- 3) Evaluating the system reliability.

A good review in these aspects can be seen in Karamchandani (1987), Lee (1989), Moses (1990), Bjerager (1990), Nikolaidis and Kapania (1990), Moses and Liu (1992), Baker and Vrouwenvelder (1992), Moan (1994). Some recent developments will be described below:

Physical modelling

In the early structural system analysis only truss and beam elements can be used. This means that a structural system should initially be idealised by truss or beam elements. Although some types of offshore structures, such as fixed jacket platforms, could be reasonably modelled by truss or beam elements, nevertheless when such

simplification is applied to a continuous structure, the results obtained from this analysis are not convincing. Lee (1989) made it possible that the ultimate strength formulae for structural assemblies, such as stiffened cylinder and box girder, could be directly used in the safety margin equations of the structure system. This improvement makes the system reliability more realistic for the continuous structures such as TLP, but on essence his method is still belong to this category.

The real breakthrough which makes system reliability methods applicable to a continuous structure is the work done by Murotsu et al (1991, 1993, 1994). In these papers, a spatial plate element model was successfully used to analyse the main hull girder of a 150,000 DWT bulk carrier. The yield and buckling failure modes are included in the failure criteria. But such a representation of failure criteria needs to be checked against experimental or numerical data.

How to consider post-failure behaviour of the structure in reliability analysis is another important issue which needs to be carefully considered. For truss structures a two-state model was initially used by many researchers. Sorensen (1987) and Moses (1988) introduced a multi-state elements and subject to proportional loads. In these methods, the possibility that the direction of incremental deformation may change and the element may regain its elastic stiffness is neglected, and load decrements are not explicitly included in the analysis. Karamchandani (1990b) presented another multi-state model in which the load decrements were explicitly taken into account and an element may change state during a load decrement. Both proportional and non-proportional loads can be applied in the approach. But the approach has only been applied to limited and highly idealised situations. Further validation is needed. Wu and Moan (1989, 1991) proposed a multi-state model by piece-wise linear relations.

For a frame structure (beam elements), development follows the sequence that only single load effect (bending moment) was first considered in the formation of plastic hinge in the structure, then combined load effect (the interaction of bending moment and axial force) was taken into account. A rigorous model, which considers the interaction of bending moment and axial force and plasticity consistent post-failure behaviour, is non-linear. If this model is directly used in the reliability analysis, the procedure is much more complicated and even impractical. Therefore some approximations need to be introduced to simplify the calculation. Thoft-Christensen and Murotsu (1986) presented a linear axial force and moment interaction model with plasticity consistent post-failure behaviour. This model was successfully applied to many real structures (Murotsu et al, 1989, 1990, 1991, 1992, etc).

Karamchandani (1990b) proposed a model in which the yield surface is non-linear as long as the section is in its initial elastic state. Once the forces reach the yield surface and a hinge forms, the non-linear yield surface is replaced by a linear surface which is tangent to the non-linear yield surface at the point where the hinge forms. The inelastic strain rates are normal to this linearized surface and the forces in the yielded section are constrained to lie along the linearized surface.

Searching for significant failure modes

Due to the great number of failure modes for a complicated structure, it is not practical to include all possible failure modes in analysis. Therefore, in practice, only the modes which mainly contribute to the system collapse are taken into account. These modes are referred to as the most likely or the most important or the most significant failure modes, or the stochastically dominant failure modes.

The existing procedures to identify the significant failure modes are Monte Carlo Simulation Method (Edwards et al, 1985); Utilisation Ratio-based Method (Moses, 1982); Truncated Enumeration Method (Melchers and Tang, 1984); β -unzipping and Branch-and-Bound method (Thoft-Christensen and Murotsu, 1986), which are two widely used methods. β -unzipping method is faster than Branch-and-Bound algorithm, but there is no guarantee that all the important failure modes are included in the final stage. Branch-and-Bound algorithm is more rigorous, but more computational time is expected.

Xiao and Mahadevan (1994) extended the truncated enumeration method for ductile structural systems. The proposed method makes use of the statistical correlations between different member limit states to impose groups of hinges at each selection level instead of one plastic hinge at a time, as used in previous studies, thus making the search for significant failure modes very rapid.

A structural system is usually modelled by a series system consisting of parallel systems. The evaluation of failure probability of such a series system is very difficult because the correlations among these parallel systems are not easy to be determined. This problem was overcome by introducing an 'equivalent safety margin' (Gollwitzer and Rackwitz, 1983).

Another problem is to evaluate multi-normal integral, which is an essential calculation in system reliability analysis. Hohenbichler and Rackwitz (1983) skilfully transformed a n-dimensional normal distribution function to n number of one-dimensional normal distribution functions, but its accuracy is not satisfactory in some cases.

Tang and Melchers (1987) extended this method by introducing an inverse Rosenblatt transformation and using Newton-Raphson method to find design point. The extended method improves the accuracy of the original method.

Gollwitzer and Rackwitz (1988) applied the findings in Hohenbichler et al (1986) to the original method of Hohenbichler and Rackwitz (1983). This is a second-order method, and its accuracy is much better than the original one.

Enevoldsen and Sorensen (1992) investigated the efficiencies of several optimisation algorithms for calculation of multi-normal integral by Gollwitzer and Rackwitz's algorithm. An optimality criteria-based algorithm was used, and efficient active set strategies were developed. The algorithm seems to be stable and fast.

Pu and Das (1993) have compared the above methods, and it was found that Tang and Melchers' algorithm has more or less the same accuracy as Gollwitzer and Rackwitz's.

In addition, Zhu (1993) derived a numerical integration method which possesses high accuracy. But its application to high dimension is not investigated in the paper.

The system reliability can finally be evaluated by Ditlevsen's bounds. Due to the development in multi-normal integration technique, the efficiency and accuracy in this aspect is improved in the past few years, and it is possible to apply high-order bound techniques to achieve narrower bounds.

Feng (1989) used one-, two- and three-order joint probabilities to calculate the failure probability of a system. It is more accurate than Ditlevsen's bounds.

A general form of the n-order upper and lower bounds was derived by Greig (1992), and an exact integration algorithm in simple recursive form was developed and used to evaluate multi-normal integral. Furthermore the third- and fourth-order bounds were calculated by the proposed method. Compared with second-order results, the method gives narrower bounds, the integration algorithm is accurate and also efficient when the dimension is less than five. For the cases that the dimension is greater than (and equal to) five, Tang and Melcher's method is preferable.

1.3 THE STATE-OF-THE-ART IN SWATH STRUCTURAL DESIGN

As can be seen in Fig. 1.1, a SWATH has more complex geometry than a mono-hull ship. As a consequence, there are more basic design parameters and more load combinations for the design. The basic design parameters for a SWATH are volume of displacement, volume of hull, length overall, breadth overall, design draught, depth, hull dimensions, hull submergence, strut thickness, etc. Normal range of these parameters are fully discussed in Gore (1985); MacGregor (1986); and Djatmiko (1992).

The midship section of a conventional mono-hull is controlled by four parameters, namely, breadth, depth, draught and area coefficient. The midship section of a SWATH is determined by nine parameters which give rise to complexity and far more choices. The definition of the nine parameters, as well as their functions in structure, are shown in Table 1.1. Among the nine parameters, only two, namely the depth of the box and depth of the haunch, are determined by strength consideration.

The results in Loscombe (1989) show that the peak stress at the haunch-box junction increases 21% with 21% reduction of box depth, and a 21% increase in box depth results in 13% reduction in peak stress. Not much difference in peak stress is observed when the depth of the haunch is changed, although the stress distribution curve shifts a little.

Table 1.1 Definition of parameters of cross-section (Loscombe, 1989)

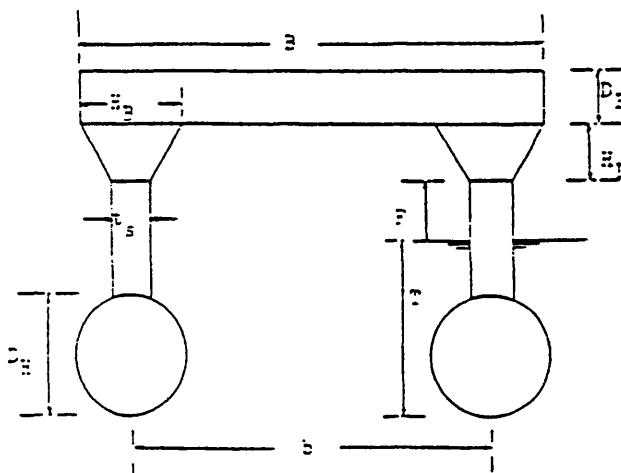
PARAMETER	DESIGN REQUIREMENT															
	A	B	C	D	E	F	G	H	I	J	K	L	M	N	O	P
B (max)					**					**						
B (min)					**											***
D _B (max)												**	***	*	*	
D _B (min)				*								**	***			
H _B (max)											*		**	*		*
H _B (min)				*							*		**			*
H _D (max)							**		*					*	*	
H _D (min)				*			**	**					***			
t _s (max)	***			*	**	**	**					**	*			
t _s (min)			*	*	**	**					**	*	*			
F (max)														*	*	
F (min)	*			*			***	**								
b (max)										**						
b (min)					***											*
T (max)		*							**	**						
T (min)	*	*					*									
D _H (max)		*												*		
D _H (min)			***								**	*				

KEY

- | | |
|---|---|
| A: minimise wavenaking resistance | I: minimise lever arm of side force |
| B: minimise wetted surface area | J: permit operation in restricted seaways |
| C: provision of adequate intact buoyancy | K: permit crew/passenger/equipment access |
| D: provision of adequate reserve buoyancy | L: ease fabrication |
| E: adequate transverse stability | M: adequate strength |
| F: acceptable tonnes per cu. immersion | N: minimise structural weight |
| G: minimise motions in rough seas | O: minimise airdraft |
| H: minimise slam forces on wet deck | P: adequate deck area |

○ REQUIREMENT HAS AN IMPACT ON THE STRUCTURAL DESIGN OF SWATH CRAFT

FACTORS INFLUENCE ON PARAMETER:	
*	SOME
**	SIGNIFICANT
***	DOMINANT



According to the stress characteristics of the structure, the whole ship can be divided into three typical parts, say, box structure, haunch/strut and lower hull. In the box structure the direct stress caused by transverse vertical moment remains more or less to the same level (Stirling, 1988; Loscombe, 1989). Based on the fact that the box structure is the main part resisting the side force, the transverse framing system is obviously preferred. The most important parameter in this part is the depth of the box.

Haunch/strut is a critical part because the peak stress occurs in the junction of haunch and strut, and the stresses in the junction of haunch and box structure are also relatively high. Because both the stress level and the weight of a longitudinal arrangement are not larger than the corresponding values when using a transverse arrangement in this area, a longitudinal framing system was recommended by Loscombe (1989) for convenience of construction.

The lower hull design is governed by two load cases, namely, hydrostatic head of water (assumed to be 1.2 meters above the main deck), and the load caused by drydocking condition (Sikora, 1988). Load cases which affect local details are:

- * slamming pressure at the intersection of lower hull and strut
- * a slow speed ship collision with a pier
- * a horizontal bending of the lower hull about the fore and aft ends of the struts.

Considering the ease of construction, the cylinder form is preferred for the lower hull. It is shown that the ring frame stiffeners were more efficient than longitudinally stiffened cylindrical structures (Sikora, 1988).

In addition, great care should be paid to the design of bulkheads, due to the fact that the maximum side force was resisted mainly by bulkheads and their associated shell, the plating and scantlings offering relatively little support. Because of shear lag effects, the effective breadth factor for the bulkhead is relatively small, less than 50 times the plating thickness either side of the bulkhead (Chalmers, 1989). Design of bulkheads was governed by maximum side force on the lower hull.

It is recognised that the demand on SWATHs by commercial operators and government (the Navy) is relatively limited due to their comparatively higher capital expenditure required for construction. Betts (1988) pointed out that the higher construction cost of a SWATH is attributed to the larger size of the ship (approximately 20-30%) compared to a mono-hull with an equivalent capability in

carrying out a certain mission. Therefore reducing structural weight is thought to be an efficient way to increase the payload of a ship. A report by Sikora and Dinsenbacher (1990) on the design study of a notional 9,000 tonne SWATH suggests that a 10% structural weight reduction could be expected to result in a 16% increase in range, or a 24% increase in payload. For this reason, various efforts were then undertaken by researchers world-wide to solve the problem of effective structural design by examining all possible alternatives on the general and detailed structures.

The possible ways to reduce structural weight or production cost are as follows:

- * The production of the structural components may be improved by slightly modifying the initial structural arrangement into a much simpler configuration (Covich, 1986; DeVries, 1991);
- * Adopting longitudinal framing is likely to achieve 3 to 12 % structural weight saving (Gupta and Schmidt, 1986);
- * Properly arranging transverse bulkhead spacing and introducing partial bulkheads in high shear areas (Sikora, 1988);
- * Use of high strength steels (Sikora, 1988; Aronne et al, 1974);
- * Use of lightweight materials, such as aluminium alloys, hybrid (steel-aluminium combination) and glass reinforced plastics (GRP) (Loscombe, 1987, 1988, 1989).

As summarised by Djatmiko (1992), there exist several general SWATH structural design programs, which are as follows:

- * DTNSRDC ASSET/SWATH program (Mulligan and Edkins, 1985);
- * US Navy Structural Synthesis design Program (SSDP) (Aronne et al, 1974);
- * DREA CEN Program for SWATH Ships (Nethercote and Schmitke, 1982);
- * UCL SWATH Structural Design Program (Walker, 1984);
- * USCG Small SWATH Structural Design (Holcomb and Allen, 1983);
- * Loscombe's Small SWATH Structural Design (Loscombe, 1987, 1988, 1989);
- * Rule-based SWATH Structural Design (ABS, 1990).

Most of these design programs can only be used in the early stages of design. In actual preliminary design, a more sophisticated design approach needs to be used.

Takeuchi et al (1985) at Japan Marine Science and Technology Center (JAMSTEC) presented a design procedure which could be used for detail design. In this program primary and secondary loads are evaluated by theoretical methods, the

global and local strength are then checked. In global analysis the three-dimensional finite element analysis was carried out.

ABS has carried out extensive research on SWATH. Based on these works a design procedure for any proposed SWATH vessel was recommended by Liu (1989) which involves the following steps:

- 1) Seakeeping and wave load analysis
- 2) Wave impact analysis
- 3) Stress analysis by finite element method
- 4) Fatigue analysis
- 5) Hull vibration analysis

In the 'stress analysis by finite element method' stage, both three-dimensional and two-dimensional models should be generated. Firstly, a coarse three-dimensional finite element model representing the whole ship including the deckhouse was generated to calculate the overall structural responses of the vessel to the predicted maximum sea loads so that appropriate boundary conditions can be obtained for input to the two-dimensional finite element analysis. Due to the coarseness of the mesh, the stresses obtained from the three-dimensional analysis could not be viewed as the actual stresses. It only provides proper boundary conditions for the finer two-dimensional finite element analysis. Secondly, in order to get the accurate stresses in the critical locations, a finer two-dimensional finite element model was performed, in which the boundary conditions are from the three-dimensional analysis. The load cases, which should be considered in the finite element analysis, are:

- 1) Still water condition
- 2) Maximum prying side force in beam sea
- 3) Maximum squeezing side force in beam sea
- 4) Yaw splitting moment in bow quartering sea

Due to the requirement of the finite element analysis, the instantaneous pressure distribution on the submerged part of the vessel must be obtained by using an 'equivalent wave system'. For load cases 2, 3 and 4, the hydrodynamic pressure distributions obtained through the equivalent wave system with the proper vertical and lateral inertial forces are superimposed on the static stillwater loads to achieve an equilibrium.

It might be said that adequate design tools already exist to build SWATH ships for any desired role now. At the moment there is a need to calibrate those design tools against full-scale data and to develop reliability-based structural design tools to permit efficient design and enable valid trade-off to be made between cost and weight. For developing rational design procedure of SWATH, the past experience in mono-hull (Faulkner and Sadden, 1979) and in offshore structures (TLP) (Lee and Faulkner, 1989) could be transformed to this case.

1.4 THE AIMS AND SCOPE OF THE THESIS

A structural design usually involves many activities, such as selection of configuration, determination of main particulars (length overall, depth, etc), selection of material, and so on. Recognising the considerable amount of work involved and limit of time, not all of these aspects are covered in the present study. The purpose of the thesis is to develop some general tools for reliability analysis, including component and system reliability methods, and reliability-based optimisation. The developed methods will be applied to a SWATH ship in order to identify the critical parts and thus establish a rational design. The flowchart of the present work is shown in Fig. 1.2.

In Chapter 2 reliability methods for both component and structural systems are developed. Because the Advanced First Order and Second Moment Method (AFOSM) is only accurate when the failure surface is linear, the Second Order Method (SORM) and Monte Carlo Simulation Method are also developed to check the accuracy of AFOSM and further decide whether or not the SORM needs to be used in SWATH structure. In structural system reliability the β -unzipping method is extended by introducing a discarding process in order to save computational time, and the combined load effect is considered in the analysis. The developed methods are then applied to a few cases to check the validity of the programs.

Prediction of primary loads on SWATH is obviously a very important aspect in structural design, which will be discussed in Chapter 3. Firstly, the motions and loads in regular waves will be calculated by the program MARCHS, which was developed and calibrated against many experimental data by Chan (1990, 1991). Then spectral analysis techniques are used to predict the design extreme loads and accelerations, and the 'equivalent wave system' is introduced to calculate the instantaneous pressure distribution on the submerged parts of SWATH, which is needed for finite element

analysis. Also discussed in this Chapter are some important issues, such as load combination, longitudinal distribution of side force, etc.

As in conventional mono-hulls, stiffened grillages are also common components in SWATH ships. To rationally determine local safety level of a SWATH, accurate prediction of ultimate strength of stiffened plates is an important task. Fortunately considerable research has been carried out in past decades. In Chapter 4 the existing formulae for prediction of ultimate strength of plate panels and stiffened plates in compression are fully calibrated and compared, and a new algorithm for stiffened plates is proposed. The best formulae (in the sense of small scatter and bias) are chosen, based on the study. Furthermore, the reliability analyses of plating and stiffened plates are carried out by AFOSM, SORM and Monte Carlo Simulation, which are developed in Chapter 2, in order to investigate the accuracy of AFOSM and SORM.

In Chapter 5 a typical transverse frame in a built SWATH is firstly idealised by a series of finite element analyses, in which three-, two-, and one-dimensional models are generated. The reliability of the idealised frame system is then calculated by an extended β -unzipping method, and the combined load effect is taken into account in the analysis. Through this analysis the critical parts and the most probable failure modes for this frame are identified. The information obtained gives good insight for the designer.

To achieve maximum safety at minimum cost is always the aim of our research. Applying reliability-based optimisation techniques to SWATH ships is the task of Chapter 6. Firstly, the algorithms for elementary and system reliability-based optimisation and the associated problems with these algorithms are discussed. An algorithm, in which the requirement of both component and system reliability can be balanced, is proposed, and it is applied to the typical frame obtained in Chapter 5. It is found that an efficient design could be achieved by using this technique.

Finally, review of the present work is made in Chapter 7. The thesis ends by describing the main conclusions of the present work and recommendations for future research in structural system reliability and reliability-based optimum design.

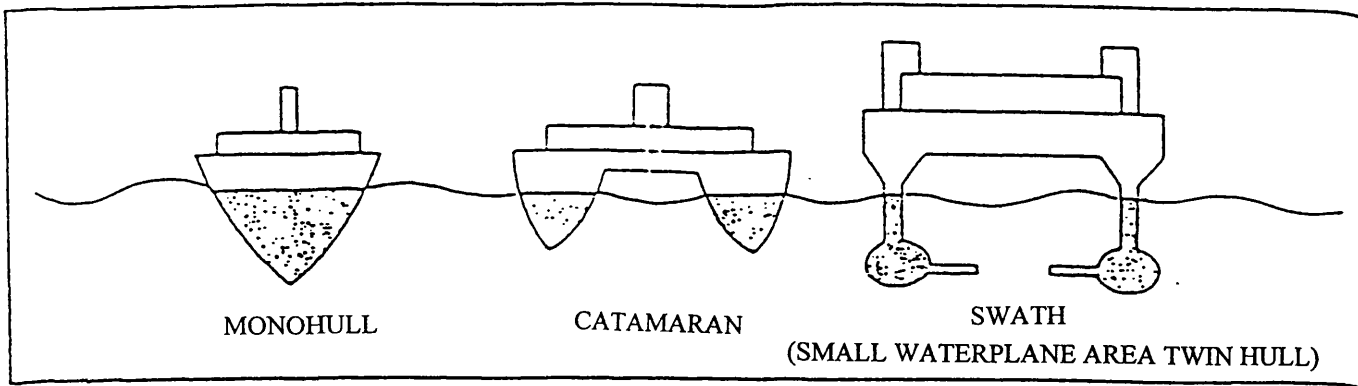


Fig. 1.1 Cross-section shape of SWATH ship (Gupta and Schmidt, 1986)

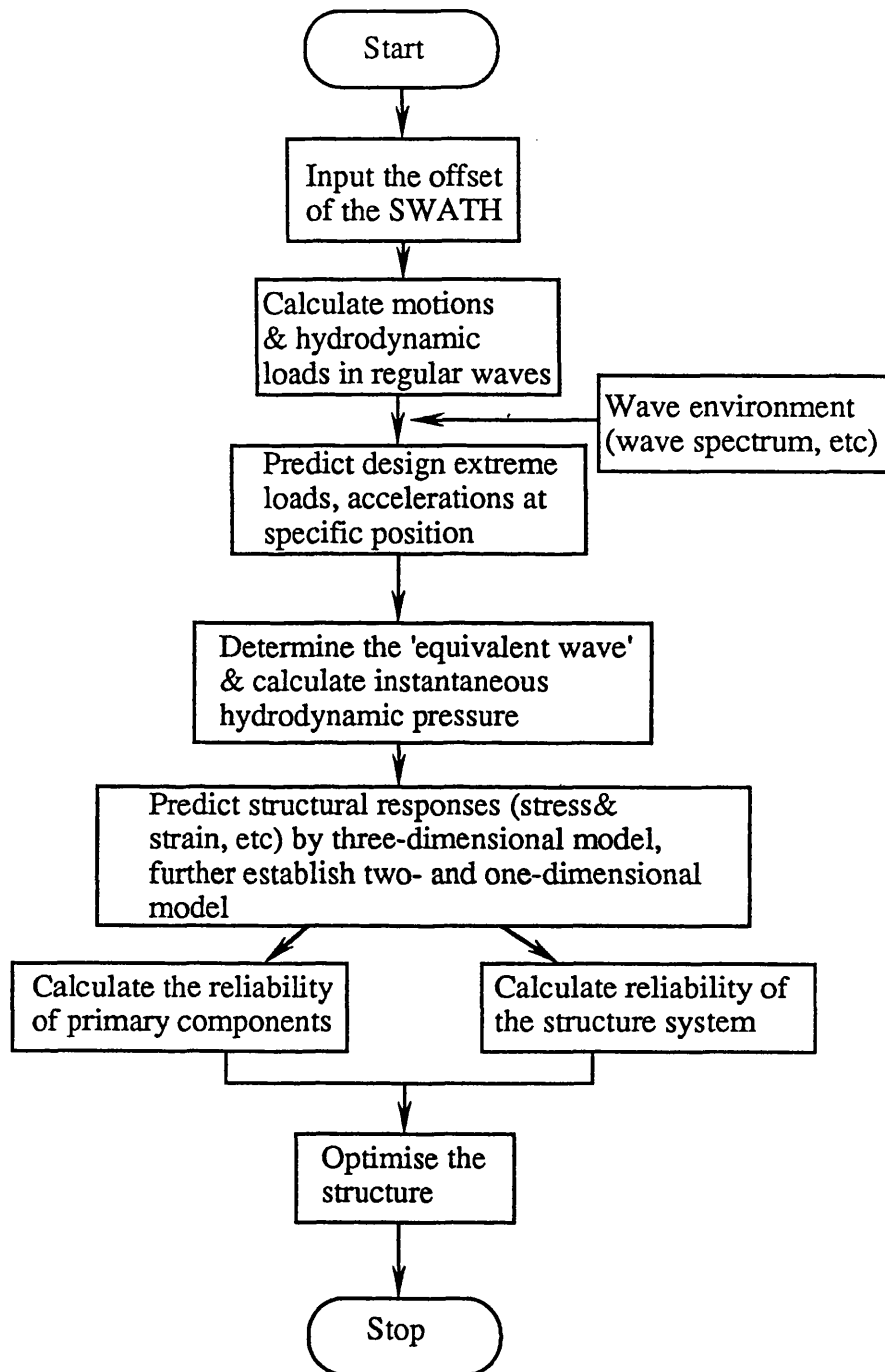


Fig. 1.2 The Flowchart of the Present Study

CHAPTER 2 RELIABILITY METHODS

2.1 INTRODUCTION

The reliability analysis concept was initially introduced in the field of aircraft, civil engineering structures and so on. Now it is widely applied in aeronautical, nuclear engineering, electrical and electronic engineering, civil engineering and marine structures. Tremendous advances have been made in the area of structural reliability methods and reliability-based design. Recently the incorporation of probabilistic concepts into design code of marine and civil structures has been observed. The probabilistic concepts were first introduced by the Norwegian Petroleum Directorate (NPD, 1977; Fjeld, 1977). In 1984 the Conoco-ABS Rule Case Committee developed a reliability-based model code which led to API RP2T and Bulletin 2U and 2V. There is a trend that developing a new design code will be based on reliability analysis, and the existing codes are re-developed based on this concept.

In this chapter, a general tool for component and structural system reliability analysis will be developed, and its validity will be checked by applying it to a few simple cases.

2.2 COMPONENT RELIABILITY METHODS

As described in Chapter 1, the failure probability of a structural component for a time-independent problem could be approximately evaluated by FORM (or AFOSM) and SORM. However Monte Carlo simulation method can give much more accurate results than those from FORM/SORM.

In this section the FORM, SORM and Monte Carlo Simulation Method will be developed, and applied to two cases to verify their validity.

2.2.1 The First-Order and Second Moment Method (FORM)

Among various algorithms for component reliability analysis, Fiessler and Rackwitz's algorithm, which shows good accuracy, efficiency and robustness, is the best. Therefore this algorithm is used in the present study. The procedure is briefly described below.

If x_1, x_2, \dots, x_n are the n independent variables involved in a structural design problem, a general expression for any limit state equation for the structure is

$$Z = g(x_1, x_2, \dots, x_n) > 0 \quad (2.1)$$

where the nature of g depends on the structural type and limit state under consideration. The failure surface is given by

$$Z=0$$

and a linear approximation to this can be found by using the Taylor series expansion

$$Z \cong g(x_1^*, x_2^*, \dots, x_n^*) + \sum_1^n (x_i - x_i^*) g_i'(x^*) \quad (2.2)$$

where

$$g_i'(x^*) = \frac{\partial g}{\partial x_i}$$

evaluated at the unknown design point

$$x^* = (x_1^*, x_2^*, \dots, x_n^*)$$

If m_i and σ_i represent the means and standard deviations of the basic variables x_i , the mean value of Z is

$$m_z \cong \sum_1^n (m_i - x_i^*) g_i'(x^*) \quad (2.3)$$

and the standard deviation

$$\sigma_z \equiv \left[\sum_1^n \{g_i'(x^*)\sigma_i\}^2 \right]^{1/2} \quad (2.4)$$

σ_z may be expressed as a linear combination of σ_i 's as follows:

$$\sigma_z = \sum_1^n \alpha_i g_i'(x^*) \sigma_i \quad (2.5)$$

where

$$\alpha_i = \frac{g_i'(x^*)\sigma_i}{\left[\sum_{j=1}^n \{g_j'(x^*)\sigma_j\}^2 \right]^{1/2}} \quad (2.6)$$

are referred to as sensitivity factors since they reflect the relative influence of each design variable on the model.

If the reliability index β of the design is defined as m_z / σ_z , then from equations (2.3) and (2.5)

$$\beta = \frac{\sum_1^n (m_i - x_i^*) g_i'(x^*)}{\sum_1^n \alpha_i g_i'(x^*) \sigma_i} \quad (2.7)$$

from which it follows

$$\sum_1^n g_i'(x^*) (m_i - x_i^* - \alpha_i \beta \sigma_i) = 0 \quad (2.8)$$

The solution of this equation is

$$x_i^* = m_i - \alpha_i \beta \sigma_i \quad \text{for all } i \quad (2.9)$$

and x_i^* is referred to as the 'design point'. It corresponds to the point of maximum probability of failure density when all the variables are normally distributed. For given values of m_i, σ_i and β , equation (2.9) can be solved in conjunction with equation (2.6).

Finally, the probability of failure for the structure is:

$$P_f = \Phi(-\beta) \quad (2.10)$$

where Φ is the normal distribution function.

If any of the design variables has non-normal distributions, a transformation is necessary.

Suppose that the variables x_i have density function $f(x_i)$ and distribution function $F(x_i)$. The basic idea of the transformation is to let the original density function and distribution function of the variable x_i be equal to that of a normal variable at the design point. That is:

$$F(x_i^*) = \Phi\left(\frac{x_i^* - m_i^N}{\sigma_i^N}\right) \quad (2.11)$$

$$f(x_i^*) = \frac{1}{\sigma_i^N} \varphi\left(\frac{x_i^* - m_i^N}{\sigma_i^N}\right) \quad (2.12)$$

so, one can get

$$m_i^N = x_i^* - \Phi^{-1}\{F(x_i^*)\} \sigma_i^N \quad (2.13)$$

$$\sigma_i^N = \frac{f^N[\Phi^{-1}\{F(x_i^*)\}]}{f(x_i^*)} \quad (2.14)$$

where m_i^N , σ_i^N are the mean and standard deviations of the equivalent normal distribution, F is the cumulative distribution function of x_i , and f^N is the normal probability density function.

2.2.2 Second-Order Method (SORM)

The point-fitting method proposed by Kiureghian et al (1987) is used because of its efficiency and compatibility to most of existing formulae. Details of this procedure will be presented below.

The Available Formulae for Second Order Methods

The existing formulae which are used to calculate the second-order reliability can be summarised as follows:

Breitung's formula

$$P_{f2} \approx \Phi(-\beta) \prod_{i=1}^{n-1} (1 + \beta k_i)^{-1/2} \quad (2.15)$$

where P_{f2} is the second order approximation of the failure probability. β is the reliability index. k_i are the main curvatures of failure surface equation. When β approaches infinity, P_{f2} approaches P_f . n is the number of random variables.

Tvedt's formulae

Tvedt (1984, 1985) has derived three formulae, which are called three term formula, single-integral formula, and double-integral formula.

If the paraboloid is defined in the rotated space by

$$y'_n = \beta + \frac{1}{2} y'^T A y' \quad (2.16)$$

then three term formula is expressed as:

$$P_{f2} \approx T_1 + T_2 + T_3 \quad (2.17)$$

where

$$T_1 = \Phi(-\beta) \prod_{i=1}^{n-1} (1 + \beta k_i)^{-1/2}$$

$$T_2 = [\beta \Phi(-\beta) - \phi(\beta)] \left\{ \prod_{i=1}^{n-1} (1 + \beta k_i)^{-1/2} - \prod_{i=1}^{n-1} (1 + (\beta + 1)k_i)^{-1/2} \right\}$$

$$T_3 = (\beta + 1) [\beta \Phi(-\beta) - \phi(\beta)] \left\{ \prod_{i=1}^{n-1} (1 + \beta k_i)^{-1/2} - \operatorname{Re} \left\{ \prod_{i=1}^{n-1} (1 + (\beta + j)k_i)^{-1/2} \right\} \right\}$$

in which $j = \sqrt{-1}$

It can be seen that the first term is the same as that in Breitung's formula. The last two terms may modify the result of Breitung's formula when β is small. Three term formula works well except for the case in which a curvature is close to the curvature of a circle with centre at the origin and radius β . This is because there are singularities in

the formula for $k_i = -\frac{1}{\beta}$ and $k_i = -\frac{1}{(\beta + 1)}$. In addition, if β is small, the results by

Breitung's formula approach the first-order results $\Phi(-\beta)$, and the last two terms do not always provide a good correction.

Single integral formula is expressed as:

$$P_{f2} \approx \phi(-\beta) \sum_{i=1}^k \omega_i \operatorname{Re} \left\{ \left[\det \left(\mathbf{I} + \left((\beta^2 + 2s_i)^{1/2} + j \right) \mathbf{A} \right) \right]^{-1/2} \right\} (\beta^2 + 2s_i)^{-1/2} \quad (2.18)$$

where the summation represents a k-point Gauss-Laguerre quadrature approximation with weight ω_i and abscissas s_i .

Double-integral formula is expressed as:

$$P_{f2} \approx \frac{2}{\sqrt{\pi}} \phi(-\beta) \operatorname{Re} \int_0^\infty \int_0^\infty \prod_{i=1}^{n-1} \left(r_p \left\{ \left[1 + (\beta^2 + 2s)^{1/2} k_i + \sqrt{2} i u k_i \right]^{-1/2} \right\} \right) (\beta^2 + 2s)^{-1/2} \exp(-s - u^2) ds du \quad (2.19)$$

where $r_p\{\cdot\}$ denotes the root with positive real part.

Exact integral formula is expressed as

$$P_{f2} \approx \Phi(\beta) \operatorname{Re} \left\{ j \left(\frac{2}{\pi} \right)^{1/2} \int_0^\infty \frac{\exp[(t + \beta)^2 / 2]}{t} \left[\prod_{i=1}^{n-1} (1 - t \times k_i)^{-1/2} \right] dt \right\} \quad (2.20)$$

Applying saddle point integration technique to this formula could achieve any accuracy in numerical sense.

Hohenbichler and Rackwitz's formula

$$P_{f2} \approx \Phi(-\beta) \prod_{i=1}^{n-1} \left(1 + \frac{\phi(-\beta)}{\Phi(-\beta)} k_i \right)^{-1/2} \quad (2.21)$$

This formula is asymptotically equivalent to Breitung's because for large β ,

$\frac{\phi(-\beta)}{\Phi(-\beta)}$ approaches β .

The Point-Fitting Procedure

For a point-fitting procedure, the basic variables $\mathbf{X} = \{x_1, \dots, x_n\}$ are first transformed into standard normalised space $\mathbf{Y} = \{y_1, \dots, y_n\}$ by

$$\mathbf{Y} = \mathbf{T}(\mathbf{X}) \quad (2.22)$$

then the variables \mathbf{Y} are transformed to a rotated space \mathbf{Y}' by an orthogonal transformation.

$$\mathbf{Y}' = \mathbf{R}\mathbf{Y} \quad (2.23)$$

This can be done by Gram-Schmidt algorithm. In the rotated space, y'_n axis passes the design point. So the n -th row of \mathbf{R} is selected to be \mathbf{Y}^* / β .

The approximate paraboloid is defined as:

$$y'_n = \beta + \frac{1}{2} \sum_{i=1}^{n-1} a_i y_i'^2 \quad (2.24)$$

$2(n-1)$ number of points, which is in the neighbourhood of the design point, are selected along the co-ordinate axes in the rotated space in the manner shown in Fig. 2.1. So, the co-ordinates of the selected points are $\{0, \dots, \pm k\beta, \dots, \eta_{\pm i}\}$. The parameter k is pre-selected as:

$$k = \begin{cases} 1 & \text{for } \beta \leq 3.0 \\ 3/\beta & \text{for } \beta > 3.0 \end{cases} \quad (2.25)$$

$\eta_{\pm i}$ is determined by the following iterative procedure.

- 1) give an initial trial point

$$y_1' = \{0, \dots, \pm k\beta, \dots, \beta\} \quad (2.26)$$

The sign of the performance function $g(\mathbf{X})$ then determines whether $\eta_{\pm i}$ are greater or

smaller than β .

2) get the second trial point

$$y_2' = \{0, \dots, \pm k\beta, \dots, (1 + 0.5k^2)\beta\} \quad \text{for } g_1 > 0 \quad (2.27a)$$

or
$$y_2' = \{0, \dots, \pm k\beta, \dots, (1 - 0.5k^2)\beta\} \quad \text{for } g_1 < 0 \quad (2.27b)$$

3) do iteration till convergence is achieved

$$\eta_3 = \eta_1 - g_1 \frac{\eta_1 - \eta_2}{g_1 - g_2} \quad (2.28)$$

This iteration generally converges within three steps.

Then the principal curvature a_i is determined by

$$\frac{1}{\sqrt{1 + \beta \times a_i}} = \frac{1}{2} \left(\frac{1}{\sqrt{1 + \beta \times a_{-i}}} + \frac{1}{\sqrt{1 + \beta \times a_{+i}}} \right) \quad (2.29)$$

where

$$a_{\pm i} = 2(\eta_{\pm i} - \beta) / (k\beta)^2 \quad (2.30)$$

Having got the principal curvatures, the second-order approximation of failure probability could be obtained by any of the formulae mentioned above.

It is worth noting that the accuracy of the point-fitting method is the worst when $a_1 = a_2 = \dots = a_{n-1}$. Therefore, if this occurs, try another transformation scheme.

2.2.3 Monte Carlo Simulation Method

The original Monte Carlo simulation method is adopted in the present study.

Assume $X_i, i=1, \dots, n$ are independent variables and their distributions are known. The limit-state function is defined as:

$$M = g(x_1, \dots, x_n) \quad (2.31)$$

It is likely to simulate the probability distribution of M by progressively building up a large sample.

Then the failure probability may be estimated in several ways. When the sample number n_s is large, a simple way is

$$P_f = P(M \leq 0) = \lim_{n_s \rightarrow \infty} k / n_s \quad (2.32)$$

where k is the number of $M \leq 0$.

2.2.4 Application to examples

The AFOSM, SORM and Monte Carlo simulation method described in the above sections have been implemented in Unix system. Validity of the program is verified by two examples.

Example 1

The first example is taken from Thoft-Christensen and Baker (1982). The safety margin equation is expressed as:

$$g(\mathbf{X}) = x_1 x_2 - 78.12 x_3 \quad (2.33)$$

all the variables are normally distributed. Their parameters are:

$\mu_{x1} = 2.0 \cdot 10^7$	kN/m ²	$\sigma_{x1} = 0.5 \cdot 10^7$	kN/m ²
$\mu_{x2} = 10^{-4}$	m ⁴	$\sigma_{x2} = 0.2 \cdot 10^{-4}$	m ⁴
$\mu_{x3} = 4$	kN	$\sigma_{x3} = 1$	kN

The reliability index $\beta=3.29$, the design point is:

$$\mathbf{X}^* = 3.29 * (-0.97, -0.18, 0.17)$$

So, the failure probability by AFOSM and SORM are respectively

$$P_{f1} = 0.4935 * 10^{-3}$$

$$P_{f2} = 0.5998 * 10^{-3}$$

In addition, Monte Carlo simulation was carried out. The sample size is 100,000. The result is:

$$P_{fmon} = 0.79 * 10^{-3}$$

From the above results, it can be seen that the second-order result is slightly better than AFOSM's. Their relative errors are:

$$e_1 = \frac{P_{f1} - P_{fmon}}{P_{fmon}} = \frac{0.5 - 0.79}{0.79} = -36.6\%$$

$$e_2 = \frac{P_{f2} - P_{fmon}}{P_{fmon}} = \frac{0.6 - 0.79}{0.79} = -24.1\%$$

Example 2

The second example is taken from Kiureghian et al (1987).

$$g(\mathbf{X}) = x_1 + 2x_2 + 2x_3 + x_4 - 5x_5 - 5x_6 \tag{2.34}$$

The variables x_i are independent and lognormally distributed with the means $\mu_1 = \dots = \mu_4 = 120$, $\mu_5 = 50$, $\mu_6 = 40$, and standard deviations $\sigma_1 = \dots = \sigma_4 = 12$, $\sigma_5 = 15$, and $\sigma_6 = 12$.

The results are:

$$P_{f1}=0.9433*10^{-2}$$

$$P_{f2}=1.213*10^{-2}$$

$$P_{fmon}=1.21*10^{-2}$$

$$e_1=-22.0\%$$

$$e_2=0.25\%$$

In this case, the results from SORM are much better than those from AFOSM.

2.3 SYSTEM RELIABILITY METHODS

In this section a structural system reliability method is developed. The β -unzipping method will be extended by introducing a discarding process, which could save computational time. The linearized plasticity condition is used to establish the safety margins which are automatically generated by computer. The significant failure modes of the structure are identified by the extended β -unzipping method, and the system reliability index is then evaluated by Ditlevsen's bounds.

2.3.1 Basic Assumptions

- 1) Only the loads and material strength of the structure are treated as random variables, the remaining, such as geometrical variables, are deterministic.
- 2) The failure of the structure is defined as the formation of a mechanism.
- 3) The members of the structure are uniform and homogeneous and to which only concentrated forces and moments are applied. So critical sections where plastic hinges may form are the joints of the members and the points at which the concentrated loads are applied. The numbers of critical sections are given in the way that for element k the number of its left and right end are $i=2*k-1$ and $j=2*k$ respectively.
- 4) A section is failed if its plasticity condition $FP_k=0$ is satisfied.

2.3.2 Automatic Generation of Safety Margins

The plasticity condition is expressed as:

$$\frac{M}{M_p} + \left(\frac{P}{P_{cr}} \right)^2 = 1 \quad (2.37)$$

It is quite complicated to directly use the above form to define the safety margins. So the linearized form is used.

The linearized plasticity condition considering the interaction of bending moment and axial force including the buckling effect can be expressed as follows:

$$FP_k = R_k - C_k^T x_t = 0 \quad (k = i, j) \quad (2.38)$$

where:

$$R_k = \sigma_{yk} w_k$$

w_k the plastic section modulus

σ_{yk} the yield stress of the member

$$C_i^T = \left(d \frac{w_i}{A_i} \text{sign}(F_{xi}), 0, \text{sign}(M_{zi}), 0, 0, 0 \right)$$

$$C_j^T = \left(0, 0, 0, d \frac{w_j}{A_j} \text{sign}(F_{xj}), 0, \text{sign}(M_{zj}) \right)$$

d is the factor to consider the effect of buckling. It is equal to

$$d = \begin{cases} 1 & \text{for tension} \\ \sigma_{yi} / \sigma_{*i} & \text{for compression} \end{cases}$$

σ_{ei} is the buckling stress of the member

A_i the cross-sectional area of the member

$\mathbf{x}_t = \left(F_{xi}, F_{yi}, M_{zi}, F_{xj}, F_{yj}, M_{zj} \right)$ is the nodal forces in the member.

The above plasticity condition is clearly shown in Fig. 2.2.

After a section of the member has yielded, the relation between the nodal forces \mathbf{x}_t and displacements δ_t vectors of the member can be derived by plastic theory.

The total displacement δ_t of the member is assumed to be comprised of an elastic displacement and a plastic displacement

$$\delta_t = \delta_t^e + \delta_t^p = \delta_t^e + \delta_i^p + \delta_j^p \quad (2.39)$$

Based on the plastic deformation theory, the plastic deformation is expressed in the form:

$$\delta_i^p = \lambda_i \frac{\partial F_i}{\partial \mathbf{x}_t} = -\lambda_i \mathbf{C}_i \quad (2.40-a)$$

$$\delta_j^p = \lambda_j \frac{\partial F_j}{\partial \mathbf{x}_t} = -\lambda_j \mathbf{C}_j \quad (2.40-b)$$

in which λ_i and λ_j are factors to indicate the magnitude of plastic deformation. When section i (or j) is elastic, λ_i (or λ_j) = 0.

The nodal forces are expressed as:

$$\mathbf{x}_t = \mathbf{K}_t \delta_t^e = \mathbf{K}_t (\delta_t - \delta_t^p) \quad (2.41)$$

Substituting Eq. (2.39) and (2.40) into Eq. (2.41)

$$\mathbf{x}_t = \mathbf{K}_t \boldsymbol{\delta}_t + \lambda_i \mathbf{K}_t \mathbf{C}_i + \lambda_j \mathbf{K}_t \mathbf{C}_j \quad (2.42)$$

Substitute equation (2.42) into equation (2.38)

$$\mathbf{R}_i - \mathbf{C}_i^T \left(\mathbf{K}_t \boldsymbol{\delta}_t + \lambda_i \mathbf{K}_t \mathbf{C}_i + \lambda_j \mathbf{K}_t \mathbf{C}_j \right) = 0 \quad (2.43-a)$$

$$\mathbf{R}_j - \mathbf{C}_j^T \left(\mathbf{K}_t \boldsymbol{\delta}_t + \lambda_i \mathbf{K}_t \mathbf{C}_i + \lambda_j \mathbf{K}_t \mathbf{C}_j \right) = 0 \quad (2.43-b)$$

Substitute the equation (2.43) into equation (2.42), then re-arrange the resulting equation in the form:

$$\mathbf{x}_t^{(r)} + \left(-\mathbf{x}_t'^{(r)} \right) = \mathbf{K}_t^{(r)} \boldsymbol{\delta}_t \quad (2.44)$$

in which

$\mathbf{x}_t'^{(r)}$ is the equivalent nodal force vector with opposite sign;

$\mathbf{K}_t^{(r)}$ is the reduced member stiffness matrix.

The expressions of $\mathbf{x}_t'^{(r)}$, $\mathbf{K}_t^{(r)}$, λ_i and λ_j depend on the status of the member.

1). when the member is elastic

$$\lambda_i = \lambda_j = 0$$

$$\mathbf{K}_t^{(r)} = \mathbf{K}_t$$

$$\mathbf{x}_t'^{(r)} = 0$$

$$\mathbf{K}_t = \begin{bmatrix} \frac{EA}{L} & 0 & 0 & -\frac{EA}{L} & 0 & 0 \\ & \frac{12EI}{L^3} & \frac{6EI}{L^2} & 0 & -\frac{12EI}{L^3} & \frac{6EI}{L^2} \\ & & \frac{4EI}{L} & 0 & -\frac{6EI}{L^2} & \frac{2EI}{L} \\ & & & \frac{EA}{L} & 0 & 0 \\ & \text{Sym.} & & & \frac{12EI}{L^3} & -\frac{6EI}{L^2} \\ & & & & & \frac{4EI}{L} \end{bmatrix} \quad (2.45)$$

2). When the left-end has failed

$$\lambda_j = 0$$

$$\lambda_i = (\mathbf{R}_i - \mathbf{C}_i^T \mathbf{K}_t \boldsymbol{\delta}_i) / (\mathbf{C}_i^T \mathbf{K}_t \mathbf{C}_i)$$

$$\mathbf{K}_t^{(r)} (= \mathbf{K}_t^{(L)}) = \begin{cases} \mathbf{K}_t - \mathbf{K}_t \mathbf{C}_i \mathbf{C}_i^T \mathbf{K}_t / (\mathbf{C}_i^T \mathbf{K}_t \mathbf{C}_i) & \text{ductile} \\ 0 & \text{brittle} \end{cases}$$

$$\mathbf{x}_t^{(r)} (= \mathbf{x}_t^{(L)}) = \begin{cases} \mathbf{R}_i \mathbf{K}_t \mathbf{C}_i / (\mathbf{C}_i^T \mathbf{K}_t \mathbf{C}_i) & \text{ductile} \\ 0 & \text{brittle} \end{cases}$$

$$\mathbf{K}_t^{(L)} = \begin{bmatrix} \frac{EA}{L} \frac{1}{1+\bar{\beta}} & -\frac{EA}{L} \frac{3C^L}{2(1+\bar{\beta})} & -EA \frac{C^L}{1+\bar{\beta}} & -\frac{EA}{L} \frac{1}{1+\bar{\beta}} & \frac{EA}{L} \frac{3C^L}{2(1+\bar{\beta})} & -EA \frac{C^L}{2(1+\bar{\beta})} \\ & \frac{3EI}{L^3} \frac{1+4\bar{\beta}}{1+\bar{\beta}} & \frac{6EI}{L^2} \frac{\bar{\beta}}{1+\bar{\beta}} & \frac{EA}{L} \frac{3C^L}{2(1+\bar{\beta})} & -\frac{3EI}{L^3} \frac{1+4\bar{\beta}}{1+\bar{\beta}} & \frac{3EI}{L^2} \frac{1+2\bar{\beta}}{1+\bar{\beta}} \\ & & \frac{4EI}{L} \frac{\bar{\beta}}{1+\bar{\beta}} & EA \frac{C^L}{1+\bar{\beta}} & -\frac{6EI}{L^2} \frac{\bar{\beta}}{1+\bar{\beta}} & \frac{2EI}{L} \frac{\bar{\beta}}{1+\bar{\beta}} \\ & \text{Sym.} & & \frac{EA}{L} \frac{1}{1+\bar{\beta}} & -\frac{EA}{L} \frac{3C^L}{2(1+\bar{\beta})} & EA \frac{C^L}{1+\bar{\beta}} \\ & & & & \frac{3EI}{L^3} \frac{1+4\bar{\beta}}{1+\bar{\beta}} & -\frac{3EI}{L^2} \frac{1+2\bar{\beta}}{1+\bar{\beta}} \\ & & & & & \frac{3EI}{L} \frac{3+4\bar{\beta}}{3(1+\bar{\beta})} \end{bmatrix}$$

$$\mathbf{x}_t^{(r)} = \mathbf{x}_t^{.L} = \begin{bmatrix} \frac{\bar{\beta}/C^L R_i'}{1+\bar{\beta}} \frac{L}{L} \\ \frac{1}{1+\bar{\beta}} \frac{3R_i'}{2L} \\ \frac{1}{1+\bar{\beta}} R_i' \\ \frac{\bar{\beta}/C^L R_i'}{1+\bar{\beta}} \frac{L}{L} \\ \frac{1}{1+\bar{\beta}} \frac{3R_i'}{2L} \\ \frac{1}{1+\bar{\beta}} \frac{R_i'}{2} \end{bmatrix} \quad (2.46)$$

3). When right end has failed

$$\lambda_i = 0$$

$$\lambda_j = (R_j - \mathbf{c}_j^T \mathbf{K}_t \boldsymbol{\delta}_t) / (\mathbf{c}_j^T \mathbf{K}_t \mathbf{c}_j)$$

$$\mathbf{K}_t^{(r)} (= \mathbf{K}_t^{(R)}) = \begin{cases} \mathbf{K}_t - \mathbf{K}_t \mathbf{c}_j \mathbf{c}_j^T \mathbf{K}_t / (\mathbf{c}_j^T \mathbf{K}_t \mathbf{c}_j) & \text{ductile} \\ 0 & \text{brittle} \end{cases}$$

$$\mathbf{x}_t^{(r)} (= \mathbf{x}_t^{.R}) = \begin{cases} R_j \mathbf{K}_t \mathbf{c}_j / (\mathbf{c}_j^T \mathbf{K}_t \mathbf{c}_j) & \text{ductile} \\ 0 & \text{brittle} \end{cases}$$

$$\mathbf{K}_t^{(R)} = \begin{bmatrix} \frac{EA}{L} \frac{1}{1+\alpha} & \frac{EA}{L} \frac{3C^R}{2(1+\alpha)} & EA \frac{C^R}{2(1+\alpha)} & -\frac{EA}{L} \frac{1}{1+\alpha} & -\frac{EA}{L} \frac{3C^R}{2(1+\alpha)} & EA \frac{C^R}{(1+\alpha)} \\ & \frac{3EI}{L^3} \frac{1+4\alpha}{1+\alpha} & \frac{3EI}{L^2} \frac{1+2\alpha}{1+\alpha} & \frac{EA}{L} \frac{3C^R}{2(1+\alpha)} & \frac{3EI}{L^3} \frac{1+4\alpha}{1+\alpha} & \frac{6EI}{L^2} \frac{\alpha}{1+\alpha} \\ & & \frac{3EI}{L} \frac{3+4\alpha}{1+\alpha} & -EA \frac{C^R}{2(1+\alpha)} & \frac{3EI}{L^2} \frac{1+2\alpha}{1+\alpha} & \frac{2EI}{L} \frac{\alpha}{1+\alpha} \\ & & & \frac{EA}{L} \frac{1}{1+\alpha} & \frac{EA}{L} \frac{3C^R}{2(1+\alpha)} & -EA \frac{C^R}{1+\alpha} \\ & \text{Sym.} & & & \frac{3EI}{L^3} \frac{1+4\alpha}{1+\alpha} & \frac{6EI}{L^2} \frac{\alpha}{1+\alpha} \\ & & & & & \frac{4EI}{L} \frac{\alpha}{1+\alpha} \end{bmatrix}$$

$$\mathbf{x}_t^{(r)} = \mathbf{x}_t^{(a)} = \begin{bmatrix} \frac{\alpha / C^R R_j'}{1 + \alpha \frac{L}{3R_j'}} \\ \frac{1 + \alpha \frac{2L}{R_j'}}{1 + \alpha \frac{2}{R_j'}} \\ \frac{\alpha / C^R R_j'}{1 + \alpha \frac{L}{3R_j'}} \\ \frac{1 + \alpha \frac{2L}{R_j'}}{1 + \alpha \frac{2}{R_j'}} \end{bmatrix} \quad (2.47)$$

4). When both ends have failed

$$\begin{Bmatrix} \lambda_i \\ \lambda_j \end{Bmatrix} = -\mathbf{G}^{-1} \mathbf{H} \delta_t + \mathbf{G}^{-1} \begin{Bmatrix} R_i \\ R_j \end{Bmatrix}$$

where

$$\mathbf{G}^{-1} = \begin{bmatrix} \mathbf{C}_i^T \mathbf{K}_t \mathbf{C}_i & \mathbf{C}_i^T \mathbf{K}_t \mathbf{C}_j \\ \mathbf{C}_j^T \mathbf{K}_t \mathbf{C}_i & \mathbf{C}_j^T \mathbf{K}_t \mathbf{C}_j \end{bmatrix}^{-1}$$

$$\mathbf{H} = \begin{bmatrix} \mathbf{C}_i^T \mathbf{K}_t \\ \mathbf{C}_j^T \mathbf{K}_t \end{bmatrix}$$

$$\mathbf{K}_t^{(r)} (= \mathbf{K}_t^{(B)}) = \begin{cases} \mathbf{K}_t - \mathbf{H}^T \mathbf{G}^{-1} \mathbf{H} & \text{ductile} \\ 0 & \text{brittle} \end{cases}$$

$$\mathbf{x}_t^{(r)} (= \mathbf{x}_t^{(B)}) = \begin{cases} \mathbf{H}^T \mathbf{G}^{-1} \begin{Bmatrix} R_i \\ R_j \end{Bmatrix} & \text{ductile} \\ 0 & \text{brittle} \end{cases}$$

$$\mathbf{K}_t^{(R)} = \begin{bmatrix}
 \frac{EA}{L} \frac{3}{\xi} & -\frac{EA}{L} \frac{3(C^L - C^R)}{\xi} & -\frac{EA}{\xi} \frac{3C^L}{\xi} & -\frac{EA}{L} \frac{3}{\xi} & -\frac{EA}{L} \frac{3(C^L - C^R)}{\xi} & \frac{EA}{\xi} \frac{3C^R}{\xi} \\
 & \frac{12EI}{L^3} \frac{\bar{\beta} + \alpha - 2\gamma}{\xi} & \frac{12EI}{L^2} \frac{\bar{\beta} - \gamma}{\xi} & -\frac{EA}{L} \frac{3(C^L - C^R)}{\xi} & -\frac{12EI}{L^3} \frac{\bar{\beta} + \alpha - 2\gamma}{\xi} & \frac{12EI}{L^2} \frac{\alpha - \gamma}{\xi} \\
 & & \frac{12EI}{L} \frac{\bar{\beta}}{\xi} & \frac{EA}{\xi} \frac{3C^L}{\xi} & -\frac{12EI}{L^2} \frac{\bar{\beta} - \gamma}{\xi} & -\frac{12EI}{L} \frac{\gamma}{\xi} \\
 & \text{Sym.} & & \frac{EA}{L} \frac{3}{\xi} & \frac{EA}{L} \frac{3(C^L - C^R)}{\xi} & -\frac{EA}{\xi} \frac{3C^R}{\xi} \\
 & & & & \frac{12EI}{L^3} \frac{\bar{\beta} + \alpha - 2\gamma}{\xi} & \frac{12EI}{L^2} \frac{\alpha - \gamma}{\xi} \\
 & & & & & \frac{12EI}{L} \frac{\alpha}{\xi} \\
 & & & & & \frac{12EI}{L} \frac{\alpha}{\xi}
 \end{bmatrix}$$

$$\mathbf{x}_t^{(r)} = \mathbf{x}_t^{,B} = \begin{bmatrix}
 \frac{4\bar{\beta} + 2\gamma}{\xi} \frac{R_i'}{C_{L,L}^L} - \frac{4\alpha + 2\gamma}{\xi} \frac{R_j'}{C_{L,L}^R} \\
 \frac{3(1 + 2\alpha + 2\gamma)}{\xi} \frac{R_i'}{L} + \frac{3(1 + 2\bar{\beta} + 2\gamma)}{\xi} \frac{R_j'}{L} \\
 \frac{3 + 4\alpha + 2\gamma}{\xi} R_i' + \frac{2(\bar{\beta} + 2\gamma)}{\xi} R_j' \\
 -\frac{4\bar{\beta} + 2\gamma}{\xi} \frac{R_i'}{C_{L,L}^L} + \frac{4\alpha + 2\gamma}{\xi} \frac{R_j'}{C_{L,L}^R} \\
 \frac{3(1 + 2\alpha + 2\gamma)}{\xi} \frac{R_i'}{L} - \frac{3(1 + 2\bar{\beta} + 2\gamma)}{\xi} \frac{R_j'}{L} \\
 \frac{2(\alpha + 2\gamma)}{\xi} R_i' + \frac{3 + 4\bar{\beta} + 2\gamma}{\xi} R_j'
 \end{bmatrix} \quad (2.48)$$

in which

$$R_i = w_i \sigma_{yi}$$

$$R_i' = \text{sign}(M_{zi}) R_i$$

$$C^L = d \frac{w_i}{A_i L} \text{sign}(M_{zi}) \text{sign}(F_{xi})$$

$$\bar{\beta} = \frac{A_i L^2}{4I} (C^L)^2$$

$$R_j = w_j \sigma_{yj}$$

$$R'_j = \text{sign}(M_{zj})R_j$$

$$C^R = d \frac{w_j}{A_j L} \text{sign}(M_{zj}) \text{sign}(F_{xj})$$

$$\alpha = \frac{A_i L^2}{4I} (C^R)^2$$

$$\gamma = \frac{A_i L^2}{4I} (C^L C^R)$$

$$\xi = 3 + 4(\bar{\beta} + \alpha + \gamma)$$

In above equations if the factor 'd' is always taken as 1, then the formulae are reduced to the case in which only interaction of bending moment and axial force is considered. Again if the $C^R = C^L = 0$, the formulae are for the case that only bending moment is considered.

In general, a safety margin M_i could be expressed as:

$$M_i = R_i - C_i^T x_t \leq 0 \quad (2.49)$$

in which

$$x_t = k_t^{(r)} \delta_t + x_t'^{(r)} \quad (2.50)$$

In the structural analysis, the equation for the structure is expressed as:

$$k^{(r)} \delta = L + R^{(r)} \quad (2.51)$$

where

$k^{(r)}$ is the reduced total stiffness matrix

δ is the displacement in global co-ordinate system

L is the external loads

$\mathbf{R}^{(r)}$ is the equivalent nodal force vector transformed to the global co-ordinate system. It is evaluated by:

$$\mathbf{R}^{(r)} = - \sum_{t=1}^n \mathbf{T}^T \mathbf{x}_t'^{(r)}$$

\mathbf{T} is the transformation matrix

From equation (2.51)

$$\delta = \mathbf{k}^{(r)-1} (\mathbf{L} + \mathbf{R}^{(r)}) \quad (2.52)$$

then the displacement for a member can be obtained by

$$\delta_t = \mathbf{T} \times \mathbf{k}_t^{(r)-1} (\mathbf{L} + \mathbf{R}^{(r)}) \quad (2.53)$$

Hence

$$\begin{aligned} \mathbf{x}_t &= \mathbf{k}_t^{(r)} \mathbf{T} \times \mathbf{k}_t^{(r)-1} (\mathbf{L} + \mathbf{R}^{(r)}) + \mathbf{x}_t'^{(r)} \\ &= \mathbf{b}_t (\mathbf{L} + \mathbf{R}^{(r)}) + \mathbf{x}_t'^{(r)} \end{aligned} \quad (2.54)$$

Finally the safety margin equation (2.49) can be expressed as:

$$\begin{aligned} M_i &= R_i - \mathbf{C}_i^T \left[\mathbf{b}_t (\mathbf{L} + \mathbf{R}^{(r)}) + \mathbf{x}_t'^{(r)} \right] \\ &= R_i - \mathbf{C}_i^T \left[\mathbf{b}_t \left(\mathbf{L} - \sum_{t=1}^n \mathbf{T}^T \mathbf{x}_t'^{(r)} \right) + \mathbf{x}_t'^{(r)} \right] \\ &= R_i - \mathbf{C}_i^T \mathbf{b}_t \mathbf{L} + \mathbf{C}_i^T \left[\mathbf{b}_t \sum_{t=1}^n \mathbf{T}^T \mathbf{x}_t'^{(r)} - \mathbf{x}_t'^{(r)} \right] \\ &= R_i - \sum_{j=1}^m b_{ij} L_j + \sum_{k=1}^{p-1} a_{ik} R_k \end{aligned} \quad (2.55)$$

where L_j are the external loads, m is the number of external loads, p is the number of hinges, b_{ij} and a_{ik} are the coefficients of external and fictitious loads respectively.

2.3.3 The Extended β -Unzipping Method

Because there are a large number of failure modes for a complex structure, it is impossible to identify all the failure modes in the system reliability. So only significant failure modes, which contribute most of the failure probability of the structure, are considered in the analysis. An extended β -unzipping method is devised to identify the significant failure modes. This consists of a selection and a discarding process. Firstly, the original β -unzipping method is used to find out the failure paths, then a discarding process is introduced to discard the failure paths whose failure probabilities are very low.

Process of selection

Firstly the structural analysis is carried out by a linear elastic finite element program. Then safety margins for all the failure elements are constructed, as described in the foregoing sections. The reliability indices for all failure elements are calculated by AFOSM, and the elements whose reliability indices fall into the interval $[\beta_{\min}^{(1)}, \beta_{\min}^{(1)} + \Delta\beta^{(1)}]$ are selected as the critical failure elements at level 1.

Secondly, each of the critical failure elements at level 1 is assumed being failed in turn, and the structural analysis is carried out again. At this stage, the stiffness matrix of the failed member is replaced by the reduced stiffness matrix and the equivalent nodal forces are applied to the structure as the fictitious loads. Then safety margins for the remaining elements are constructed and reliability indices are calculated again, and the elements whose reliability indices fall into the interval $[\beta_{\min}^{(2)}, \beta_{\min}^{(2)} + \Delta\beta^{(2)}]$ are selected as the critical failure elements at level 2.

Thirdly, the above operations are repeated until the formation of a mechanism. The criteria for the formation of mechanism is:

$$|\mathbf{k}^{(p)}| / |\mathbf{k}^{(0)}| \leq \epsilon_1$$

where $\mathbf{k}^{(p)}$ is the total structure stiffness matrix at pth failure stage, and $\mathbf{k}^{(0)}$ is the original total stiffness matrix. ϵ_1 is a constant for determining the plastic failure of the structure. ϵ_1 is chosen as 0.01 in the study.

Process of discarding

If the failure probability of the identified failure path is very small, the failure path is excluded. The failure probability of a failure path could be expressed as:

$$P'_f = P\left(\bigcap_{j=1}^{m_i} M_j \leq 0\right) = P\left(\bigcap_{j=1}^{m_i} F_j\right) \quad (2.56)$$

where m_i is the number of components in the i th parallel system, M_j is the safety margin of the j th component in the parallel system, F_j is the set of events corresponding to $M_j \leq 0$. Due to the fact that:

$$P\left(\bigcap_{j=1}^{m_i} F_j\right) \leq \min[P(F_i \cap F_j)] \quad (2.57)$$

the criterion for discarding is that if any $P(F_i \cap F_j)$ in a failure path is less than ϵ_2 then the failure path is precluded. Now ϵ_2 is set to be 10^{-24} .

It is worth mentioning that the discarding process introduced here does not need any more computation, because $P(F_i \cap F_j)$ are evaluated in the calculation of multi-normal distribution function, which is needed in finding the equivalent safety margin of a parallel system. Details are explained in the following section.

2.3.4 Multi-Normal Integration

The evaluation of multi-normal integral is frequently required in structural system reliability. It is defined as:

$$\Phi_n(\boldsymbol{\beta}, \boldsymbol{\rho}) = P\left(\bigcap_{i=1}^n x_i \leq \beta_i\right) \quad (2.58)$$

where:

$\Phi_n(\bullet)$ is n-dimensional normal distribution function

$$\boldsymbol{\beta} = (\beta_1, \dots, \beta_n)$$

$\boldsymbol{\rho}$ is the correlation matrix among the variables X_i

$P(\cdot)$ is the failure probability of an event.

Although it is possible to estimate the exact value by a numerical integration technique, it is impractical when the dimension is large. For example, if five-point integration for one-dimension is adopted, the number of evaluation of function will be 5^{10} for a ten-dimensional multi-normal integration. Therefore in practice, if n is greater than 5, an approximate method is preferred. Much effort has gone into finding an efficient approximate method with acceptable accuracy for last decade (Hohenbichler and Rackwitz, 1983; Hohenbichler, 1981; Gollwitzer and Rackwitz, 1988; Tang and Melcher, 1987).

The basic idea for these methods is to transform a n-dimensional integration to n number of one-dimensional integrations. Therefore in these cases the number of evaluation of function is 5 times n , instead of 5 to power n (it is assumed that a five-point integration is used for one-dimensional integration).

The existing methods are fully discussed by Pu and Das (1994). Based on this investigation, Tang's algorithm is used in the present study. Besides its accuracy and efficiency, another advantage of this method is that the intermediate results in the method could be fully used in the discarding process of the extended β -unzipping method. The method will be briefly described below.

Firstly, the correlated variables \mathbf{X} were transformed into an independent standard normal space \mathbf{U} by the so-called Rosenblatt transformation.

$$\mathbf{X} = \mathbf{b} \times \mathbf{U} \quad (2.59)$$

where

$$\mathbf{b} = \begin{bmatrix} b_{11} & & & \\ b_{21} & b_{22} & & \\ \cdot & \cdot & \cdot & \\ b_{n1} & b_{n2} & \dots & b_{nn} \end{bmatrix}$$

$$b_{11}=1$$

$$b_{21} = \rho_{21} , \quad b_{22} = \sqrt{1 - \rho_{21}^2}$$

$$b_{i1} = \rho_{i1} , \quad i=3, \dots, n$$

$$b_{ij} = \frac{\left(\rho_{ij} - \sum_{k=1}^{i-1} b_{ik} b_{jk} \right)}{b_{jj}} , \quad i=3, \dots, n$$

$$b_{ii} = \left(1 - \sum_{j=1}^{i-1} b_{ij}^2 \right)^{1/2} , \quad j=2, \dots, i-1$$

So, substituting equation (2.59) to (2.58)

$$\begin{aligned} \Phi_n(\boldsymbol{\beta}, \boldsymbol{\rho}) &= P\left(\bigcap_{i=1}^n x_i \leq \beta_i \right) = P\left(\bigcap_{i=1}^n \left\{ \sum_{j=1}^i b_{ij} u_j - \beta_i \right\} \leq 0 \right) \\ &= P\left(\bigcap_{i=2}^n \left\{ \sum_{j=1}^i b_{ij} u_j - \beta_i \leq 0 \right\} \mid u_1 \leq \beta_1 \right) P(u_1 \leq \beta_1) \end{aligned} \quad (2.60)$$

Because u_1 is independent to u_i ($i=2, \dots, n$), the conditional probability in equation (2.60) can be expressed as:

$$\begin{aligned}
& P\left(\bigcap_{i=2}^n \left\{ \sum_{j=1}^i b_{ij} u_j - \beta_i \leq 0 \mid u_1 \leq \beta_1 \right\}\right) \\
&= P\left(\bigcap_{i=2}^n \left\{ b_{i1} \tilde{u}_1 + \sum_{j=2}^i b_{ij} u_j - \beta_i \leq 0 \right\}\right) \\
&= P\left(\bigcap_{i=2}^n \left\{ b_{i1} \Phi^{-1}[\Phi(\beta_1)\Phi(u_1)] + \sum_{j=2}^i b_{ij} u_j - \beta_i \leq 0 \right\}\right) \\
&= P\left(\bigcap_{i=2}^n h_i(\mathbf{u}) \leq 0\right) \\
&\approx P\left(\bigcap_{i=2}^n \sum_{j=1}^i \alpha_{ij} u_j - \beta_{i,Ex}^{(2)} \leq 0\right) \tag{2.61}
\end{aligned}$$

where

$$h_i(\mathbf{u}) = b_{i1} \Phi^{-1}[\Phi(\beta_1)\Phi(u_1)] + \sum_{j=2}^i b_{ij} u_j - \beta_i \tag{2.62}$$

$i=2, \dots, n$

For estimation of the conditional probability in equation (2.60), a reverse Rosenblatt transformation was carried out as follows:

$$\begin{aligned}
P_{i,Ex} &= P\left(\left\{ \sum_{j=1}^i b_{ij} u_j - \beta_i \leq 0 \mid u_1 \leq \beta_1 \right\}\right) \\
&= P(x_i - \beta_i \leq 0 \mid x_1 \leq \beta_1) \\
&= P(x_i \leq \beta_i \cap x_1 \leq \beta_1) / P(x_1 \leq \beta_1)
\end{aligned}$$

$$= \Phi(\beta_1, \beta_i, \rho_{i1}) / \Phi(\beta_1) \quad (i=2, \dots, n) \quad (2.63)$$

$$\beta_{i,Ex}^{(2)} = \Phi^{-1}(P_{i,Ex}) \quad (2.64)$$

The joint failure probability in Eq. (2.63) is used for discarding process in the extended β -unzipping method. For the calculation of new correlation coefficients, the Newton-Raphson algorithm is used. $h_1(\mathbf{u})$ in equation (2.62) can be rewritten as:

$$h(u_1, V) = d_1 \Phi^{-1}(\Phi(\beta_1)\Phi(u_1)) + d_2 V - \beta_i \quad (2.65)$$

where

$$d_1 = b_{i1} \quad , \quad d_2 = \sqrt{1 - b_{i1}^2} \quad \text{and} \quad V = \sum_{j=2}^i b_{ij} u_j / d_2$$

assume

$$g(u_1) = \Phi^{-1}(\Phi(\beta_1)\Phi(u_1)) \quad (2.66)$$

The problem of finding β^* in equation (2.65) is equivalent to

$$\min \beta^{*2} = u_1^2 + V^2 \quad (2.67)$$

subject to

$$h(u_1, V) = 0$$

Therefore

$$G(u_1) = d\beta^{*2} / du_1 = d_2^2 u_1 + (-\beta_i + d_1 g(u_1)) d_1 g'(u_1) = 0 \quad (2.68)$$

The Newton-Raphson algorithm is used to find the root of equation (2.68).

$$u_1^{k+1} = u_1^k - G(u_1^k) / G'(u_1^k) \quad (2.69)$$

$$G'(u_1) = d_2^2 - d_1 \beta_i g''(u_1) + d_1^2 [g(u_1)g''(u_1) + g'(u_1)^2] \quad (2.70)$$

where

$$g'(u_1) = \Phi(\beta_1) \exp\left[\left(g(u_1)^2 - u_1^2\right) / 2\right] \quad (2.71)$$

$$g''(u_1) = g'(u_1) \{g(u_1)g'(u_1) - u_1\} \quad (2.72)$$

Having got the point u_1^* , at which β^{*2} reaches its minimum, the sensitivity factors for Eq. (2.65) can be obtained by:

$$\alpha_{ij} = \frac{-\frac{\partial h_i}{\partial u_j}}{\left[\sum_{k=1}^n \left(\frac{\partial h_i}{\partial u_k}\right)^2\right]^{1/2}} \quad (2.73)$$

where

$$\frac{\partial h_i}{\partial u_j} = b_{ij} \quad \text{for } j=2, \dots, n$$

$$\frac{\partial h_i}{\partial u_1} = b_{i1} g'(u_1^*)$$

then the correlation factors r_{kl} between $h_i(\mathbf{u})$ can be calculated by:

$$r_{kl} = \alpha_k^T \alpha_l \quad k, l = 2, \dots, n$$

repeat the procedure, one can get

$$\Phi_n(\boldsymbol{\beta}, \boldsymbol{\rho}) = \Phi(\beta_1) \Phi(\beta_{2,Ex}^{(2)}) \dots \Phi(\beta_{n,Ex}^{(n)}) \quad (2.74)$$

2.3.5 Equivalent Safety Margin

As mentioned in the foregoing section, the structural system is modelled as a series system of parallel systems. In order to evaluate the reliability index of the structural system, the probability of failure of each parallel system and the correlation between the parallel systems need to be calculated. For evaluation of the probability of a parallel system the multi-normal integration techniques can be used. Correlation of a pair of parallel systems is not easily evaluated because the safety margins of the parallel systems are in general not linear. So the equivalent safety margin of a parallel system, suggested by Gollwitzer and Rackwitz (1983), is used.

Suppose that there are n elements in the parallel system, and the safety margins for each element are expressed as:

$$M_i = \alpha_{i1}U_1 + \alpha_{i2}U_2 + \dots + \alpha_{im}U_m + \beta_i = \sum_{j=1}^m \alpha_{ij}U_j + \beta_i \quad (2.75)$$

in which U_j are independent standard normally distributed variables, β_i are reliability indices for all safety margins.

The failure probability of the parallel system can be evaluated by:

$$P_{fp} = \Phi_n(-\boldsymbol{\beta}, \boldsymbol{\rho}) \quad (2.76)$$

So, the reliability index for the parallel system is:

$$\beta_p = -\Phi^{-1}(\Phi_n(-\beta, \rho)) \quad (2.77)$$

where:

$$\beta = (\beta_1, \beta_2, \dots, \beta_n)$$

$$\rho = [\rho_{ij}] = [\alpha_i^T \alpha_j]$$

The equivalent safety margin is defined in the form of:

$$M^e = \alpha_1^e U_1 + \alpha_2^e U_2 + \dots + \alpha_m^e U_m + \beta^e = \sum_{i=1}^m \alpha_i^e U_i + \beta^e \quad (2.78)$$

its reliability index β^e is equal to β_p and its sensitivity factors against changes in basic variables are the same as the original parallel system.

Let the basic variables vector \mathbf{U} be increased by a small increment $\boldsymbol{\varepsilon} = (\varepsilon_1, \varepsilon_2, \dots, \varepsilon_m)$. The corresponding reliability index for the parallel system is:

$$\begin{aligned} \beta_p(\boldsymbol{\varepsilon}) &= -\Phi^{-1} \left(P \left(\bigcap_{i=1}^n \left\{ \sum_{j=1}^m \alpha_{ij} (U_j + \varepsilon_j) + \beta_i \leq 0 \right\} \right) \right) \\ &= -\Phi^{-1}(\Phi_n(-\beta - \boldsymbol{\alpha}\boldsymbol{\varepsilon}, \rho)) \end{aligned} \quad (2.79)$$

Apply the similar operation to equivalent safety margin M^e ,

$$\begin{aligned} \beta^e(\boldsymbol{\varepsilon}) &= -\Phi^{-1} \left(\Phi(-\beta^e - \boldsymbol{\alpha}^e \boldsymbol{\varepsilon}) \right) \\ &= \beta^e + \boldsymbol{\alpha}^e \boldsymbol{\varepsilon} = \alpha_1^e \varepsilon_1 + \alpha_2^e \varepsilon_2 + \dots + \alpha_m^e \varepsilon_m + \beta^e \end{aligned} \quad (2.80)$$

in Eq. (2.79) and (2.80), let $\beta^e(\mathbf{0}) = \beta_p(\mathbf{0})$, one can get

$$\alpha_i^e = \frac{\left. \frac{\partial \beta_p}{\partial \varepsilon_i} \right|_{\boldsymbol{\varepsilon} = \mathbf{0}}}{\sqrt{\sum_{j=1}^m \left(\left. \frac{\partial \beta_p}{\partial \varepsilon_j} \right|_{\boldsymbol{\varepsilon} = \mathbf{0}} \right)^2}} \quad i=1, \dots, m \quad (2.81)$$

The values of α_i^e are evaluated by numerical differentiation in the following way:

- 1). giving $\boldsymbol{\varepsilon} = (0, \dots, \varepsilon_i, 0, \dots, 0)$ in turn for all basic variables where $\varepsilon_i = 0.1$, evaluate the

$$\beta_p(\boldsymbol{\varepsilon}) = -\Phi^{-1}(\Phi_n(-\boldsymbol{\beta} - \boldsymbol{\alpha}\boldsymbol{\varepsilon}, \rho)) \quad , \quad \text{and}$$

$$\frac{\partial \beta_p}{\partial \varepsilon_i}$$

- 2). Normalise the $\frac{\partial \beta_p}{\partial \varepsilon_i}$ according to Eq. (2.81).

2.3.6 Evaluation of Structural System Reliability

Finally the structural system reliability is defined as a series system of parallel systems. The failure probability of the system is expressed as:

$$P_f = P \left(\bigcup_{i=1}^n \left(\bigcap_{j=1}^{m_i} M_j^{(i)} \leq 0 \right) \right) = P \left(\bigcup_{i=1}^n \left(\bigcap_{j=1}^{m_i} F_j^{(i)} \right) \right) \quad (2.82)$$

where n is the number of mechanisms, m_i is the number of failure events in a parallel system. Because there are many mechanisms for a complex structure, the value of n is taken as the number of significant mechanisms identified in the analysis.

It is difficult to calculate the exact failure probability, Ditlevson's bounds

technique is used in the present study.

Due to the fact that multi-normal integration is time-consuming, some researchers set the m_j equal to one, so Eq.(2.82) become a weakest link system. Although such a definition could avoid to do any multi-normal integration, it is too conservative for the high redundant structures. A better approximation is proposed here, which is expressed as:

$$P_f = \max_{i=1}^n P \left(\bigcap_{j=1}^{m_i} F_j^i \right) \quad (2.83)$$

This definition could save much computational effort and the result would be better than a weakest link system.

Let's compare Eq.(2.82) and (2.83). If equation (2.82) is used, in order to get the equivalent safety margin the number of evaluation of multi-normal integration is (m_i+1) for each parallel system, so for the system, the number of evaluation of multi-

normal integration is $\sum_{i=1}^n (m_i + 1)$. On contrary, if equation (2.83) is used, for every

parallel system only one multi-normal integration is expected, so for the system only n integration is needed. Moreover there is no need to calculate the bounds, which is also time-consuming.

2.3.7 Application to a Frame Structure

The program has been used to calculate the system reliability of a portal frame structure to show its validity. This frame was frequently investigated by many researchers to validate their methods and was also used to check the program. The results for three conditions, a) only bending moment is considered; b). interaction of bending moment and axial force is considered; c). interaction of bending moment axial force including buckling effect, are obtained in order to find out the difference among these assumptions.

In the analyses, only the loads and the strength of the sections are treated as

random variables, the remaining variables are assumed deterministic. All the loads and resistances of sections are assumed to be independent.

The frame is shown in Fig. 2.3, and the parameters are listed in Table 2.1.

Table 2.1: Parameters for the portal frame

Element ends No.	Cross-sect. area $A_i(\text{m}^2)$	Inertia moment $I_z(\text{m}^4)$	Resistance (mean value) $R_i(\text{kNm})$
1,2	4.0×10^{-3}	3.58×10^{-5}	75
3,4	4.0×10^{-3}	4.77×10^{-5}	101
5,6	4.0×10^{-3}	4.77×10^{-5}	101
7,8	4.0×10^{-3}	3.58×10^{-5}	75

$P_1=20 \text{ kN}$	$P_2=40 \text{ kN}$	$\text{cov}(R_i)=0.05$	$\text{cov}(P_i)=0.3$
$E=210 \text{ GPa}$	$\sigma_y=276 \text{ MPa}$		

1) The case where only bending moment is considered

$\Delta\beta^{(1)}$ is set to be 3.0, and $\Delta\beta^{(i)}$ ($i=2,3,\dots$) 1.0. The system reliability of the portal frame is 2.49, while the reliability index at level 1 is 1.296. So it is obvious that the structural system reliability is much higher than those of components. The failure tree is shown in Fig. 2.4. The total number of mechanisms is 25. The failure modes identified in the analysis are shown in Fig. 2.5.

The values of $\Delta\beta^{(i)}$ are very important in the β -unzipping method. If the values are too small, it is possible to fail to identify all the significant failure paths. If the values are too large, the number of mechanisms identified in the analysis will be too many, this would waste computational resources. There are no rules in selecting a

proper value of $\Delta\beta^{(i)}$, which is determined by trial.

For the portal frame if $\Delta\beta^{(i)}$ ($i=2,3\dots$) is set to be 1.8 instead of 1.0 in the previous analysis, the total mechanisms identified are 55. The reliability index for the structure system is the same as that in the previous analysis.

It is found that although the number of mechanisms in the second analysis is much larger than that in the first one, the final failure probability of the system is almost the same. This is because the reliability indices of the extra mechanisms in the second analysis are so large that they hardly influence the failure probability of the structural system.

2) The cases where interaction is considered

As described in the foregoing sections, the linearized plasticity condition is used in the analysis. $\Delta\beta^{(1)}$ is set to be 3.0 and $\Delta\beta^{(i)}=1.0$. For simplicity the buckling strength of the section is assumed to be seventy percent of the yield stress.

The failure trees in these cases are similar to the previous one, so they are not shown here. The results are summarised in Table 2.2.

Comparing the results in Table 2.2, it can be seen that:

- * The results agree well with those in the published papers. The failure probability of the most critical failure path is 6.580×10^{-3} for bending moment only in Thoft-Christensen and Murotsu (1986).
- * The reliability index of the system by considering the interaction of bending moment and axial force is slightly smaller than that when only bending moment is considered.
- * The system reliability index in the case where interaction of bending moment and axial force including buckling effect is considered is smaller than the others. This is mainly due to the fact that the failure element 7, which has the highest failure probability, is in compression in this case.
- * The system reliability index evaluated by Eq. (2.83) is slightly larger than that by Eq. (2.82). It is obvious that it is a good approximation.

Table 2.2: Results of the portal frame

	BO*	B+A*	B+A+B*
β_S	2.48881	2.31999	2.25090
P_{fu}	6.4099e-3	1.0171e-2	1.2197e-2
P_{fL}	6.4098e-3	1.0170e-2	1.2196e-2
β_1	1.296	1.166	1.101
β_S^{28}	2.48874	2.32011	2.25104

* BO means bending moment only

B+A for interaction of bending moment and axial force

B+A+B for interaction of bending moment axial force including buckling effect

β_1 is the reliability of the structure at level 1

β_S^{28} is the reliability index evaluated by Eq.(2.83)

2.4 DISCUSSIONS

The structural system reliability analysis of a portal frame is carried out. The safety margins of the structure are automatically generated by computer, in which the effect of interaction of bending moment and axial force including the buckling effect is investigated. It is found that:

- 1) The results obtained by the program agree well with those in published papers. The failure probability of the most critical failure path is 6.580×10^{-3} for bending moment only in Thoft-Christensen and Murotsu (1986).
- 2) The reliability index under pure bending is much larger than those when the interaction is considered. So the interaction must be considered in the analysis.
- 3) The effect of buckling strength on system reliability depends on whether the element with the highest failure probability is in compression. It is recommended that the effect of buckling is always taken into consideration, and such calculation does not need much computational time.
- 4) The system reliability evaluated by the methods in Eq. (2.83) is a good approximation, although it is slightly over-estimated.

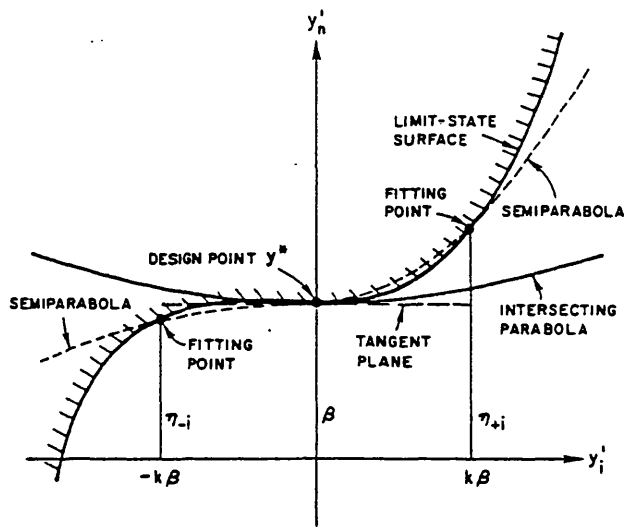


Fig. 2.1 Fitting of paraboloid in rotated standard space (Kiureghian et al, 1987)

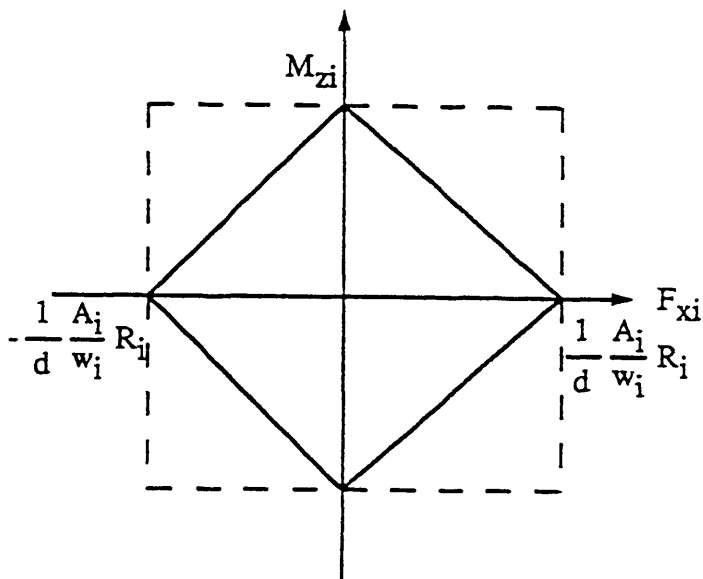


Fig. 2.2 Linearised plasticity condition

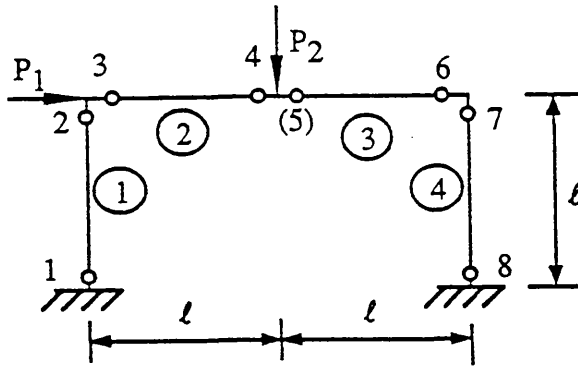


Fig. 2.3 Portal frame

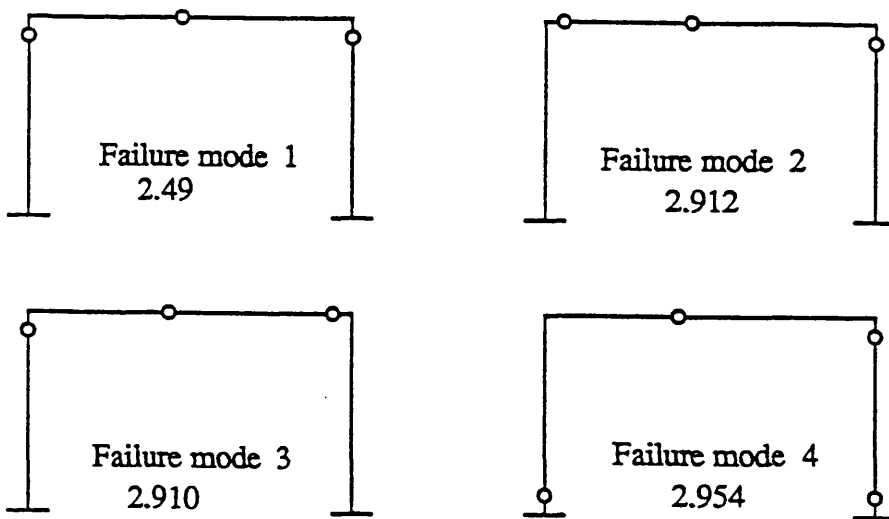


Fig. 2.5 Identified failure modes of the portal frame

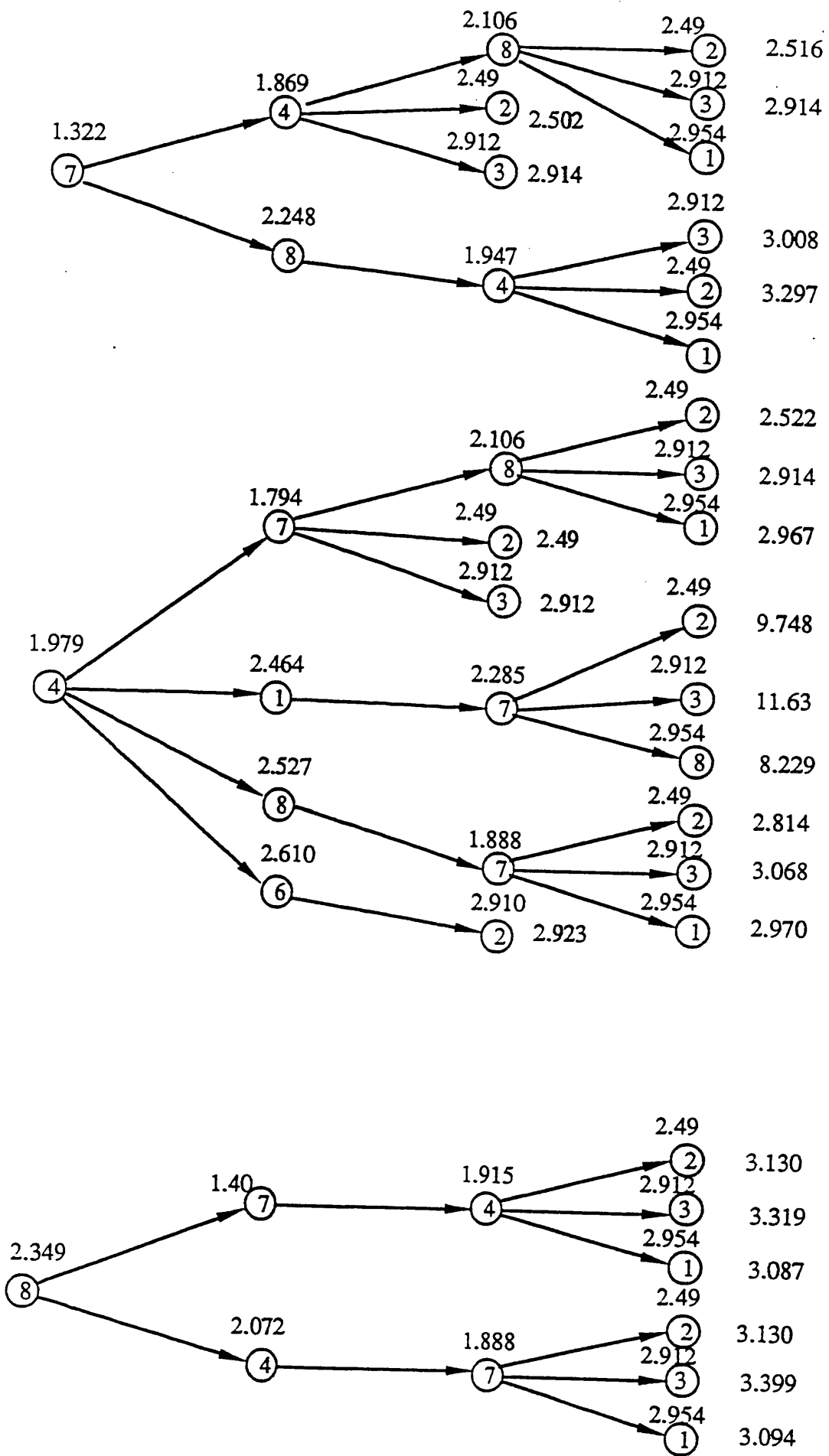


Fig. 2.4 The failure tree of portal frame (bending only)

CHAPTER 3 PRIMARY LOADS ON SWATH SHIPS

3.1 INTRODUCTION

To design a structure with adequate but not excessive safety, one of the important problems is to accurately predict the loads on the structure. It is found that the structural weight heavily depends on the loads exerted on it (Stirling et al, 1988).

The loads on the SWATH can be classified as primary loadings and secondary loadings. The primary loadings are those which affect the structure as a whole and determine the general configuration and scantlings of the vessel. The secondary loadings govern the local scantlings and structural details. It may be said that the primary loads could be accurately predicted by existing methods (Chan et al, 1992) from the engineering point of view, while for the determination of secondary loads considerable work still needs to be done.

The Naval Architecture and Ocean Engineering department of the University of Glasgow has been actively involved in the research of SWATH ships since the early 80's. Chan (1990, 1991) has developed a program, MARCHS, which can be used to predict the motions and loads of both mono- and twin hull ships. But for the purpose of structural design, gaps still exist. Firstly, in structural design various extreme values are needed. A spectral analysis method is expected. Secondly, the horizontal and vertical inertia forces are two important components. If the horizontal inertia force is in the same direction as hydrodynamic side force, the situation could be worse. For the same reason the vertical inertia force could increase the maximum shear force at the junction of cross-structure and haunch. So the horizontal and vertical accelerations should be calculated. Finally, if the concentrated loads are directly applied to the structure in the finite element analysis, the stress concentration in the lower hulls is severe. So the instantaneous pressure distribution should be used when high accuracy is expected.

The aims of the chapter are to fill these gaps and extend the existing programs to a module which could generate the data for finite element analysis. Therefore, firstly the program, MARCHS, was used to calculate the response amplitude operators of primary loads on a built SWATH (PATRIA) in regular waves. Another program was then developed to carry out spectral analysis of motion responses, accelerations and loads. In addition, due to the requirement of finite element analysis,

a so-called 'equivalent wave system', as suggested by Reilly et al (1988), was adopted to calculate the instantaneous pressure distribution at the submerged part of the hull. Furthermore, several other factors which should be considered in structural analysis are also discussed in the chapter.

3.2 PRIMARY LOADS

3.2.1 Components of Primary Loads

Like all conventional monohull ships, there exists a longitudinal bending moment which can be calculated by static balance. But it is not so important as in the monohull. The primary loads, which govern the structural design in SWATH, are the transverse loads acting in the longitudinal plane through the centreline. They are defined as longitudinal shear F1, side force F2, vertical shear force F3, prying moment F4, pitch torsional moment F5, and yaw splitting moment F6, as shown in Fig. 3.1.

Considerable work has been carried out over the years to predict the primary loads on SWATH. It was found that the most critical loading is the side force in beam seas at zero forward speed. Although the side force in quartering seas is not the largest, the yaw splitting moment is likely to cause problems since the superposition of the side force and yaw splitting moment. It was recommended that both the side force in beam seas and the yaw splitting moment should be considered in the structural analysis (Reilly et al, 1988; Liu, 1989; ABS, 1990).

Another important component of wave induced loads in structural design is the vertical shear in box structure. It is caused by the pitch difference between the two lower hulls and the vertical inertial force of the structure. The maximum occurs at the junction of the cross structure and the haunch.

As to the combination of all the primary loads, Chalmers (1989) suggested that the combination listed in Table 3.1 can be used, but no sufficient evidence supports this combination. The best way to take into account the load combination is to use the 'equivalent wave system' (Reilly et al, 1988) in structural analysis. Firstly, a finite element model, which represents the whole ship including superstructures, is carried out for both critical load cases in association with the 'equivalent wave

system'. A finer mesh representing some critical structures is then generated. In the finer model, its boundary conditions were taken from the results of the coarse model.

Table 3.1: Combination of loads

Heading	Transverse Bending	Transverse Box Shear	Longitudinal Bending	Torsion
Beam	Design	Design	0.15 Design	0.25 Design
Bow quarter	0.8 Design	Design	0.8 Design	Design
Head/Following	0.15Design	Design	0.1 Design	0.1 Design

The 'equivalent wave system' is the wave, whose period is that at which the largest critical load occurs, and it results in the same extreme design value obtained from the spectral analysis. At the same time, by using the 'equivalent wave system' the instantaneous pressure distribution at the submerged part of the hull can be obtained. Details will be discussed in the following sections.

3.2.2 Available Methods for Determination of Primary Loads

The existing techniques, which are used to calculate the primary loads, can be classified as empirical formula, analytical method, and experimental test.

There are several empirical methods (Sikora et al, 1983; ABS, 1990; Sikora, 1988; Luedeke et al, 1985; Betts, 1988) to predict maximum expected design side force for SWATH, among which Sikora's algorithm was recognized as the best one.

Theoretical prediction of wave loads was pioneered by Lee and Curphey at the David Taylor Naval Ship Research and Development Center (DRNSRDC) (Lee and Curphey, 1977). Later Reilly et al (1988) combined the strip theory and sink source distribution methods to calculate the wave induced loads. It has good agreement with the results from the model tests. Because of the interaction between the two lower hulls, the strip theory was not suitable for SWATHs from a theoretical point of view.

In the late 80's three-dimensional panel theory appeared (Chan, 1991; Kobayashi and Shimada, 1990). It was confirmed that the interaction between the two lower hulls is strong, especially when the ship is at zero speed and in beam sea. The forward speed reduces the effect of this interaction (Kobayashi and Shimada, 1990).

In addition, experimental tests, thought to be the most reliable tool, could be carried out to determine the loads. Since it is a costly activity no sufficient experimental data was available until now. No attempt was made here to comprehensively summarize the existing methods. It has been done by Miller (1991).

Since the 1980's, the Naval Architecture and Ocean Engineering department of the University of Glasgow has been actively involved in the SWATH research. In the early 90's Chan developed a program, MARCHS, in which three dimensional potential theory was used. It was verified that the program developed by Chan (1990, 1991) can accurately predict the wave induced loads.

In the present study, the program MARCHS was used to calculate the wave induced loads on a built SWATH 'PATRIA'. A three dimensional oscillating source distribution method, in association with linearised potential theory, was used in the program. The local co-ordinate system is defined in Fig. 3.1. The x-axis points at the ship bow and the o-xy plane is at the mean free surface, and the z-axis vertically upward through the centre of gravity of the ship. The wetted body surface was discreted into many panels in which the oscillating sources were assigned to simulate the fluid field.

The viscous damping has also been considered by using an empirical method based on the cross-flow approach because the viscous damping effect is of importance when wave-making damping is no longer the dominant factor. Because of the peculiar shape of SWATH the surface waves in vertical oscillation are not so large that the viscous effect should be considered in the seakeeping calculation.

The program consists of HULSUR, HULPLOT, HULDAT, MOTION, and WVLOAD. The program HULSUR is used to expedite the discretisation of the wetted body surface for general hull form of a marine vehicle having one longitudinal plane of symmetry. The HULPLOT is for plotting the surface on the screen to check if there is any irregular and erratic input. The HULDAT is for inputting the data which will be used in the MOTION. After running the MOTION, first- and second-order hydrodynamic forces and the first-order motion responses can be obtained. For

SWATH, the program WVLOAD should be run to get the forces in the longitudinal cut through the centerline. Details are shown in Chan (1991, 1990).

Because of the symmetry of the hull, the expression of lateral loads can be simplified at the midpoint in the longitudinal plane through the centreline. Either part of the twin-hull could be used in calculation of lateral loads in longitudinal cut. At present the port was used in the computation, and the effect of the starboard was replaced by the six components of the lateral loads.

Wave induced loads consist of:

- a) Mass or inertia force, including acceleration effect
- b) Incident wave or Froude-Krylov force
- c) Diffracted wave force
- d) Radiated force
- e) Quasi-hydrostatic force due to vertical motion.

The first item is obtained by multiplying the mass by acceleration. The rest are calculated by integration of the hydrodynamic pressure over the wetted hull surface.

As presented by Chan (1991), the six components of primary loads defined in Fig. 3.1 can be expressed as follows:

$$F_1 = -\frac{1}{2} \left(M\bar{y}_G \ddot{\xi}_6 + F_{1p} - F_{1s} \right) \quad (3.1a)$$

$$F_2 = -\frac{1}{2} \left(F_{2p} - F_{2s} \right) \quad (3.1b)$$

$$F_3 = \frac{1}{2} M\bar{y}_G \ddot{\xi}_4 - \frac{1}{2} \left(F_{3p} - F_{3s} \right) \quad (3.1c)$$

$$F_4 = \frac{1}{2} M\bar{y}_G \ddot{\xi}_3 - i_{45} \ddot{\xi}_5 - \frac{1}{2} \left(F_{4p} - F_{4s} \right) \quad (3.1d)$$

$$F_5 = -i_{54}\ddot{\xi}_4 - i_{56}\ddot{\xi}_6 - \frac{1}{2}(F_{5p} - F_{5s}) \quad (3.1e)$$

$$F_6 = -\frac{1}{2}M\bar{y}_G\ddot{\xi}_1 - i_{65}\ddot{\xi}_5 - \frac{1}{2}(F_{6p} - F_{6s}) \quad (3.1f)$$

In which

- M is the ship's mass
 \bar{y}_G the transverse distance of the centre of gravity of one hull to the ship's centreline
 $i_{kl} = i_{lk}$
 i_{45} the product moment of inertia of one hull about the longitudinal and vertical ship centrelines
 i_{56} the product moment of inertia of one hull about the vertical ship centreline and the neutral axis of the cross-deck
 $\ddot{\xi}_j$ the acceleration of body motion in j th direction
 F_{jp}, F_{js} fluid forces on port and starboard hulls due to quasi-hydrostatic and hydrodynamic pressures in j th direction.

3.2.3 Extreme Value and Spectral Analysis

For structural design, it is necessary to predict the possible maximum value of loads to which a vessel may be subject during its lifetime. The extreme value must be determined by considering all sea conditions, ship speed and heading combinations which might be encountered during the vessel's lifetime, together with the frequency of occurrence of each of these combinations.

At the moment there are two approaches which could be used to do such work, namely long term and short term prediction. It seems that the long term prediction is more reasonable. It was also found that the extreme values predicted by the short term method has good agreement with those by the long term techniques (Ochi, 1978). Therefore the short term method was adopted in the study.

Spectral analysis techniques can be used to calculate the various statistical averages of structural responses. If a sea energy spectral density function is denoted by $S(\omega)$, then the response spectral density function can be obtained by:

$$S_r(\omega) = (RAO)^2 S(\omega) \quad (3.2)$$

In which

$S_r(\omega)$ is the response spectral density function;

RAO the response amplitude operator.

then the various orders of moment of response spectrum can be calculated

$$m_j = \int_0^{\infty} \omega^j \times S_r(\omega) d\omega$$

In the spectral analysis the Pierson-Moskowitz spectrum, which is based on the wave measurement in the Atlantic Ocean, was used. The spectral density function is expressed as:

$$S(\omega) = \frac{\alpha g^2}{\omega^5} \exp \left[-\beta \left(\frac{g}{U\omega} \right)^4 \right] \quad (3.3)$$

in which

$$\alpha = 0.0081$$

$$\beta = 0.74$$

$$g = 9.81 \text{ ms}^{-1}$$

U is the characteristic wind speed at 19.5 meters above sea level in ms^{-1} .

A relationship exists between wind speed and significant wave height for a particular sea. The relations of these two parameters at Atlantic Ocean are shown in Table 3.2 (Lewis, 1967).

Table 3.2: Relation of wind speed and wave height

Wind speed(knots)	Wave height(m)
16	2
24	3
31	4
42.5	6
49.0	7

A program was developed to perform spectral analysis and to calculate the extreme values by Ochi's formulae (1973, 1978).

It is assumed that: (a) random sea is a steady-state Gaussian (normal) process with zero mean, (b) response to waves is linear, (c) the spectrum bandwidth is less than 0.9.

The most probable extreme value is expressed as:

$$\bar{\gamma}_n = \left(2 \ln \left\{ \frac{2\sqrt{1-\epsilon^2}}{1+\sqrt{1-\epsilon^2}} N \right\} \right)^{0.5} \sqrt{m_0} \quad (3.4a)$$

The design extreme value is:

$$\gamma_n = \left(2 \ln \left\{ \frac{2\sqrt{1-\epsilon^2}}{1+\sqrt{1-\epsilon^2}} \frac{N}{(\alpha/k)} \right\} \right)^{0.5} \sqrt{m_0} \quad (3.4b)$$

where

N is the number of observations,

$$N = \frac{3600T}{4\pi} \left(\frac{1+\sqrt{1-\epsilon^2}}{\sqrt{1-\epsilon^2}} \right) \sqrt{\frac{m_2}{m_0}} \quad (3.5)$$

ϵ is the bandwidth parameter $\epsilon = \sqrt{1 - \frac{m_2^2}{m_0 m_4}}$

T is duration of specified sea in hours

m_0 is area under response spectrum

m_2, m_4 are 2nd and 4th moment of response spectrum respectively

α is risk parameter

k is number of encounters with a specified sea in ship's lifetime

Substituting Eq.(3.5) into Eqs.(3.4a and 3.4b), the most probable extreme value and the design extreme value are expressed as:

$$\bar{\gamma}_n = \left(2 \ln \left\{ \frac{3600T}{2\pi} \sqrt{\frac{m_2}{m_0}} \right\} \right)^{0.5} \sqrt{m_0} \quad (3.6a)$$

$$\gamma_n = \left(2 \ln \left\{ \frac{3600T}{2\pi(\alpha/k)} \sqrt{\frac{m_2}{m_0}} \right\} \right)^{0.5} \sqrt{m_0} \quad (3.6b)$$

It is of interest to note that the extreme values are no longer a function of the bandwidth parameter.

3.2.4 Instantaneous Pressure Distribution

Due to the requirement of the finite element analysis, the instantaneous pressure distribution calculation is carried out. An 'equivalent wave system' suggested by Reilly et al (1988) was adopted.

The 'equivalent wave system' is a wave with the period at which the maximum response of critical loads occurs, and it will give rise to the same extreme wave-induced load obtained from short-term extreme value statistics. It is recommended that both the side force in the beam sea and the yaw splitting moment in quartering sea should be treated as critical loads (Reilly et al, 1988). At present only side force in beam sea was considered since the side force is worse than the yaw splitting moment in most cases.

3.3 RESULTS OF PATRIA

In this section a case study was described. All calculations were carried out on a built SWATH (PATRIA), which was designed by FBM Marine Company and launched in 1989. It is now in operation as a passenger ferry between Madenia and Porto Santo, off the Spanish coastline. Its principal dimensions are shown in Fig. 3.2, and its main particulars listed in Table 3.3.

Table 3.3: Particulars of PATRIA

Displacement	169 tonnes
Mean draught, t	2.7 m
Lower hull length	31.05 m
Length of the strut	28.6 m
Overall length	36.50 m
Lower hull diameter H_D	1.8 m
Single strut	
Strut width T_S	1.0 m
Submerged strut height D_S	1.1 m
Box width B	13.0 m
C_{wp} (water plane coefficient)	0.80
Strut height S_H	1.65 m
Box depth D_B	1.0 m
Section depth D	5.9 m

3.3.1 Seakeeping

The motion responses of the ship were calculated by the program MOTION. Five headings, namely, 0° , 45° , 90° , 135° and 180° were considered. The speed of the ship is zero. The significant wave height is 3 metres. The motion responses in different wave directions are shown in Figs. 3.3 to 3.7 and the different average values of the responses are listed in Table 3.4.

It was shown that the motion characteristics of PATRIA are good. The significant heave is just 1.67 metres and roll 0.158 rad.

Table 3.4: Motion responses

Dir.	Mode	m_0	Average *	Significant **
0°	Surge	0.676	1.0275	1.644
	Sway	0.00	0	0
	Heave	0.524	0.905	1.448
	Roll	0.00	0	0
	Pitch	0.0086	0.11625	0.186
	Yaw	0.00	0	0
45°	Surge	0.39	0.78	1.248
	Sway	0.2	0.55875	0.894
	Heave	0.58	0.9525	1.524
	Roll	0.004	0.07875	0.126
	Pitch	0.0057	0.09375	0.15
	Yaw	0.0005	0.0275	0.044
90°	Surge	0.0201	0.1775	0.284
	Sway	0.44	0.82875	1.326
	Heave	0.69	1.03875	1.662
	Roll	0.0063	0.09875	0.158
	Pitch	0.0018	0.0525	0.084
	Yaw	4.2E-06	0.0025	0.004
135°	Surge	0.302	0.6875	1.1
	Sway	0.207	0.56875	0.91
	Heave	0.697	1.04375	1.67
	Roll	0.0036	0.075	0.12
	Pitch	0.0027	0.065	0.104
	Yaw	0.00049	0.0275	0.044
180°	Surge	0.582	0.95375	1.526
	Sway	0.00	0	0
	Heave	0.675	1.0275	1.644
	Roll	0.00	0	0
	Pitch	0.0048	0.08625	0.138
	Yaw	0.00	0	0

* Average = $1.25\sqrt{m_0}$

** Significant = $2.0\sqrt{m_0}$

3.3.2 Loads

The response amplitude operators of the six force components defined in section 3.2.1 were calculated and shown in Figs. 3.8 to 3.12 and the different extreme values are shown in Table 3.5 in which the Max1 is the 'most probable extreme value', the Max2 'design extreme value' with a value of 0.01 of the risk parameter in one sea state and Max5 'design extreme value' in the lifetime (it is supposed that the ship meets ten times the specified sea in its life time). m_0 is the area under the response spectrum.

It is indicated that :

- * The largest side force and bending moment occur in the beam seas.
- * The side force in beam seas is 2180 kN, which is in good agreement with the design value (2030 kN) previously used by design company. A similar check is made for the maximum transverse bending moment at mid transverse frame with the 2-D FE model result. A bending moment of $7.98 \cdot 10^3$ kNm obtained from the wave loading program compares well with the FE output of $8.13 \cdot 10^3$ kNm.
- * The results obtained from the first group of formulae are slightly smaller than those from the second group. The difference in the results may be caused by the bandwidth effect of the response spectrum which was considered only in the second group of formulae.
- * The largest yaw splitting moment occurs at bow quartering sea.
- * Although the side force in beam sea is 2.76 times that in the bow quartering sea, nevertheless the yaw splitting moment in bow quartering sea is 6.9 times that in the beam sea. So it is possible that the combination of the loads in bow quartering sea is also as critical as in beam sea.
- * The largest pitch torsional moment, which is relatively small, also occurs at beam sea. It is not therefore so important as the side force and yaw splitting moment.

Table 3.5: Extreme values

Dir.	Force	m_0	Max1	Max2	Max3
0°	Force1	0	0	0	0
	Force2	2.3E+08	62000	78000	84000
	Force3	0	0	0	0
	Force4	7.6E+09	360000	440000	480000
	Force5	0	0	0	0
	Force6	2.9E+10	700000	870000	950000
45°	Force1	3.5E+08	76000	95000	100000
	Force2	2.2E+10	600000	750000	810000
	Force3	2E+09	180000	220000	240000
	Force4	2.9E+11	2100000	2700000	2970000
	Force5	1.22E+10	444000	556000	605000
	Force6	1.6E+12	5200000	6460000	7010000
90°	Force1	167000	1650	2070	2250
	Force2	1.55E+11	1610000	2010000	2180000
	Force3	4.61E+09	273000	342000	372000
	Force4	2.09E+12	5910000	7360000	7980000
	Force5	1.76E+10	534000	669000	727000
	Force6	3.61E+10	782000	971000	1050000
135°	Force1	3.45E+08	75800	94400	103000
	Force2	2.05E+10	585000	729000	791000
	Force3	2.7E+09	208000	261000	284000
	Force4	2.34E+11	1980000	2460000	2670000
	Force5	1.07E+10	416000	521000	566000
	Force6	1.7E+12	5380000	6680000	7240000
180°	Force1	0	0	0	0
	Force2	6.26E+08	103000	128000	139000
	Force3	0	0	0	0
	Force4	1.93E+10	569000	708000	768000
	Force5	0	0	0	0
	Force6	1.6E+10	520000	647000	701000

Combinations of transverse bending moment (F4), side force (F2), vertical shear (F3), and yaw splitting moment (F6) are shown in Table 3.6, based on the results in Table 3.5. Although it is too early to give a simplified load combination for design, it is suggested that the combination shown in Table 3.1 is too conservative.

Table 3.6: Combination of loads

Heading	Transverse bending	Side force	Vertical shear	Yaw splitting moment
0°	0.06M	0.04M	0.0F _s	0.13M _y
45°	0.37M	0.37F	0.65F _s	0.97M _y
90°	M	F	F _s	0.15M _y
135°	0.33M	0.36F	0.76F _s	M _y
180°	0.10M	0.06F	0.0F _s	0.10M _y

3.3.3 Accelerations

Due to the requirement of the determination of the inertia force in structural analysis, the vertical and lateral accelerations were calculated.

Because only motion responses were outputs from the program 'MOTION', an interface needs to be developed to calculate the accelerations, which are evaluated by the following procedure:

Since the motions can be expressed by:

$$\xi_j = |\xi_j| \times e^{-i(\omega t + \varepsilon_j)} \quad (3.7)$$

in which

$j = 1,6$ for six directions of motion

ξ_j are motion amplitudes for each direction

ε_j are phase angles for each direction

ω is encountered frequency

So, accelerations in each direction can be calculated by:

$$\ddot{\xi}_j = -\omega^2 |\xi_j| \times e^{-i(\omega t + \epsilon_j)} \quad (3.8)$$

where $\ddot{\xi}_j$ are accelerations for each direction

Therefore, the vertical and lateral accelerations at a location with co-ordinates (x,y) can be obtained by:

$$a_v = \ddot{\xi}_3 + \ddot{\xi}_4 \times y - \ddot{\xi}_5 \times x \quad (3.9)$$

$$a_L = \ddot{\xi}_2 + \ddot{\xi}_6 \times x \quad (3.10)$$

where

a_v is vertical acceleration

a_L is lateral acceleration

To investigate the effect of the roll on the vertical acceleration in the beam sea, the accelerations at four points were calculated and their maximum values are shown in Table 3.7. The co-ordinates of the four points are (0.0, 0.0), (-6.8, 0.0), (-6.8, 5.0), (-6.8, 2.5) respectively.

From Table 3.7 it can be seen that the vertical acceleration in point 3 is larger than those in points 4 and 2 at the wave incident angles 45° and 135° , but is even smaller than those in points 4 and 2 in beam sea. At heading and following seas, they are equal to each other. This means that the effect of roll on vertical acceleration does not always increase the vertical acceleration due to the difference in phase angles of different motion modes. In addition, because the sea condition used in structural analysis is beam sea, only the heave and pitch accelerations were considered in the later calculation.

Table 3.7: Accelerations at different points

Dir.	Accel.	m0	Max1	Max2	Max3
0°	Point1	0.264	2.075	2.595	2.82
	Point2	0.911	3.872	4.836	5.252
	Point3	0.911	3.872	4.836	5.252
	Point4	0.911	3.872	4.836	5.252
45°	Point1	0.315	2.269	2.837	3.083
	Point2	0.636	3.226	4.033	4.381
	Point3	0.782	3.571	4.466	4.853
	Point4	0.696	3.373	4.218	4.583
90°	Point1	0.455	2.73	3.42	3.71
	Point2	0.47	2.78	3.47	3.77
	Point3	0.418	2.62	3.27	3.55
	Point4	0.424	2.64	3.3	3.58
135°	Point1	0.475	2.789	3.487	3.788
	Point2	0.59	3.109	3.886	4.221
	Point3	0.645	3.247	4.06	4.411
	Point4	0.606	3.149	3.937	4.277
180°	Point1	0.525	2.943	3.674	3.989
	Point2	0.671	3.323	4.15	4.507
	Point3	0.671	3.323	4.15	4.507
	Point4	0.671	3.323	4.15	4.507

It was also indicated that the significant values of the vertical and lateral accelerations at point 2 in beam sea, at which the mid-frame was taken in structural analysis, are 1.37 (m/s²) and 0.95 (m/s²), only 14% and 9.7% of gravity acceleration respectively.

In addition, the accelerations at fore and after perpendiculars as well as the gravity centre are shown in Table 3.8 and typical RAO of accelerations at above points are shown in Fig. 3.13. In Table 3.8 the 'G.C.' is the gravity centre, 'F.P.' the fore perpendicular, and 'A.P.' the after perpendicular.

The results in Table 3.8 show that the largest vertical acceleration occurs at the after perpendicular in following sea. Its significant value is 3.734(m/s²), reaching 38% of gravity acceleration. But the vertical acceleration in beam sea is not so large

as that in following sea. The maximum, which occurs at fore perpendicular, is 2.332 (m/s^2), about 23.8% of gravity acceleration.

The lateral accelerations in quartering and beam seas do not vary rapidly, especially in beam seas. Their significant values are around 1.0 (m/s^2), 10% of gravity acceleration.

Table 3.8: Accelerations

Dir.	Position	Vertical Acceleration			Lateral Acceleration		
		m_0	Average	Signif.	m_0	Average	Signif.
0°	G.C.	0.264	0.6425	1.028	0	0	0
	F.P.	2.315	1.9025	3.044	0	0	0
	A.P.	3.484	2.33375	3.734	0	0	0
45°	G.C.	0.315	0.70125	1.122	0.092	0.37875	0.606
	F.P.	2.083	1.80375	2.886	0.181	0.53125	0.85
	A.P.	2.266	1.88125	3.01	0.326	0.71375	1.142
90°	G.C.	0.455	0.84375	1.35	0.229	0.59875	0.958
	F.P.	1.36	1.4575	2.332	0.236	0.6075	0.972
	A.P.	0.937	1.21	1.936	0.223	0.59	0.944
135°	G.C.	0.475	0.86125	1.378	0.097	0.38875	0.622
	F.P.	1.102	1.3125	2.1	0.273	0.6525	1.044
	A.P.	1.171	1.3525	2.164	0.234	0.605	0.968
180°	G.C.	0.525	0.90625	1.45	0	0	0
	F.P.	1.745	1.65125	2.642	0	0	0
	A.P.	1.61	1.58625	2.538	0	0	0

3.3.4 Instantaneous Pressure Distribution

The pressure distribution was calculated by using the equivalent wave system mentioned in the above section. As can be seen in Fig. 3.9, the peak position of side force RAO is at the $\omega=1.2$, which corresponds to the wave period of 5.236 second, and the maximum value is 1.62e3(kN). So a wave of 5.236 second wave period and 1.25 metres wave amplitude, which results in a total of 2.03e3(kN) side force, was used to calculate the pressure distribution. In order to seek the worst wave position the resultant force of pressure distribution at five phase angles, namely, $\omega t=0, \pi/2,$

π , $2\pi/3$ and 2π , were calculated. The resultant force of the hydrodynamic pressure of the port hull at $x=-6.8$ meters at five phase angles are 48.33, 22.68, -48.33, -22.68, and 48.33 kN respectively. The pressure distributions corresponding to the five phase angles were shown in Fig. 3.14. The positions of the points in the figure are shown in Fig. 3.15. It is found that the largest side force occurs at $\omega t=0$ and π corresponding to the prying and squeezing force respectively. The results agree well with those in Reilly et al (1988).

Another important parameter which should be considered in the design is the longitudinal distribution of the side force. Due to a lack of experimental data one can not get it from the existing experiment now. Sikora and Dinsbacher (1990) carried out a sensitivity study of the stresses to variations in longitudinal distribution of side force. Three types of distributions, namely, uniform, trapezoidal and sinusoidal, were assumed to calculate the stresses at different points. There was not much difference in the stresses for three kinds of distributions. So Sikora and Dinsbacher suggested that the uniform distribution could be used when analysing the whole ship. For conservative consideration, 10 percent of margin could be added when only one section was analysed.

Because the stresses are strongly dependant on the geometry of the structure it was not expected that the conclusion would be applicable to all structures. To investigate the longitudinal distribution of the side force, the longitudinal distribution of the hydrodynamic pressure in the port hull was calculated and the results are shown in Fig. 3.16. It can be seen that the largest force (55.75kN) occurs near the mid-ship and decreases toward the ends. The average is 36.11 kN, so the maximum is 1.54 times the average value. The results agree well with those in Kobayashi and Shimada (1990) except for a little fluctuation near the mid-ship. Therefore it may be said that the sinusoidal distribution is more realistic than the uniform distribution.

For completeness, the pressure distributions at $x=-15.77$, -14.05 , -9.35 , -1.85 , 0.65 , 3.15 , 5.65 , 8.15 , 12.75 , 14.65 meters were also shown in Figs. 3.17 to 3.26, and their resultant forces in different phase angles shown in Table 3.9. Z_{sf} is the exertion point of resultant force.

Table 3.9: Resultant force of hydrodynamic pressure at port hull

Posi.(m)						
-15.77	ωt	0	$\pi / 2$	π	$3\pi / 2$	2π
	Resultant force	0.392e3	0.082e3	-0.392e3	-0.082e3	0.392e3
	Z_{sf}	-1.797	-1.797	-1.797	-1.797	-1.797
-14.05	ωt	0	$\pi / 2$	π	$3\pi / 2$	2π
	Resultant force	0.1813e5	0.0713e5	-0.1813e5	-0.0711e5	0.1813e5
	Z_{sf}	-0.967	-0.924	-0.967	-0.924	-0.967
-9.35	ωt	0	$\pi / 2$	π	$3\pi / 2$	2π
	Resultant force	0.421e5	0.1841e5	-0.421e5	-0.1835e5	0.421e5
	Z_{sf}	-1.048	-1.019	-1.048	-1.019	-1.048
-6.85	ωt	0	$\pi / 2$	π	$3\pi / 2$	2π
	Resultant force	0.4833e5	0.2268e5	-0.4833e5	-0.2267e5	0.4833e5
	Z_{sf}	-1.05	-1.022	-1.05	-1.022	-1.05
-1.85	ωt	0	$\pi / 2$	π	$3\pi / 2$	2π
	Resultant force	0.5521e5	0.2756e5	-0.5521e5	-0.2749e5	0.5521e5
	Z_{sf}	-1.041	-1.017	-1.041	-1.017	-1.041
0.65	ωt	0	$\pi / 2$	π	$3\pi / 2$	2π
	Resultant force	0.5575e5	0.2277e5	-0.5575e5	-0.277e5	0.5575e5
	Z_{sf}	-1.041	-1.017	-1.041	-1.017	-1.041
3.15	ωt	0	$\pi / 2$	π	$3\pi / 2$	2π
	Resultant force	0.5496e5	0.2678e5	-0.5496e5	-0.2672e5	0.5496e5
	Z_{sf}	-1.041	-1.016	-1.041	-1.016	-1.041
5.65	ωt	0	$\pi / 2$	π	$3\pi / 2$	2π
	Resultant force	0.5292e5	0.2476e5	-0.5292e5	-0.2496e5	0.5292e5
	Z_{sf}	-1.031	-1.005	-1.031	-1.005	-1.031
8.15	ωt	0	$\pi / 2$	π	$3\pi / 2$	2π
	Resultant force	0.5067e5	0.2261e5	-0.5067e5	-0.2255e5	0.5067e5
	Z_{sf}	-0.9901	-0.9624	-0.9901	-0.9623	-0.9901
12.75	ωt	0	$\pi / 2$	π	$3\pi / 2$	2π
	Resultant force	0.1844e5	0.074e5	-0.1844e5	-0.074e5	0.1844e5
	Z_{sf}	-0.9571	-0.9257	-0.9571	-0.9256	-0.9571
14.65	ωt	0	$\pi / 2$	π	$3\pi / 2$	2π
	Resultant force	0.2561e3	0.056e3	-0.2561e3	-0.056e3	0.2561e3
	Z_{sf}	-1.802	-1.817	-1.802	-1.817	-1.802

From Figs. 3.17 to 3.26 it was shown that :

- * The pressure distributions keep more or less the same nature near the central parts, except for the far ends.
- * The pressure distributions at phase angle $\omega t = 0.0$ and π , which correspond to prying and squeezing force respectively, are symmetric to the x-axis. Hence in structural analysis when the loadcase is switched from prying to squeezing, only the sign of the pressure needs to be changed.

3.4 DISCUSSIONS

Prediction of primary loads on SWATH is of prime importance in structural design. In the present study the primary loads were calculated by a validated program developed by Chan. Another program, SPEC, was developed to carry out spectral analysis and to calculate extreme design values. Several factors which are important in structural analysis were discussed. Based on these analyses the following conclusions may be drawn:

- * The largest side force occurs in beam seas. The wave length, at which the largest RAO of side force occurs, is about four times the width of the ship.
- * Although no experimental data is available to verify the analytical results, good agreement exists between the calculated side force and that used by the FBM Marine Company.
- * The longitudinal distribution of the hydrodynamic forces shows that the interaction between the two hulls is strong, and the uniform distribution of side forces suggested by Sikora and Dinsenbacher (1990) is not suitable in this case. A sinusoidal distribution is preferred based on the results.
- * Load combinations suggested by Chalmers (1989) seem to be too conservative in this case. More cases need to be calculated to establish simple and accurate load combinations for design.

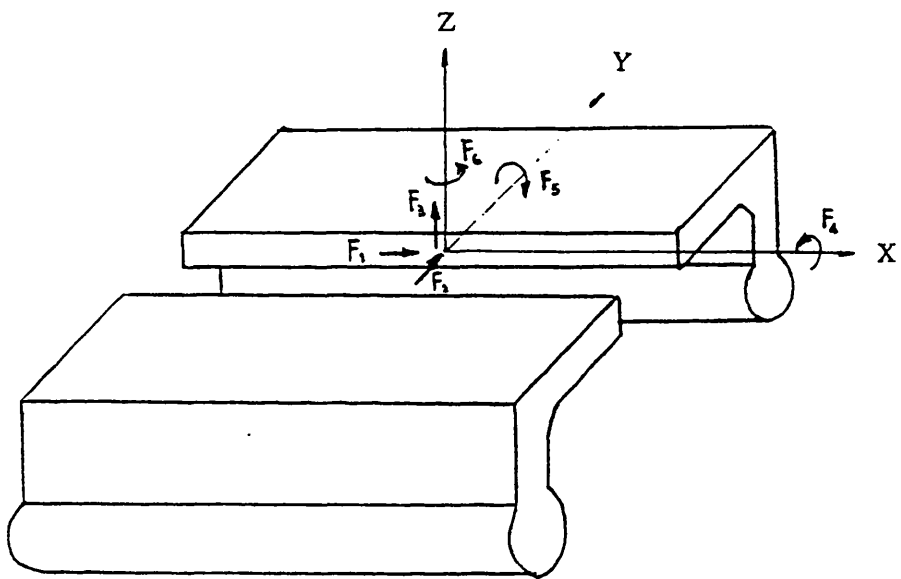


Fig. 3.1 Definition of primary loads and co-ordinates system

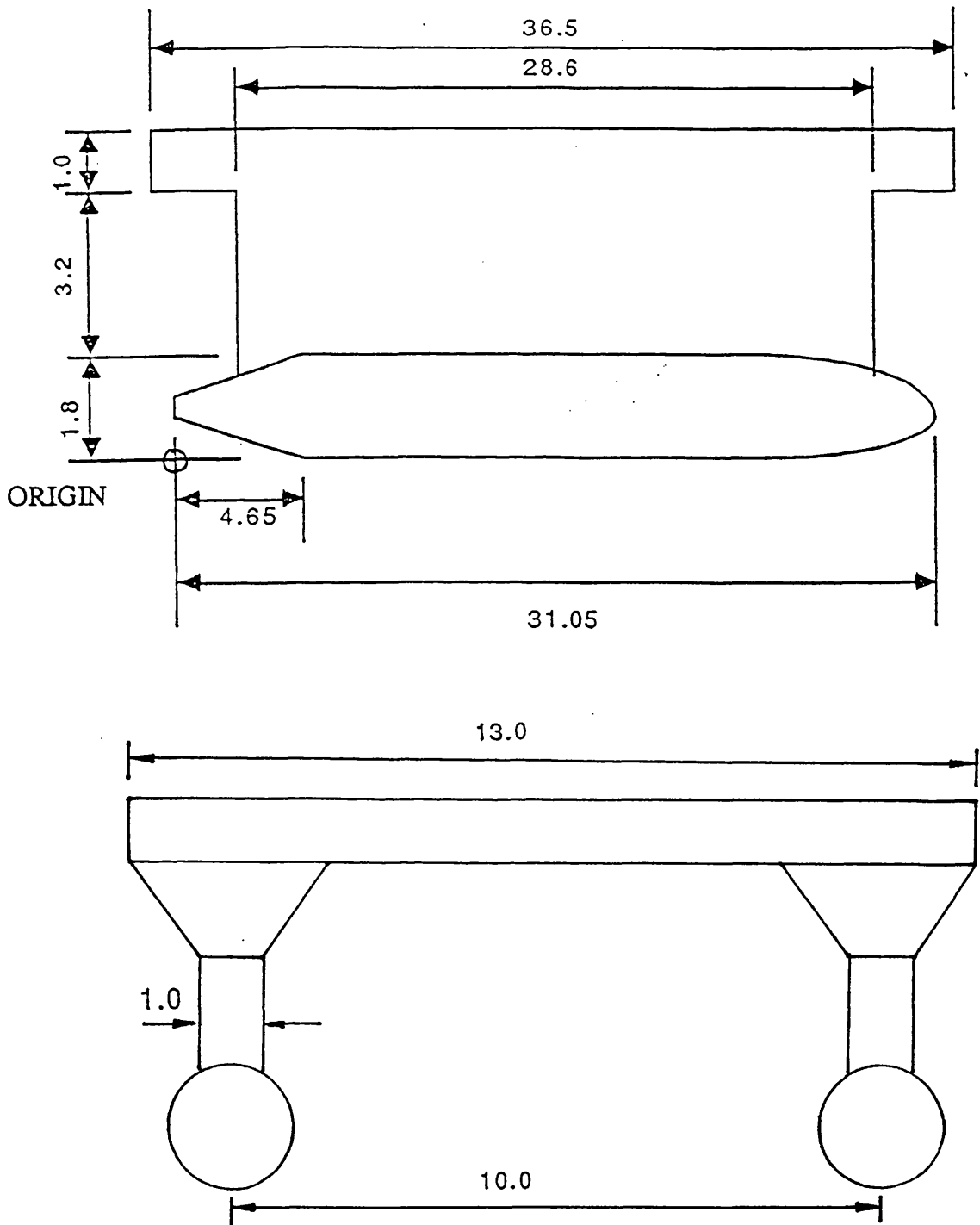


Fig. 3.2 Dimensions of the PATRIA model (in meters)

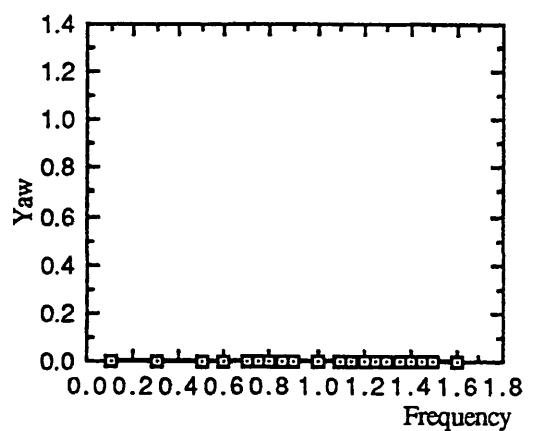
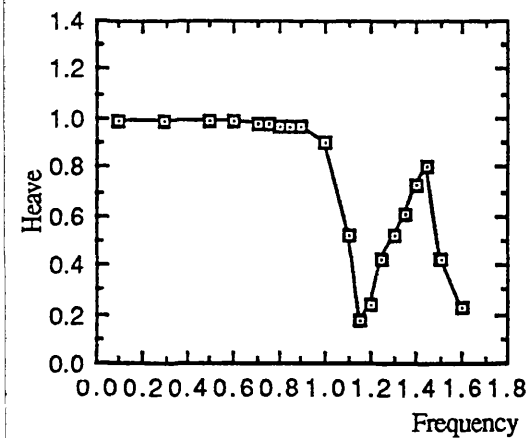
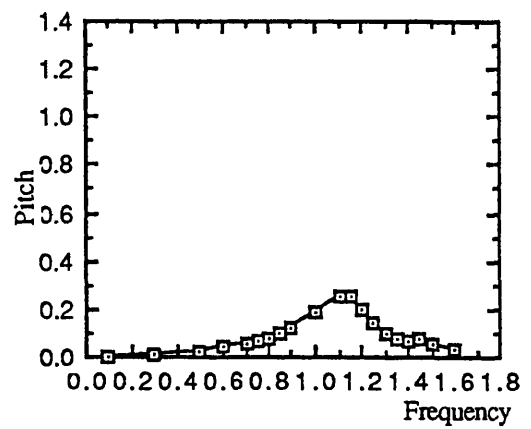
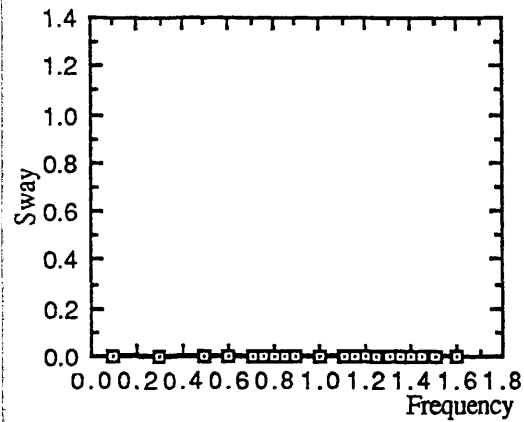
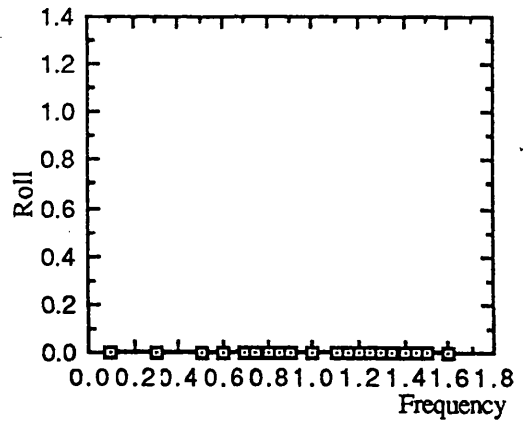
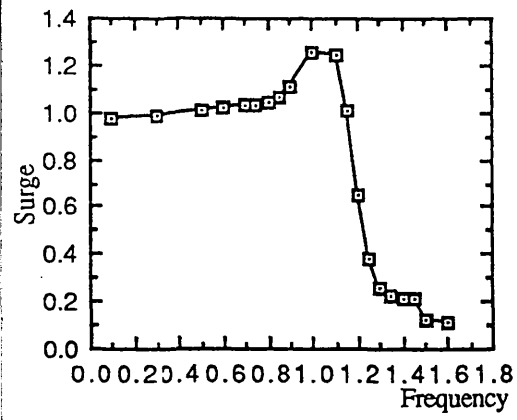


Fig. 3.3 RAO of motion responses in wave incident angle 0°

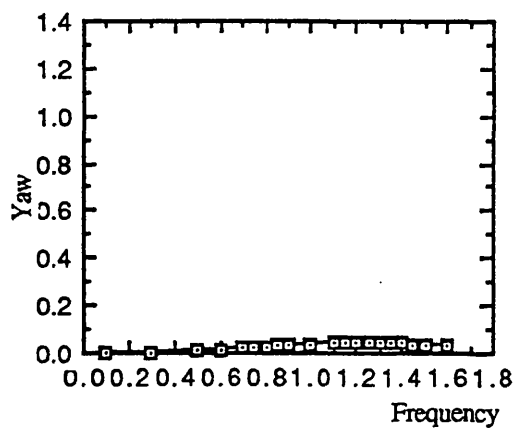
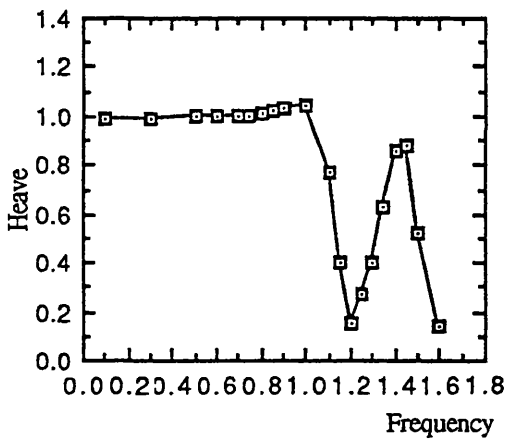
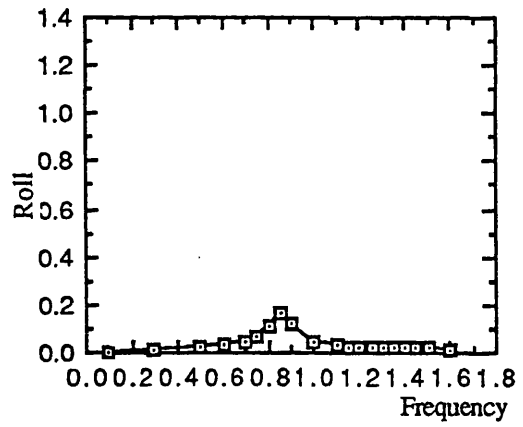
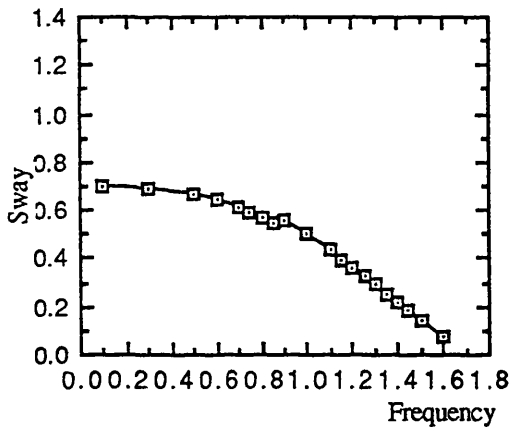
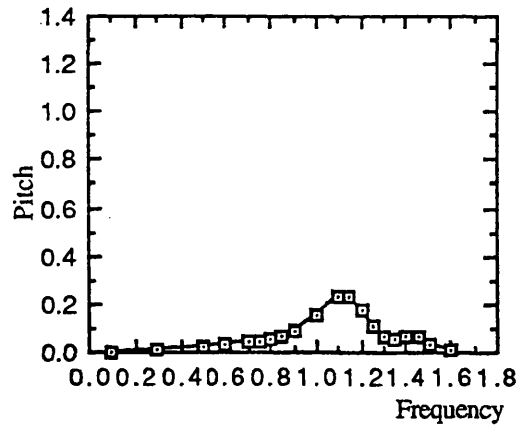
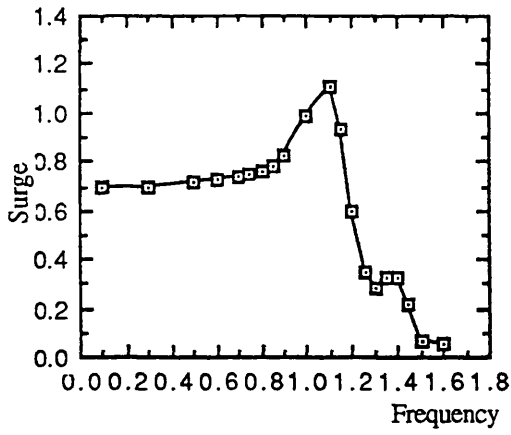


Fig. 3.4 RAO of motion responses in wave incident angle 45°

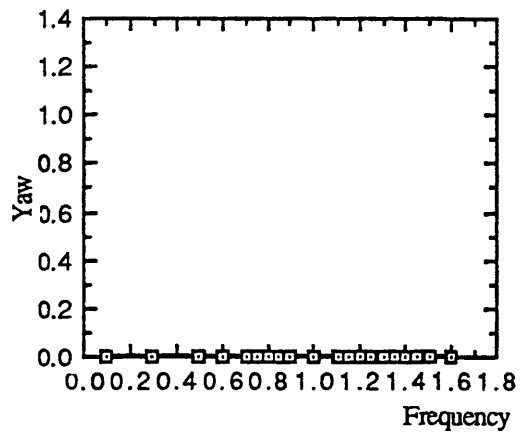
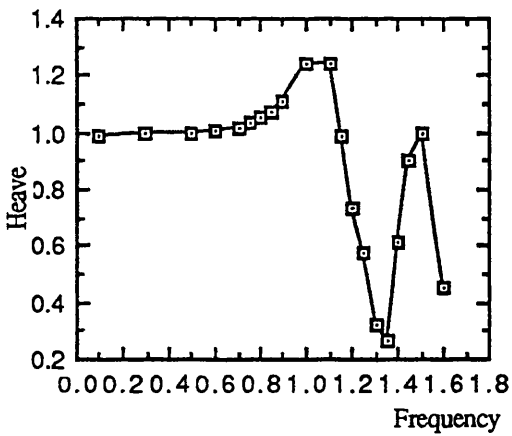
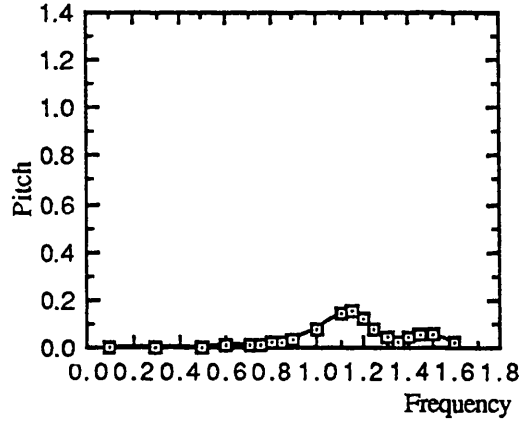
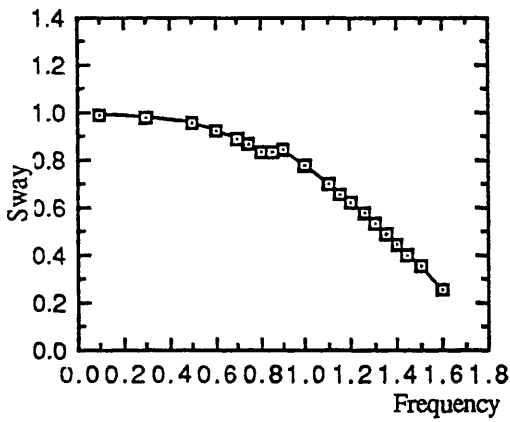
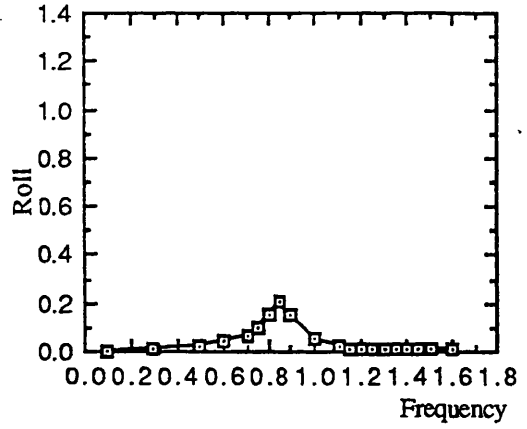
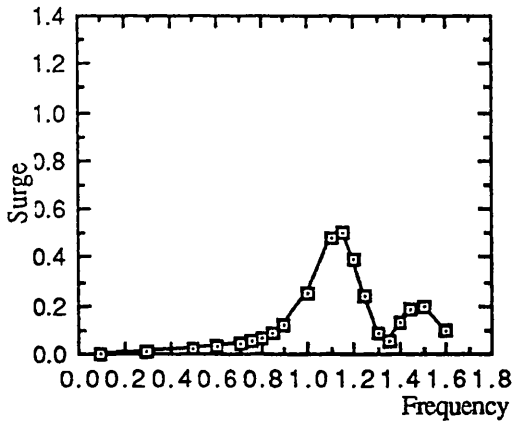


Fig. 3.5 RAO of motion responses in wave incident angle 90°

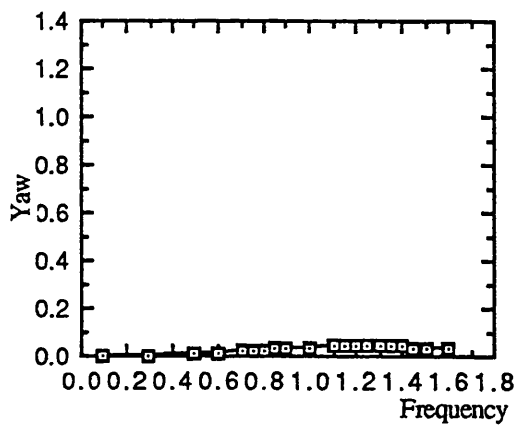
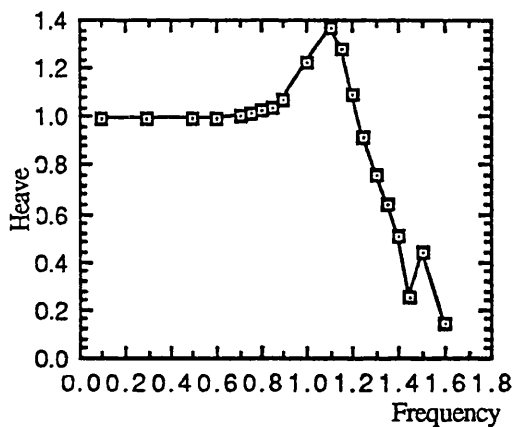
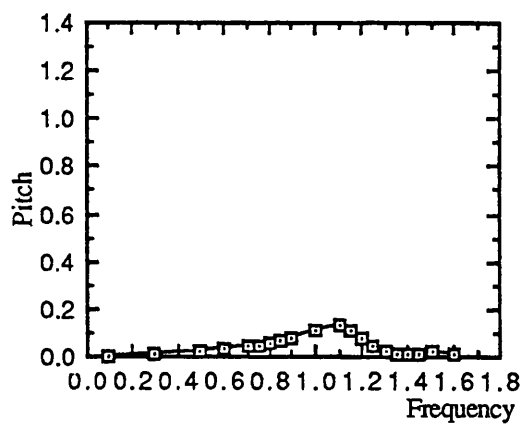
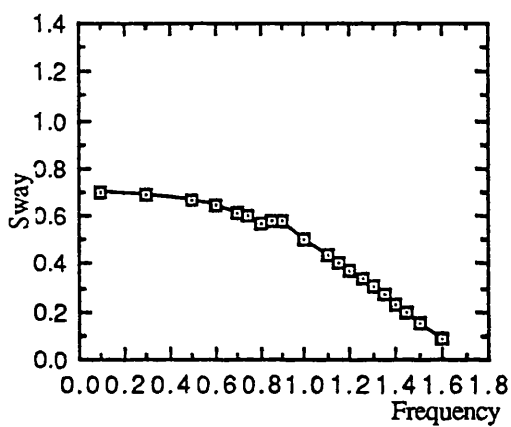
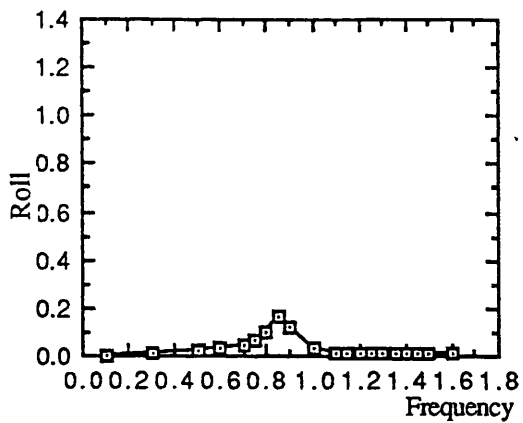
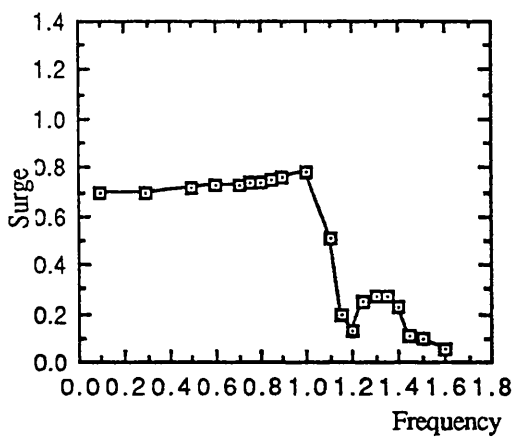


Fig. 3.6 RAO of motion responses in wave incident angle 135°

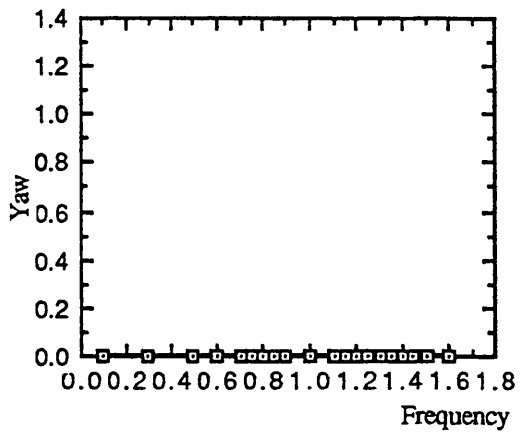
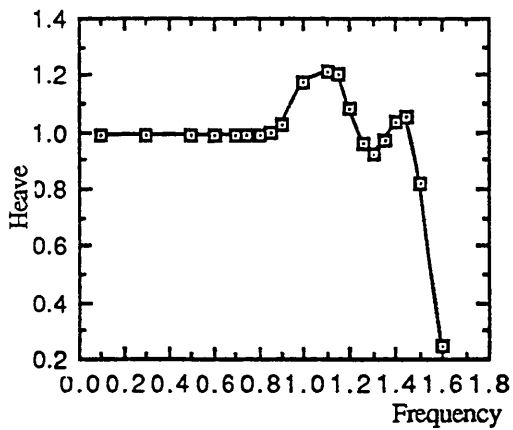
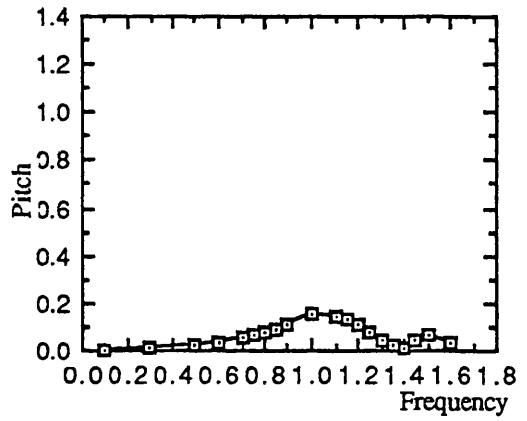
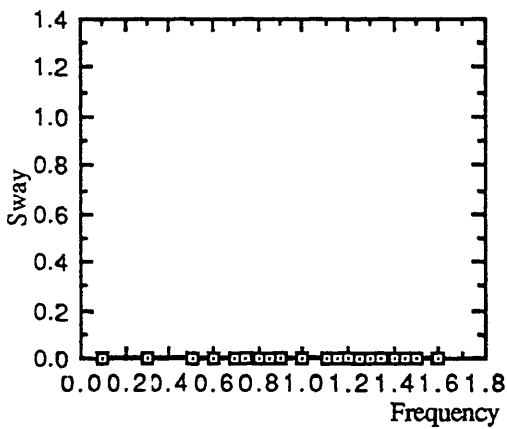
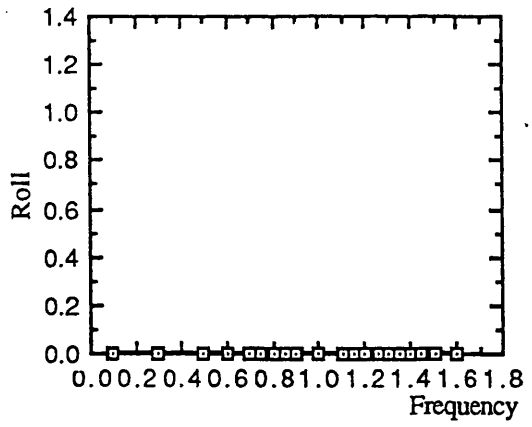
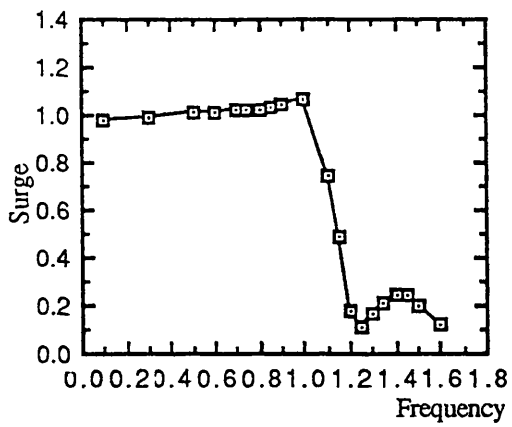


Fig. 3.7 RAO of motion responses in wave incident angle 180°

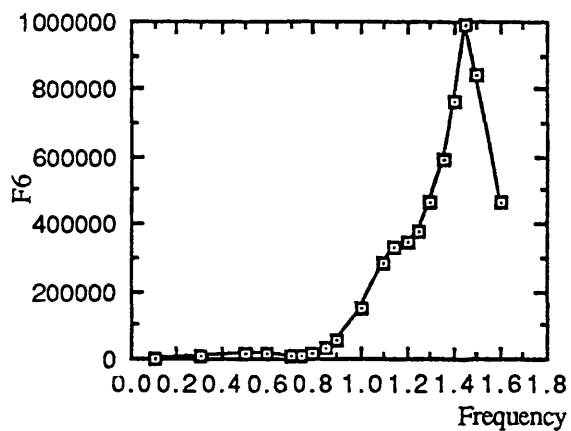
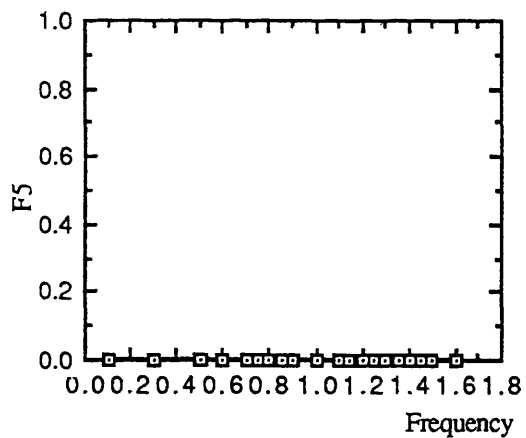
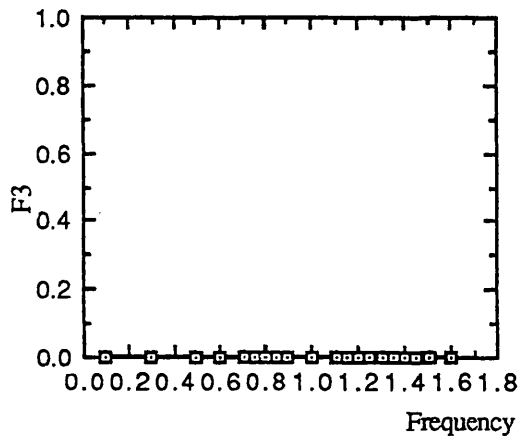
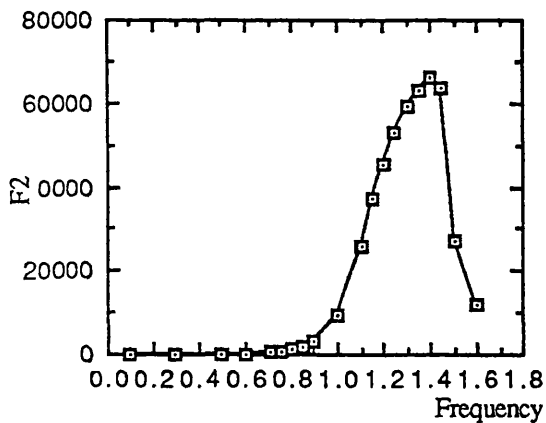
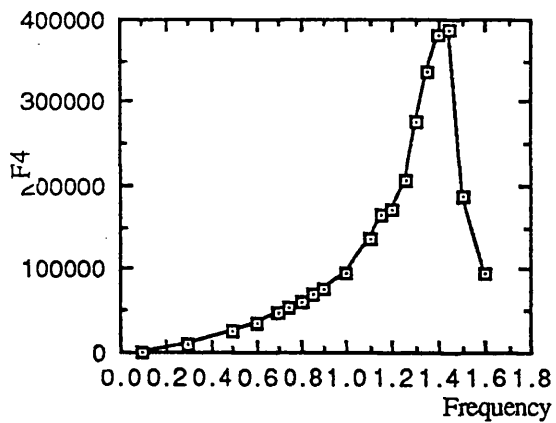
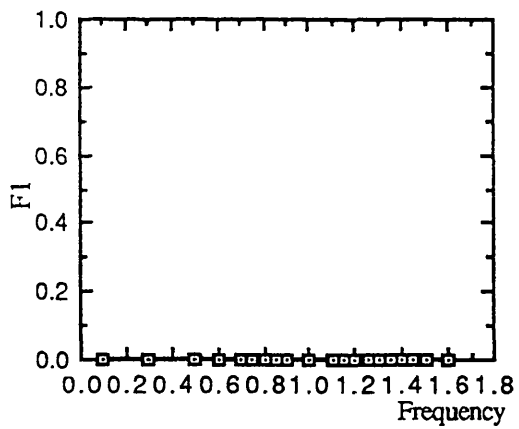


Fig. 3.8 RAO of loads in wave incident angle 0°

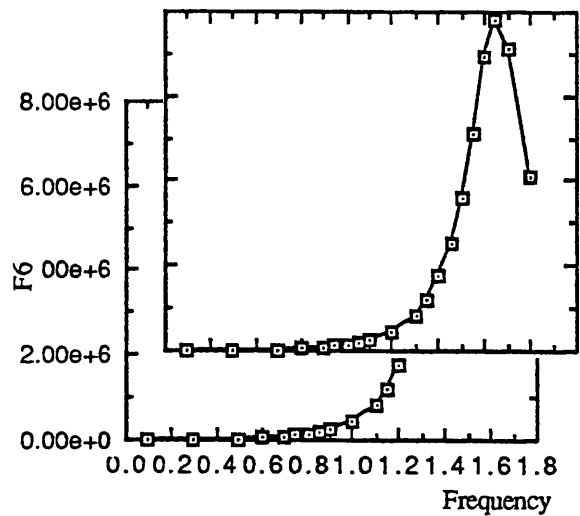
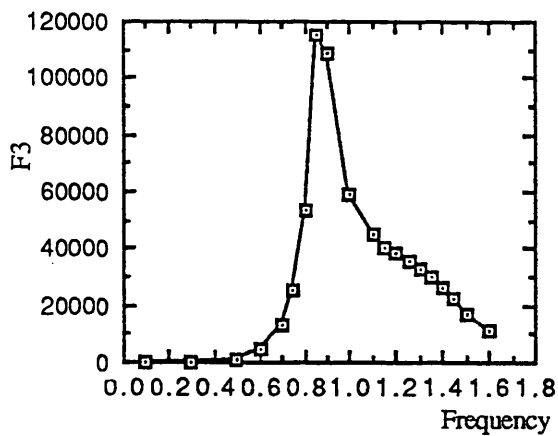
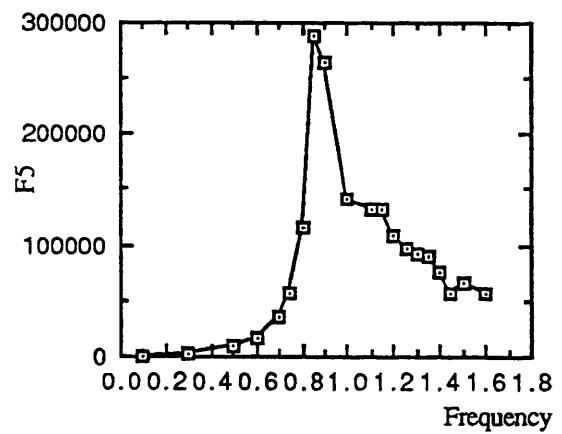
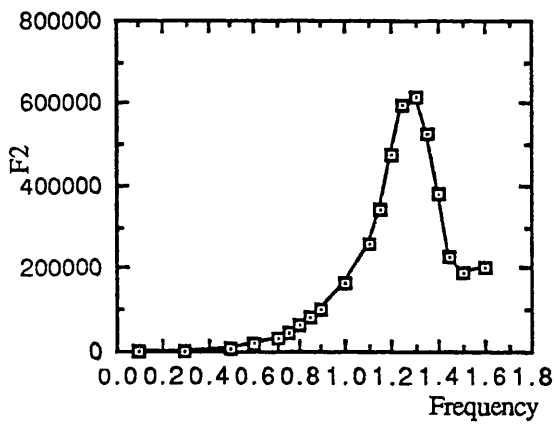
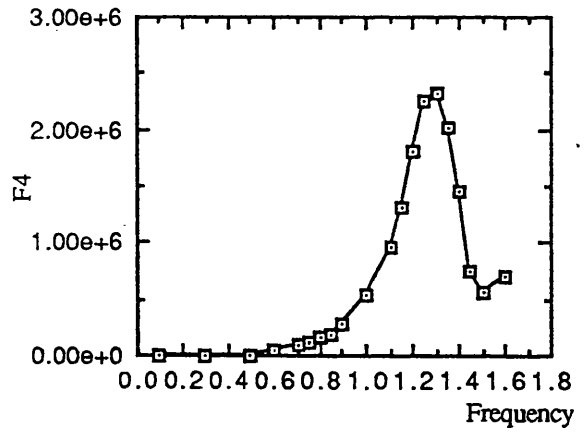
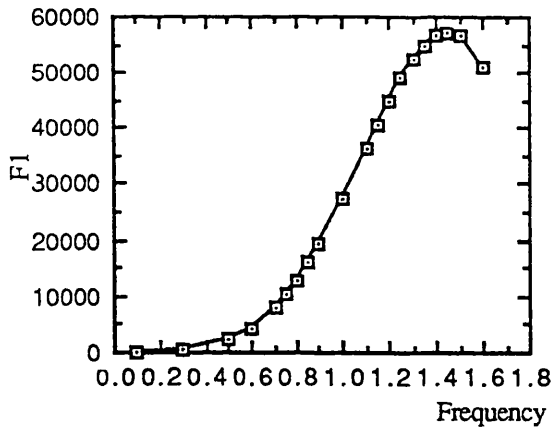


Fig. 3.9 RAO of loads in wave incident angle 45°

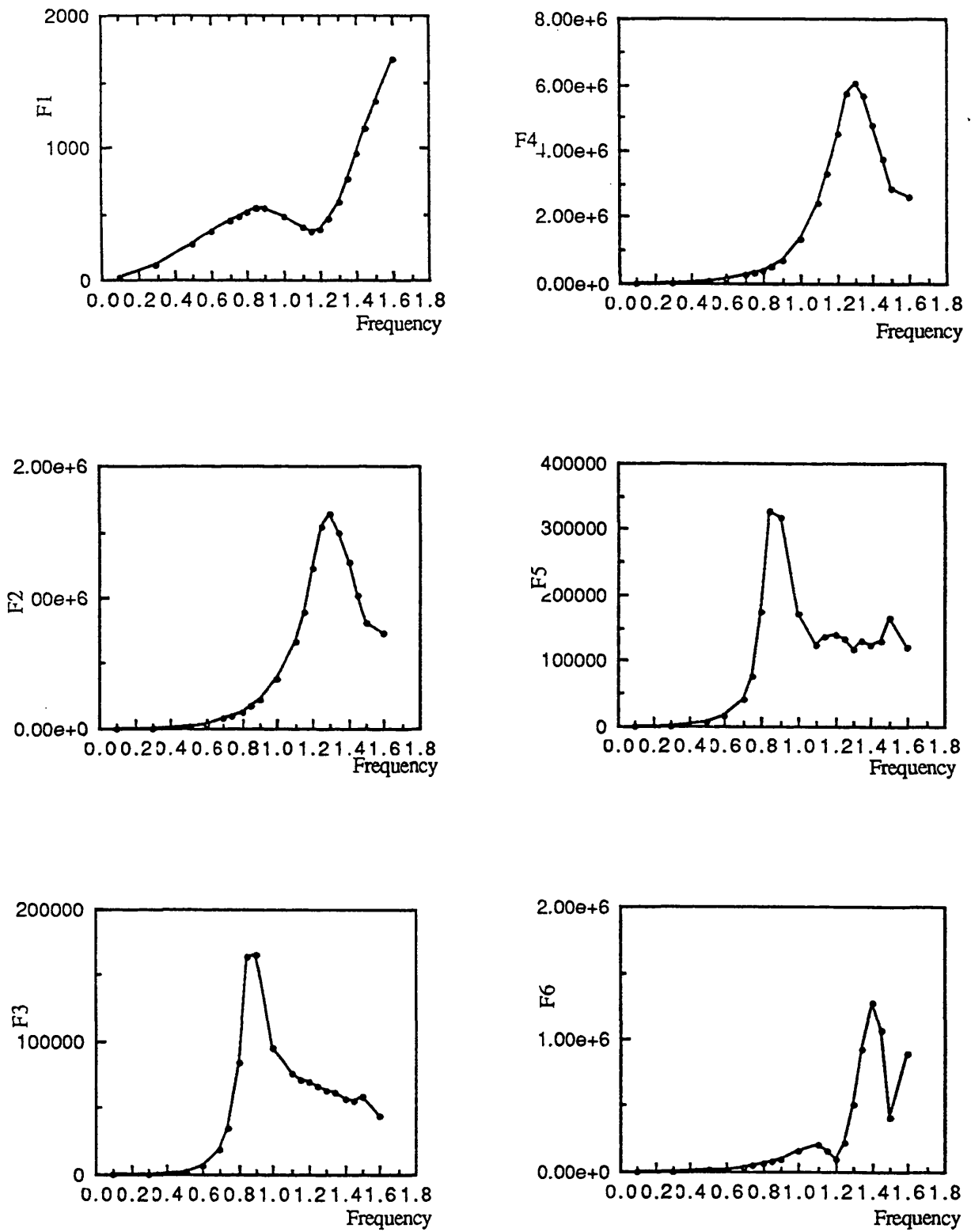


Fig. 3.10 RAO of loads in wave incident angle 90°

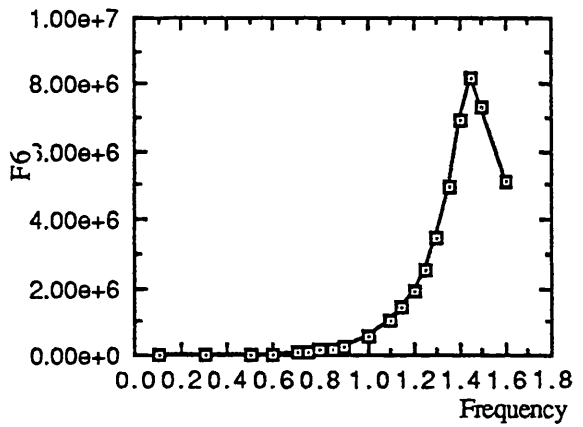
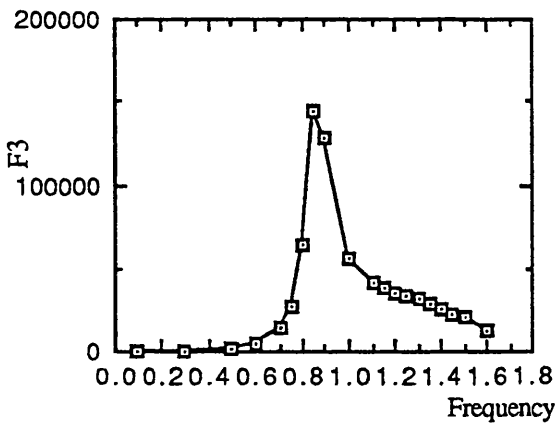
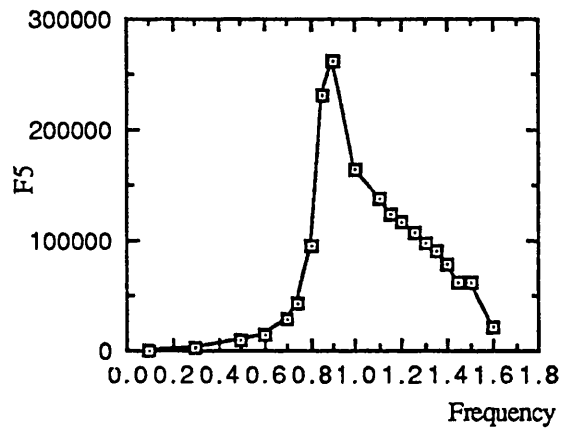
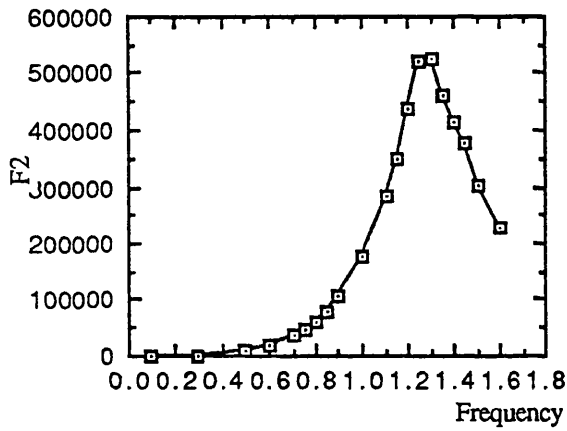
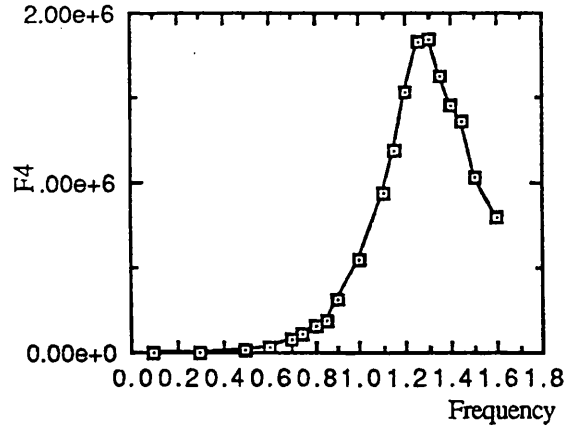
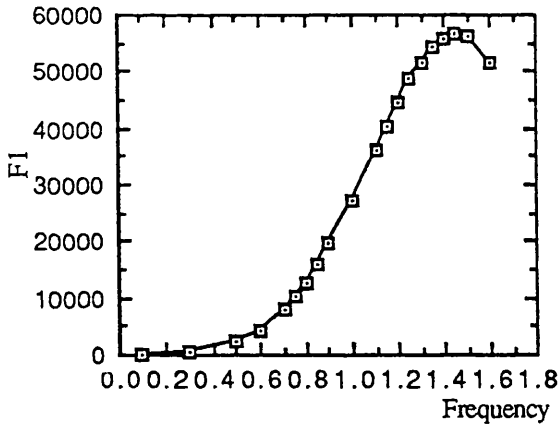


Fig. 3.11 RAO of loads in wave incident angle 135°

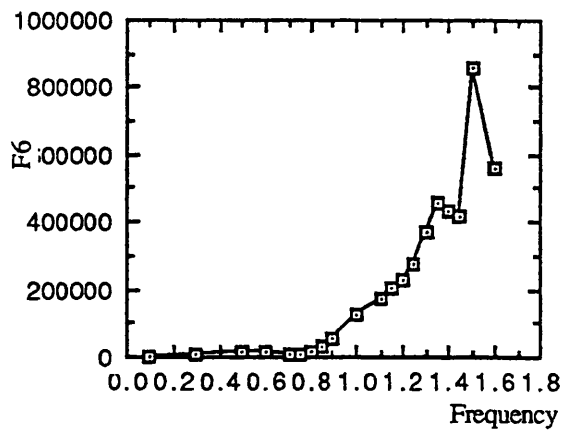
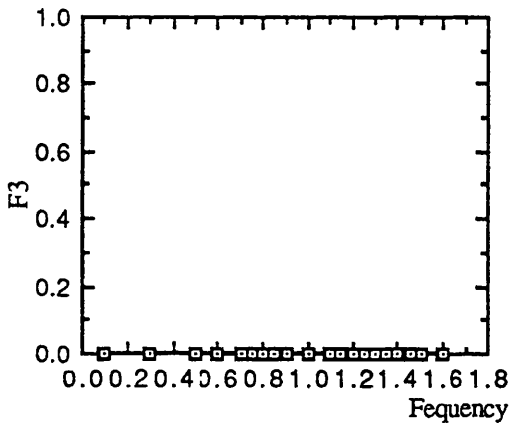
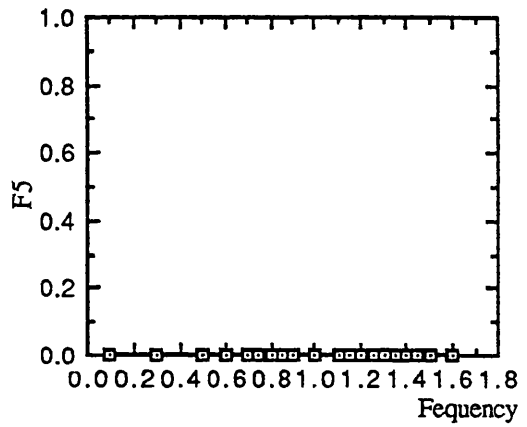
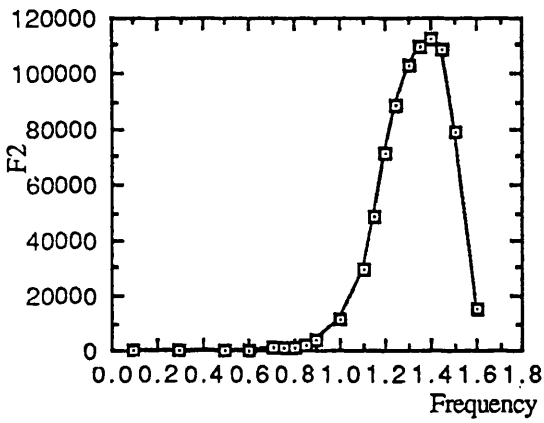
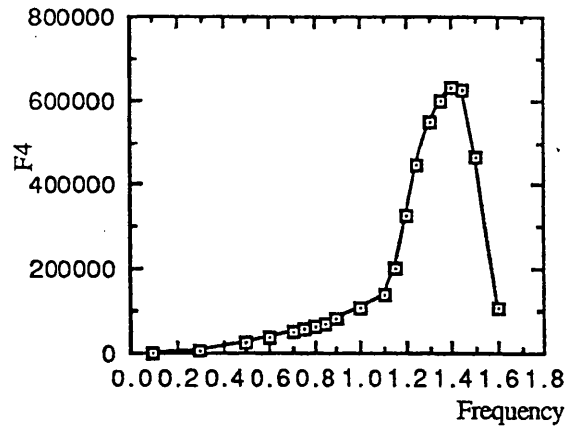
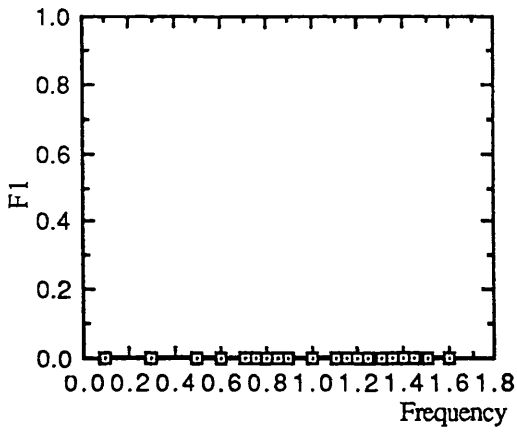


Fig. 3.12 RAO of loads in wave incident angle 180°

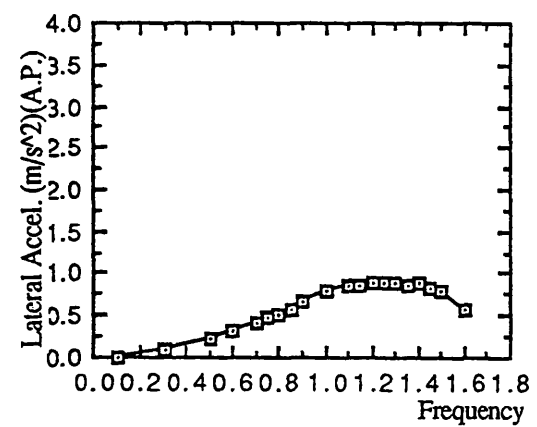
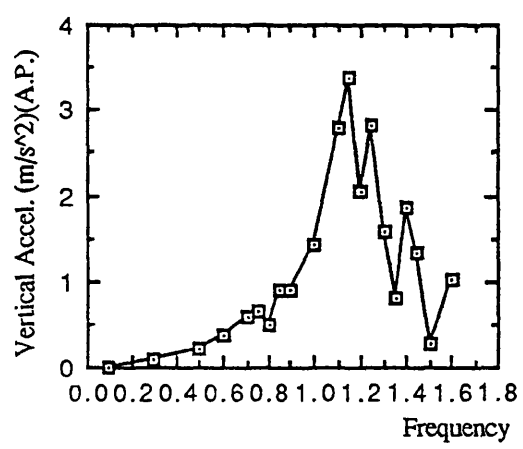
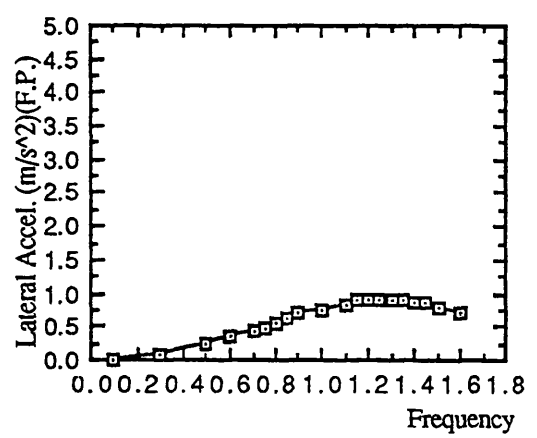
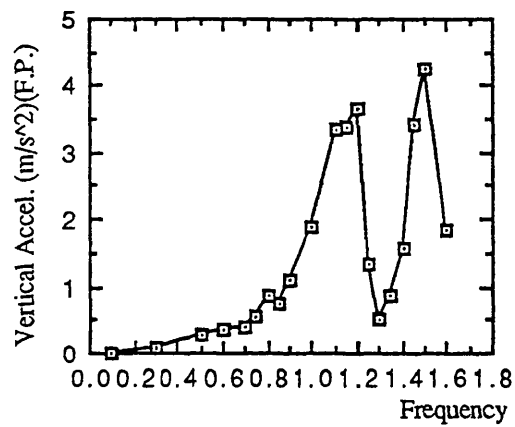
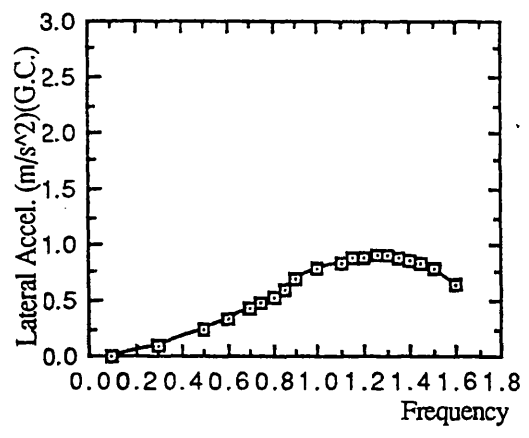
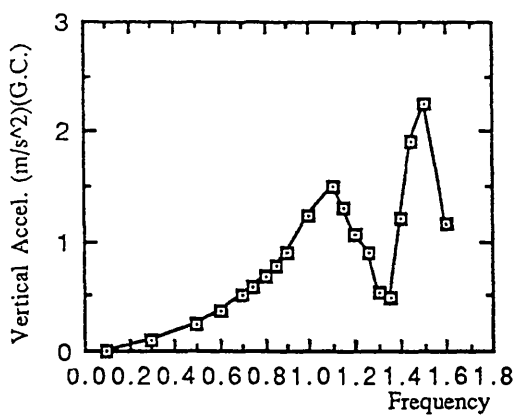
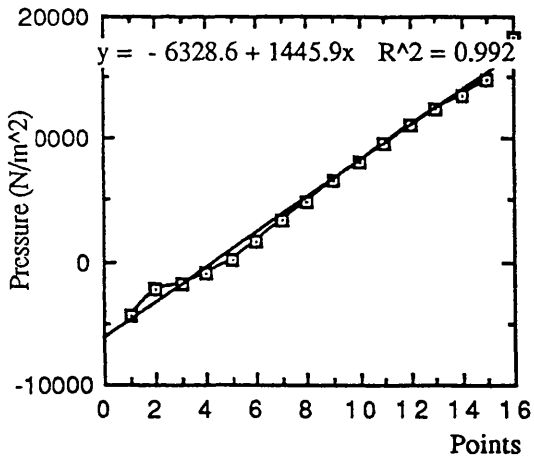
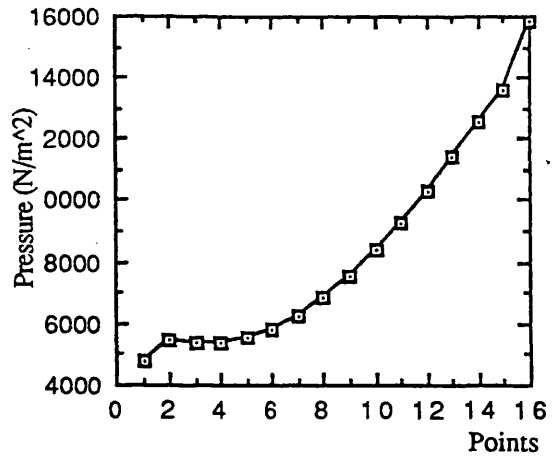


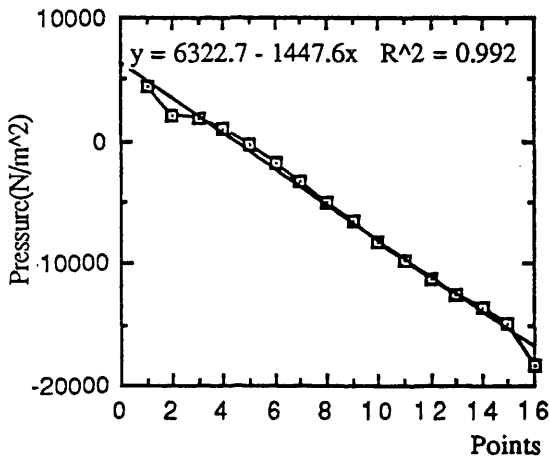
Fig. 3.13 RAO of acceleration at G.C., F.P. and A.P. in beam sea



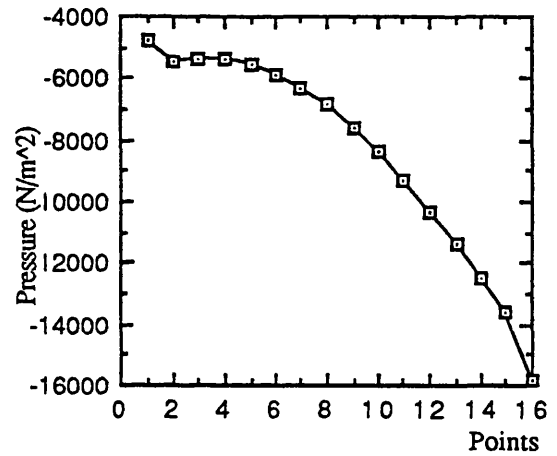
PRESSURE DISTRIBUTION AT T=0.0



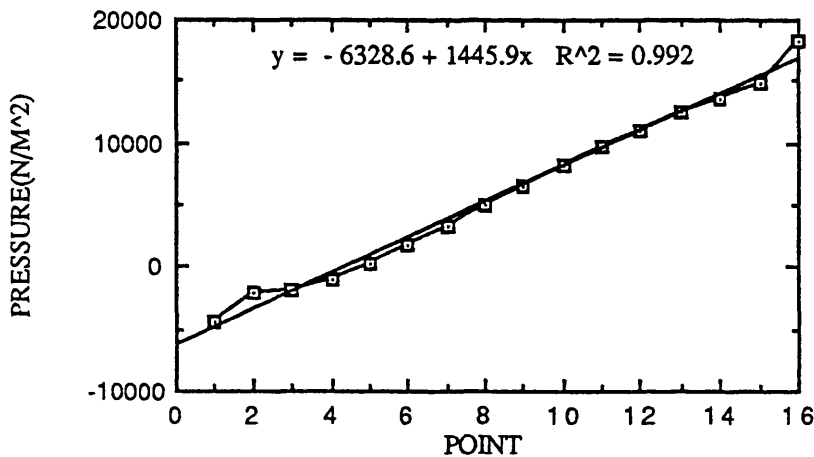
PRESSURE DISTRIBUTION AT T=1.309



PRESSURE DISTRIBUTION AT T=2.62



PRESSURE DISTRIBUTION AT T=3.927



PRESSURE DISTRIBUTION AT T=5.236

Fig. 3.14 Instantaneous pressure distributions at X=-6.8 meters

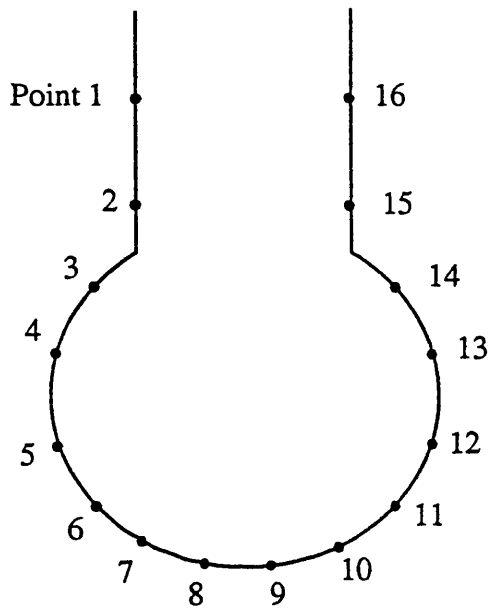


Fig. 3.15 Definition of points

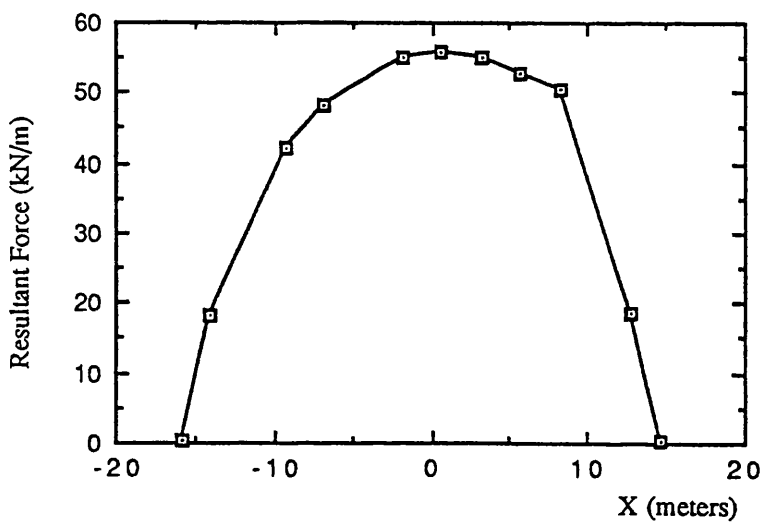
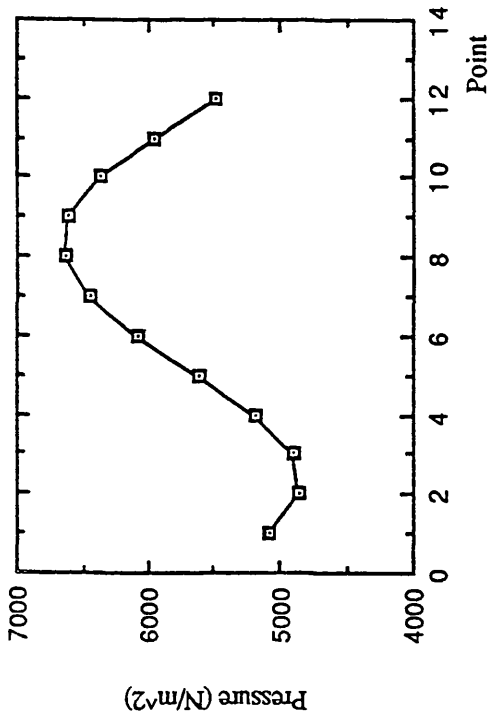
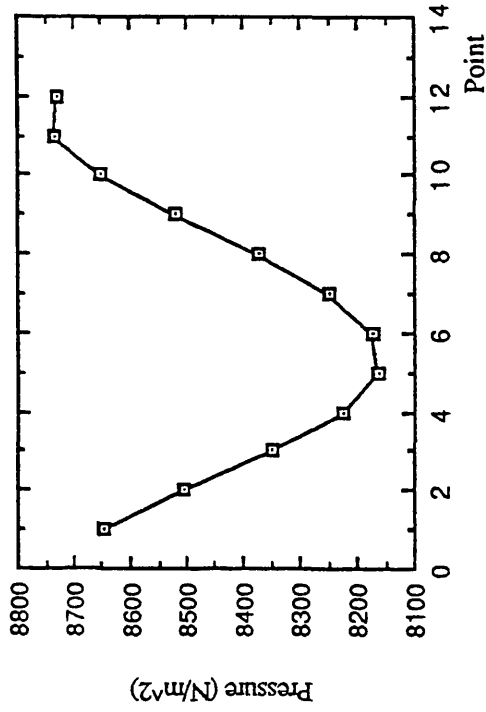


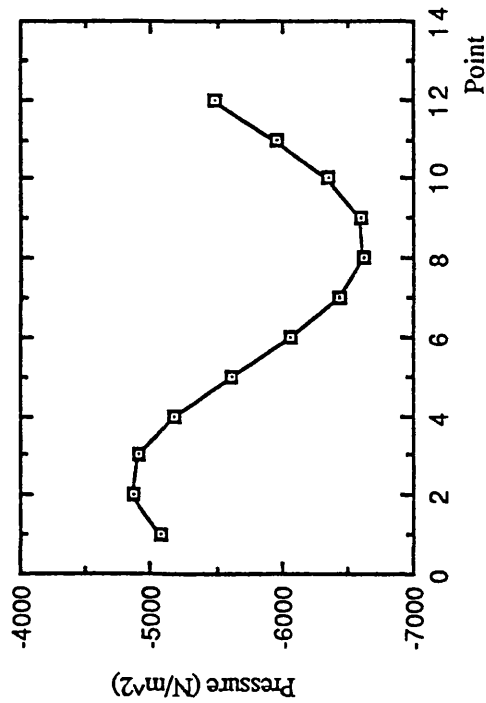
Fig. 3.16 Longitudinal distribution of resultant force of hydrodynamic pressure on port



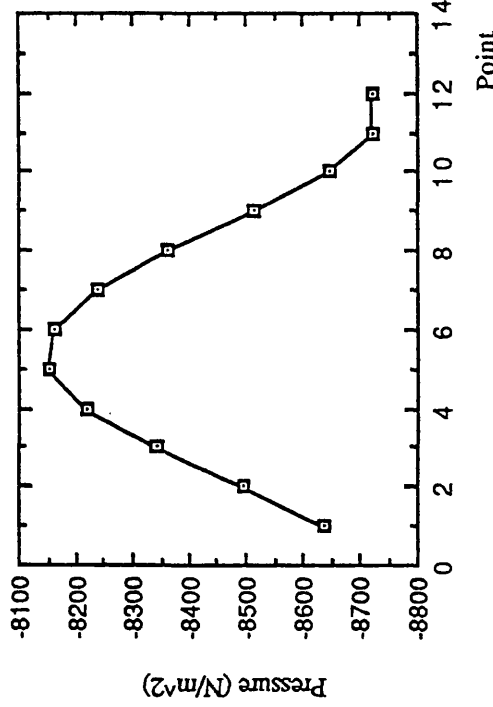
(a) Pressure Distribution at t=0.0



(b) Pressure Distribution at t=1.308

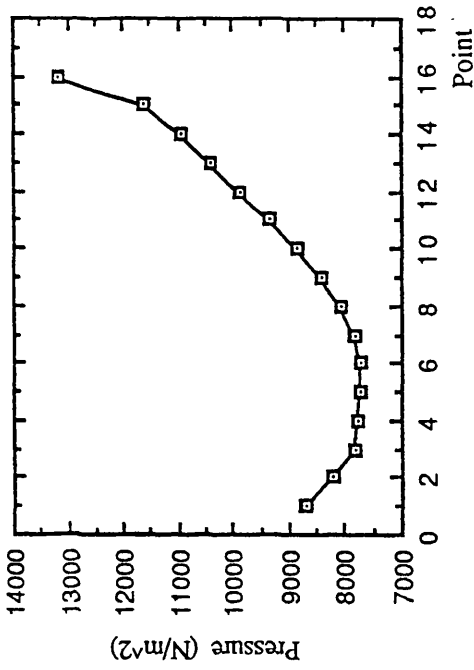


(c) Pressure Distribution at t=2.618

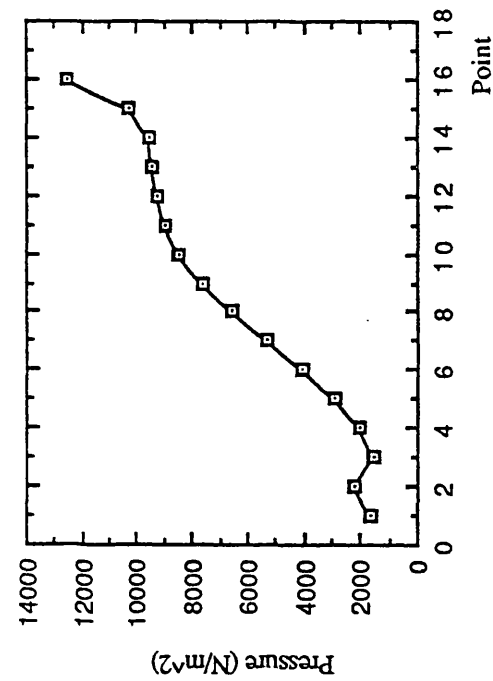


(d) Pressure Distribution at t=3.927

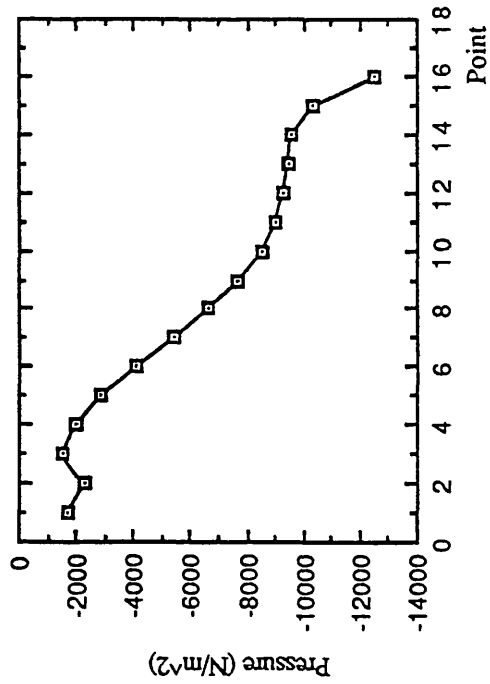
Fig. 3.17 Instantaneous pressure distributions at X=15.77 meters



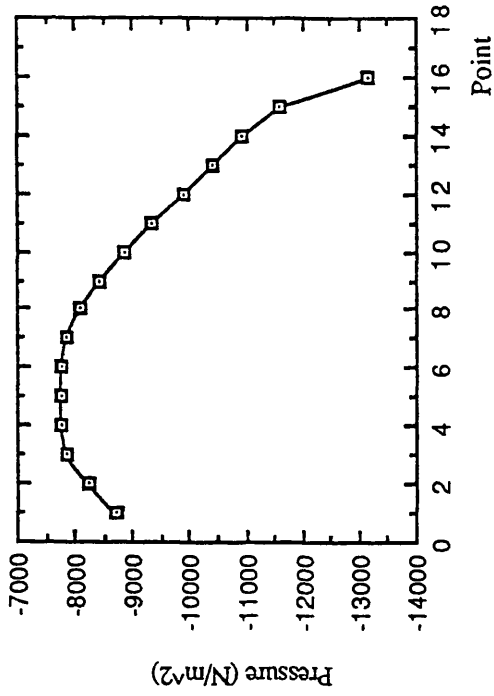
(a) Pressure Distribution at t=0.0



(b) Pressure Distribution at t=1.308

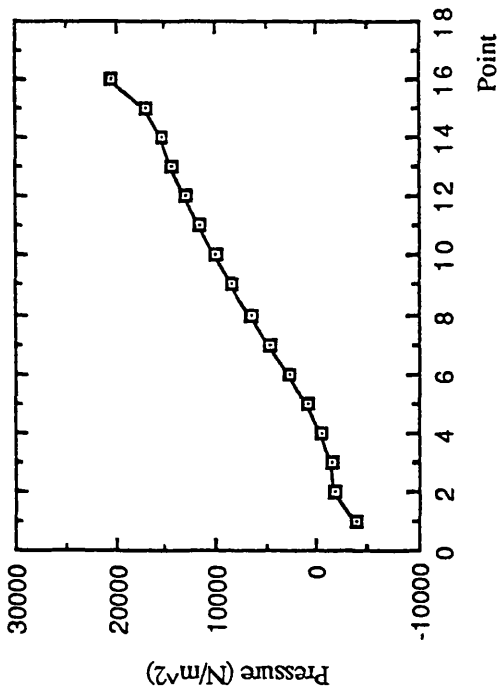


(c) Pressure Distribution at t=2.618

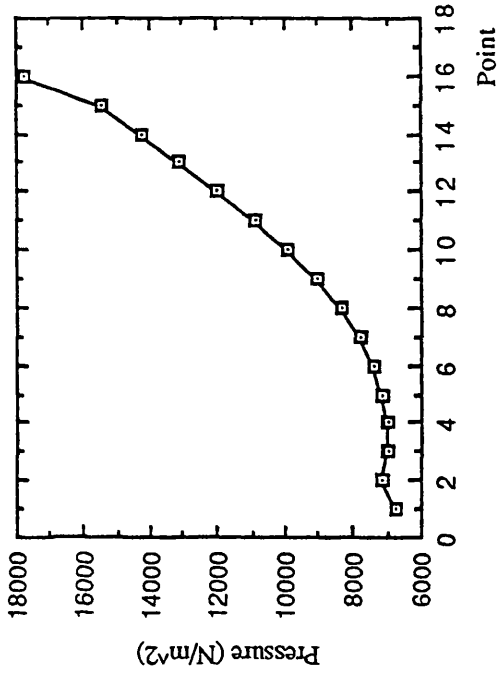


(d) Pressure Distribution at t=3.927

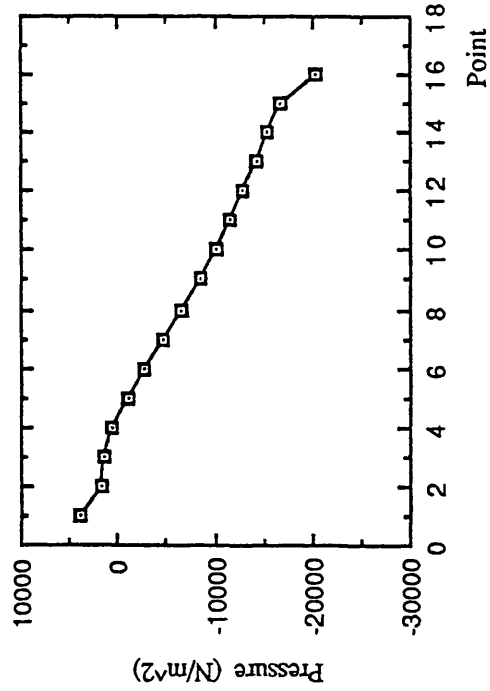
Fig. 3.18 Instantaneous pressure distributions at X=-14.05 meters



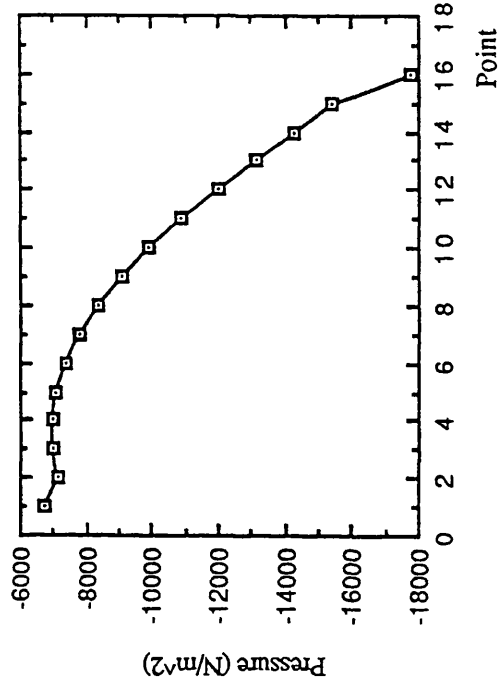
(a) Pressure Distribution at $t=0.0$



(b) Pressure Distribution at $t=1.308$

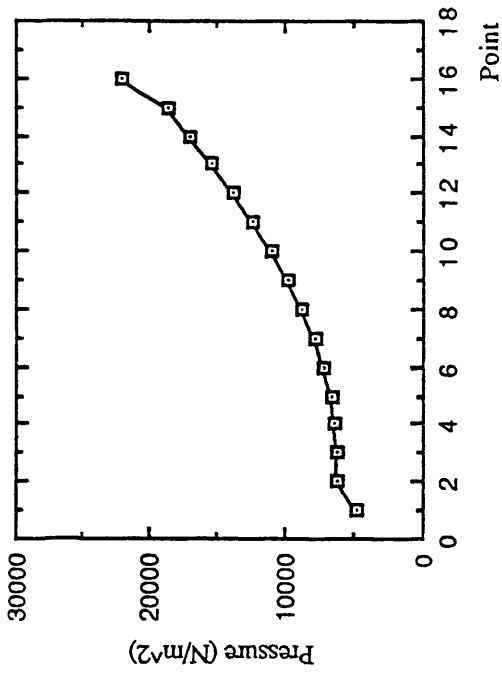


(c) Pressure Distribution at $t=2.618$

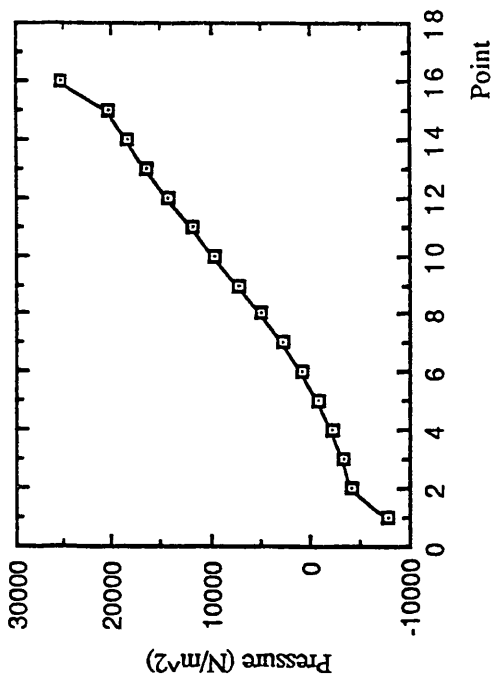


(d) Pressure Distribution at $t=3.927$

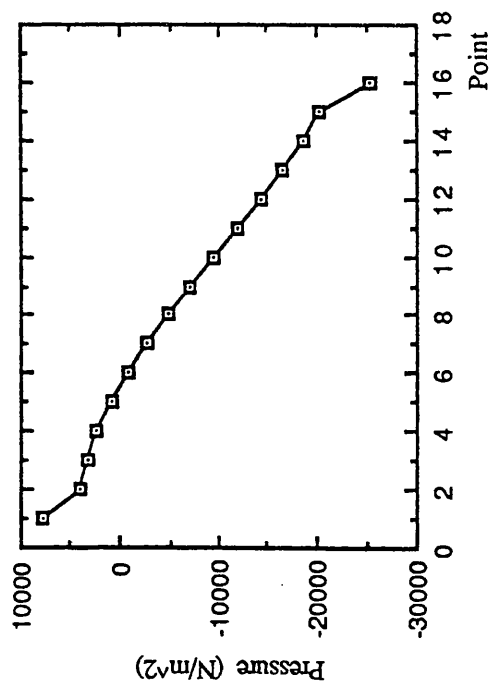
Fig. 3.19 Instantaneous pressure distributions at $X=-9.35$ meters



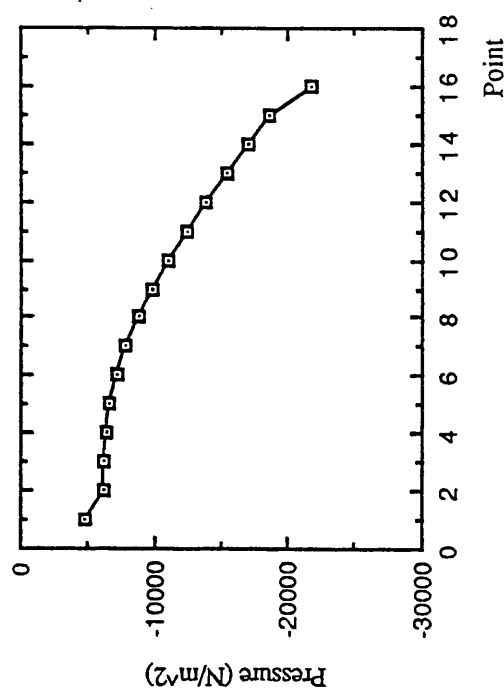
(a) Pressure Distribution at $t=0.0$



(b) Pressure Distribution at $t=1.308$

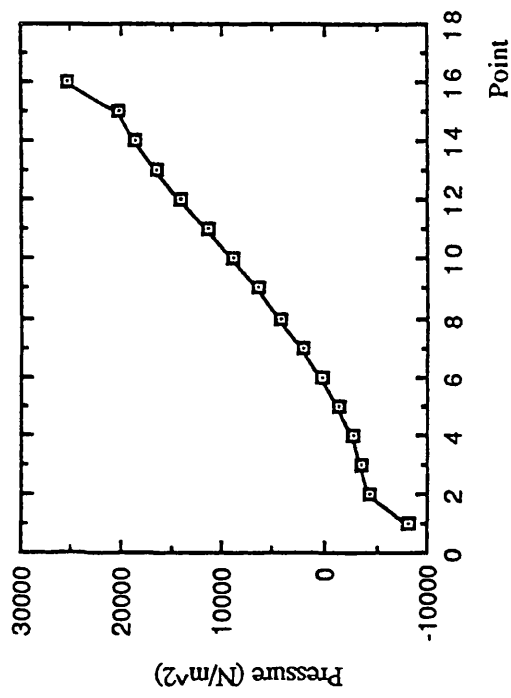


(c) Pressure Distribution at $t=2.618$

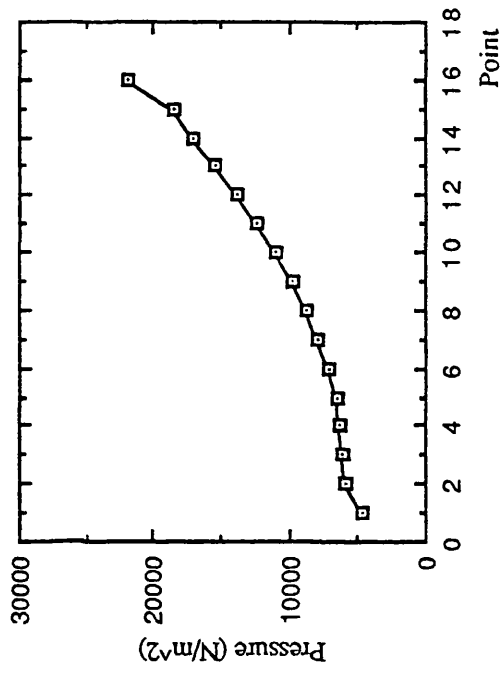


(d) Pressure Distribution at $t=3.927$

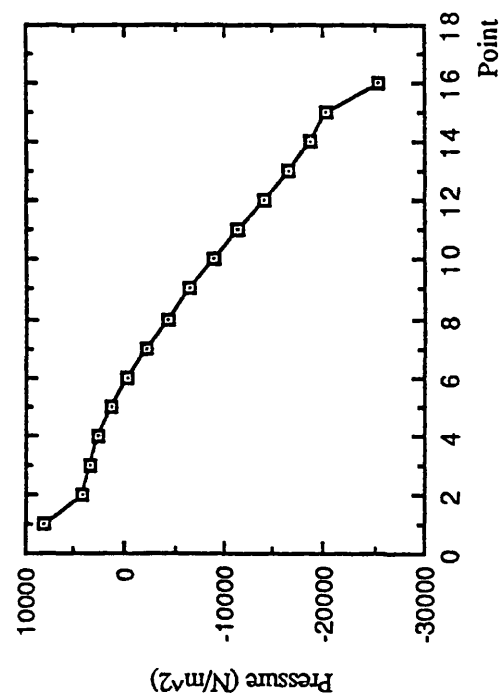
Fig. 3.20 Instantaneous pressure distributions at $X=-1.85$ meters



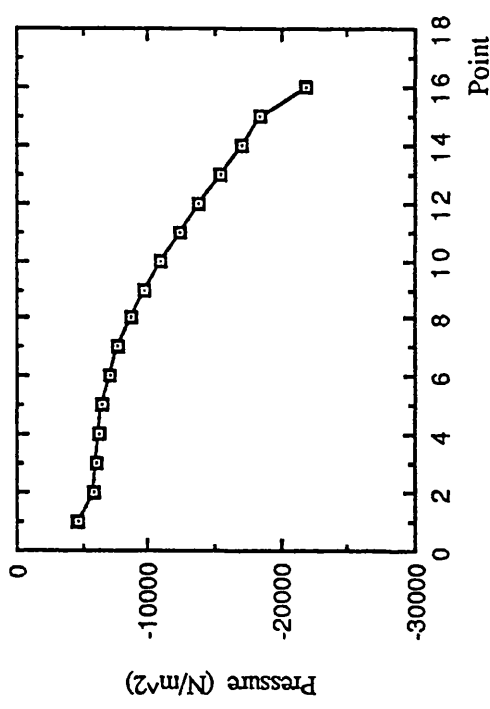
(a) Pressure Distribution at $t=0.0$



(b) Pressure Distribution at $t=1.308$

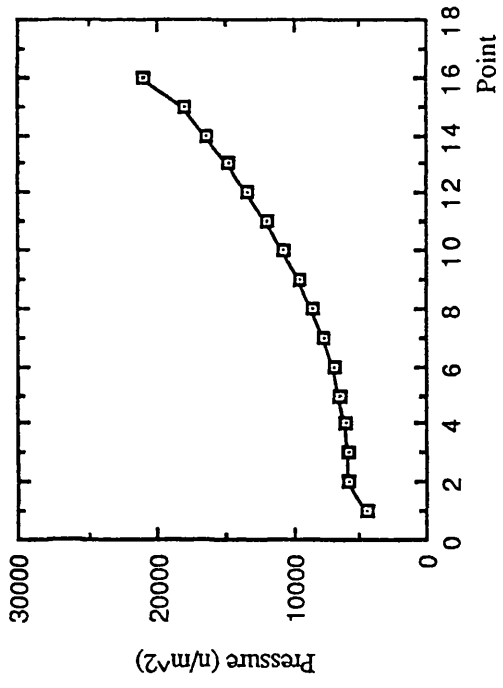


(c) Pressure Distribution at $t=2.618$

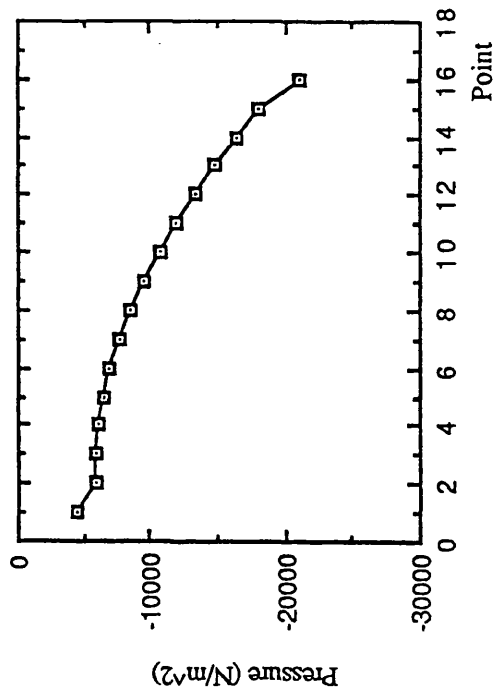


(d) Pressure Distribution at $t=3.927$

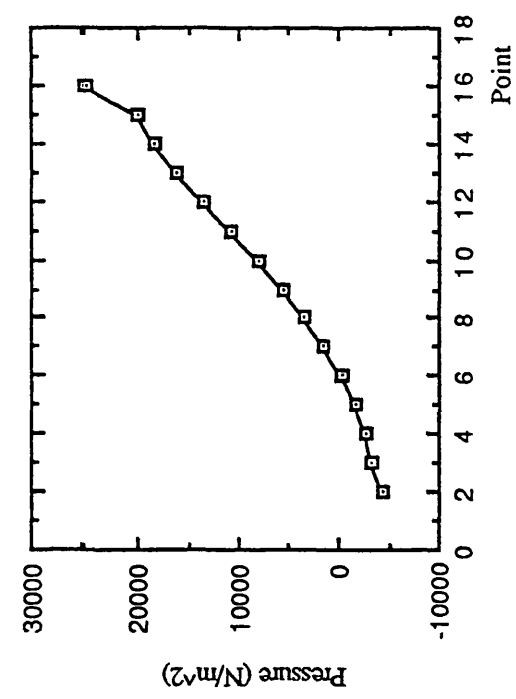
Fig. 3.21 Instantaneous pressure distributions at $X=0.65$ meters



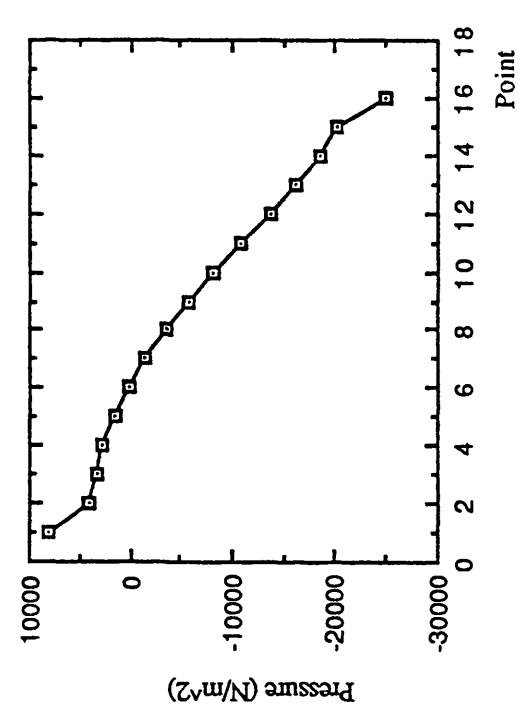
(a) Pressure Distribution at $t=0.0$



(b) Pressure Distribution at $t=1.308$



(c) Pressure Distribution at $t=2.618$



(d) Pressure Distribution at $t=3.927$

Fig. 3.22 Instantaneous pressure distributions at $X=3.15$ meters

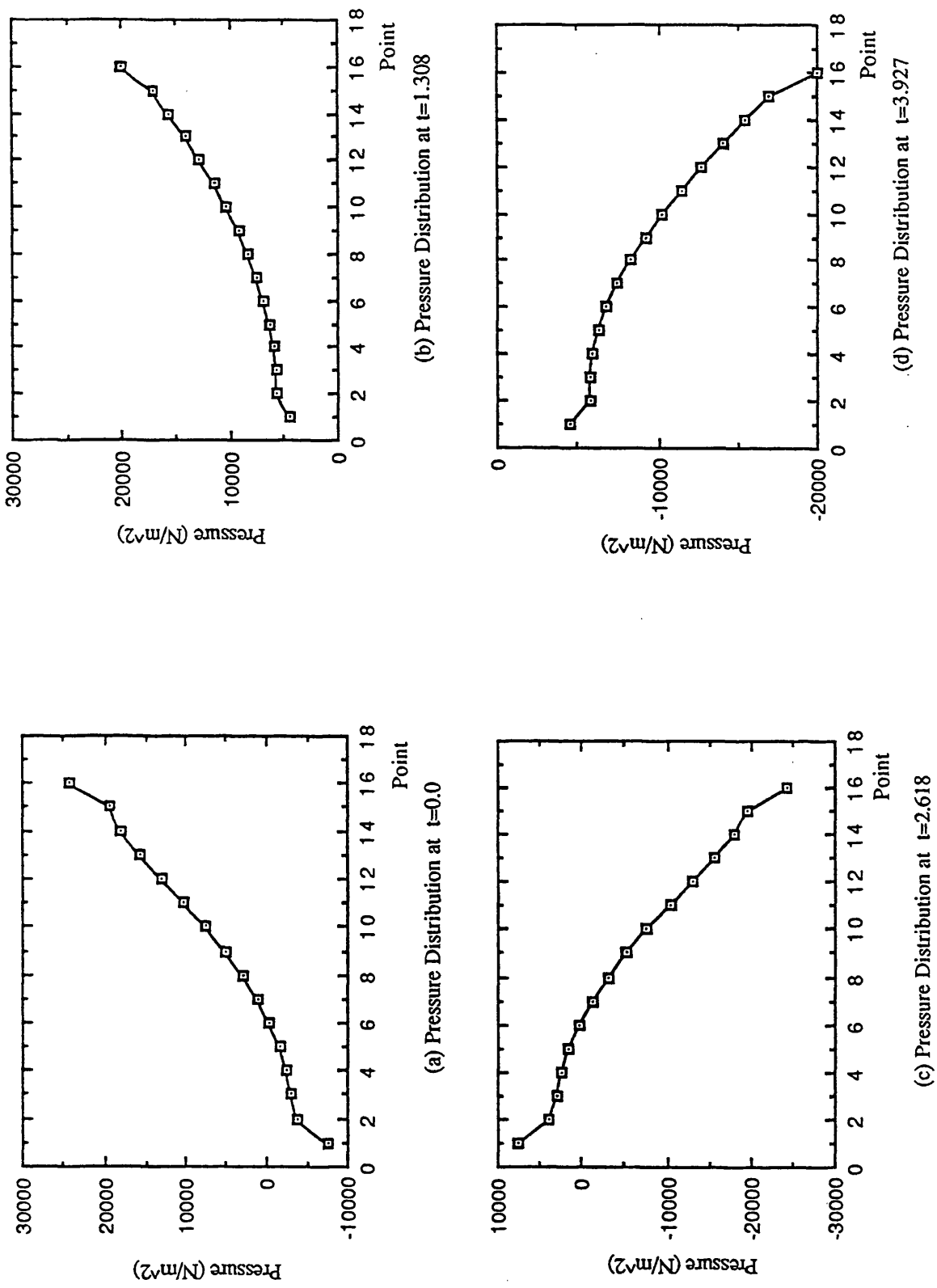


Fig. 3.23 Instantaneous pressure distributions at X=5.65 meters

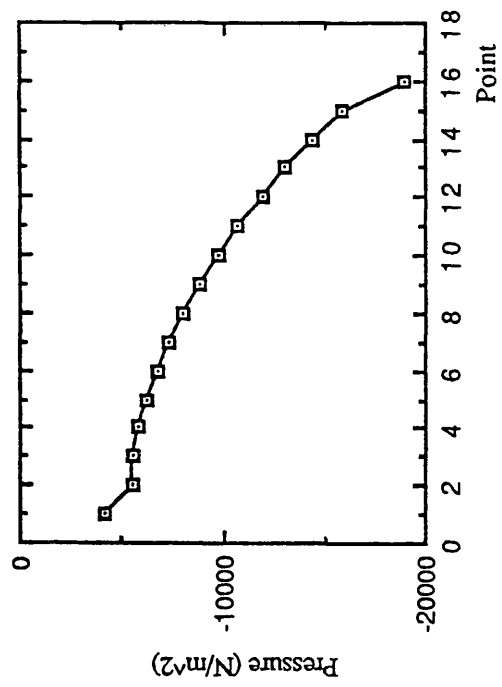
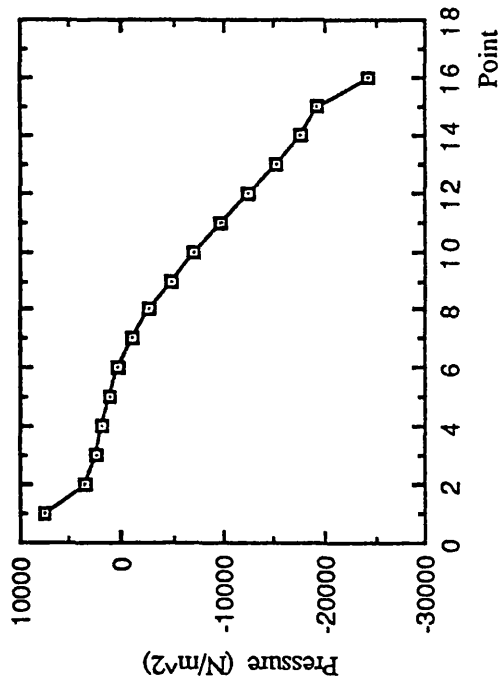
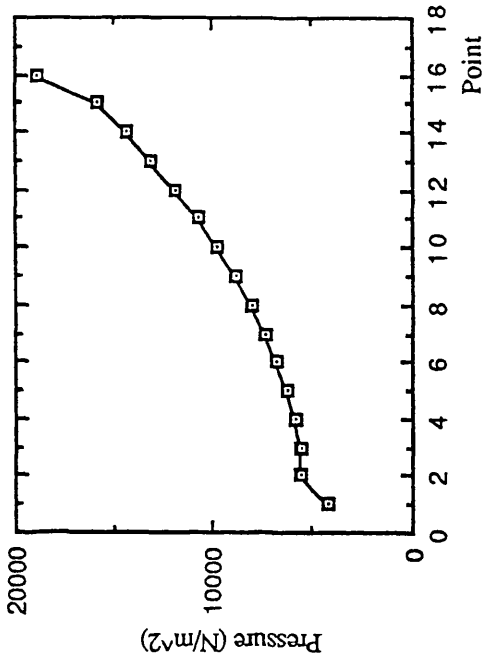
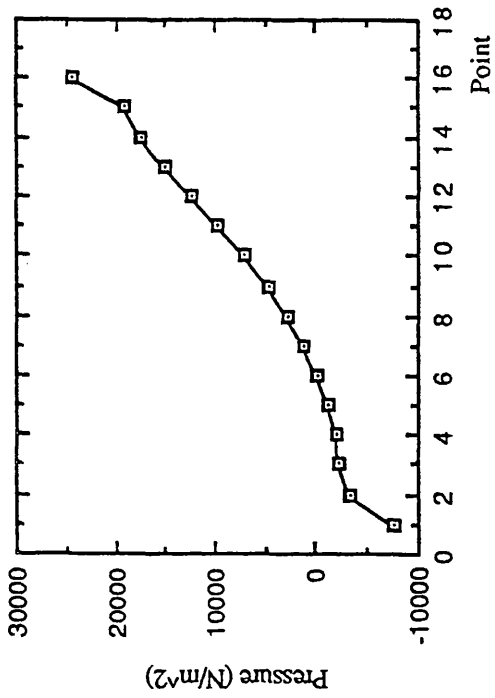
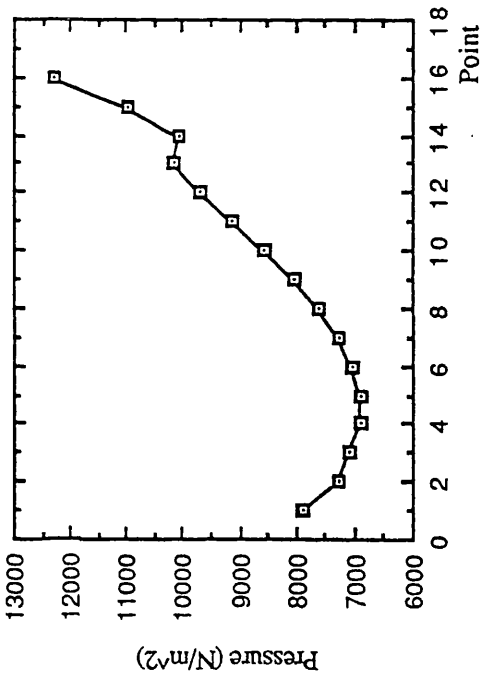
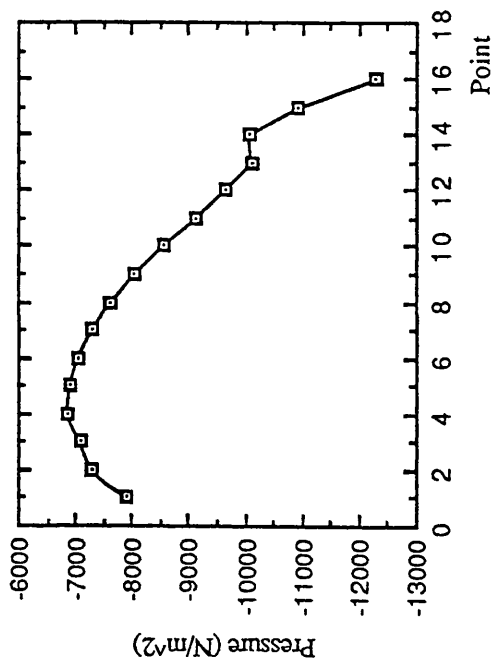


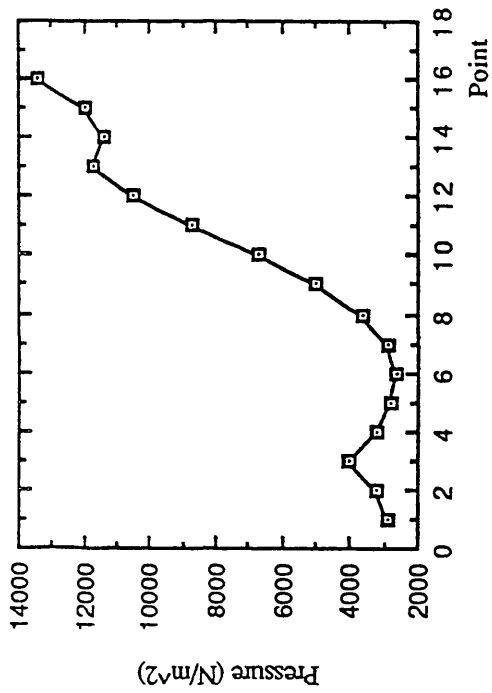
Fig. 3.24 Instantaneous pressure distributions at $X=8.15$ meters



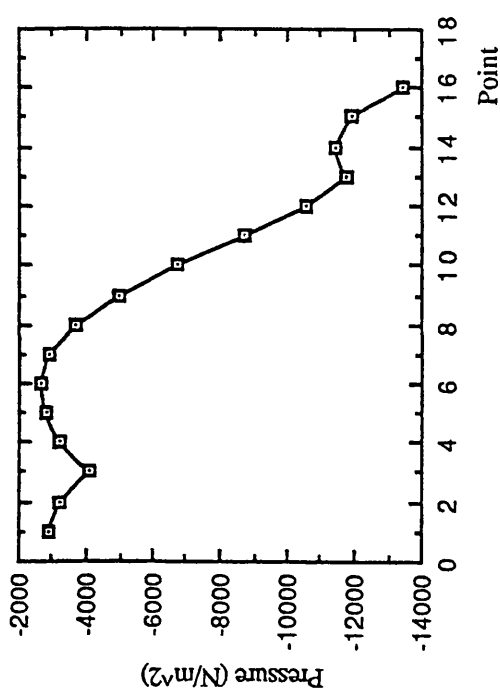
(b) Pressure Distribution at $t=1.308$



(d) Pressure Distribution at $t=2.618$

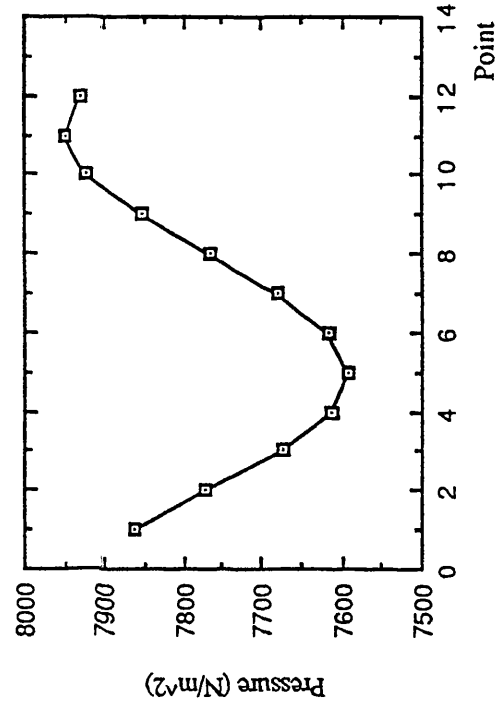


(a) Pressure Distribution at $t=0.0$

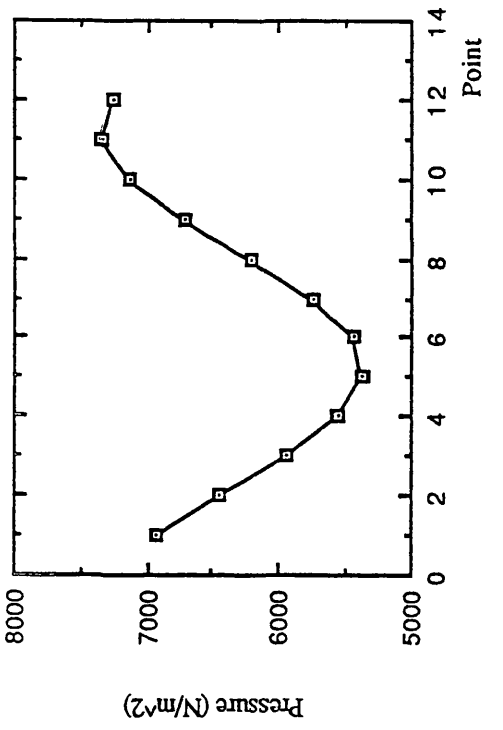


(c) Pressure Distribution at $t=2.618$

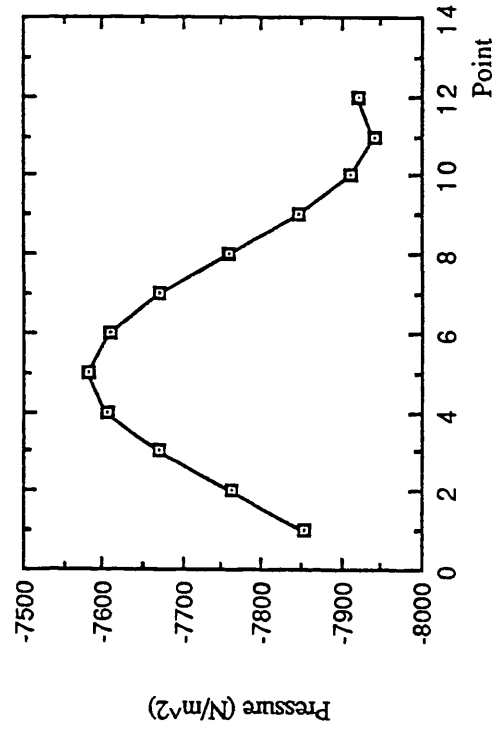
Fig. 3.25 Instantaneous pressure distributions at $X=12.75$ meters



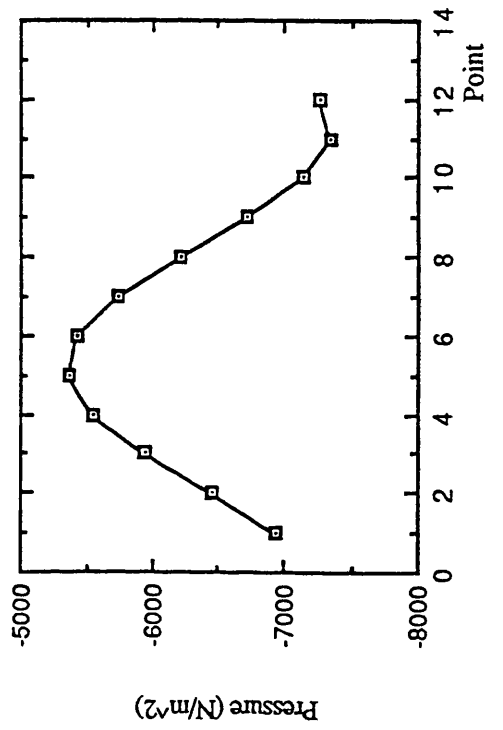
(a) Pressure Distribution at $t=0.0$



(b) Pressure Distribution at $t=1.308$



(c) Pressure Distribution at $t=2.618$



(d) Pressure Distribution at $t=3.927$

Fig. 3.26 Instantaneous pressure distributions at $X=14.65$ meters

CHAPTER 4 ULTIMATE STRENGTH AND RELIABILITY

ANALYSIS OF STIFFENED PLATES

4.1 INTRODUCTION

Stiffened plates are common structural units in bridges, ships and offshore structures. Although research into stiffened plates started back in the last century, a large number of notable theoretical and numerical studies have been carried out since 1970.

Shown in Fig. 4.1 is a typical stiffened plate which consists of plate and longitudinal stiffeners as well as strong transverse stiffeners (girders).

The failure modes of a stiffened plate in compression are:

- 1) plate failure
- 2) stiffener-plate column failure; it can be divided into two modes
 - a) plate_induced failure
 - b) stiffener_induced failure
- 3) torsional failure of the stiffener
- 4) overall grillage buckling.

The plate failure may occur before or after the failure of column-like failure, which affects the stiffness and the effective width of the plating associated with the stiffener. Failure modes 3 and 4 should be avoided due to the quick loss of strength in the post-buckling region. To prevent torsional buckling, the ratio of the web height to thickness is generally kept being less than 10. Overall grillage buckling is usually avoided by provision of stiff transverse frames and support from minor bulkheads and pillars.

Since the behaviour of the plating strongly influences the performance of stiffened plates, the features of the plating will be studied first in the following section.

A vast amount of research has been carried out since 1970. The state-of-the-art in this field was well summarised by Faulkner (1975b) and Guedes Soares and Soreide (1983). Since then, some new formulae have been published. Unfortunately

all these formulae were calibrated separately and it is difficult to compare these works. Therefore it is necessary to calibrate the strength formulae on the same database because the uncertainty in strength formulation is important in structural reliability analysis. In addition, with the increasing understanding of plate panels, it is possible to incorporate the recent research results in plating into the formulation of stiffened plates.

Probabilistic methods are increasingly being used in the analysis of plating and stiffened plates. But all the analysis were carried out usually by Advanced First Order Second Moment method without investigating its accuracy of results. With the development of reliability techniques, the Second Order Method (SORM) is not so time-consuming as before. It was recommended that in practice the accuracy of the AFOSM and SORM needs to be checked for a particular problem first, and then one can decide whether or not the SORM should be used.

In this chapter the existing formulae for prediction of ultimate strength of plate panels and stiffened plates under compression are calibrated by using a large amount of experimental and numerical data. A new formula for stiffened plates is proposed. Secondly, the reliability analysis of plate panels and stiffened plates is carried out by using AFOSM, SORM and Monte Carlo simulation to investigate the accuracy of the methods.

4.2 BEHAVIOUR OF UNSTIFFENED PLATES

Plate elements are the main parts in stiffened panels. Because the global failure of the stiffened panels is usually avoided by design, the interframe failure of the plate stiffener assembly or failure of the plate elements between stiffeners are main failure modes. The prediction of plate strength is also a prerequisite for assessing the strength of stiffened plates.

4.2.1 The Parameters which Influence the Strength

The parameters which influence the strength of plates are plate slenderness, residual stress, initial distortion, boundary condition, plate aspect ratio and types of loads.

1) Influence of plate slenderness

Plate slenderness is the most important factor, which is the non-dimensional variable that results from the Bryan expression for critical buckling load σ_c of an infinitely long thin, elastic plate with simply supported edges.

$$\frac{\sigma_c}{\sigma_0} = \frac{4\pi^2 E}{12(1-\nu^2)\sigma_0} \left(\frac{t}{b}\right)^2 = \frac{3.61}{\beta^2} \quad (4.1)$$

In ship plates β can vary from 1 to 5 with the corresponding value of plate strength changing from yield strength to 40% of its value. So the plate strength can change by as much as 60% over the useful range of slenderness.

2) Influence of distortion and residual stress

Stiffeners are usually connected to the plate by welding. This action results in the distortion and residual stress, which are called initial imperfections.

A widely used residual stresses distribution is shown in Fig. 4.2. To obtain equilibrium in the plate, the residual stress is expressed as:

$$\frac{\sigma_r}{\sigma_0} = \frac{2\eta}{b/t - 2\eta} \quad (4.2)$$

A typical initial deflection profile is shown in Fig. 4.3. The initial deflection gives rise to a decrease in the rigidity and ultimate strength of plates. It is found that the same deflection shape as the buckling mode has the most significant weakening effect.

In some cases the local deformation in plates is likely to have a much more significant influence in compressive strength than the overall distortion, even if its amplitude is smaller than overall deflection (Dow and Smith, 1984; Smith, 1981).

Through a large number of experiments on frigates, Faulkner (1975) suggested that the mean value of plate central deflection can be calculated by:

$$\frac{\delta_0}{t} = 0.12\beta^2 \left(\frac{t_w}{t}\right) \quad \text{for } t_w \leq t, \beta \leq 3 \quad (4.3a)$$

$$\frac{\delta_0}{t} = 0.15\beta^2 \left(\frac{t_w}{t} \right) \quad \text{for } t_w \leq t, \beta > 3 \quad (4.3b)$$

$$\frac{\delta_0}{t} = K\beta^2 \left(\frac{t_w}{t} \right) \quad \text{for } t_w > t \quad (4.3c)$$

where $K=0.12$ for frigates and 0.15 for merchant ships.

Carlsen (1977) pointed out the initial deflection in most cases meets:

$$\frac{\delta_0}{t} \leq \frac{1}{200} \frac{b}{t} \quad (4.4)$$

Based on the experimental measurements, Smith and Davidson et al (1987) classified the initial imperfection as slight, average and severe, which is shown in Table 4.1.

Table 4.1: Assumed imperfection levels

Level	Initial deflection δ'_0	Residual stresses σ'_r
Slight	$0.025\beta^2$	0.05
Average	$0.1\beta^2$	0.15
Severe	$0.3\beta^2$	0.3

It is shown that in the practical range of plate slenderness the reduction of plate strength due to the presence of distortions or of residual stress can be as much as 20% to 23% of the perfect plate strength. If both types of imperfections exist simultaneously, it leads to up to 50% reduction of plate strength. It is worth mentioning that the effect of both imperfections is not equal to the sum of the effect of each imperfection considered separately.

3) Influence of boundary condition

The boundary conditions for loaded edges are classified into two extreme situations: simple supports and clamped supports. Other conditions can be treated in

between them. For unloaded edges, the conditions are grouped into three : constrained, restrained, and unrestrained. In the first two cases the edges are forced to remain straight, which does not happen in the unrestrained case. For restrained conditions no displacements are allowed in the transverse direction as opposed to the other two situations.

Boundary condition is another relatively important factor. As shown by Guedes Soares (1988b), the ratio of the strength of clamped plates ϕ_c to the strength of the corresponding simply supported ones ϕ_s has the mean value of 1.09 with a standard deviation of 0.08. A good regression was obtained relative to the slenderness.

$$\frac{\phi_c}{\phi_s} = 0.82 + 0.14\beta \quad (4.5)$$

with a correlation coefficient of 0.85. It shows that when the β varies from 2.5-3.5, the strength of clamped plates is 15% to 30% higher than simply supported ones.

The effect of the unloaded edges is shown in Fig. 4.4. It shows that in-plane restraint has a strengthening effect of 5 to 10%, depending on plate slenderness and magnitude of initial imperfections.

4) Influence of the aspect ratio

Plate aspect ratio also needs to be considered. The strength of plates is not very sensitive to the changes of aspect ratio. Typically the plate strength changes by 5% as the aspect ratio varies from 0.6 to 1.0. But the aspect ratio of the plate becomes important when dealing with the shape of initial imperfections.

As shown in Fig. 4.5, the minimum buckling load occurs between 0.7 and 0.8 of aspect ratio. In the situation that the aspect ratio is greater than one, the plates tend to be stiffer and stronger but have a steeper post-collapse unloading as shown in Fig. 4.6.

5) Influence of combined loading

Generally the loads which should be considered in the design are longitudinal compression, transverse in-plane compression, shear, bending moment and lateral loading.

Although the effect of the combined loading can be reasonably predicted by numerical methods, the formulae for design still need to be improved further.

Effect of biaxial compression

Based on the experimental results of Becker et al (1970), a parabolic interaction relationship was proposed as follows (Faulkner et al, 1973):

$$\frac{\sigma_x}{\sigma_{xu}} + \left(\frac{\sigma_y}{\sigma_{yu}} \right)^2 = 1 \quad (4.6)$$

where

$$\sigma_{yu} = \sigma_0 \left[\frac{0.9}{\beta^2} + \frac{1.9}{\alpha\beta} \left(1 - \frac{0.9}{\beta^2} \right) \right], \quad \beta \geq 1, \quad \alpha\beta \geq 1.9 \quad (4.7)$$

taken from the French Bureau Veritas solution for a pinned plate.

The load-capacity is considered to be reached when the stress field at any edge satisfies the plasticity condition:

$$\sigma_{cy}^2 = \sigma_x^2 + \sigma_y^2 - \sigma_x \sigma_y \quad (4.8)$$

On this principle, Becker and Colao (1977) proposed an interaction curve

$$R_x^2 + R_y^2 - R_x R_y = 1 \quad (4.9)$$

in which:

$$R_x = \frac{\sigma_x}{\sigma_{xu}}, \quad R_y = \frac{\sigma_y}{\sigma_{yu}} \quad (4.10)$$

A more general interaction relation is recommended by Davidson et al (1989)

$$R_x^2 + \eta R_x R_y + R_y^2 = 1 \quad (4.11)$$

where η is defined to vary with plate slenderness from -1 (the von Mises ellipse) at plate slenderness 0.5 to -1 at plate slenderness 3.3.

Bradfield et al (1993) have recently presented a group of experimental data. Having compared the existing interaction curves with their experimental data, they suggested that a two-segments interaction relation may be better than a single one. At the moment Davidson's method is preferable.

Effect of lateral load

The lateral load will cause a deflection of cylindrical shape with dimensions equal to the plate side. So the effect of lateral load could be in either direction. For square plate, it weakens the strength because the caused deflection has the same shape as the dominant buckling mode, for rectangular, its effect is adverse.

For the large lateral load, 12% reduction in strength was found when the hydrostatic pressure is up to 190 m water column (Carlsen, 1977).

Smith et al (1991) utilised finite element models to investigate the influence of lateral load. The effect of lateral load is shown in Fig. 4.7. It can be seen that its effect is remarkable in panels with high column slenderness and plate slenderness.

When the lateral pressure is above a critical load, a linear interaction curve was assumed by Faulkner et al (1973) as follows:

$$\frac{\sigma_{c(p,y)}}{\sigma_{c(y)c}} + \frac{q_x}{q_{xp}} = 1 \quad (4.12)$$

and the fix-ended boundary condition should be used in this region.

4.2.2 Available Strength Formulae

Post buckling behaviour of plates loaded in compression has been studied in great detail. Many design methods using empirical solutions are now available. A good review can be found in Faulkner (1975b). Since then, several new methods have been published. Vilnay and Rockey (1981) proposed a generalised effective width formula based on the numerical results of Frieze et al (1976). A good agreement with Frieze's results was found. Rhodes (1981) employed a simple method to generate the load-shortening curve of plate loaded in compression. Although there is good agreement with some numerical methods for perfect plates, the results for imperfect plates, especially when initial deflection is over 30% of plate thickness, are not so satisfactory. Adopting the same idea as Vilnay, Bonello et al (1991) presented a strength modelling for unstiffened plates in which two characteristic points in load-shortening curves were defined. Because two parameters (b'_{ec} and b'_{eb}) in the procedure are still obtained from two groups of curves derived from numerical load-shortening curves, this method seems to be unsuitable for design. Guedes Soares (1988b) developed a formula, in which the initial deflection and residual stress could be explicitly considered, based on the existing experimental and numerical data. Chapman and Dowling associates (1991) derived an empirical formula for plating.

Because the main purpose of Rhodes and Bonello's methods is to establish the post-buckling curves, they are not suitable for design. The discussion will therefore be focused on other methods.

4.2.2.1 Faulkner's method

The strength of a welded rectangular plate is given by:

$$\phi_F = \frac{\sigma_m}{\sigma_0} = \phi_b - \Delta\phi_b \quad (4.13)$$

$$\Delta\phi_b = \frac{\sigma_r E_t}{\sigma_0 E} \quad (4.14)$$

where σ_m and σ_0 are the plate compressive strength and the yield stress respectively, ϕ_b is the strength of an unwelded plate, and $\Delta\phi_b$ represents the reduction of strength due to the weld induced residual stress.

$$\phi_b = \frac{a_1}{\beta} - \frac{a_2}{\beta^2} \quad \text{for } \beta \geq 1.0 \quad (4.15)$$

where

$$\beta = \frac{b}{t} \sqrt{\frac{\sigma_0}{E}} \quad \text{---the plate slenderness;}$$

E ---Young's modulus

the constants are:

$$a_1=2.0 \quad \text{and} \quad a_2=1.0 \quad \text{for simply supports} \quad (4.15a)$$

$$a_1=2.5 \quad \text{and} \quad a_2=1.56 \quad \text{for clamped supports} \quad (4.15b)$$

The residual stress σ_r can be obtained by:

$$\frac{\sigma_r}{\sigma_0} = \frac{2\eta}{(b/t) - 2\eta} \quad (4.16)$$

$$\frac{E_t}{E} = \left(\frac{a_3\beta^2}{a_4 + p_r(1-p_r)\beta^4} \right)^2 \quad \text{for } 0 \leq \beta \leq 1.9 / \sqrt{p_r} \quad (4.17a)$$

$$\frac{E_t}{E} = 1.0 \quad \text{for } \beta \geq 1.9 / \sqrt{p_r} \quad (4.17b)$$

In which

$$p_r = \frac{\sigma_p - \sigma_r}{\sigma_0} \quad (4.18)$$

σ_p --- proportional limit stress

Faulkner (1975a) advised that the p_r is generally adopted 0.5.

The constants a_3 and a_4 depend on the boundary conditions

$a_3=3.62$ $a_4=13.1$ for simple supports

$a_3=6.31$ $a_4=39.8$ for clamped supports

Faulkner's method does not account explicitly for the level of initial imperfection.

4.2.2.2 Carlsen's method

His method is expressed as:

$$\phi_{ca} = \phi_b \left(\frac{1}{1 + \sigma_r / \sigma_0} \right) \left(1 - \frac{0.75\delta'_0}{\beta} \right) \quad (4.19)$$

where

$\frac{\sigma_r}{\sigma_0}$ is given by Eq. (4.16), ϕ_b is given by Eq. (4.15), but the constants in which are:

$a_1=2.1$ $a_2=0.9$ for simple supports

$$\delta'_0 = \frac{\delta_0}{t}$$

δ_0 ---the maximum amplitude of distortions.

In this method the plate slenderness, residual stress and initial imperfection are explicitly accounted for.

4.2.2.3 Guedes Soares' method

The method presented by Guedes Soares is based on a refined Faulkner's method and has two forms. One is:

$$\phi_G = [1.08\phi_b] \left[1.07 - 0.99 \frac{\Delta\phi_b}{\phi_b} \right] \left[1 - (0.626 - 0.121\beta) \frac{\delta_0}{t} \right] \left[0.76 + 0.01\eta + 0.24 \frac{\delta_0}{t} + 0.1\beta \right] \quad \text{for } \beta > 1.0 \quad (4.20)$$

The other form is:

$$\phi_G = [1.08\phi_b] \left[\left(1 - \frac{\Delta\phi_b}{1.08\phi_b} \right) (1 + 0.0078\eta) \right] \left[1 - (0.626 - 0.121\beta) \frac{\delta_0}{t} \right] \left[0.665 + 0.006\eta + 0.36 \frac{\delta_0}{t} + 0.14\beta \right] \quad \text{for } \beta > 1.0 \quad (4.21)$$

The method can account explicitly for β , η and δ_0 . The terms in the first bracket predict the strength of perfect plates, the first and second bracket predict the strength of plates with residual stress, the first and third bracket indicate the strength of plates with initial deflections and the fourth term should be used for plates that have both initial deflections and residual stress.

The ϕ_b and $\Delta\phi_b$ are calculated by Eq. (4.15) and (4.14) respectively.

Strictly speaking, these equations should only be applicable to simply supported plates. However, when using the coefficient in Eq. (4.15b) to quantify ϕ_b , they can also be applicable to the clamped plates.

The disadvantage of the method is that it estimates the maximum strength, ignoring the strain at which the maximum value occurs, which is very important for the case with sharp load shortening curves.

4.2.2.4 Vilnay's method

Vilnay and Rockey (1981) designed a procedure to generate the generalised effective width by using the load-shortening curves from well controlled numerical analysis. This method can theoretically calculate the effective width at any strain.

When there are no residual stresses, the maximum effective width occurs at the strain equal to 1.0. It is expressed as:

$$\frac{b_{em}}{b} = B_0(1.75 - 0.5\beta) + 0.262\beta - 0.4 \quad (4.22)$$

where

$$B_0 = 0.3625\delta'_0 + 0.9425 \quad \text{when } \delta'_0 < 0.7 \quad (4.23a)$$

$$B_0 = 0.2\delta'_0 + 0.83 \quad \text{when } \delta'_0 > 0.7 \quad (4.23b)$$

and the effective width at strain equal to zero is:

$$\frac{b_{e0}}{b} = 1.063 - 0.533\delta'_0 \quad \text{when } \delta'_0 < 0.4 \quad (4.23a)$$

$$\frac{b_{e0}}{b} = 0.943 - 0.233\delta'_0 \quad \text{when } \delta'_0 > 0.4 \quad (4.23b)$$

subject to limit that $\frac{b_{e0}}{b}$ is not great than 1.0.

The effective width at large strain is:

$$\frac{b_{e\infty}}{b} = 0.72 - 0.06\beta$$

When residual stresses exist, the effective widths at different strains are presented as follows:

The effective width at strain equal to zero is:

$$\frac{b_{e0R}}{b} = \frac{b_{e0}}{b} - 2 \left(\frac{b_{e0}}{b} - \frac{b_{em}}{b} \right) \sigma'_r \quad (4.25)$$

and at strain equal to 1.0 is:

$$\frac{b_{emR}}{b} = \frac{b_{em}}{b} - \left(\frac{b_{e0}}{b} - \frac{b_{em}}{b} \right) (6.075\beta^2 - 28.957\beta + 36.067) \sigma'_r \quad (4.26)$$

and the effective width at strain equal to 2.0 is:

$$\frac{b_{e2R}}{b} = \frac{b_{e\infty}}{b} + \left(\frac{b_{em}}{b} - \frac{b_{e\infty}}{b} \right) \exp(-k) \quad (4.27)$$

where

$$k = 0.8\beta - 0.5$$

The maximum effective width is determined by comparing the values at strain equal to 1.0 and 2.0.

4.2.2.5 Imperial College's method

Chapman et al (1991) presented a strength formula which consists of two parts. The first part is used to calculate the strength of simply supported constrained panels with sinusoidal imperfections of amplitude of $\delta'_0 = 0.1\beta^2$ and compressive residual stresses of 20% of yield stress (based on a yield stress of 245 N/mm², and Young's Modulus of 205000 N/mm²). It is expressed as:

$$\sigma'_{xu} = \frac{\sigma_{xu}}{\sigma_0} = 0.23 + \frac{1.16}{\beta} - \frac{0.48}{\beta^2} + \frac{0.09}{\beta^3} \quad (4.28)$$

The second part aims to get a modification factor which takes into account the effect of the imperfection and residual stresses other than those assumed in the above equation. The average non-dimensional uniaxial compressive stress in a constrained panel buckling in a square plate mode is:

$$\bar{\sigma}_x = \frac{k}{1+k} \frac{4\pi^2 E}{12(1-\nu^2)} \left(\frac{t}{b}\right)^2 \frac{1}{\sigma_0} + \frac{\pi^2 E}{8\sigma_0} \left(\frac{\delta_0}{b}\right)^2 (k^2 + 2k) \quad (4.29)$$

and the non-dimensional stress at the longitudinal edges of the panel is given by:

$$\sigma'_{xe} = \bar{\sigma}_x + \frac{\pi^2 E}{8\sigma_0} \left(\frac{\delta_0}{b}\right)^2 (k^2 + 2k) \quad (4.30)$$

The effective width is expressed as the ratio of the average stress ($\bar{\sigma}_x$) to the edge stress (σ'_{xe}). For residual stresses greater than 10% of yield, the value of this ratio at twice yield strain is considered to be the maximum value. For the zero residual stresses the ratio is at yield strain. For intermediate levels of residual stress, linear interpolation between the two values is used.

Therefore the modification factor applied to the first part is defined as the ratio of the maximum effective width obtained from the second part for the real initial imperfection (including the deflection and residual stresses) to that for the average initial imperfection assumed in the first part.

The value obtained from the above procedure is for simply supported constrained panels. For unconstrained panels the following expression can be used (Smith et al, 1987):

$$\frac{\text{constrained}}{\text{unconstrained}} = 0.95 + 0.05\beta \quad (4.31)$$

4.2.3 Calibration and Comparison of the Existing Methods

In order to evaluate the existing methods, all the formulae mentioned above are calibrated against the existing experimental and numerical results (Smith et al, 1987; Moxham, 1971; Dwight and Moxham, 1969; Ueda et al, 1975). The results are shown in Tables 4.2-4.6 and Fig. 4.8-4.12.

Table 4.2: Model uncertainty factor of Faulkner's method

Experiments Source	Number of Cases	Minimum Value	Maximum Value	Mean Value	C.O.V
Moxham	56	1.05	1.64	1.22	0.109
Dwight	33	0.93	1.55	1.09	0.155
Ueda	54	0.77	1.65	1.03	0.214
Smith	57	0.996	1.42	1.26	0.084
Total	200	0.77	1.65	1.159	0.163

Table 4.3: Model uncertainty factor of Carlsen's method

Experiments Source	Number of Cases	Minimum Value	Maximum Value	Mean Value	C.O.V
Moxham	56	0.87	1.68	1.15	0.154
Dwight	33	0.83	1.23	1.02	0.101
Ueda	54	0.85	1.28	1.011	0.084
Smith	57	1.06	1.44	1.246	0.06
Total	200	0.829	1.68	1.117	0.138

Table 4.4: Model uncertainty factor of Guede Soares' method

Experiments Source	Number of Cases	Minimum Value	Maximum Value	Mean Value	C.O.V
Moxham	56	0.92	1.33	1.06	0.086
Dwight	33	0.84	1.32	0.99	0.126
Ueda	54	0.77	1.22	0.98	0.091
Smith	57	0.85	1.212	1.073	0.07
Total	200	0.774	1.329	1.031	0.101

Table 4.5: Model uncertainty factor of Vilnay's method

Experiments Source	Number of Cases	Minimum Value	Maximum Value	Mean Value	C.O.V
Moxham	56	0.83	1.23	1.053	0.117
Dwight	33	0.778	1.134	0.989	0.098
Ueda	54	0.62	1.174	0.871	0.188
Smith	57	0.868	1.202	1.047	0.069
Total	200	0.62	1.231	0.99	0.147

Table 4.6: Model uncertainty factor of IC's method

Experiments Source	Number of Cases	Minimum Value	Maximum Value	Mean Value	C.O.V
Moxham	56	0.532	1.02	0.788	0.209
Dwight	33	0.454	1.015	0.794	0.197
Ueda	54	0.469	1.015	0.864	0.132
Smith	57	0.834	1.083	1.015	0.053
Total	200	0.454	1.170	0.893	0.200

From the above Tables and Figures, it is clearly shown that:

- 1) In the whole range Guedes Soares' method is the best. Its mean value is 1.031 and coefficient of variation 10.1%. Its skewness is fairly small [see Fig. 4.10(b)]. The slope of the linear regression line is only -0.042.
- 2) Although IC's method showed very good results compared to Smith's numerical data nevertheless, on the whole, it is not as good as Guede Soares' formula. The method presents very good accuracy for plates with moderate initial deflection and residual stresses. But when initial deformation is equal to zero, its accuracy is questionable. From Eqs. (4.27) and (4.28) it is shown that, when the initial distortion is equal to zero, the average compressive stress is always equal to the edge stress. This means that b_e is equal to 1.0, which leads to an unacceptable modification factor defined in the procedure. In addition, the method showed very large skewness [see Fig. 4.12(b)].
- 3) Vilnay's method [Fig. 4.11(b)] shows almost no skewness, and its mean value is the closest to one (0.990) among all the methods. But its coefficient of variation (0.147) almost reaches the margins (0.150) recommended by Faulkner (1991). From Fig. 4.11 (b) it can be seen that a few of the points lie far away from the unit (say, below 0.75).

4.3 BEHAVIOUR OF STIFFENED PLATES

Due to the interaction of different failure modes, the situation for stiffened plates is much more complicated than for plate panels. As pointed out in the section 4.1, if the failure modes 3 and 4 are excluded by properly selecting the dimensions of the stiffened plates, the behaviour of the stiffened plates can be represented by assemblage of the stiffener and its associated plate with effective width. In this way the problem is simplified.

The behaviour of the column assemblage can now be exactly (in numerical sense) analysed by numerical methods (finite difference or finite element). Some researchers (Chalmers and Smith, 1992; Smith et al, 1991) advocated that the numerical methods could be directly used in design in the way that the whole load shortening curves are generated and stored in the computer in advance, then the ultimate strength of a stiffened plate can be obtained by interpolation from the stored data. Furthermore, the numerical method was directly used to establish the safety margin equation in reliability analysis (Bonello and Chryssanthopoulos, 1993b).

Although it is likely that the numerical analysis could be directly used in design in the near future, nevertheless, the relatively simple analytical formulations are still preferable in the design at present. So discussions will focus on these simple formulae.

4.3.1 Parameters influencing the strength

The parameters might be classified as geometrical and imperfection parameters. The main geometrical parameters which influence the strength are as follows:

Geometrical parameters

- a) stiffener slenderness λ
- b) plate slenderness β
- c) ratio of stiffener to cross-sectional area A_s / A_t
- d) ratio of top flange to web area A_f / A_w
- e) cross-sectional slenderness of the stiffener

Imperfection parameters

- f) initial stiffener deflection δ_{0s}
- g) relative stiffener deflection $\delta_{0s1} / \delta_{0s2}$
- h) initial plate deflection δ_0
- i) compressive plate welding stresses σ_{rp}
- j) axial welding stresses in the stiffener σ_{rs}
- k) yield stress

1) Slenderness of plate and stiffener

These are the most important parameters which influence the strength of the stiffened plates. Their effects are shown in Figs. 4.13, 4.14, 4.15. For low stiffener slenderness, failure is attributed to plastic crushing of the cross-section while, for high slenderness, failure with rapid load relaxation occurred beyond initial compressive yielding at the top of the stiffener. Rapid increase of stress on top of the stiffener occurs when the stiffness is reduced due to loss of plate stiffness, i.e. plate buckling. Such interaction is considerable for low stiffener slenderness, 0.3-0.5. For high stiffener slenderness 1.5, the magnification of the stiffener stresses is primarily due to general column instability (σ_m / σ_0 just reaches 0.5).

Smith et al (1991) suggested that the stiffener slenderness used in the structures is better to be less than 0.4 due to a sharply peaked form of load-shortening curves when λ is great than 0.6, and plate slenderness is less than 1.5 in order to reduce the sensitivity to the variation of some parameters. Such restriction will result in a cost and structural weight penalty.

2) Ratio of stiffener to cross-sectional area

The effect of this factor is shown in Fig. 4.16. Its influence on strength is remarkable at the low stiffener slenderness and high plate slenderness reaching 40% in some cases, but is small in most cases. A value of $A_s / A_t = 0.2$ is typical of ship construction.

3) Ratio of top flange to web cross-sectional area

The effect is shown in Table 4.7. The increase of the ratio does not mean an increase in the strength. The effect is quite small.

Table 4.7: Strength of stiffened panels (Carlsen, 1980)

Geometry				Strength, σ_y/σ_0				Notes
				Modified Perry-Robertson (P-R)		Numerical	$\frac{\sigma_{P-R}}{\sigma_{Num}}$	
$\bar{\lambda}$	b/t_p	A_t/A_p	A_t/A_w	PI	SI			
0.3	30	0.3	0.8	0.931	0.897	0.872	1.029	
0.5	30	0.3	0.8	0.913	0.826	0.807	1.024	
1.0	30	0.3	0.8	0.740	0.571	0.575	0.993	
1.5	30	0.3	0.8	0.397	0.335	0.325	1.031	
0.3	55	0.3	0.8	0.663	0.827	0.667	0.994	
0.5	55	0.3	0.8	0.644	0.762	0.618	1.042	
1.0	55	0.3	0.8	0.506	0.527	0.473	1.070	Basic cases T-profile
1.5	55	0.3	0.8	0.291	0.309	0.303	0.960	
0.3	80	0.3	0.8	0.512	0.758	0.540	0.948	
0.5	80	0.3	0.8	0.494	0.698	0.516	0.957	
1.0	80	0.3	0.8	0.385	0.483	0.393	0.980	
1.5	80	0.3	0.8	0.230	0.283	0.264	0.871	
0.3	30	0.125	0.8	0.938	0.858	0.889	0.965	Reduced A_t/A_p ratio
1.0	30	0.125	0.8	0.776	0.509	0.523	0.973	
1.5	30	0.125	0.8	0.405	0.305	0.318	0.959	
0.3	80	0.048	0.8	0.489	0.645	0.536	0.912	
1.0	80	0.048	0.8	0.402	0.349	0.335	1.042	
1.5	80	0.048	0.8	0.216	0.214	0.238	0.899	
0.3	55	0.3	0	0.670	0.802	0.710	0.944	$A_t/A_w =$
1.0	55	0.3	0	0.514	0.484	0.463	1.045	Flat bar

Imperfections: plate, $\sigma_{rp}/\sigma_0 = 0.2$, $w_{op} = 0.01b$
 Stiffener, $\sigma_{rs}/\sigma_0 = 0$, $w_{os} = 0.0015a$
 Yield stress, $\sigma_0 = 320 \text{ N/mm}^2$

4). Initial stiffener deflection

The effect of the parameter is shown in Fig. 4.17. The strength decreases with the increase of the initial stiffener deflection. Such effect is small when $\lambda=0.3$, but obvious when $\lambda=1.0$ and 1.5 . Up to 26% strength reduction was found at $\lambda=1.5$ and $b/t=55$ (Rhodes, 1981).

5) Relative stiffener deflection $\delta_{0s1} / \delta_{0s2}$.

The definitions of δ_{0s1} and δ_{0s2} are shown in Fig. 4.18. This parameter is used to measure the interaction between adjacent stiffeners. The ratio $\delta_{0s1} / \delta_{0s2}$ was found to have a mean value of 0.25. Its effect on compressive strength is shown in Fig. 4.19. Such effect is high when the structure is slender. When stiffener slenderness is less than 0.4, the effect is relatively small. The severest effect occurs at $\delta_{0s1} / \delta_{0s2} = -1$.

6) Initial plate deflection

The effect of the initial plate deflection is primarily reflected by reducing the maximum strength of the plate, further the effective width associated with the stiffener. Its effect is shown in Fig. 4.20. The strength reduces 5-10% when the plate distortion increases from $0.005b$ to $0.015b$, the smaller percentage reduction for slender structures, i.e. for high values of λ and β .

7) Compressive residual stresses in plating

The primary influence of the plate welding stresses is to reduce the axial stiffness of the plates and the effective width associated with the stiffener. The effect of plate welding stress is shown in Figs. 4.21 and 4.22.

For the cases with low plate slenderness, the effect of increasing the welding stresses beyond $(0.1-0.2) \sigma_0$ is negligible, while the strength continues to drop for increasing residual stresses in the cases with slender plates.

For slender plates, residual stresses reduce the stiffness of the plate even for low compression, causing magnification of the bending stresses, while for stocky plates, reduced stiffness occurs only for high compression. In the case with a slender stiffener, $\lambda=1.0$, and stocky plate, $b/t=30$, the plate residual stresses did not influence the strength at all because stiffener-induced failure occurred before the plate reached its buckling compression.

8) Residual stresses in the stiffener

Residual stresses in the stiffener are difficult to determine due to their randomness nature. Both compression and tension may occur in the top of the stiffener. There are three types of assumed residual stress distributions shown in Fig. 4.23.

Assuming constant compressive welding stress in the web, a 3 to 5% of yield stress reduction in the strength was obtained (Carlsen, 1980) when the $\sigma_{rs} / \sigma_0=0.1$.

9) Yield stress

Yield stress has little effect on the non-dimensional compressive strength, shown in Fig. 4.24.

Two important issues involved in the selection of different parameters in the design formula should be considered.

a) Determine the effective width for the stiffened plate

Although there are some good formulae to determine the effective width in maximum compression of the plate, few formulae can be used to calculate the effective width when the compression is below the maximum compression. Unfortunately, for plates with moderate residual stress, the maximum strength is reached for in-plane compression when $\varepsilon / \varepsilon_0=1.5-2.0$ while, except for very stocky stiffeners, the stiffener itself will collapse by compressive yielding on top of the stiffener before the plate has reached its maximum load. Therefore, from a theoretical point of view, the effective width should be determined by iterative equilibrium analysis or incremental analysis.

b) Interaction between adjacent stiffener span

The primary interaction effect between adjacent stiffener spans is due to the plate flange buckling, causing a larger reduction in out-of-plane stiffness for the stiffener element deflection away from the plate flange than for the adjacent elements deflecting in the opposite direction. The former element will thereby cause deteriorating end moments on the stiffener-induced elements and is itself somewhat restrained by the end moments.

The increased out-of-plane deflection magnification due to plate buckling may be considered as the result of:

- i) reduced effective Euler stress giving larger magnification factor;
- ii) eccentricity of end loads due to larger buckling induced shift of neutral axis at the midspan than at the ends;
- iii) restraining end moment due to smaller lateral deflection in the SI span.

The eccentricity effect could be treated as a modified initial stiffener deflection.

4.3.2 Existing Methods

Guedes Soares and Soreide (1983) has comprehensively studied all the existing methods. From their study, it was concluded that Faulkner's method gives better prediction. Since then, two methods have been presented by Gordo and Guedes Soares (1993) and Chapman et al (1991). Because the main purpose of Gordo's method was to derive approximate load-shortening curves of stiffened plates, it is not discussed here.

In addition, Faulkner's formulae are extended by incorporating the recent research results in plate panels. It is called the 'proposed method' later.

4.3.2.1 Faulkner's formula

This method is based on that of Johnson-Ostenfeld's formula. The ultimate strength is expressed as:

$$\phi = \frac{\sigma_u}{\sigma_0} = \frac{\sigma_e}{\sigma_0} \left[\frac{A_s + b_e \times t}{A_s + b \times t} \right] \quad (4.32)$$

where

$$\frac{\sigma_e}{\sigma_0} = 1 - \frac{1}{4} \frac{\sigma_0}{\sigma_E} \quad \sigma_E \geq 0.5\sigma_0 \quad (4.33a)$$

$$\frac{\sigma_e}{\sigma_0} = \frac{\sigma_E}{\sigma_0} \quad \sigma_E \leq 0.5\sigma_0 \quad (4.33b)$$

where

$$\sigma_E = \frac{\pi^2 \times E \times r_{ce}^2}{a^2}$$

$$r_{ce}^2 = \frac{I'_e}{A_s + b_e \times t} \quad (4.34)$$

and EI'_e is the buckling flexural rigidity of the stiffener. The tangent effective width of the plate (b'_e) is given by:

$$\frac{b'_e}{b} = \begin{cases} \frac{1}{\beta_e} \times R_r & \beta_e \geq 1 \\ R_r & 0 \leq \beta_e \leq 1 \end{cases} \quad (4.35)$$

The effective width of the plate is related to the slenderness as follows:

$$\frac{b_e}{b} = \begin{cases} \left[\frac{2}{\beta_e} - \frac{1}{\beta_e^2} \right] \times R_r & \beta_e \geq 1 \\ R_r & 0 \leq \beta_e \leq 1 \end{cases} \quad (4.36)$$

where

$$\beta_e = \frac{b}{t} \sqrt{\frac{\sigma_e}{E}}$$

$$R_r = \begin{cases} 1 - \left(\frac{2\eta}{b/t - 2\eta} \right) \left(\frac{\beta^2}{2\beta - 1} \right) \frac{E_t}{E} & , \beta \geq 1 \\ 1 - \left(\frac{2\eta}{b/t - 2\eta} \right) \frac{E_t}{E} & , 0 \leq \beta < 1 \end{cases} \quad (4.37)$$

when the biaxial compression and the shear stress are in the presence, the effective width should be reduced by the factors R_y and R_τ .

$$R_y = 1 - \left(\frac{\sigma_y}{\sigma_{yu}} \right)^2 \quad (4.38)$$

$$R_\tau = \left\{ 1 - \left(\frac{\tau}{\tau_0} \right)^2 \right\}^{1/2} \quad (4.39)$$

where

$$\frac{E_t}{E} = \begin{cases} \left(\frac{3.62\beta^2}{13.1 + 0.25\beta^4} \right)^2 & \text{for } 0 \leq \beta \leq 2.7 \\ 1 & \text{for } \beta > 2.7 \end{cases} \quad (4.40)$$

4.3.2.2 Carlsen's Method

Carlsen (1980) proposed a formulation which is based on the Perry-Roberston formula adopting the criteria of initial yielding in the outer fibres. The mean stress for plate-stiffener combination is given by:

$$\phi = \frac{\sigma_u}{\sigma_0} = \frac{A_e}{A_t} \frac{\left(1 + \zeta + \psi - \sqrt{(1 + \zeta + \psi)^2 - 4\zeta}\right)}{2\zeta} \quad (4.41)$$

where

$$\zeta = \frac{\sigma_0}{\sigma_E} \quad (4.42)$$

$$\psi = \frac{A_t \times \delta_{0s}}{W} = \frac{\delta_{0s} \times z}{r^2} \quad (4.43)$$

$$\sigma_E = \frac{\pi^2 E \times r^2}{a^2} \quad (4.44)$$

The plate is considered to be fully effective when calculating σ_E and the section modulus W . Both plate-induced and stiffener-induced failure should be considered.

For plate-induced failure

Considering the effect of eccentricity of end loads due to larger buckling induced shift of neutral axis at the midspan than at the ends, the ψ in the equation (4.43) should be expressed as:

$$\psi = \frac{\delta_{0se} \times z_p}{r^2} \quad (4.45)$$

where

$$\delta_{0se} = \delta_{0s} + z_p \left(\frac{A_t}{A_e} - 1 \right) \quad (4.46)$$

in which,

z_p is the distance from the neutral axis to the plate, and

$$\delta_{0s} = 0.0015a \quad (4.47)$$

$$A_t = b \times t + A_s \quad (4.48)$$

$$A_e = b_e \times t + A_s \quad (4.49)$$

$$\frac{b_e}{b} = \frac{1.8}{\beta} - \frac{0.8}{\beta^2} \quad , \max 1.0 \quad (4.50)$$

For stiffener-induced failure

$$\psi = \frac{\delta_{0s} \times z_t}{r^2} \quad (4.51)$$

where

z_t : distance from the neutral axis to the top of the stiffener.

$$\frac{b_e}{b} = 1.1 - 0.1 \times \beta \quad , \max 1.0 \quad (4.52)$$

Assumptions adopted in the method are as follows:

- Full plate width is used in the calculation of the Euler stress and radius of gyration.
- The eccentricity effect due to the shift of neutral axis caused by plate buckling is considered as the initial stiffener deflection for plate induced failure, but not for stiffener-induced failure.

$$e = z_p \left(\frac{A_t}{A_e} - 1 \right)$$

- The stiffener deflection amplitude is always equal to 0.0015a.
- The effective width of the plate is calculated by different formulae for plate and

stiffener induced failure. The initial deflection and residual stress of the plate are assumed as $0.01b$ and $0.2\sigma_0$ respectively.

- e) A reduction factor of 0.95 is introduced to reflect the effect of the residual stress in stiffener ($\sigma_{rs} / \sigma_0 = 0.1$).

4.3.2.3 Imperial College's formulation

This formula proposed by Imperial College is also based on the Perry-Robston's formulation. Both compression and lateral pressure were considered in the method. Only the formulae in compression are presented here.

The ultimate stress of a single column is expressed as:

$$\sigma_u = \frac{1}{2} \left\{ \sigma_{oe} + (1 + \psi)\sigma_E - \sqrt{[\sigma_{oe} + (1 + \psi)\sigma_E]^2 - 4\sigma_{oe}\sigma_E} \right\} \quad (4.53)$$

where

σ_{oe} : the effective yield stress of the material

σ_E : the Euler buckling stress of the effective column

ψ : parameter pertain to the effective imperfection in the column

$$\psi = \frac{\delta_{0se} \times z}{r_e^2} \quad (4.54)$$

in which

z distance from the neutral axis to the point where the check is applied

δ_{0se} the effective imperfection which consists of two parts

(a) initial imperfection (column mode) $\delta_{0s} = \text{specified tolerance} = a/\text{constant}$

(b) loading eccentricity due to overall girder bending $e = r_e^2 / H$

where H is the distance from neutral axis of box to mid-thickness of plate. For isolated stiffened plates, H is taken as zero.

The ultimate stress will be taken as the minimum value from the plate-induced failure and stiffener-induced failure.

For plate-induced failure

Two points should be checked in this failure mode. One is the plate yielding in compression, another is the stiffener yielding in tension. So, the parameter z in equation (4.54) should be both z_p and z_t .

$$\delta_{0se} = \delta_{0s} + a_c \times e \quad \text{for plate check} \quad (4.55)$$

$$\delta_{0se} = -(\delta_{0s} + a_c \times e) \quad \text{for stiffener check} \quad (4.56)$$

where

a_c is the factor for taking account of the reduced effect of loading eccentricities in continuous (multi-bay) stiffened plates. It is assumed to be 0.5.

σ_{oe} in equation (4.53) will be:

$$\sigma_{oe} = \sigma_{op} \quad \text{for plate check}$$

$$\sigma_{oe} = -\sigma_{os} \quad \text{for stiffener check}$$

where

σ_{op} : the nominal yield stress of the plate material (in compression)

$-\sigma_{os}$: the nominal yield stress of the stiffener material (in tension).

For stiffener-induced failure

The point at which check should be applied is the stiffener yielding in compression.

$$\delta_{0se} = \delta_{0s}$$

$$\sigma_{oe} = \sigma_{os}$$

where

σ_{os} : the nominal yield stress of the stiffener material (in compression).

The parameters concerning the effective section are defined in Fig. 4.25, and b_e is obtained by:

$$\frac{b_e}{b} = 0.23 + \frac{1.16}{\beta} - \frac{0.48}{\beta^2} + \frac{0.09}{\beta^3} \quad (4.57)$$

4.3.2.4 Proposed method

With increasing understanding of the behaviour of plate panels, it is important to incorporate the recent research results in plating into the formulae of stiffened plates to achieve better prediction. As seen in the previous sections, Guedes Soares's formulation gives the best ultimate strength prediction of plate panels. So these formulae were adapted to Faulkner's formulation.

For completeness, all the formulae are presented here. The ultimate strength of stiffened plates is expressed as:

$$\phi = \frac{\sigma_u}{\sigma_0} = \frac{\sigma_e}{\sigma_0} \left[\frac{A_s + b_e \times t}{A_s + b \times t} \right] \quad (4.58)$$

where

$$\frac{\sigma_e}{\sigma_0} = 1 - \frac{1}{4} \frac{\sigma_0}{\sigma_E} \quad \sigma_E \geq 0.5\sigma_0 \quad (4.59a)$$

$$\frac{\sigma_e}{\sigma_0} = \frac{\sigma_E}{\sigma_0} \quad \sigma_E \leq 0.5\sigma_0 \quad (4.59b)$$

where

$$\sigma_E = \frac{\pi^2 \times E \times r_{ce}^2}{a^2}$$

$$r_{ce}^2 = \frac{I_e'}{A_s + b_e \times t} \quad (4.60)$$

and EI_e' is the buckling flexural rigidity of the stiffener. The tangent effective width of the plate (b_e') is given by:

$$\frac{b_e'}{b} = \begin{cases} \frac{1}{\beta_e} \times R_\eta \times R_\delta \times R_{\eta\delta} & \beta_e \geq 1 \\ R_\eta \times R_\delta \times R_{\eta\delta} & 0 \leq \beta_e \leq 1 \end{cases} \quad (4.61)$$

The effective width of the plate is related to the slenderness as follows:

$$\frac{b_e}{b} = \begin{cases} 1.08 \times \phi_b \times R_\eta \times R_\delta \times R_{\eta\delta} & \beta_e \geq 1 \\ 1.08 \times R_\eta \times R_\delta \times R_{\eta\delta} & 0 \leq \beta_e \leq 1 \end{cases} \quad (4.62)$$

where

$$\beta_e = \frac{b}{t} \sqrt{\frac{\sigma_e}{E}}$$

$$\phi_b = \frac{2}{\beta_e} - \frac{1}{\beta_e^2} \quad (4.63)$$

$$R_\eta = \left(1 - \frac{\Delta\phi_b}{1.08 \times \phi_b} \right) (1 + 0.0078\eta) \quad (4.64)$$

$$R_\delta = 1 - (0.626 - 0.121\beta_e) \frac{\delta_0}{t} \quad (4.65)$$

$$R_{\eta\delta} = 0.665 + 0.006\eta + 0.36\frac{\delta_0}{t} + 0.14\beta_e \quad (4.66)$$

in which $\Delta\phi_D$ is obtained by Eq. (4.14).

4.3.3 Calibration and Comparison of the Methods

As done in the foregoing section, the above methods are calibrated against the existing experimental and numerical data. The results are listed in Table 4.8-4.11 and Fig. 4.26-4.32.

Table 4.8: Model uncertainty factor of Faulkner's method

Experiments Sources	Number of cases	Minimum value	Maximum value	Mean value	C.O.V.
Horne(1976,77)	20	0.822	1.562	1.039	0.158
Faulkner(1976)	24	0.924	1.146	1.030	0.066
Dorman(1973)	12	0.835	1.024	0.943	0.060
Smith(1975)	7	0.924	1.534	1.228	0.197
Total exp.	63	0.822	1.562	1.039	0.143
Smith(1991)	70	0.881	1.013	0.948	0.031
Smith(1991)	70	0.969	1.259	1.135	0.063
Total numer.	140	0.881	1.259	1.041	0.104
Total	203	0.822	1.562	1.041	0.117

Table 4.9: Model uncertainty factor of Carlsen’s method

Experiments Sources	Number of cases	Minimum value	Maximum value	Mean value	C.O.V.
Horne(1976,77)	20	0.980	1.404	1.133	0.108
Faulkner(1976)	24	1.014	1.715	1.215	0.127
Dorman(1973)	12	0.928	1.081	1.007	0.044
Smith(1975)	7	0.917	1.498	1.202	0.191
Total exp.	63	0.917	1.715	1.148	0.137
Smith(1991)	70	0.911	1.230	1.040	0.063
Smith(1991)	70	0.992	1.795	1.354	0.129
Total numer.	140	0.911	1.795	1.197	0.171
Total	203	0.911	1.795	1.182	0.163

Table 4.10: Model uncertainty factor of Imperial’s method

Experiments Sources	Number of cases	Minimum value	Maximum value	Mean value	C.O.V.
Horne(1976,77)	20	0.772	1.293	1.018	0.118
Faulkner(1976)	24	0.795	1.660	1.030	0.204
Dorman(1973)	12	0.843	1.022	0.953	0.062
Smith(1975)	7	0.881	1.214	1.030	0.105
Total exp.	63	0.772	1.660	1.012	0.151
Smith(1991)	70	0.712	0.894	0.808	0.075
Smith(1991)	70	0.913	1.064	0.993	0.043
Total numer.	140	0.712	1.064	0.901	0.118
Total	203	0.712	1.574	0.931	0.132

Table 4.11: Model uncertainty factor of the Proposed method

Experiments Sources	Number of cases	Minimum value	Maximum value	Mean value	C.O.V.
Horne(1976,77)	20	0.809	1.345	1.004	0.109
Faulkner(1976)	24	0.806	1.128	0.965	0.080
Dorman(1973)	12	0.840	1.062	0.973	0.075
Smith(1975)	7	0.926	1.264	1.085	0.116
Total exp.	63	0.806	1.345	0.992	0.099
Smith(1991)	70	0.747	1.011	0.887	0.075
Smith(1991)	70	0.898	1.258	1.079	0.090
Total numer.	140	0.747	1.258	0.983	0.129
Total	203	0.747	1.345	0.986	0.120

From these Tables and Figures, it can be seen that:

- Faulkner's method is the best one with the mean value of 1.041 and coefficient of variation of 11.7%, although it shows slight skewness with the slope of -0.268.
- Imperial College's method has relatively large coefficient of variation which reaches 0.142, although it shows no skewness at all.
- Although the proposed method shows the best prediction if only the experimental data are included in the calibration [Fig. 4.30-4.32], on the whole, the results only have more or less the same accuracy as Faulkner's method.

Having studied the details of the calculation, the following points are worth mentioning:

- The coefficient of variation is very small for a single source of experimental or numerical data, but it becomes large when all sources are included in the

calibration. So any low C.O.V. from relatively few sources needs to be checked, because any unrealistic low C.O.V. could lead to an untruly high reliability index in reliability analysis.

- In recent years there is a trend to use the numerical data to calibrate the strength formulae without considering the errors involved in the numerical calculation. Although it is an acceptable way when experimental data are not sufficient, nevertheless two points should be kept noted. Firstly, the numerical data have also uncertainty. Figure 4.33 and Table 4.12 taken from Smith et al (1991) clearly show the accuracy of the numerical calculation. If these data are used to regress the mean and C.O.V. of the numerical method (of course the sample is too less, but one can get insight from it), it gives the mean of 1.121 and C.O.V. of 0.071. Secondly, a numerical method usually has better consistency, which no doubt leads to low C.O.V.

- The differences between Carlsen's method and Imperial College's method are:

a) In IC's method, the check applied to outer fibre of the stiffener is introduced for plate-induced failure.

b) For consideration of column imperfection, initial imperfection of the stiffener is assumed to be always $0.0015a$ in Carlsen's method. In IC's method either the actual initial imperfection of the stiffener or the tolerance in Rules (when the actual imperfection is unknown) is used.

c) For consideration of eccentricity due to the loss of plate effectiveness in plate-

induced failure, an item $e = z_p \left(\frac{A_t}{A_e} - 1 \right)$ is introduced in Carlsen's method. A similar term is used to take account of the effect of box girder height in IC's method. But from the formula it can be seen that, for an isolated plate eg. $H=0.0$ this term is equal to zero. This means that in this case the effect of the loss of the plate effectiveness is not considered in IC's method.

- In some cases, the failure mode in experiment is plate-induced failure, but the failure mode calculated by Carlsen's method is the stiffener-induced failure. Such mismatch is caused by the assumption that the initial stiffener deflection is equal to $0.0015a$.

- Although Faulkner's method is the best one, it gives poor prediction when the initial imperfection (including residual stress in plate, initial deflection in stiffener and load eccentricity) is large.

Table 4.12: Details of test panels and correlation of theoretical and experimental compressive strength (Smith et al, 1991)

Source	Panel No	n_s	n_c	Initial Deformation			Plating Residual Stress ϵ_{2c}/ϵ_0	A_1/A	β	λ	Lateral Pressure $Q(m)$	Compressive Strength σ_c		
				Plating mean w_{0max}/t	Stringers							Expt.	Theoretical Values	
					mean δ_{01}/a	δ_{02}/δ_{01}							Average Imperfections	Actual Imperfection
Ref 19	1a	4	4	0.0060	0.0007	0.7	-	0.30	2.67	0.24	0	0.76	0.65	0.69
	1b	4	4	0.0077	0.0011	-	-	0.30	2.72	0.23	10.2	0.73	0.57	0.57
	2a	9	3	0.0044	0.0025	-	0.48	0.29	1.42	0.42	4.8	0.91	0.81	0.81
	2b	9	3	0.0060	0.0010	-	0.33	0.30	1.48	0.42	0	0.83	0.82	0.82
	3a	9	3	0.0093	0.0028	0.2	0.38	0.19	1.68	0.70	2.0	0.69	0.69	0.63
	3b	9	3	0.0150	0.0019	-0.8	0.43	0.19	1.68	0.70	0	0.61	0.71	0.60
	4a	11	4	0.0081	0.0023	0.5	0.38	0.22	1.41	0.54	0	0.82	0.80	0.75
	4b	11	4	0.0063	0.0008	0.5	0.41	0.22	1.43	0.53	5.5	0.83	0.73	0.76
	5	4	4	0.0100	0.0008	-0.4	0.16	0.19	3.31	0.45	0	0.72	0.51	0.55
	7	4	4	0.0094	0.0007	-	0.08	0.19	3.42	0.52	0	0.65	0.49	0.53
Ref 24	A1	4	4	-	0.0028	-0.67	0.08	0.43	1.47	0.28	0	0.90	0.86	0.76
	A2	3	4	-	0.0028	-0.67	0.06	0.38	1.94	0.30	0	0.68	0.76	0.68
	A3*	4	4	-	0.0028	-0.67	0.11	0.43	1.50	0.33	0	0.84	0.86	0.75
	A4*	3	4	-	0.0028	-0.67	0.06	0.38	1.90	0.34	0	0.73	0.77	0.67
	B1	4	4	-	0.0028	-0.67	0.09	0.43	1.47	0.28	0	0.88	0.86	0.77
	B2	3	4	-	0.0028	-0.67	0.09	0.38	1.98	0.31	0	0.70	0.77	0.66
	B3*	4	4	-	0.0028	-0.67	0.12	0.43	1.56	0.35	0	0.79	0.84	0.73
	B4*	3	4	-	0.0028	-0.67	0.14	0.38	1.90	0.35	0	0.73	0.79	0.66
	C1	5	4	-	0.0028	-0.67	0.14	0.48	1.22	0.27	0	0.94	0.89	0.80
	C2	4	4	-	0.0028	-0.67	0.19	0.43	1.49	0.28	0	0.87	0.86	0.77
	C3	3	4	-	0.0028	-0.67	0.17	0.38	1.84	0.29	0	0.81	0.79	0.70
	C4	5	4	-	0.0028	-0.67	0.46	0.48	1.24	0.28	0	0.90	0.88	0.79

* Flat-bar stiffeners

4.4 RELIABILITY ANALYSIS OF STIFFENED PLATES

Some researchers have been applying the probabilistic methods to stiffened plates, but they only used the Advanced First Order Second Moment Method (AFOSM) to calculate the reliability index without investigating the accuracy. It is well known that the AFOSM is only accurate when the safety margin equation is linear. When the non-linearity in the limit state expression is large, the results from AFOSM are usually very poor. So, in practice, for a specific problem, a wise way to carry out reliability analysis is first to investigate the accuracy of the AFOSM and SORM (Second Order Reliability Method), then decide whether or not the results from the AFOSM are acceptable from an engineering point of view. Therefore the programs developed in Chapter 2 are used to evaluate the failure probability of stiffened plates.

The safety margin equation is expressed as follows:

$$M = \sigma_0 X_m \phi_m - \sigma_s \quad (4.67)$$

where

- σ_0 yield stress of the material
- X_m model uncertainty factor
- ϕ_m non-dimensional strength of the structure
- σ_s external loads effect

4.4.1 Reliability Analysis of Unstiffened Plates

Six cases, whose plate slendernesses vary from 1.011 to 3.111, are selected to carry out the reliability analysis, in which both Faulkner's and Guedes Soares' strength formulae are studied. The values and probability distribution types of the basic variables used in the analysis are listed in Table 4.13. The reason for the selection is stated below.

Table 4.13: Values and types of the basic variables

Basic variables	Prob. distrib.	COV (%)	Mean Values					
			Case1	Case2	Case3	Case4	Case5	Case6
b (mm)	Normal	1	800	700	600	400	320	260
t (mm)	Normal	4	10	10	10	10	10	10
σ_0 (N / mm ²)	Log-Normal	8	313	313	313	313	313	313
E (N / mm ²)	Log-Normal	4	207000	207000	207000	207000	207000	207000
η	Normal	7	4.5	4.5	4.5	4.5	4.5	4.5
δ_0 / t	Log-Normal		1.161	0.889	0.653	0.290	0.186	0.123
X_m	Normal	10.1	1.031	1.031	1.031	1.031	1.031	1.031
σ_s (N / mm ²)	Gumbel I	20.0	75	75	75	115	125	130

1) Width and thickness of the plate

It is widely recognised that the width of the plate has very low C.O.V. Some researchers treated it as a deterministic variable. It might be more reasonable to assume one percent of C.O.V., and a four percent of C.O.V for thickness of plate sounds reasonable.

2) Yield stress and Young's modulus

There is not much argument for these two parameters. It is agreed that they have lognormal probability distributions with 8 and 4 percent of C.O.V. respectively.

3) Residual stress

There are two possible ways to determine it. One way is to assume a constant value of η across the b/t range, which leads to a rapid decrease of residual stress σ'_r . Faulkner (1975b) suggested mean values of η of 4.5 - 6.0 with a coefficient of variation of 0.07 - 0.10 for marine structures after fabrication and low values of 3.0-4.5 after shake-out at sea.

Recently Bonello et al (1991) presented another way to determine the η , based on the regression from experimental data. The η is expressed as:

$$\eta = \eta_R + \Delta\eta \quad (4.68)$$

where

η_R is the mean value of η which is treated as deterministic and determined by:

$$\eta_R = 1.40 + 0.06 \left(\frac{b}{t} \right) \quad (4.69)$$

$\Delta\eta$ is a normal zero-mean basic variable with a standard deviation calculated by:

$$\sigma_{\Delta\eta} = 0.04 \left(\frac{b}{t} \right) \quad (4.70)$$

This means that the coefficient of variation of η could reach 0.52 when $b/t=100$. It is quite high.

In the present study, η is assumed to be constant with coefficient of variation of 0.07.

4) Initial imperfection δ_0 / t

Faulkner (1973, 1975b) suggested that the mean value of δ_0 / t could be obtained by:

$$\frac{\delta_0}{t} = 0.12\beta^2 \left(\frac{t_w}{t} \right) \quad \text{for } t_w \leq t \quad (4.71)$$

Its coefficient of variation varies typically from 0.60 for stocky plates to 0.30 for slender plating.

Another model was derived by Bonello et al (1991). The δ_0/b is divided into two parts:

$$\frac{\delta_0}{b} = \left[\frac{\delta_0}{b} \right]_R + \Delta \left[\frac{\delta_0}{b} \right] \quad (4.72)$$

where

$\left[\frac{\delta_0}{b} \right]_R$ is the mean value and deterministic

$$\left[\frac{\delta_0}{b} \right]_R = 0.12 \left(\frac{b}{t} \right) \left(\frac{\sigma_0}{E} \right) \quad (4.73)$$

$\Delta \left[\frac{\delta_0}{b} \right]$ has a zero-mean and its standard deviation is:

$$\sigma_{\Delta(\delta_0/b)} = \left[\frac{\delta_0}{b} \right]_R \left(0.675 - 0.004 \left(\frac{b}{t} \right) \right) \quad (4.74)$$

In the present study Bonello's model was adopted.

5) Model uncertainty factor

The model uncertainty factor is assumed to have normal distribution. Its mean and coefficient of variation are obtained from the previous section.

6) External loads effect

Because the long-term extreme values are usually used in ship design the Gumbel I distribution is adopted in this case. The mean values are determined in the way that

the reliability index obtained in the calculation is near 3.0, which is the target reliability in most situations. The coefficient of variation of the external load effect is assumed to be 20%.

The results of the reliability analyses are presented in Table 4.14 and Figures 4.34 and 4.35. In the Table the e_i ($i=1,2$) are the relative errors of the AFOSM and SORM, which are evaluated by:

$$e_i = \frac{P_{fi} - P_{fm}}{P_{fm}} \times 100 \quad (4.75)$$

where P_{fi} ($i=1,2$) are failure probabilities of first and second order calculation. P_{fm} is the value from Monte Carlo simulation.

From the Table and the Figures, it is found that:

- The results from SORM are much better than from AFOSM. The AFOSM and SORM underestimate the failure probability in all the cases. The largest relative error reaches -45.1% for AFOSM and -26.4% for SORM in the high plate slenderness when Guedes Soares' formula is used.
- In most cases the relative errors of SORM are nearly half of those of AFOSM.
- The relative errors of reliability index are within ten percent for all the cases. The largest errors are 7.4% for AFOSM and 3.8% for SORM.

Table 4.14: Results of reliability analysis of plating

		Case1	Case2	Case3	Case4	Case5	Case6	
		Guede Soares' Method		1st order	0.2113e-2	0.1751e-2	0.8076e-3	0.1034e-2
2nd order	0.2830e-2			0.2284e-2	0.1026e-2	0.1601e-2	0.1056e-2	0.1183e-2
Simulation	0.3846e-2			0.306e-2	0.1432e-2	0.1506e-2	0.1168e-2	0.1324e-2
P_f								
e1	-45.1			-42.8	-43.6	-31.3	-29.9	-24.2
e2	-26.4			-25.4	-28.4	6.3	-9.6	-10.6
1st order	2.861			2.920	3.153	3.080	3.149	3.089
2nd order	2.767			2.836	3.083	2.948	3.074	3.040
Simulation	2.665			2.741	2.982	2.967	3.044	3.006
β_T								
e1	7.4	6.5	5.7	3.8	3.4	2.8		
e2	3.8	3.5	3.4	-0.6	1.0	1.1		
Faulkner's Method		1st order	0.6757e-2	0.3098e-2	0.1041e-2	0.1241e-2	0.6499e-3	0.5321e-3
		2nd order	0.8338e-2	0.3857e-2	0.1321e-2	0.1646e-2	0.8759e-3	0.7083e-3
		Simulation	0.799e-2	0.366e-2	0.1228e-2	0.1536e-2	0.788e-3	0.652e-3
		P_f						
		e1	-15.4	-15.4	-15.2	-19.2	-17.5	-18.4
		e2	4.4	5.4	7.6	7.2	11.2	8.6
		1st order	2.470	2.737	3.078	3.026	3.216	3.273
		2nd order	2.394	2.664	3.007	2.939	3.129	3.191
		Simulation	2.409	2.682	3.029	2.960	3.160	3.215
		β_T						
e1	2.5	2.1	1.6	2.2	5.6	1.8		
e2	-0.6	-0.7	-0.7	-0.7	-1.0	-0.7		

4.4.2 Reliability Analysis of Stiffened Plates

Similarly, the reliability analyses of stiffened plates are carried out. Ten cases, shown in Table 4.15, are selected. The principle for such selection is the same as that in section 4.4.1. The strength of a stiffened plate is predicted by Faulkner's method and the proposed method. The results are shown in Tables 4.16 and 4.17 and Figures 4.36 and 4.37.

From the tables and figures, it is observed that:

- The failure probabilities obtained from SORM are much better than those from AFOSM. The relative errors of the SORM are usually very small, the largest is 3.7%, while the largest relative error of AFOSM is -22.8%.
- The differences in reliability index between the two methods are not remarkable.
- The AFOSM always underestimates the failure probability in these situations.
- The relative errors of Faulkner's and the proposed method have the similar level for AFOSM, but for SORM the former has better accuracy. A possible reason for this is that, in the proposed method, the deflection of plate is explicitly considered, and the deflection is assumed to be log-normally distributed in the reliability analysis. So the failure surface in the standard space might have stronger non-linearity in the latter case. This would lead to a larger error.

Basic variables	Probability distribution	COV (%)	Mean Values											
			Case1	Case2	Case3	Case4	Case5	Case6	Case7	Case8	Case9	Case10		
b (mm)	Normal	1	508	508	508	508	508	508	508	508	508	400	300	600
t _p (mm)	Normal	4	9.5	9.5	9.5	9.5	9.5	9.5	9.5	9.5	9.5	10	10	10
h _w (mm)	Normal	4	150	150	150	150	150	150	150	150	150	150	150	150
t _w (mm)	Normal	4	10	10	10	10	10	10	10	10	10	10	10	10
a (mm)	Normal	1	2000	2500	3000	3500	4000	4500	5000	4000	4000	4000	4000	4000
σ _{0p} (N / mm ²)	Log-Normal	8	313	313	313	313	313	313	313	313	313	313	313	313
σ _{0s} (N / mm ²)	Log-Normal	8	313	313	313	313	313	313	313	313	313	313	313	313
E (N / mm ²)	Log-Normal	4	207e3	207e3	207e3	207e3	207e3	207e3	207e3	207e3	207e3	207e3	207e3	207e3
η	Normal	7	4.5	4.5	4.5	4.5	4.5	4.5	4.5	4.5	4.5	4.5	4.5	4.5
δ ₀ *	Log-Normal	eq.(74)	0.1	0.1	0.1	0.1	0.1	0.1	0.1	0.1	0.1	0.1	0.1	0.1
X _m **	Normal	11.7/	1.041/	1.041/	1.041/	1.041/	1.041/	1.041/	1.041/	1.041/	1.041/	1.041/	1.041/	1.041/
σ _s (N / mm ²)	Gumbel I	12.0	0.986	0.986	0.986	0.986	0.986	0.986	0.986	0.986	0.986	0.986	0.986	0.986
		20	90	90	80	80	75	70	50	80	100	80	100	65

* These values are only used for the proposed method

** These values are taken from table 8 and 11.

The upper one is for Faulkner's method, the lower one for the proposed method

Table 4.15: Values and types of basic variables of stiffened plates

	Case1	Case2	Case3	Case4	Case5	Case6	Case7	Case8	Case9	Case10	
P_f	1st order	0.7331e-3	0.1148e-2	0.5541e-3	0.1221e-2	0.1681e-2	0.3245e-2	0.6243e-3	0.4123e-3	0.1096e-2	0.1275e-2
	2nd order	0.8431e-3	0.1325e-2	0.6506e-3	0.1450e-2	0.2063e-2	0.4116e-2	0.7518e-3	0.5238e-3	0.1349e-2	0.1580e-2
	Simulation	0.850e-3	0.1342e-2	0.658e-3	0.1440e-2	0.2052e-2	0.397e-2	0.7540e-3	0.5340e-3	0.1376e-2	0.1540e-2
	e1	-13.8	-14.5	-15.8	-15.2	-18.1	-18.3	-17.2	-22.8	-20.3	-17.2
	e2	-0.8	-1.3	-1.1	1.0	0.5	3.7	-0.3	-1.9	-2.0	2.6
	1st order	3.181	3.049	3.262	3.031	2.933	2.722	3.228	3.344	3.063	3.017
β_r	2nd order	3.141	3.006	3.216	2.978	2.868	2.642	3.174	3.277	3.000	2.952
	Simulation	3.138	3.002	3.212	2.980	2.870	2.652	3.173	3.272	2.994	2.960
	e1	1.4	1.6	1.6	1.7	2.2	2.6	1.7	2.2	2.3	1.9
	e2	0.1	0.1	0.1	-0.1	-0.1	-0.4	0.03	0.2	0.2	-0.3

Table 4.16: Reliability of stiffened plates by Faulkner's formulation

	Case1	Case2	Case3	Case4	Case5	Case6	Case7	Case8	Case9	Case10	
P_f	1st order	0.5886e-3	0.900e-3	0.4239e-3	0.9538e-3	0.1452e-2	0.3781e-2	0.8196e-3	0.7285e-3	0.2957e-2	0.9449e-3
	2nd order	0.6896e-3	0.1059e-2	0.5099e-3	0.1167e-2	0.1869e-2	0.4650e-2	0.9881e-3	0.9350e-3	0.3667e-2	0.1254e-2
	Simulation	0.640e-3	0.1002e-2	0.482e-3	0.1116e-2	0.1802e-2	0.4518e-2	0.942e-3	0.882e-3	0.3552e-2	0.121e-2
	e1	-8.03	-10.18	-12.05	-14.53	-19.42	-16.31	-12.99	-17.4	-16.75	-21.91
	e2	7.75	5.69	5.79	4.57	3.72	2.92	4.89	6.01	3.24	3.64
	1st order	3.244	3.121	3.337	3.104	2.978	2.671	3.149	3.183	2.752	3.107
β_r	2nd order	3.199	3.073	3.285	3.044	2.900	2.601	3.094	3.110	2.681	3.022
	Simulation	3.220	3.090	3.301	3.057	2.911	2.611	3.108	3.127	2.692	3.033
	e1	0.75	1.00	1.09	1.54	2.30	2.30	1.32	1.79	2.23	2.44
	e2	-0.65	-0.55	-0.48	-0.43	-0.38	-0.38	-0.45	-0.54	-0.41	-0.36

Table 4.17: Reliability of stiffened plates by proposed formulation

4.5 CONCLUSIONS

Stiffened plates are common components in ships and offshore structures. It is very important to accurately predict the strength of stiffened plates. Because the uncertainty in strength is very important in reliability analysis of a structure, it is crucial to find out the correct model uncertainty factor in the reliability analysis.

The behaviour of plate panels and stiffened plates are fully discussed. The existing strength formulae were then calibrated by a large number of experimental and numerical data. It is found that Guedes Soares' formulae and Faulkner's method are the best for plate panels and stiffened plates respectively. A new formulation for prediction of the strength of a stiffened plate was proposed which combines these two.

Furthermore, the reliability analyses of plate panels and stiffened plates were carried out in which the AFOSM, SORM and Monte Carlo simulation are applied. It is found that the results for failure probability from SORM are much better than those from AFOSM. In these cases the AFOSM always underestimates the failure probability. The largest relative errors of failure probability and reliability index reach -45.1% and 7.4% respectively. Considering the nominal nature of reliability index the difference between the two methods is so small that the values obtained from AFOSM are acceptable in practice.

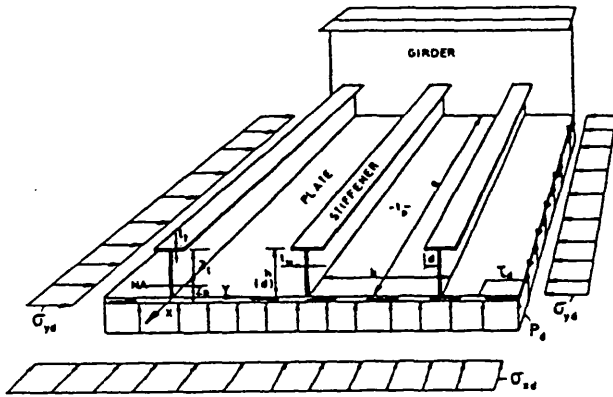


Fig. 4.1 Definition of stiffened plates (DNV,1982)

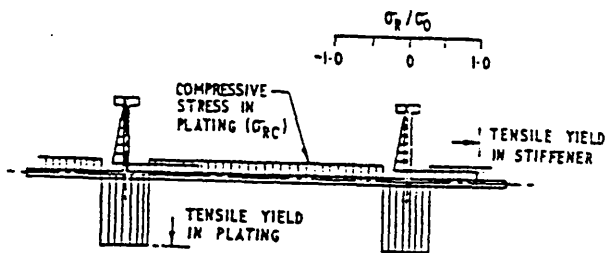
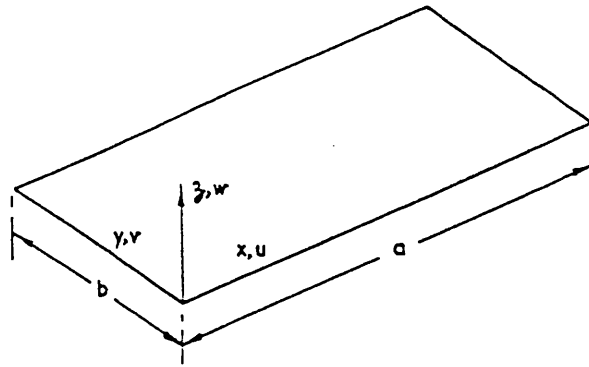
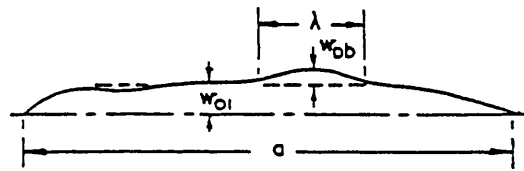


Fig. 4.2 Residual stress in stiffened panels (Smith et al, 1991)



(a) REFERENCE AXES FOR PLATE ELEMENT



(b) TYPICAL INITIAL DISTORTION PROFILE

Fig. 4.3 Initial deformation of plating (Smith et al, 1991)

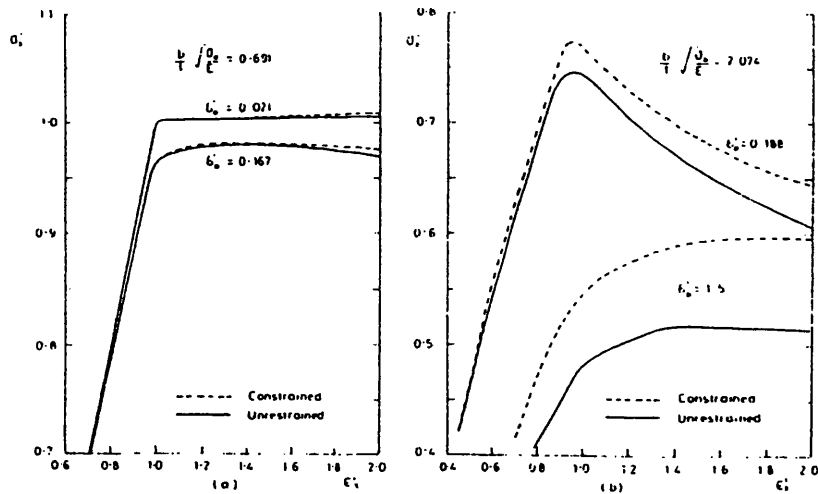


Fig. 4.4 Effect of unloaded edge in-plane restraint on square plates in uniaxial compression (Frieze et al, 1976)

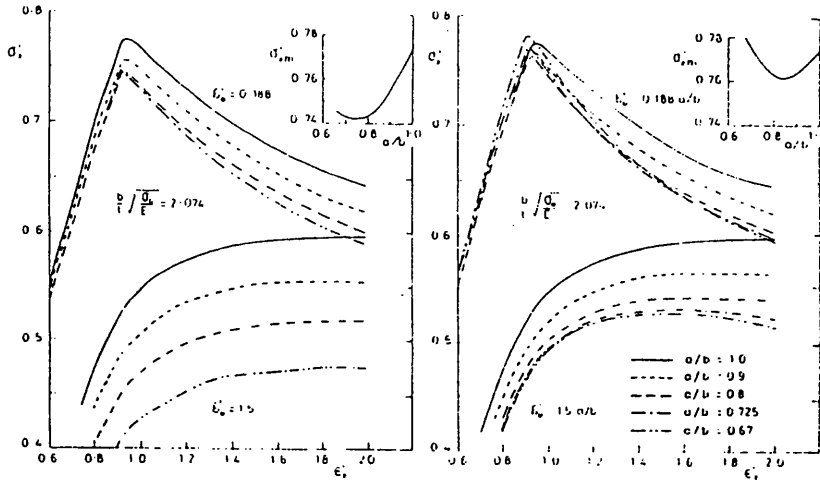


Fig. 4.5 Effect of aspect ratio on constrained plates (Frieze et al, 1976)

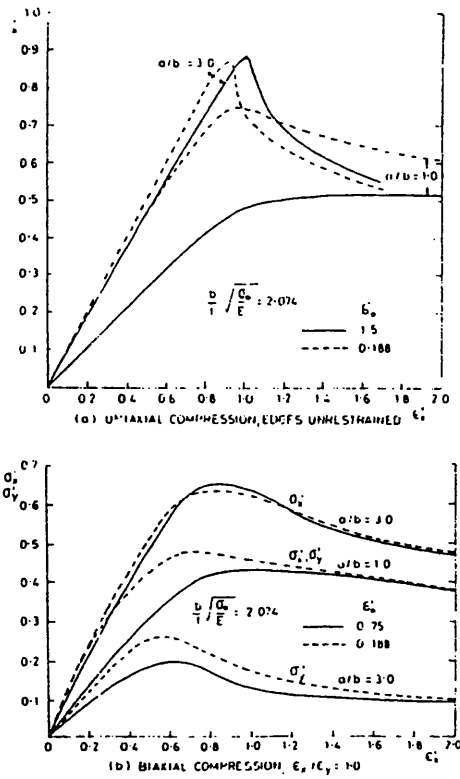


Fig. 4.6 Load-shortening curves of platings (Frieze et al, 1976)

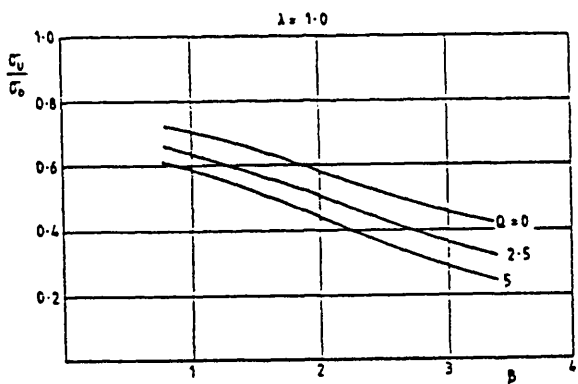
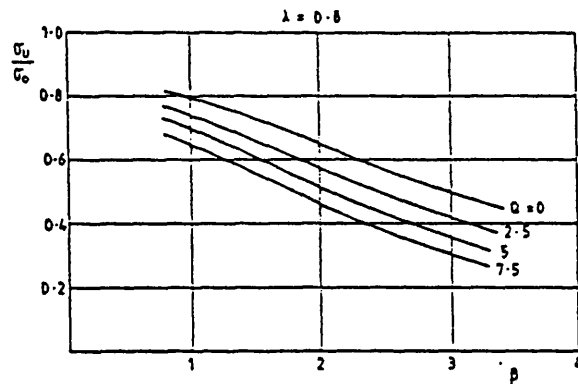
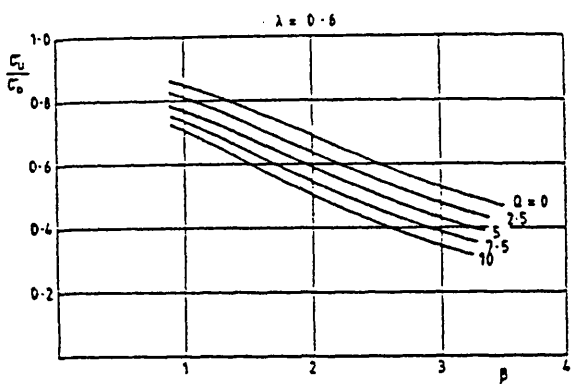
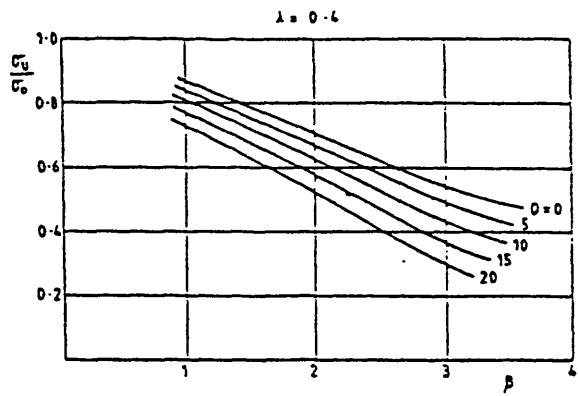
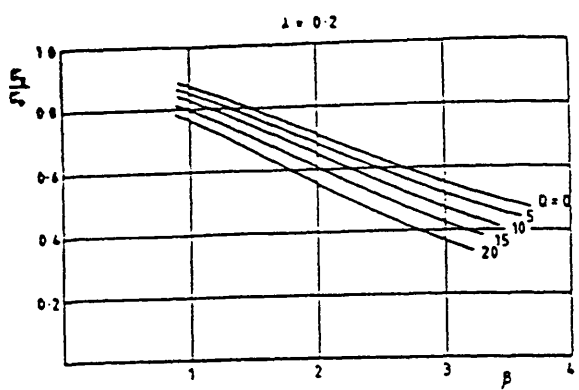


Fig. 4.7 Influence of lateral pressure on compressive strength (tee-bar stiffeners $A_S/A=0.2$, average imperfection) (Smith et al, 1991)

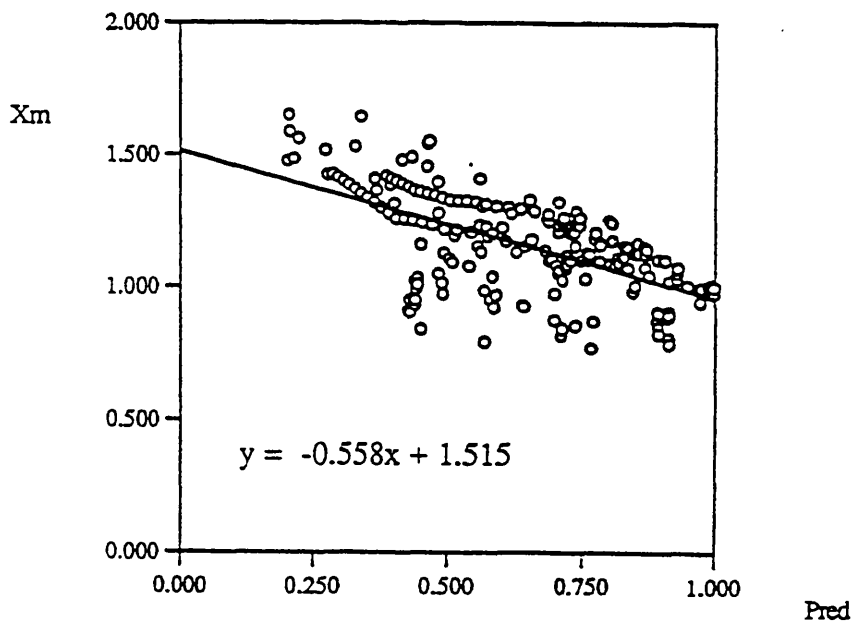
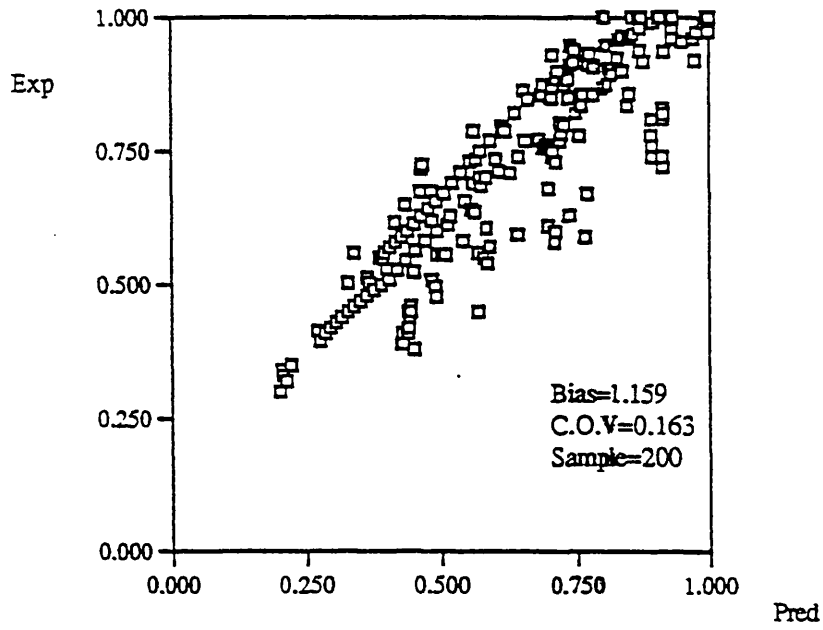


Fig. 4.8 Results of Faulkner's method

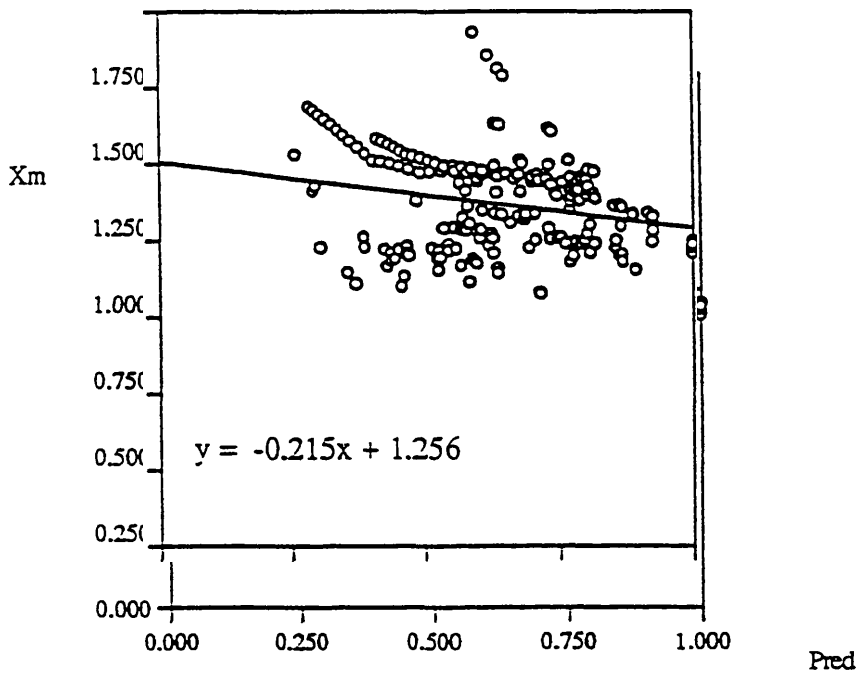
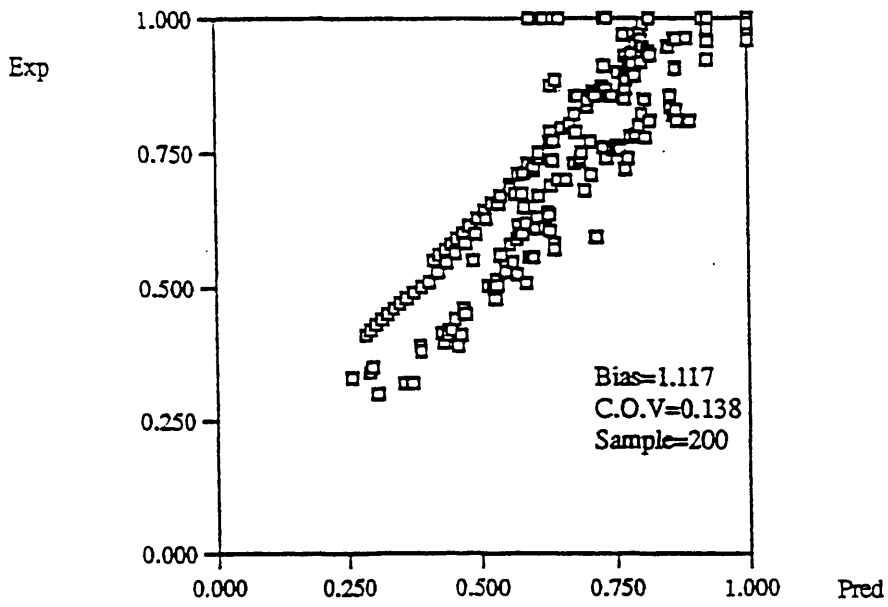


Fig. 4.9 Results of Carlsen's method

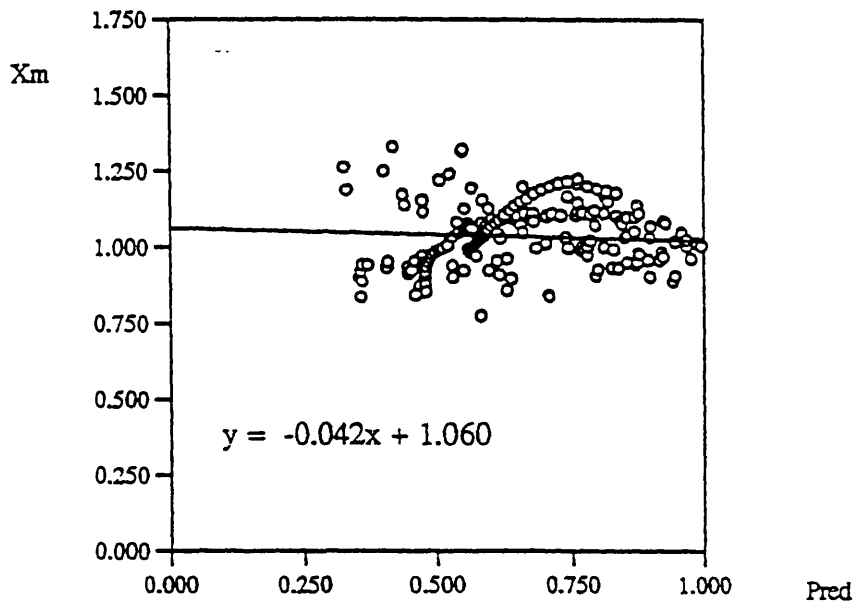
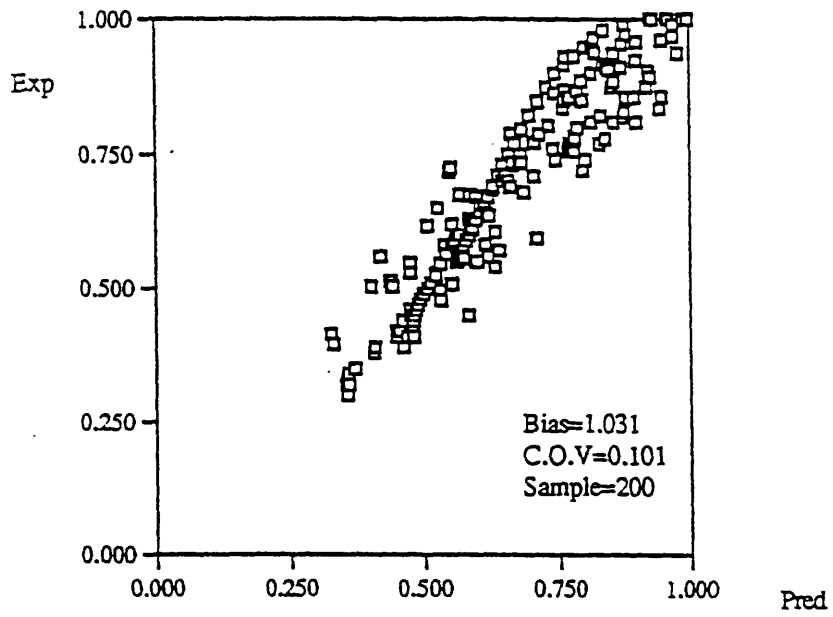


Fig. 4.10 Results of Guede Soares' method

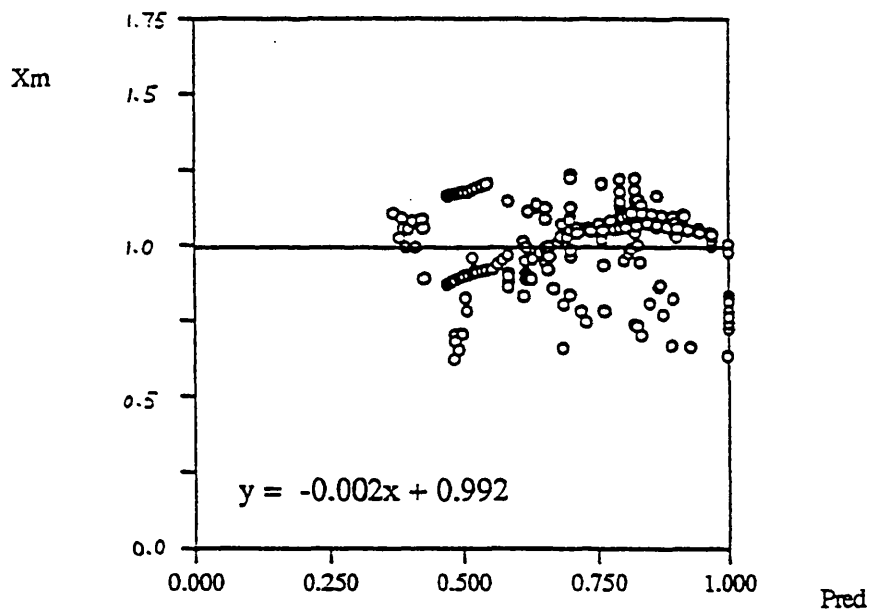
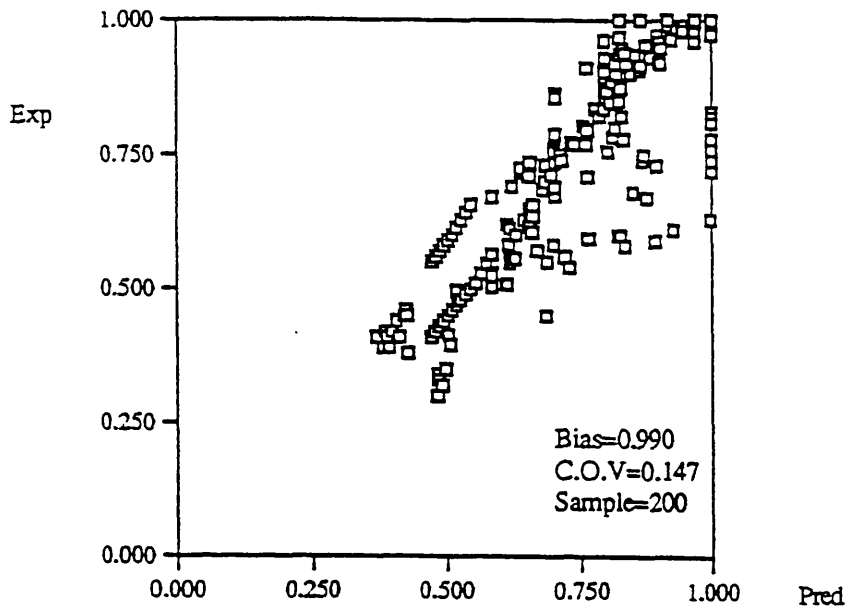


Fig. 4.11 Results of Vilnay's method

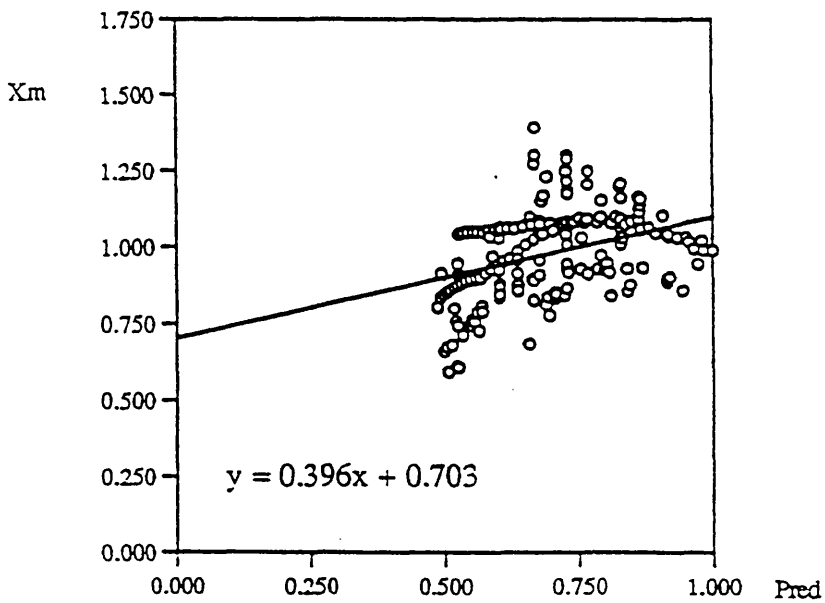
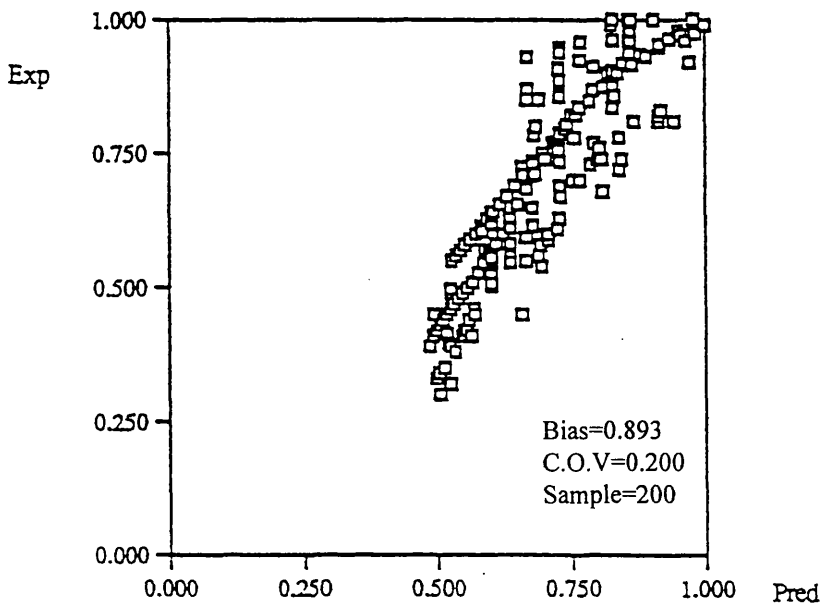


Fig. 4.12 Results of Imperial College's method

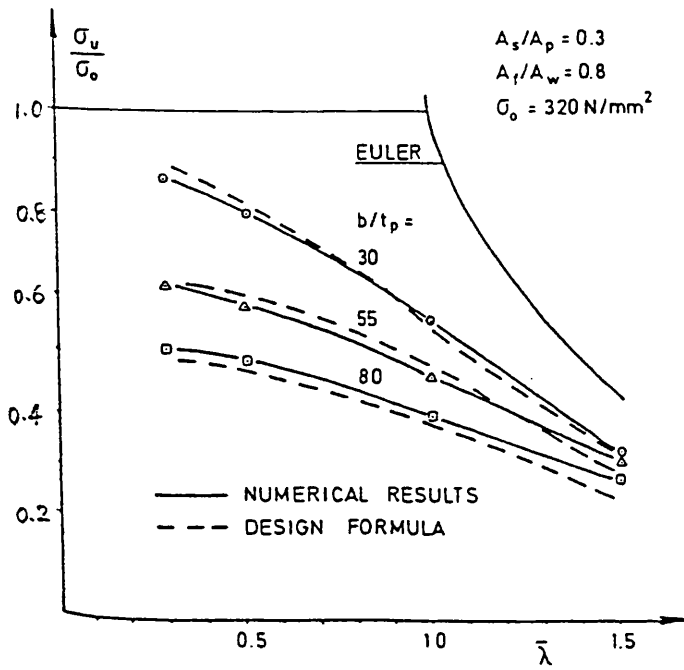


Fig. 4.13 Effect of stiffener and plate slenderness (Carlsen, 1980)

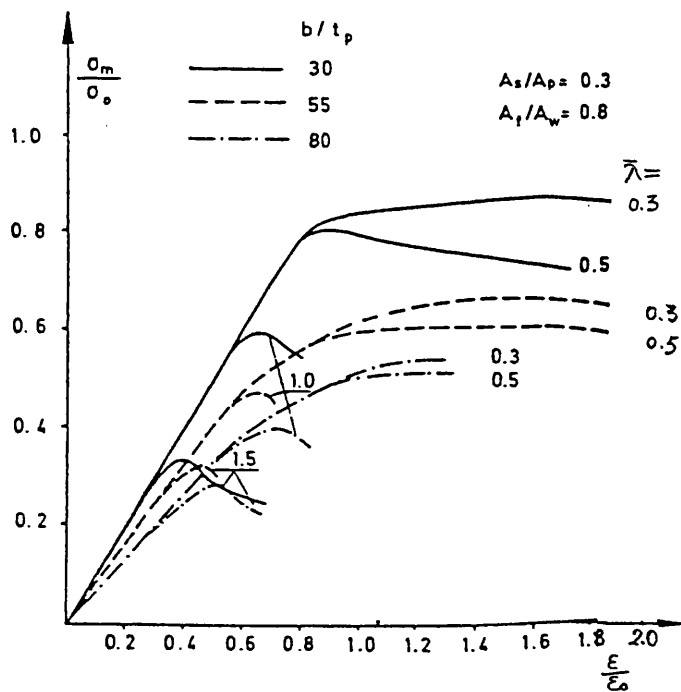


Fig. 4.14 Effect of stiffener and plate slenderness (Carlsen, 1980)

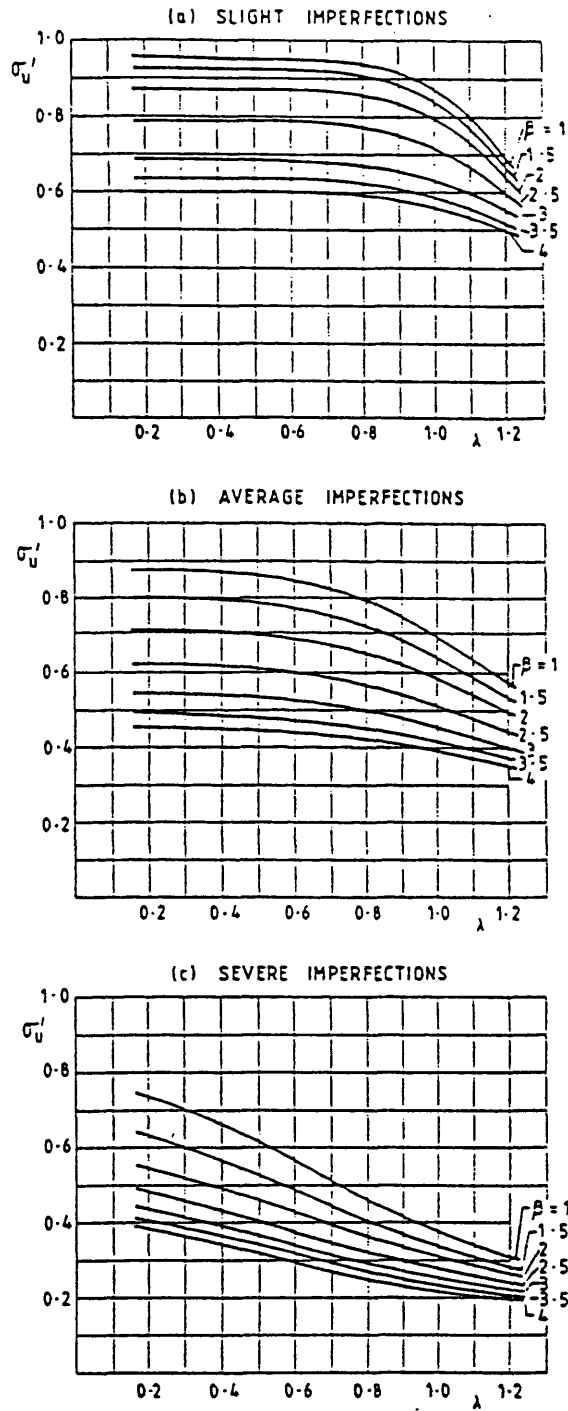


Fig. 4.15 Effect of stiffener and plate slenderness (Smith et al, 1991)

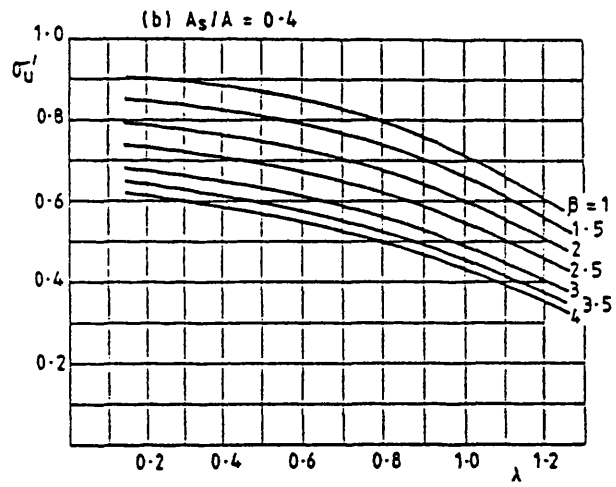
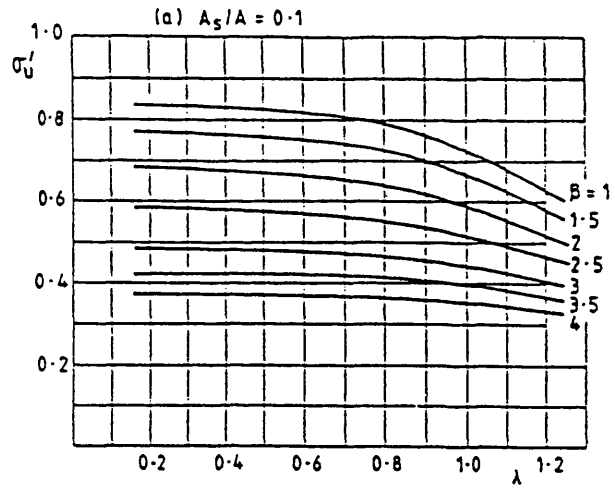


Fig. 4.16 Effect of ratio of stiffener to cross-sectional area (Smith et al, 1991)

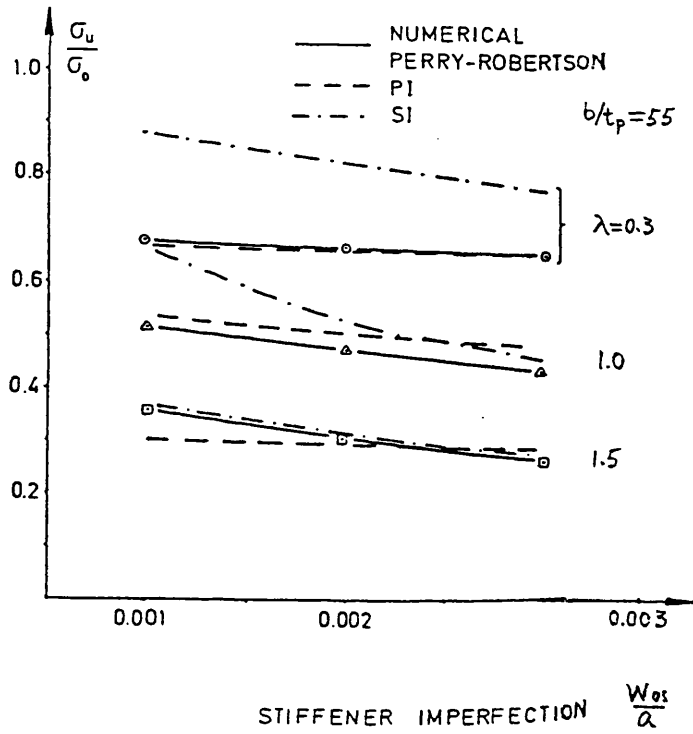


Fig. 4.17 Effect of top flange to web cross-sectional area (Carlsen, 1980)

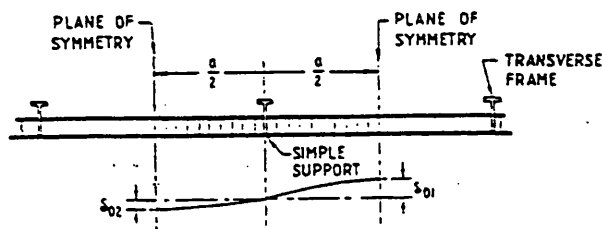


Fig. 4.18 Definition of initial deformation of stiffener in adjacent spans (Smith et al, 1991)

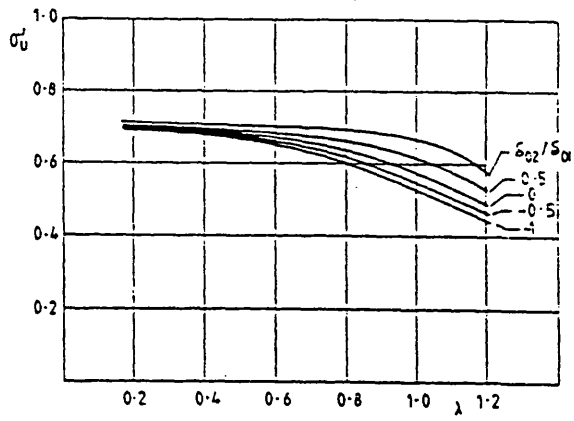


Fig. 4.19 Effect of initial stiffener deformation in adjacent spans on compressive strength (Smith et al, 1991)

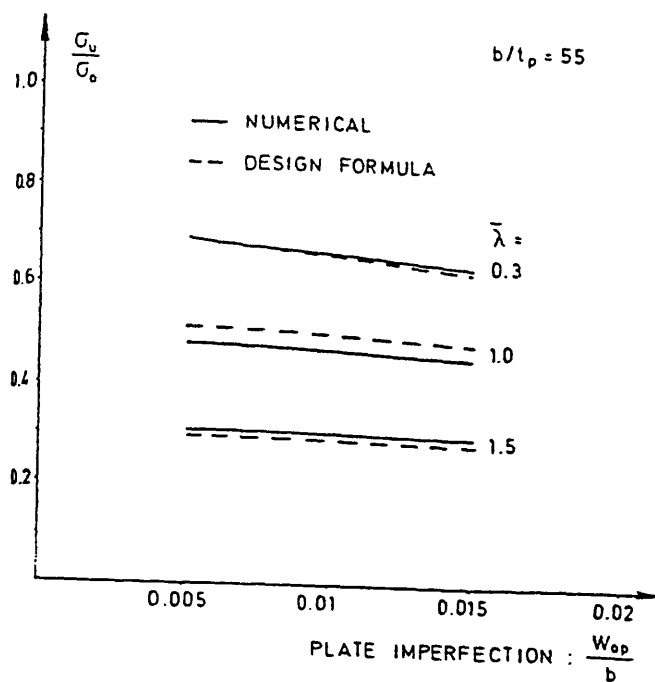


Fig. 4.20 Effect of initial plane deflection on compressive strength (Carlsen, 1980)

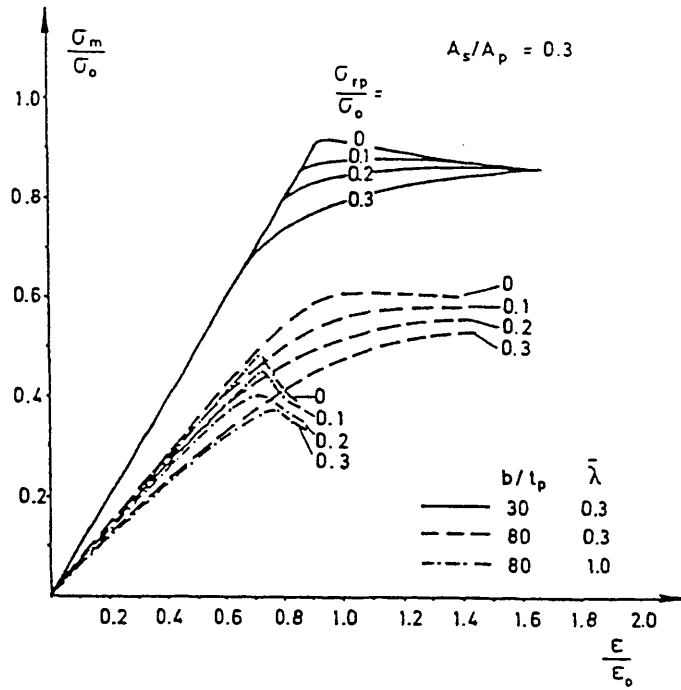


Fig. 4.21 Effect of residual stress in plating on compressive strength (Carlsen, 1980)

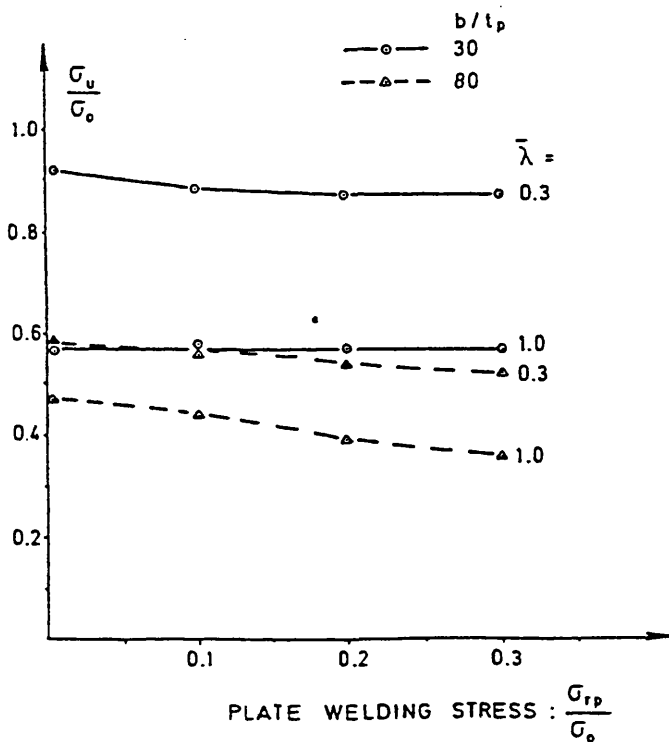


Fig. 4.22 Effect of residual stress in plating on compressive strength (Carlsen, 1980)

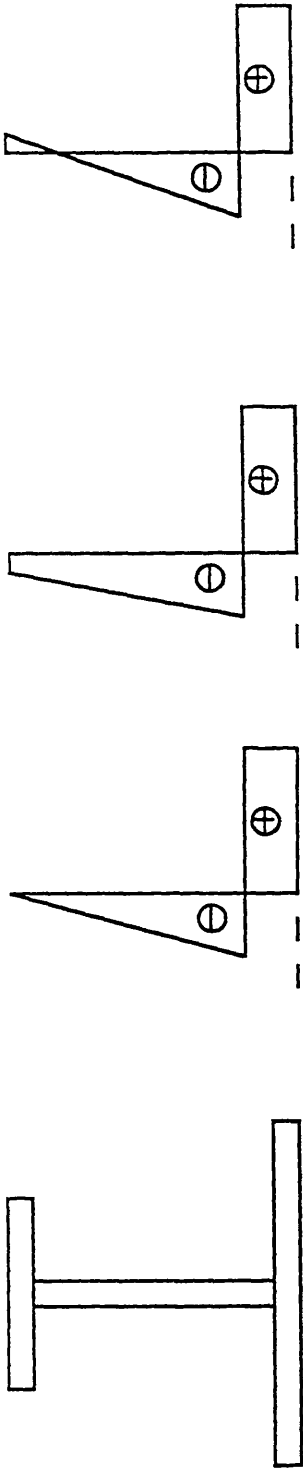


Fig. 4.23 Different assumptions in residual stress distribution of stiffeners

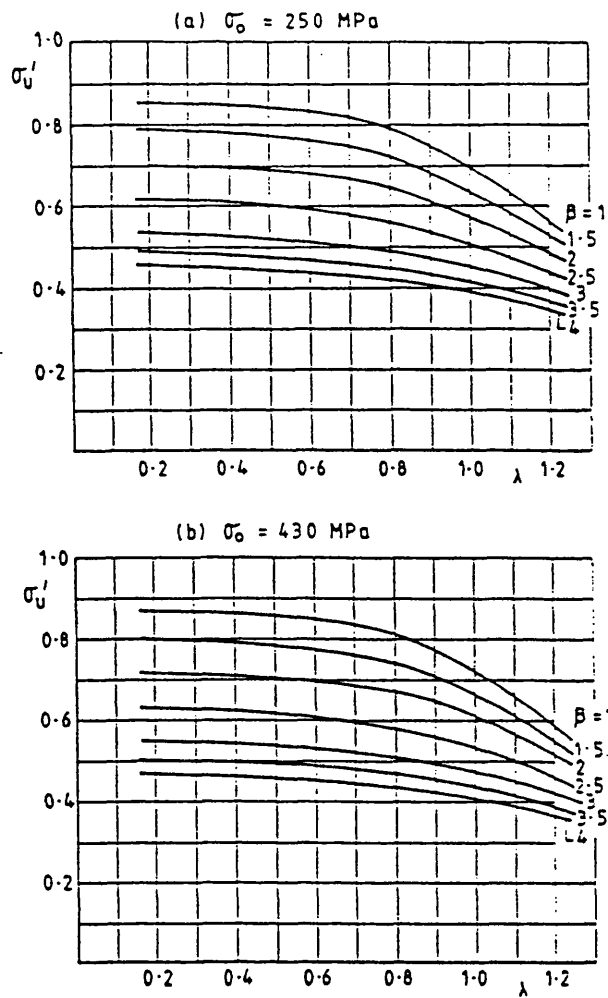


Fig.4.24 Effect of yield stress on compressive strength (Smith et al, 1991)

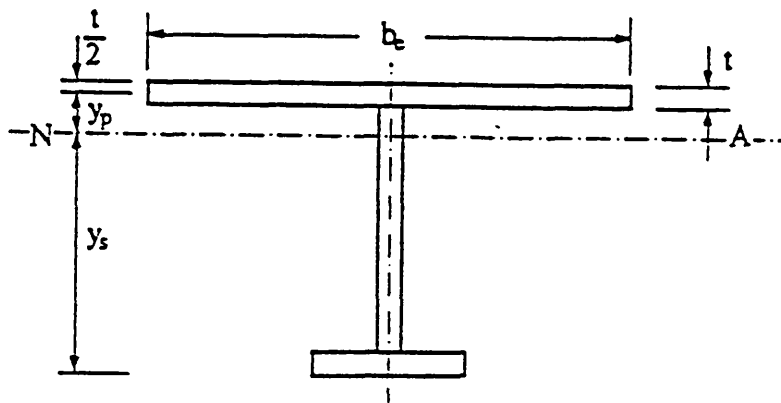


Fig. 4.25 Definition of some parameters for cross-section of column (Chapman et al, 1991)

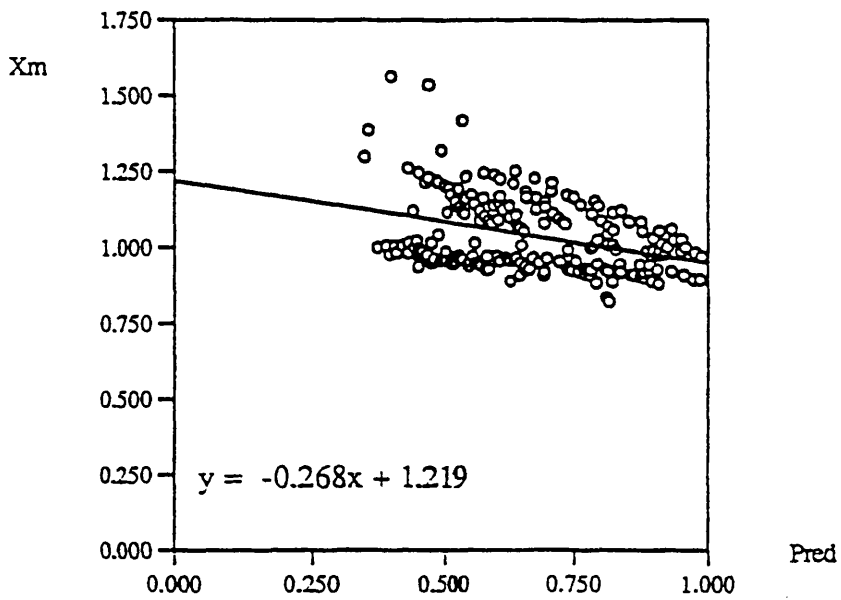
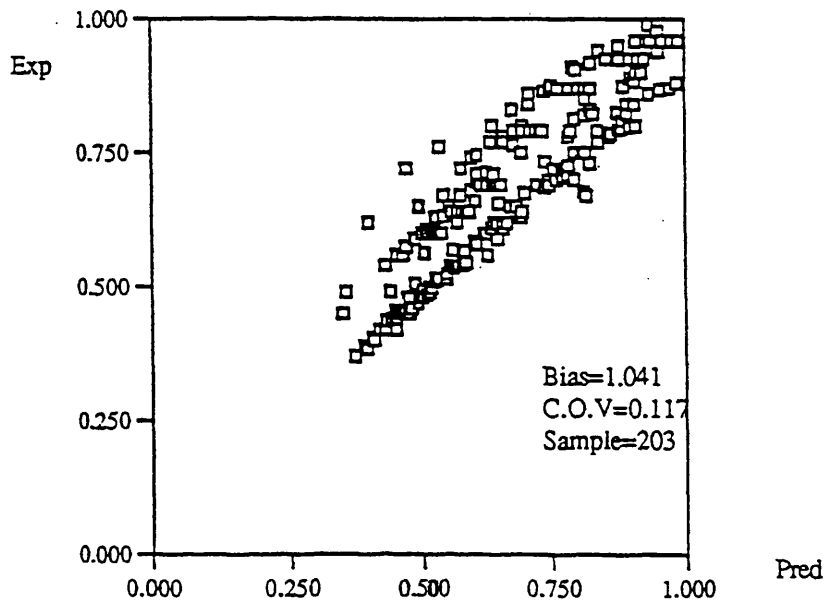


Fig. 4.26 Results of Faulkner's method

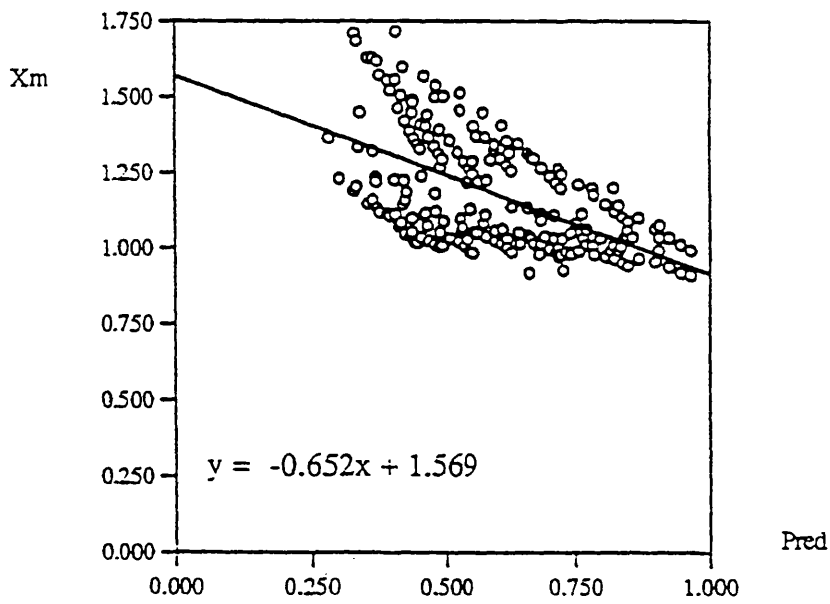
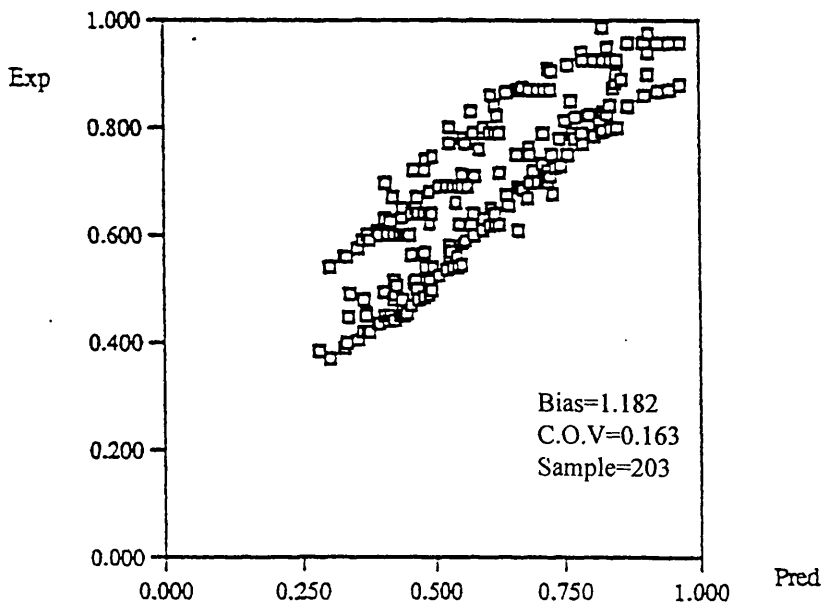


Fig. 4.27 Results of Carlsen's method

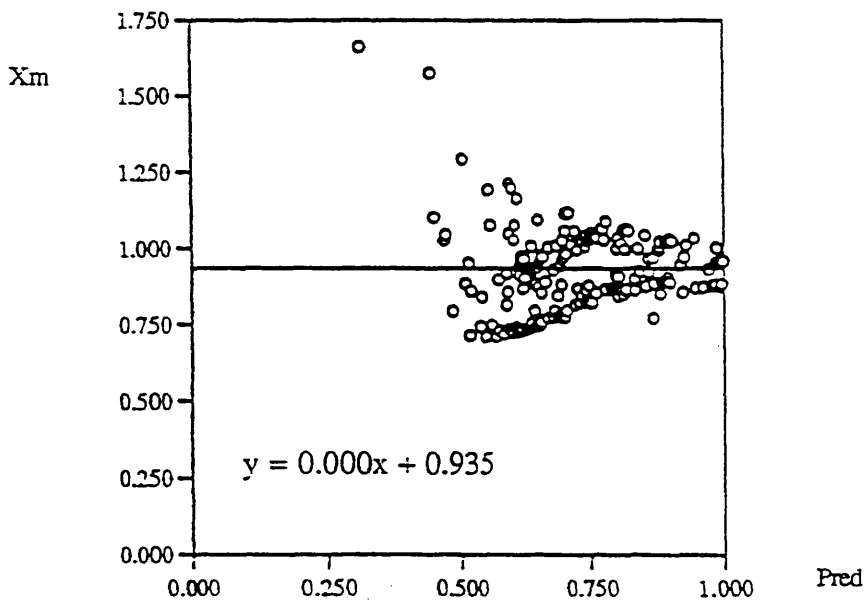
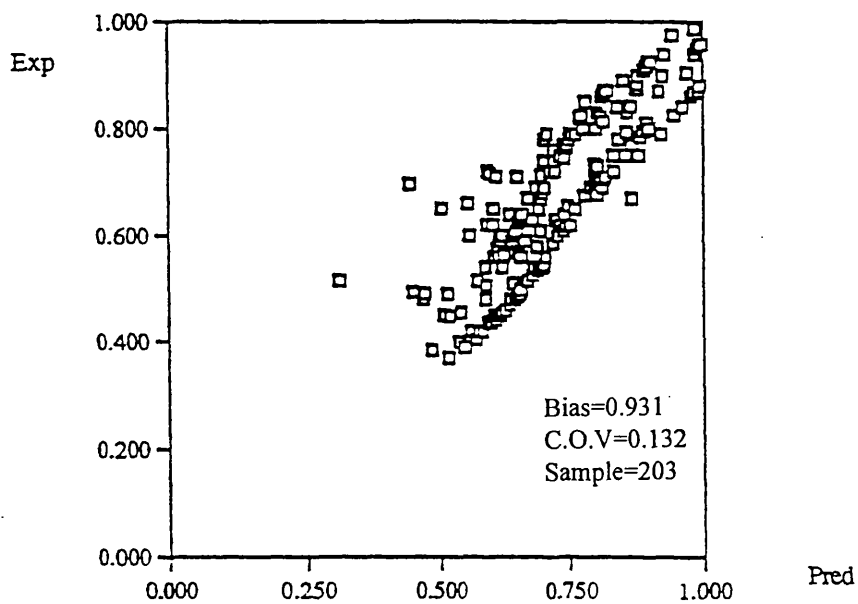


Fig. 4.28 Results of Imperial College's method

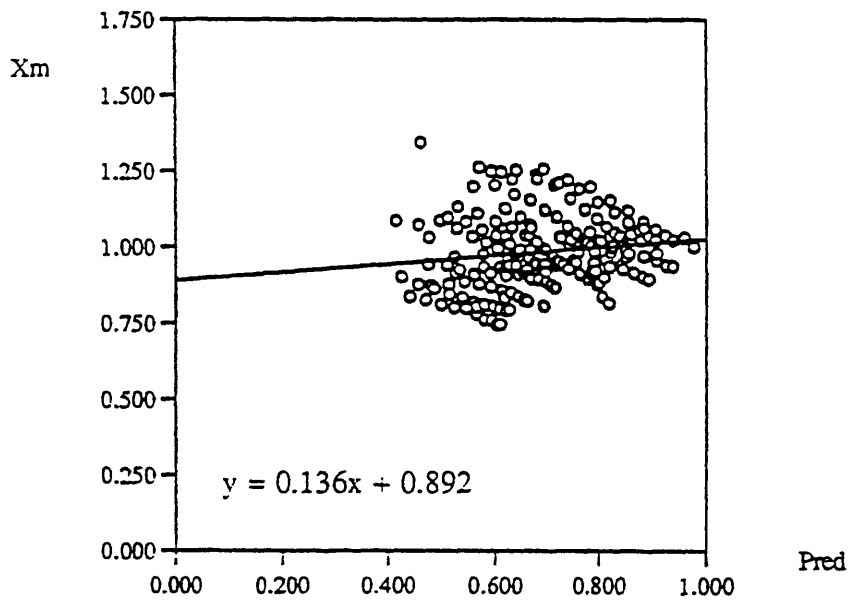
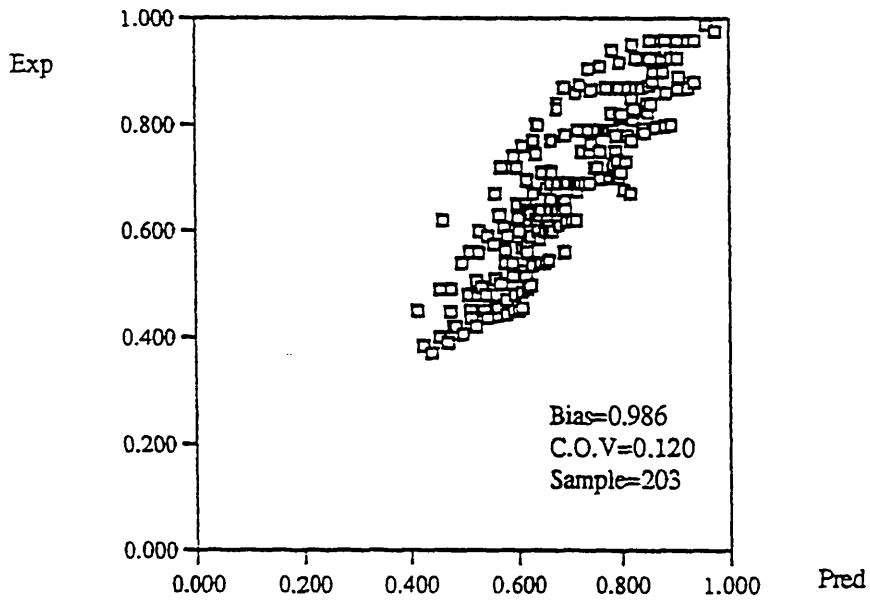


Fig. 4.29 Results of proposed method

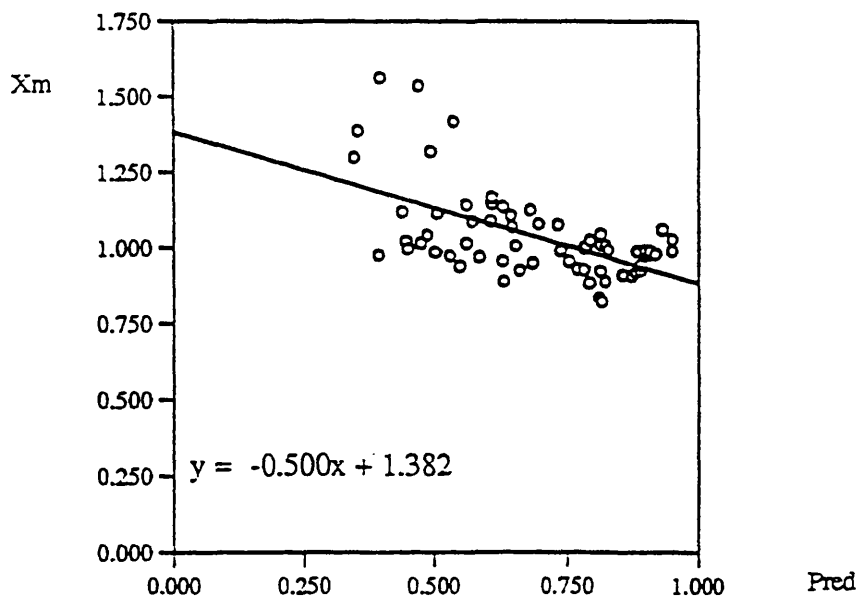
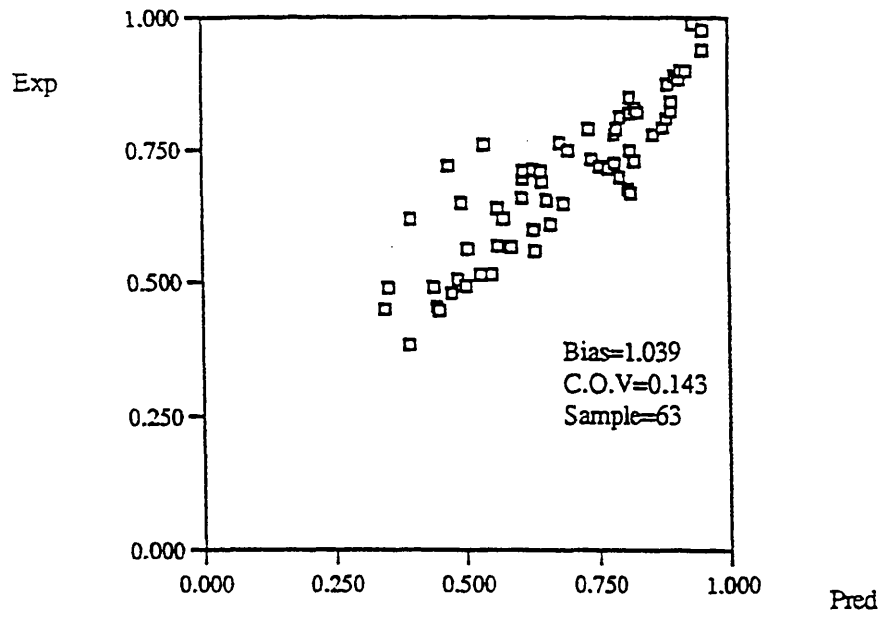


Fig. 4.30 Results of Faulkner's method from experimental data

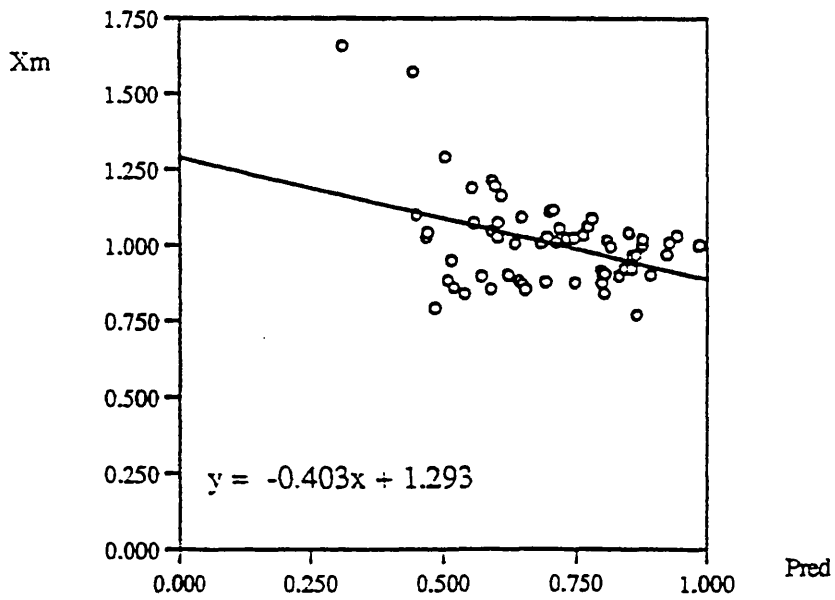
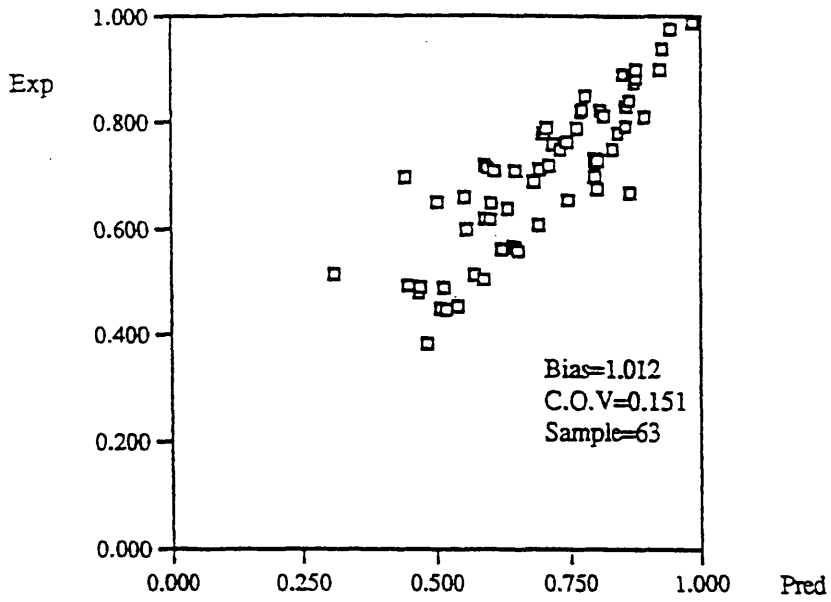


Fig. 4.31 Results of Imperial College's method from experimental data

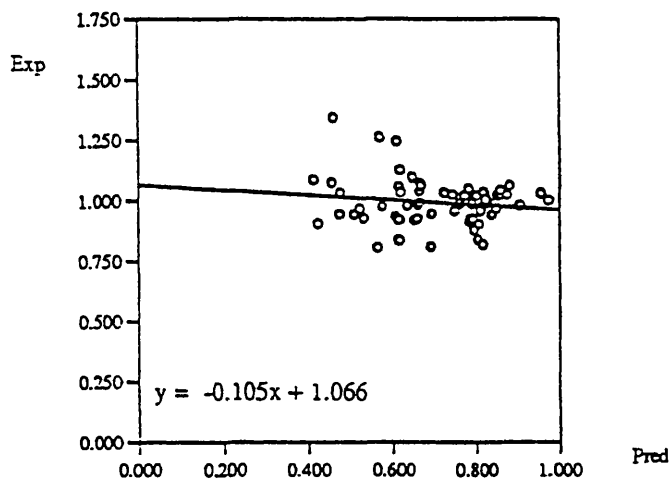
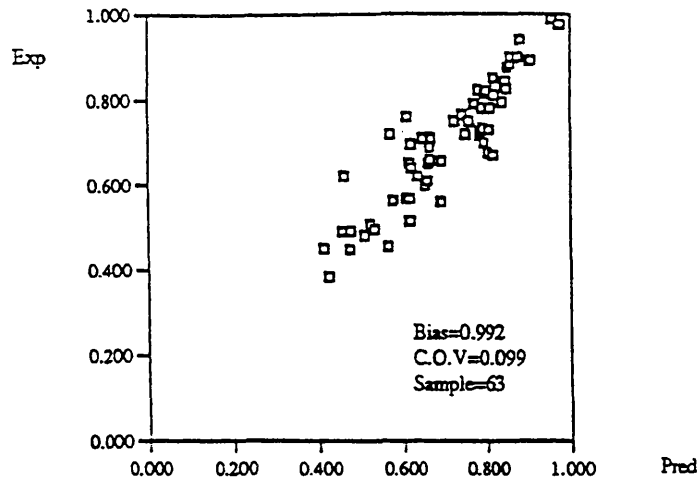


Fig. 4.32 Results of proposed method from experimental data

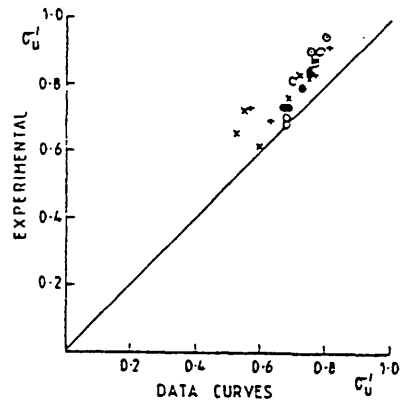


Fig. 4.33 Correlation of numerical and experimental results (Smith et al, 1991)

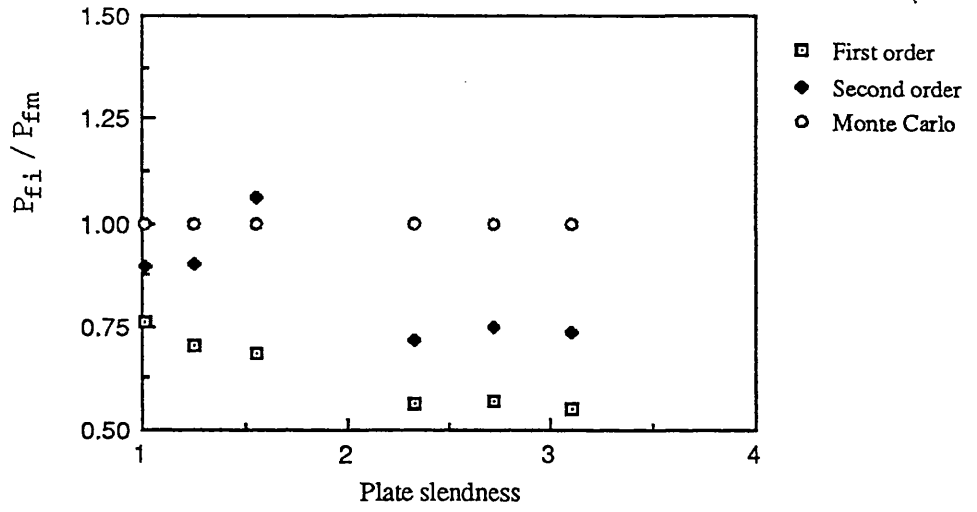


Fig. 4.34 Reliability of plate panels by Guede Soares' formulae

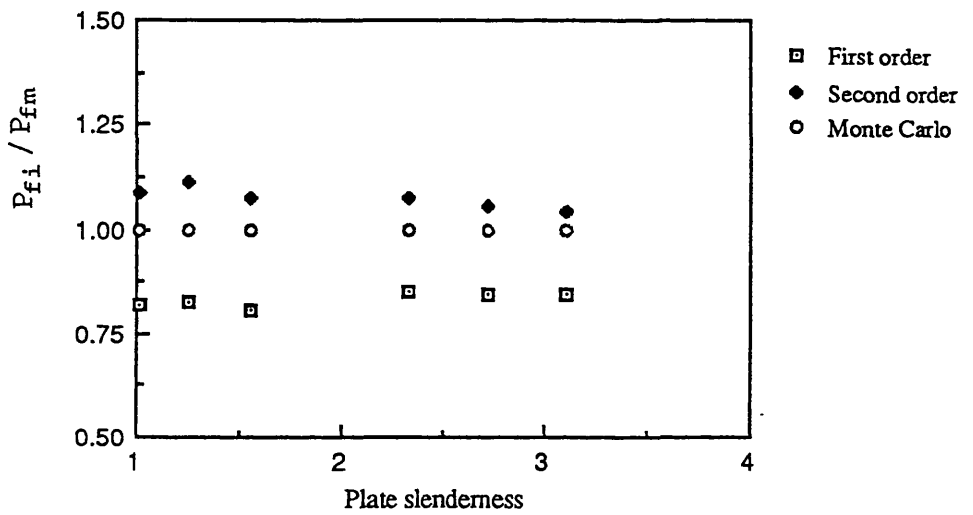


Fig. 4.35 Reliability of plate panels by Faulkner's formulae

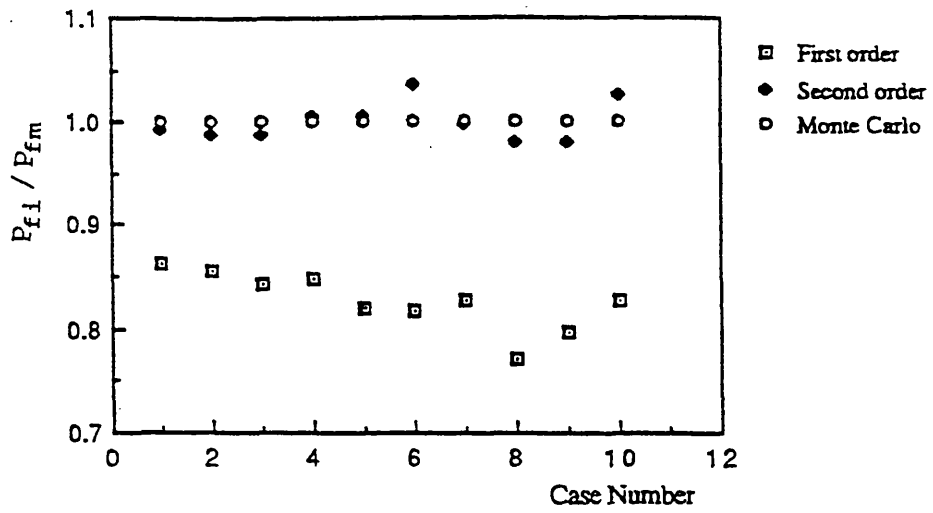


Fig. 4.36 Failure probability of stiffened plates by Faulkner's method

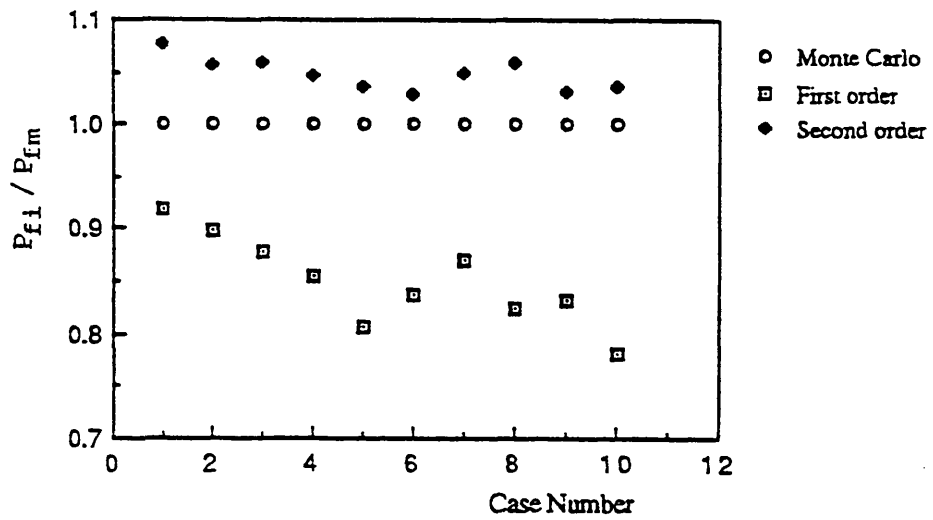


Fig. 4.37 Failure probability of stiffened plates by proposed method

CHAPTER 5 STRUCTURAL SYSTEM RELIABILITY ANALYSIS OF PATRIA

5.1 INTRODUCTION

Due to the complexity of the geometry of SWATH, the simple beam theory could no more be easily applied to calculate even the primary stresses in the structure. It is necessary to carry out the finite element method to fulfil such work. Since the appearance of the finite element method, it has gradually been recognised as a reliable and powerful tool in the structural analysis and other fields. With the improvement of commercial FE software and the emergence of the high speed computer, it is possible to evaluate the stresses in a complicated structure. But because there is a considerable amount of work involved in the preparation of input data and post-processing of the obtained results, three dimensional computation is extremely time-consuming and costly.

Although some researchers have tried to model the whole ship by finite element method, the meshes used in their analyses were so coarse that the results from this work can only be used as the boundary condition in a finer mesh. For the purpose of getting realistic stresses in the structure, further finer finite element analysis should be carried out.

As can be seen in Chapter 2, structural system reliability analysis is a powerful tool, but it is computationally time-consuming and costly. During the system reliability analysis the finite element analysis is repeatedly carried out to automatically establish the safety margins at different stages. For a complex structure, such as SWATH, it is impossible to carry out system reliability analysis by directly using a three-dimensional model. So some simplifications have to be introduced.

Murotsu et al (1990, 1991) has applied the system reliability techniques to a SWATH ship. In the analysis the whole ship was modelled by spatial beam frames to which only the wave induced side force was applied. The transverse sections were modelled by a series of transverse beam elements and the lower hull, as well as the decks, were modelled by longitudinal beam elements. The critical failure paths were shown to be around the middle part of the ship.

The aim of this chapter is to apply the system reliability techniques developed in Chapter 2 to a typical transverse frame in the middle part of a built SWATH ship. Firstly, the selected frame structure will be idealised by a one-dimensional model through a series of finite element analyses. Then a structural system reliability method will be applied to the one-dimensional model. The critical sections in the transverse frame are identified through this analysis.

5.2 MODELLING OF A TYPICAL FRAME SECTION OF PATRIA

5.2.1 Ship Particulars

The various particulars of the PATRIA are:

Displacement	169 tonnes
Mean draught, t	2.7 m
Lower hull length	31.05 m
Overall length	36.50 m
Lower hull diameter H_D	1.8 m
Single strut	
Strut width T_S	1.0 m
Submerged strut height D_S	1.1 m
Box width B	13.0 m
C_{wp} (water plane coefficient)	0.80
Strut height S_H	1.65 m
Box depth D_B	1.0 m
Section depth D	5.9 m

The dimensions of the ship are shown in Fig. 5.1.

5.2.2 Materials

The structure is made up of aluminium and the various allowable stresses in frame structure for structural design are as follows. This will depend on the location of the material, i.e. whether it is at welded zones or not.

Alloy	Bending (N/mm ²)	Shear (N/mm ²)
AlMg4.5Mn(5083)NS8	145	82
AlMg4.5Mn(heated zone)	97	54
AlMgSi 1-T6(6082)HE30	145	81
AlMgSi 1-T6(heated zone)	70	40

A stress usage factor of 0.67 has been used in the design.

Stress usage factor = design stress / 0.2% welded proof stress.

5.2.3 Three-Dimensional Model

A three-dimensional model, which represents the structures between frame 8-12 of PATRIA, is shown in Fig. 5.2. The model includes four frames and one bulkhead spaced at 1250 mm. Thus the length considered is 5 meters between frames 8-12. Due to symmetry of the structure, only half hull extending to the mid-point is considered. Both the upper and lower decks are of 4 mm stiffened extruded sections, the stiffeners being spaced longitudinally at 333 mm approximately. Between frames and bulkhead, there are two transverse stiffeners of aluminium section bulb extending up to just outboard of the haunch. The arrangement of the stiffeners in the upper and lower deck is shown in Fig. 5.3, and the dimensions of all the stiffeners used in the structure are shown in Table 5.1. The geometric properties of the stiffeners are shown in Table 5.2, in which K_t is torsional constant, I_{yy} second area moment about y-axes, I_{zz} second area moment about z-axes, A section area, SA_y effective shear area in y-direction, SA_z effective shear area in z-direction.

Table 5.1: Dimensions of stiffeners

Designation	<u>365</u>	<u>243</u>	<u>184</u>	<u>161</u>
Overall width (mm)	300	300	300	300
Plating thicknesses (mm)	3	4	4	6
Total depth (mm)	68	52	52	52
T-bar width (mm)	25	20	50	50
Web thickness (mm)	3	3	4	4
Flange thickness (mm)	5	4	5	9
Weight (kg/m)	3.27	4.05	4.61	6.82
Inertia (cm ⁴)	59.05	24.85	53.14	75.7
Modulus (cm ³)	10.71	4.99	12.20	18.31

Table 5.2: Geometric properties of stiffeners

Stiffener Type	Kt(mm ⁴)	I _{yy} (mm ⁴)	I _{zz} (mm ⁴)	A(mm ²)	SA _y (mm ²)	SA _z (mm ²)
161	12939	93950	78840	598	148	148
184	3001	52310	85720	422	172	172
243	822.7	2766	50090	212	132	132
Bulb Angle	22680	8899	270800	529	244	244
Type 3	853.3	213.3	21333.3	160	160	160

The model consists of QSI4 shell elements and BMS3 beam elements. The total element number is 4360, and total node number is 4558. The loads were applied to the lower hull of frames and bulkhead as concentrated loads.

Apart from the enormous amount of time spent on the preparation of input data and processing of obtained results, computation time at a PC 486 is around seven hours.

The deformation of the structure is shown in Fig. 5.4. Figures 5.5(a) and 5.5(b) show the transverse stress distribution in the upper deck at mid-frame and bulkhead respectively. The transverse bending stresses remain more or less uniform inboard of the haunch, while the maximum occurs just after the junction of cross-structure and inner haunch due to decrease in stiffness of deck in the absence of

transverse stiffeners. The stress decreases afterwards which follows the bending moment in the deck structure. The stress distributions in the lower deck at mid-frame and bulkhead are also shown in Figs 5.6(a) and 5.6(b).

Distributions of transverse stresses at various sections of $x=-475, -2650, -3400, -4390, -5400, -6000, 6480$ mm, as well as of $y=-10, -500, -990, -1010, -1800, -2200, -2580, -2620, -3400, -4100$ mm, are shown in Figs 5.7(a) to 5.7(r) respectively. From these Figures, shear lag effect can be investigated and the effective breadth at any transverse section can be calculated using the following formula:

$$\sigma_{\max} \times b_e = \int_{-b/2}^{b/2} \sigma_{\text{nom}} \times dz$$

where σ_{\max} and σ_{nom} are the maximum and average transverse stress respectively in the deck, b and b_e are the hull breadth and effective breadth at transverse section. The effective breadth at mid-frame in the upper deck is shown in Fig 5.8. It can be seen that there is not much decrease in effective breadth of deck inboard of haunch, while there is some effect at just outboard of haunch. An interesting phenomenon, which is worth mentioning here, is that the stresses of the upper deck outboard of haunch at the frames and bulkhead are less than those at mid-space in the Figs 5.7(d) and 5.7(e). To investigate this effect, another three-dimensional model, in which the transverse stiffeners in the decks were deleted, was created. It is found that this phenomenon is attributed to the discontinuity of transverse stiffeners in the decks.

Transverse stress distributions along inside and outside haunch at bulkhead are shown in Figs 5.9(a) and 5.9(b). The maximum transverse bending stresses at different areas are shown in Table 5.3 along with the results from two-dimensional and one-dimensional model for comparison, which will be discussed later. The equivalent stresses contours at longitudinal bulkhead are shown in Figs 5.10.

Table 5.3: Maximum Transverse Bending Stresses at Different Areas

Location		3D Model	2D Model	1D Model
End Frame	Upper Deck	65.9		
	Lower Deck	-60.3		
Mid Frame	Upper deck	55.3	51	51.8
	Lower Deck	-60.1	-61.1	-59.9
Bulkhead	Upper Deck	59		
	Lower Deck	-63		
Inside Haunch	(at midframe)	98/-59.0	132.6/-59.6	104.6/-54.9
Outside Haunch	(at midframe)	-98.5/59.3	-156.8/63.3	-151/65
Inside Strut		-56.0	-55.06	
Outside Strut		57.9	59.28	

5.2.4 Two-Dimensional Model

Having obtained effective breadth from three-dimensional calculations, a two-dimensional model representating the mid-frame in the three-dimensional model was generated. The mesh was shown in Fig. 5.12, and the deflection in Fig. 5.13. The web plate was represented by membrane and the flange and associated shell by bar elements. Total element number is 467, and total node number is 375. Computation time is only about 10 minutes on a PC 486.

The key step in making the two-dimensional model equivalent to the three-dimensional model is to get the correct effective breadths 'b_e' at different parts in transverse direction. Under the condition that no three-dimensional results are available, the following empirical formula can be used to estimate the effective breadth.

$$b_e = \left[1 - \left(\frac{7 - l/b}{7} \right)^3 \right] \times b \leq b$$

In which b_e is effective breadth, b full breadth, l spacing of the frames considered. The effective breadths at decks inboard and outboard of cross-structure, inner and out haunch, inside and outside strut, and lower hull were calculated by using the above formula and listed in Table 5.4. The locations in Table 5.4 were marked in Fig. 5.12. Details are shown in Das and Pu (1993).

Table 5.4: Effective breadths at different parts

Location	By Formula	By 3D results	Error (%)
1	6058	6058	0
2	3580	5000	28
3	3862.5	4550	15
4	3493	3384	3
5	3052	-----	-----
6	1525	-----	-----

In addition, the effective breadths have been calculated based on the three-dimensional results, and listed in Table 5.4 for comparison. Unfortunately, the stress distribution can not be used to calculate the effective breadth at lower hull because the side force was applied as a concentrated force at the hull, so the stress concentration at these areas is strong.

From Table 5.4 it is shown that the empirical formula is accurate in the area where the stress level changes slowly, but not in the area where stresses change rapidly. Furthermore, the effective breadths were compared with the results in Stirling (1988). There is much difference due to the discrepancy in the geometry of the two structures.

In Figs 5.14(a) and (b) the transverse stress distributions along the top and bottom decks of the mid-frame are shown respectively. It is shown that there is good agreement of the stress distribution between the three- and two-dimensional model. The stresses at various positions of the structure for the two-dimensional are shown in Fig. 5.15, and the maximum value in Table 5.3.

The results in Table 5.3 show that the stresses in decks and shell of haunch agree well, but there is much difference in the flange of the haunch. The difference was caused by adopting average effective breadth in the haunch area. In fact, as can be seen in Fig. 5.8(b), the effective breadth at the junction of haunch and strut is smaller than average. This means that the actual neutral line of the beam near the junction of haunch and strut is closer to the central point of the web plate. In other words, the actual difference between the stress at flange and shell is not as large as that shown in two-dimensional analysis. So, it may be said that the two-dimensional analysis exaggerates the stress concentration in haunch area. Whereas, on the whole, the two-dimensional results agree well with three-dimensional results.

5.2.5 One-Dimensional Model

A one-dimensional model was created to represent the mid-frame. Its mesh is shown in Fig. 5.16. There are thirty four two-dimensional beam elements. Total node number is thirty two. Computation time is about 2 minutes on a PC 486.

Strictly speaking, some parts of the frame are not suitable to use the beam elements to simulate, some techniques need to be adopted in the process. Because the junctions of the lower deck and the haunch and the junctions of the haunch and the strut are much stronger than the other parts, rigid ends elements (Hughes, 1983) should be used. Unfortunately, such elements are not accommodated in LUSAS, so in the present study, these parts were represented by beam elements with larger geometric properties. In addition, from Fig. 5.15, it can be seen that the strut behaves like a whole beam. Hence, the geometric shape was changed to a single line, as seen in Fig. 5.16. Furthermore, the properties of the elements 9, 10, 14 and 15 were assigned an extremely large value in order to simulate the real situation.

The moment diagram of the one-dimensional model is shown in Fig. 5.17. The stress distribution in the deck line is shown in Fig. 5.18. There is a good agreement between the two- and one-dimensional results. In addition, the largest stress value in the haunch is -151, which is close to the two-dimensional result. The deformation of the one-dimensional model is shown in Fig. 5.19. The deflections of several points of one- and two-dimensional models are listed in Table 5.5. The positions of these points are marked in Fig. 5.18.

Table 5.5: The deflections of different points

Location	Deformation 2D(u/v)(mm)	Deformation 1D(u/v)(mm)	Error(u/v)(%)
Point 1	0.24/-35.6	0.3/-33.4	20/6
Point 2	80.3/-23.7	65.2/-22.7	19/4
Point 3	58.6/-5.4	54.1/-9.1	8/68
Point 4	0.14/-9.62	0.25/-9.28	78/4
Point 5	13.4/-14.9	13.9/-21.6	4/45

5.3 LOADS

The loads considered in the system reliability analysis are wave induced loads, buoyancy, structural weight and superimposed loads including acceleration effects. Details of the calculation are presented in Chapter 3.

The statistical properties of the loads are listed in Table 5.6. How to apply the above loads is shown in Fig. 5.20. The boundary conditions are due to symmetry for central line node and restrained in vertical direction at ship side node to absorb unbalanced vertical force. All the loads are applied in the form of concentrated loads in order to reduce the total number of load cases, which is an important factor affecting the computational time.

Because the haunch and upper box parts are crucial parts in the SWATH the lower hull and strut were excluded from the system analysis.

Table 5.6: Loads used in the analysis

Type of the loads	Mean value(N)	COV
Side force (F_{10} , F_{11})	81636	0.2
Buoyancy (F_9)	56567.5	0.2
Weight of upper part (F_1 , F_2)	18798.8	0.0
Weight of lower part (F_3)	18798.8	0.0
Vertical inertial force of upper part (F_4 , F_5)	1642.3	0.2
Vertical inertial force of lower part (F_6)	1642.3	0.2
Lateral inertial force of upper part (F_7)	1149.8	0.2
Lateral inertial force of lower part (F_8)	1149.8	0.2

5.4 SYSTEM RELIABILITY ANALYSIS OF THE 1D-MODEL

The method developed in Chapter 2 is used in the present analysis. The configuration and element number of the one-dimensional model used in the calculation are shown in Fig. 5.20 (it is noted that the total number of elements in this model is different from the model shown in Fig. 5.16). The model in Fig. 5.16 was originally generated for the multiple criteria optimisation in Zanic et al (1993), where the wave induced load and buoyancy were applied in the form of instantaneous pressure distribution. In system reliability analysis all the loads are applied in the form of concentrated loads, so the element number can be further reduced. The parameters of the structure are presented in Table 5.7.

To simulate the stiff joints in the structure, the following elements, 9, 10, 14, 15, 16, 17, 20 and 21 are assigned a very large geometrical properties. In order to investigate the effect of buckling strength, both cases, interaction of bending moment and axial force, interaction of bending moment and axial force including buckling effect are calculated. The results are shown in Table 5.8. The system reliability indices for both cases are 4.113 and 3.756 respectively, and the failure paths identified in the calculation for the case B+A are shown in Fig. 5.21, in which the number inside the circle is the number of critical section, the value above the circle is

for that critical section, the value on the right of the last circle for a failure path is the reliability index for that failure path.

It is seen that the most critical section in the structure is section 35 which is in the haunch area, and the failure path with the highest failure probability is 35-37-36-38. It is interesting to note that all the sections included in the identified failure paths are in the haunch area. This is attributed to the fact that the dominant load in the structure is side force, the remaining components of the loads play a less important role.

Table 5.7: Parameters of the model

Element No.	Cross-sect. area $A_i(\text{mm}^2)$	Inertia moment $I_z(\text{mm}^4)$	Resistance (mean value) $R_i(\text{N} \cdot \text{mm})$	Coef. of correl. ρ
1,2,3,4, 5,6,7,8	0.4803e4	0.324e8	2.6207e7	0.0
11,12,13	1.177e4	0.2129e10	1.0073e9	0.0
18,19	0.650e4	0.3717e8	6.1716e7	0.0
22,23	1.400e4	0.285e10	1.2900e9	0.0
24,25,26	1.6120e4	0.3392e10	1.5179e9	0.0

Table 5.8: Results of SWATH

	B+A*	B+A+B*
β_S	4.113	3.756
P_{fu}	0.19498e-4	0.862625e-4
P_{fL}	0.19498e-4	0.862622e-4

- * B+A for interaction of bending moment and axial force
 B+A+B for interaction of bending moment and axial force including buckling effect
 P_{fu} is the upper bound of the system
 P_{fL} is the lower bound of the system
 β_S is the reliability index of the system

5.5 CONCLUSIONS

Structural system reliability method is applied to a typical cross-deck frame in a built SWATH ship. The interaction of bending moment and axial force including the buckling effect is considered in the analysis. It is found that:

- * The two-dimensional model is less time-consuming than the three-dimensional model, and has good results when the effective breadth can be accurately obtained from the empirical formula. So for a conceptual study of a new type of design, it is suggested that a three-dimensional model between critical parts of the structure should be carried out first to establish the effect of shear lag for eventual feedback to a two-dimensional model. Thus a rational design procedure, both for the frame and bulkhead, can be established, which is less time consuming and cost effective.
- * The most critical part in the typical frame is section 35 in the haunch area. The finding is the same as that by the conventional deterministic method.
- * The buckling has a moderate effect on system reliability in this particular case, and should be considered in the analysis.
- * All the critical sections included in the significant failure paths are in the haunch area. Hence it may be said that more attention should be paid to the haunch area.

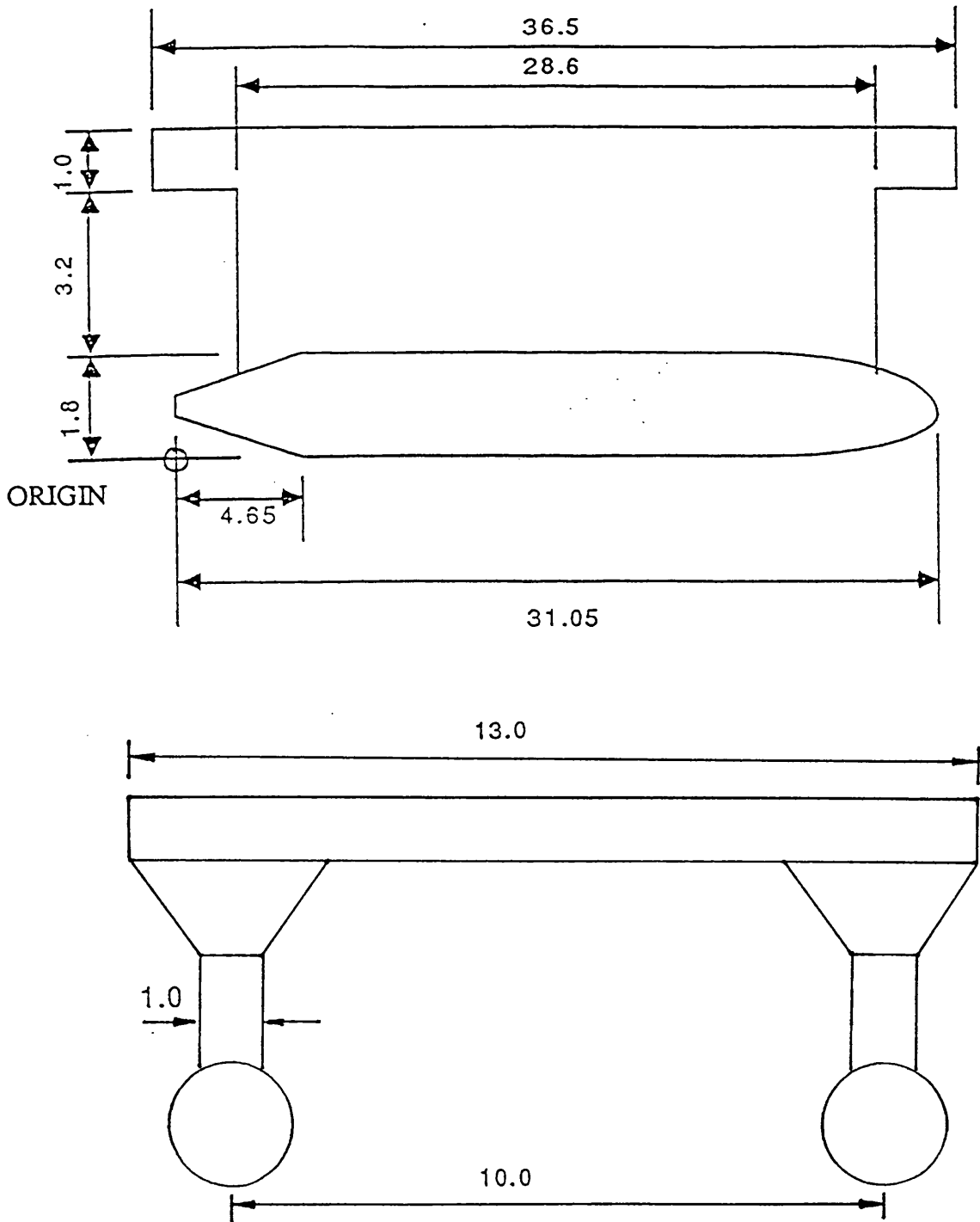


Fig. 5.1 Dimensions of the PATRIA model (in meters)

FEA

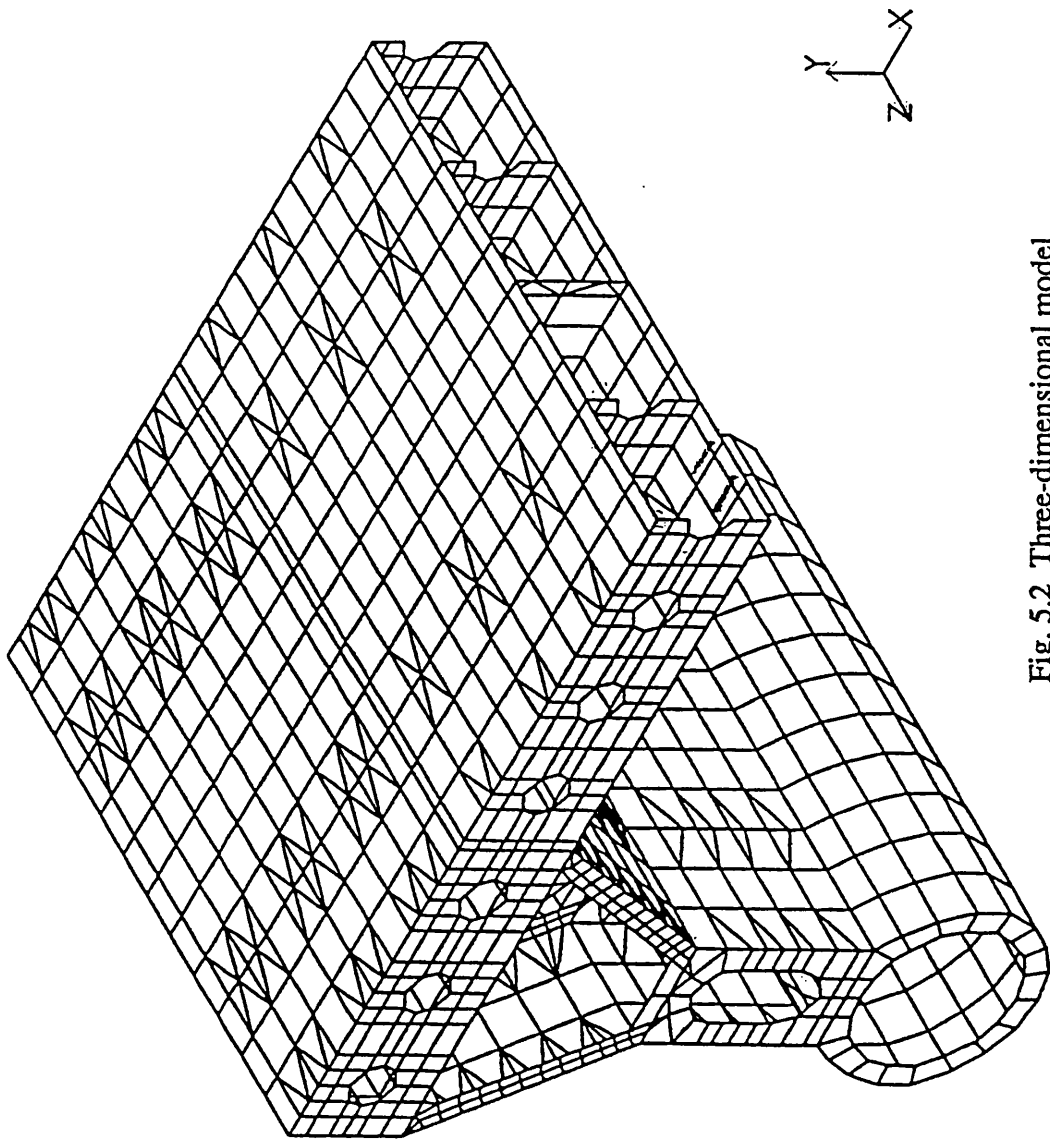


Fig. 5.2 Three-dimensional model

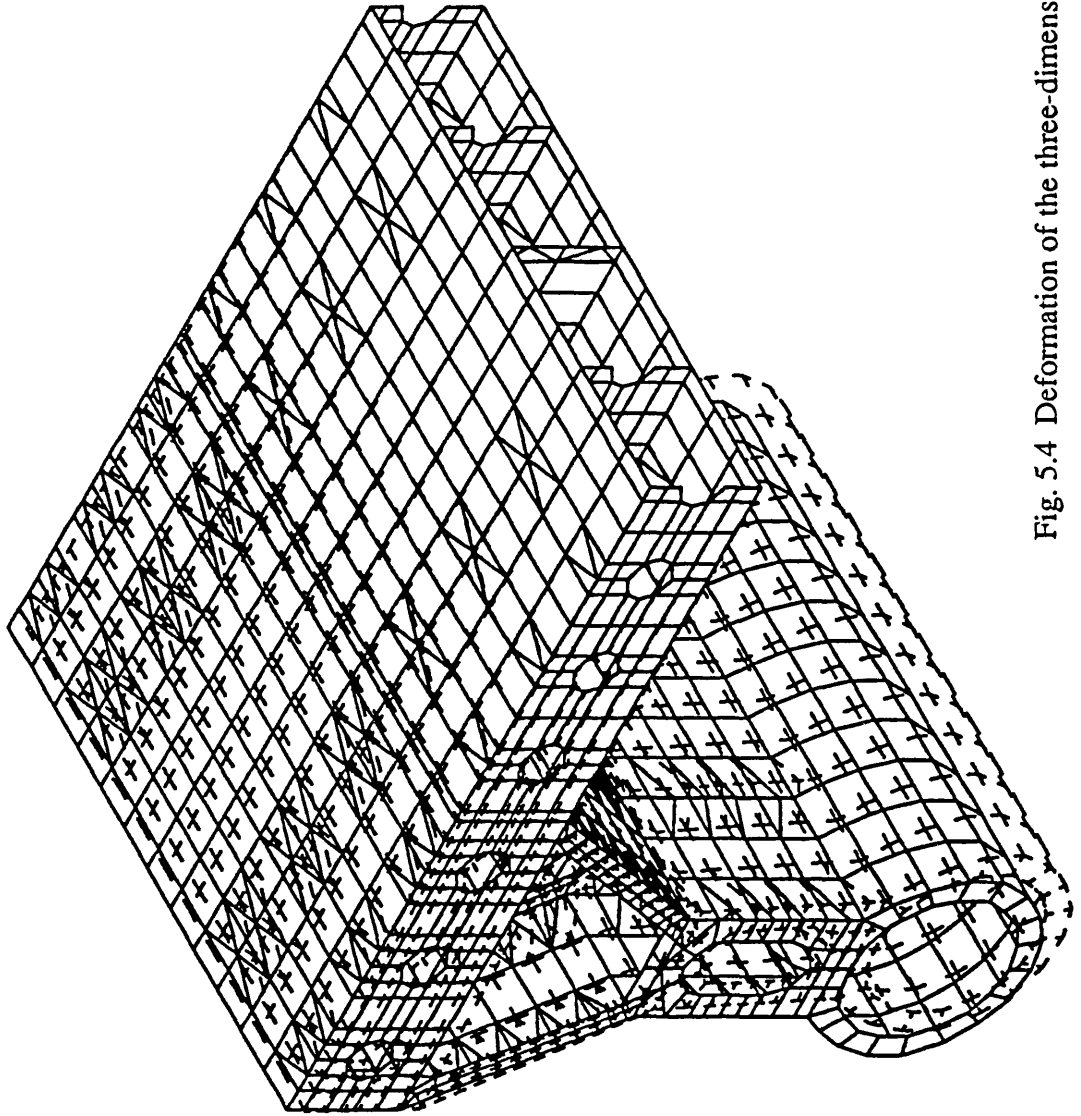


Fig. 5.4 Deformation of the three-dimensional model

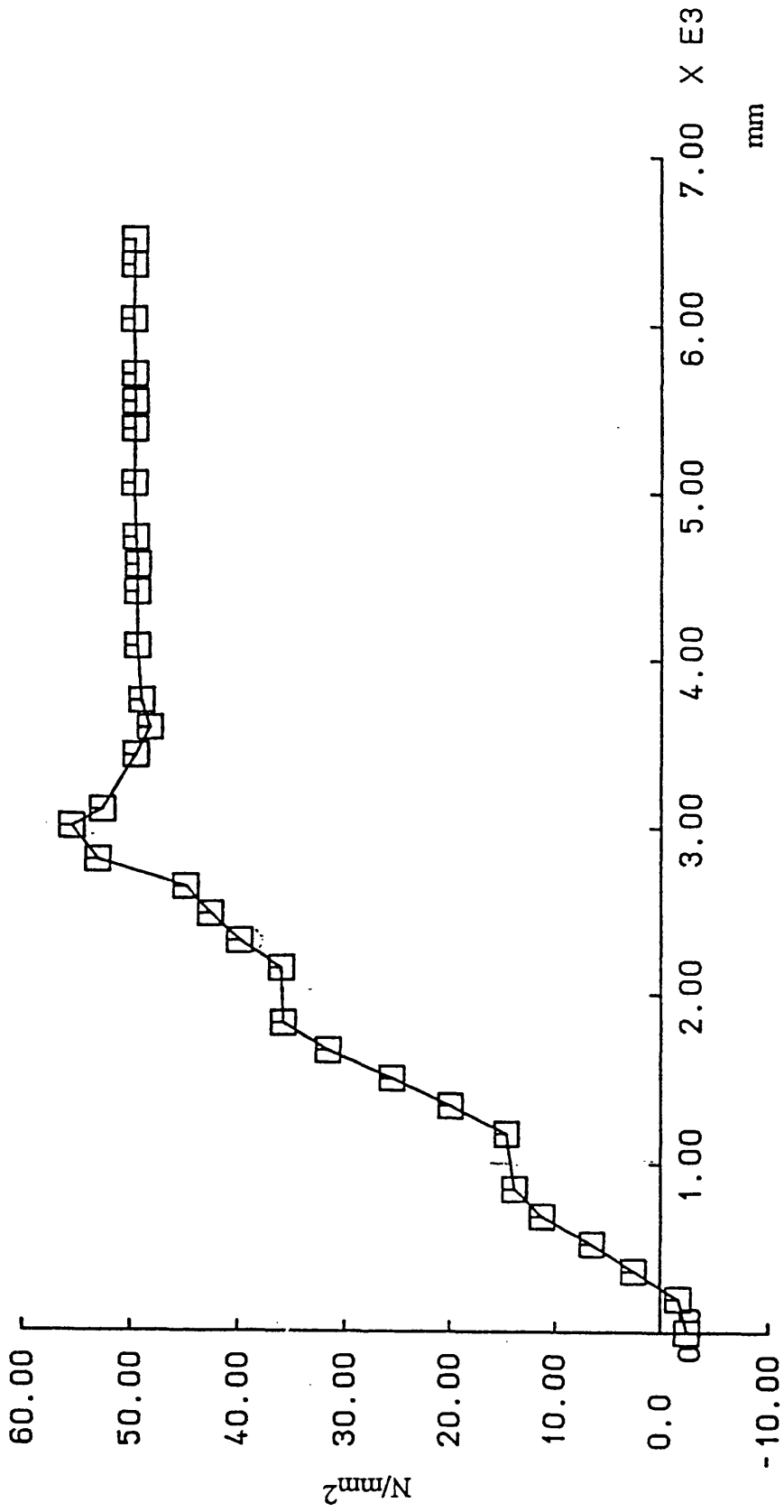


Fig. 5.5(a) Transverse stress distribution at $z=-1250$ mm on upper deck

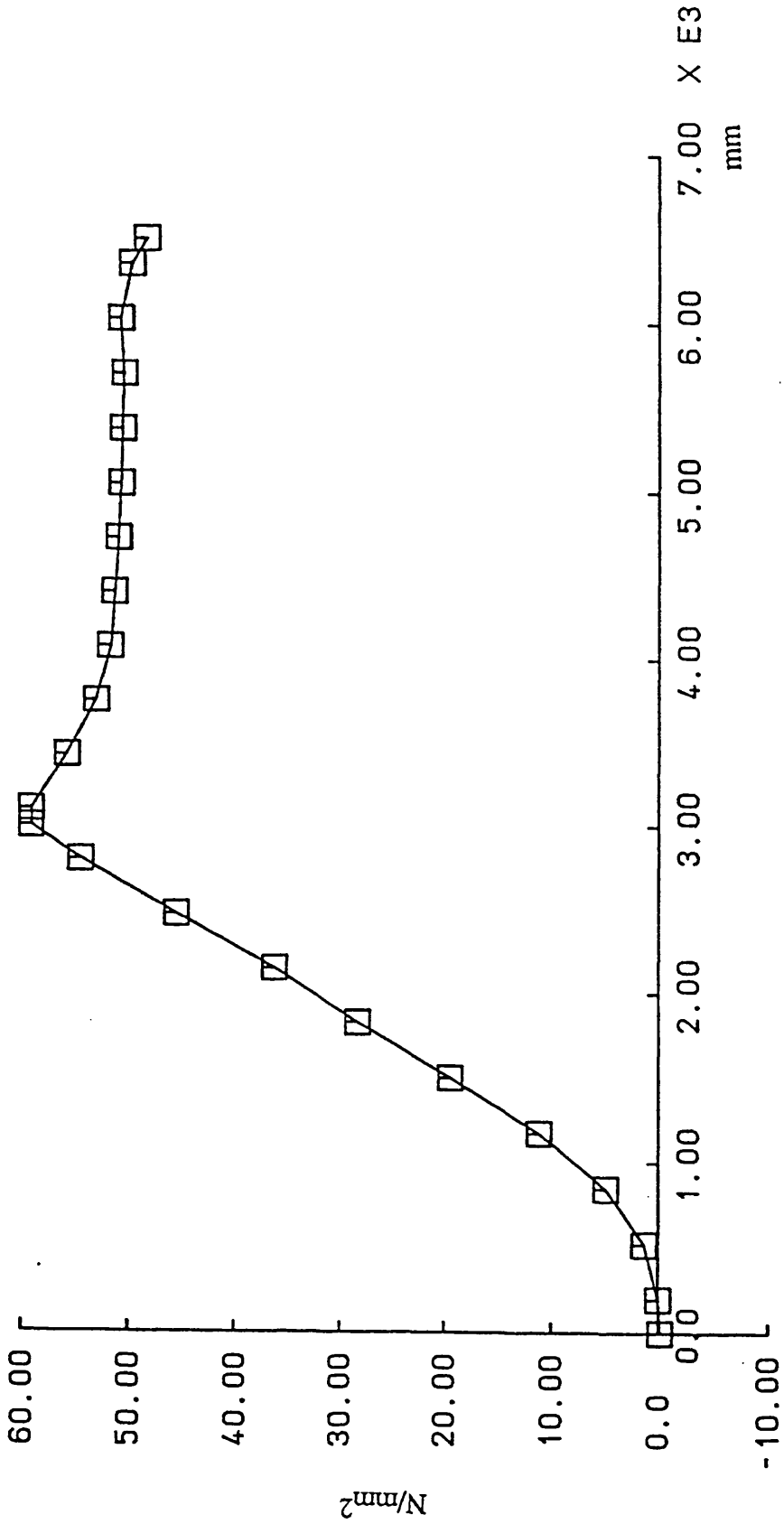


Fig. 5.5(b) Transverse stress distribution at z=-2500 mm on upper deck

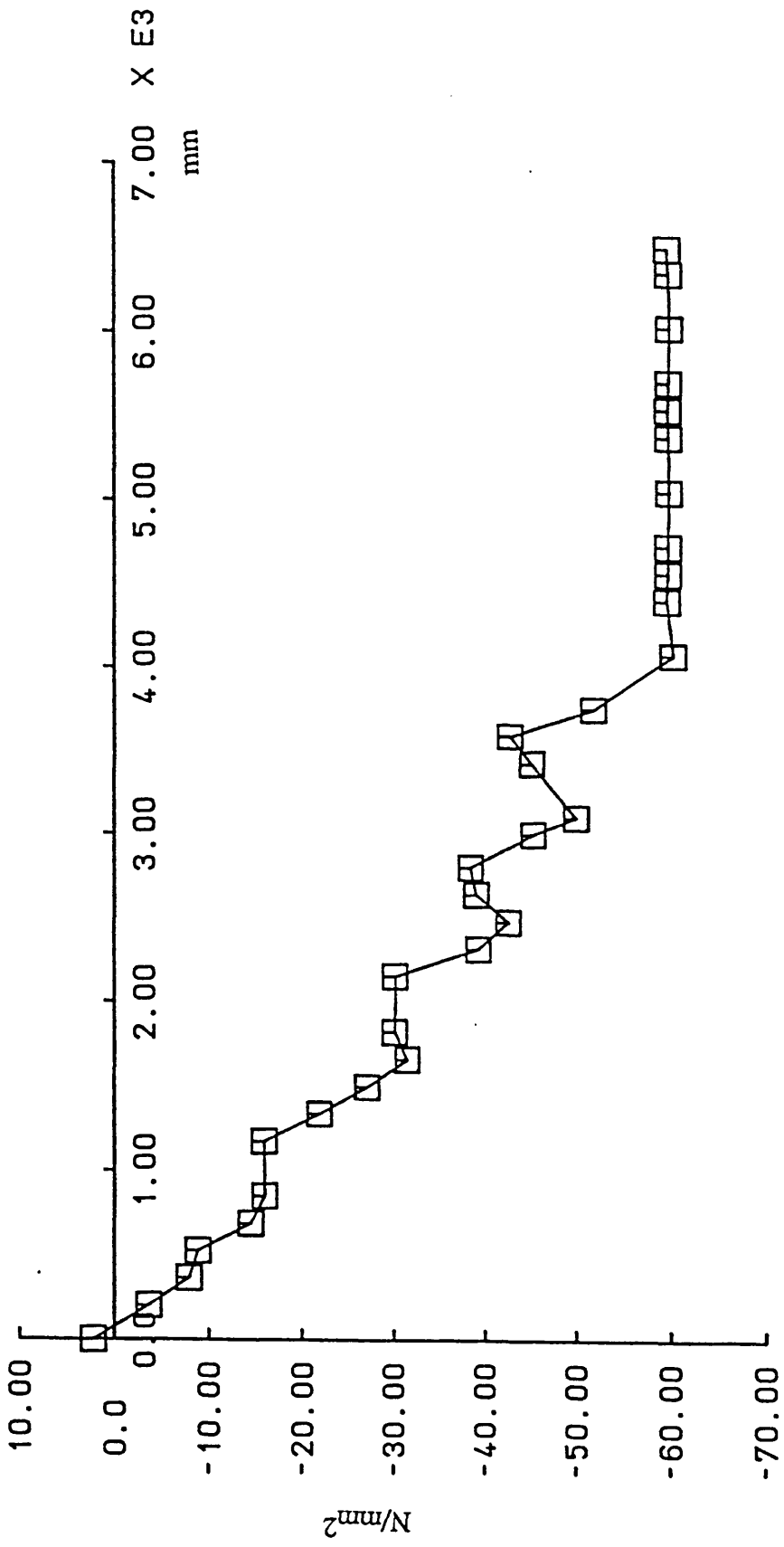


Fig. 5.6(a) Transverse stress distribution at z=-1250 mm on lower deck

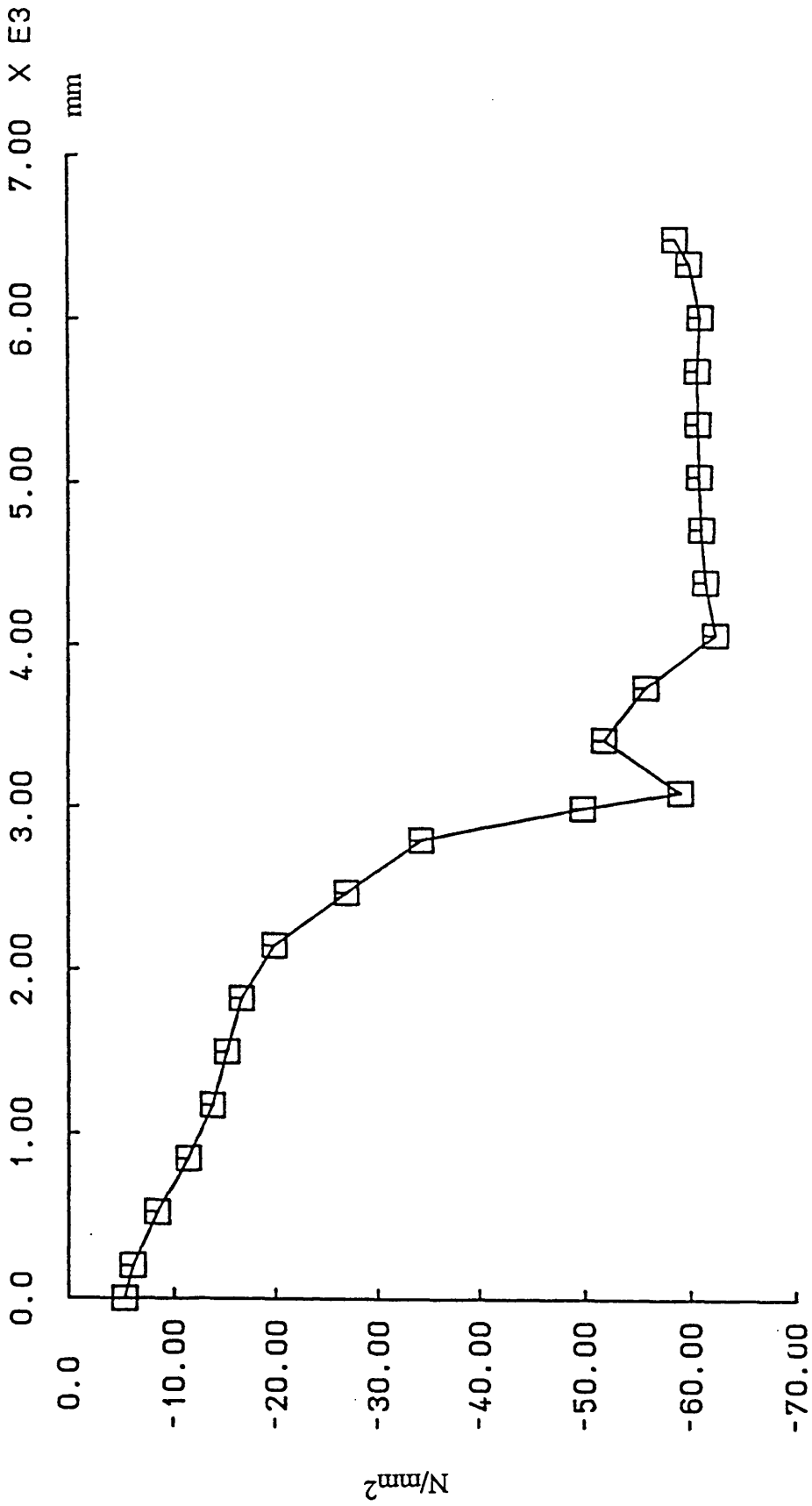


Fig. 5.6(b) Transverse stress distribution at $z=-2500$ mm on lower deck

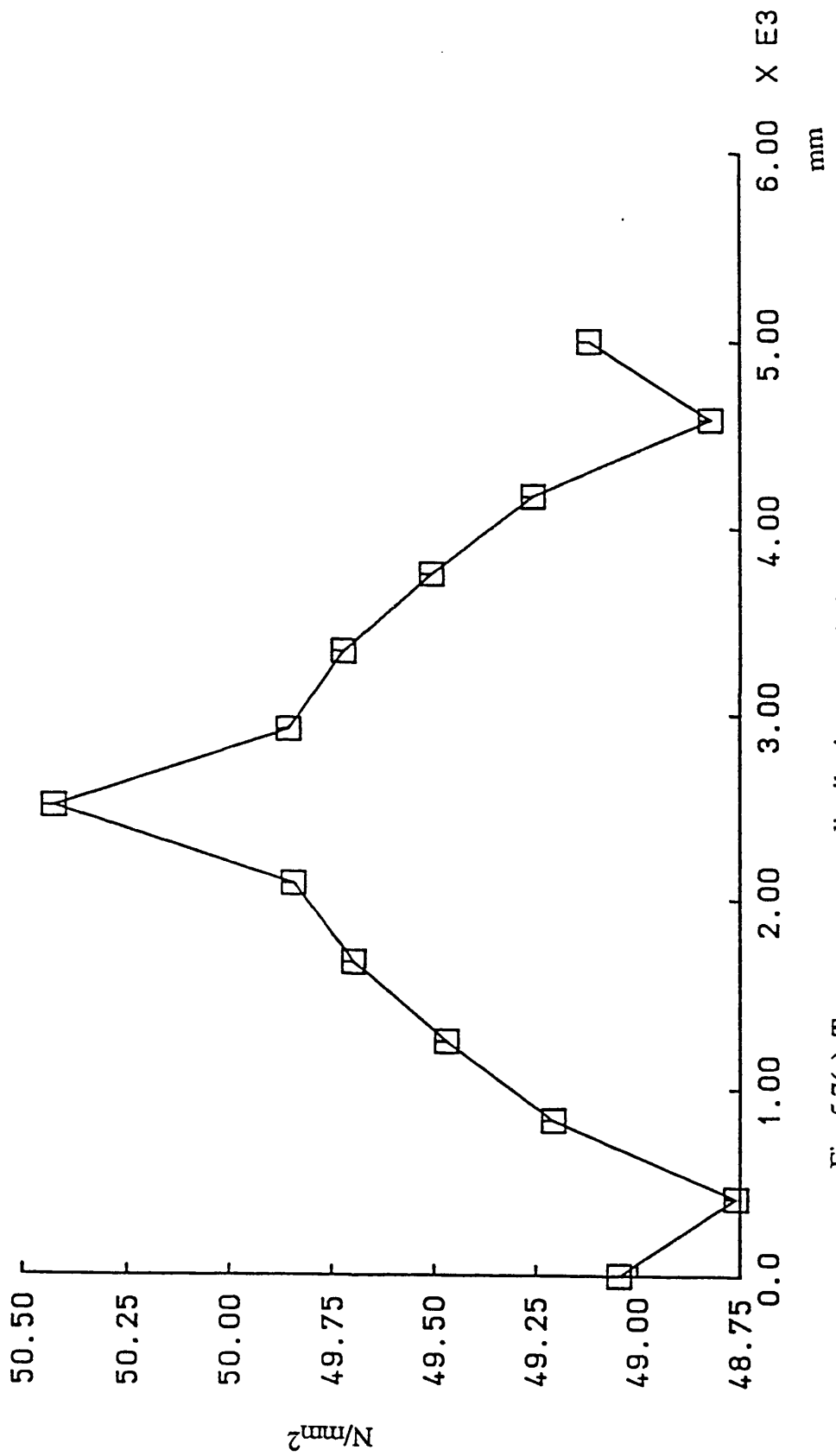


Fig. 5.7(a) Transverse stress distribution at x=-475 mm on upper deck

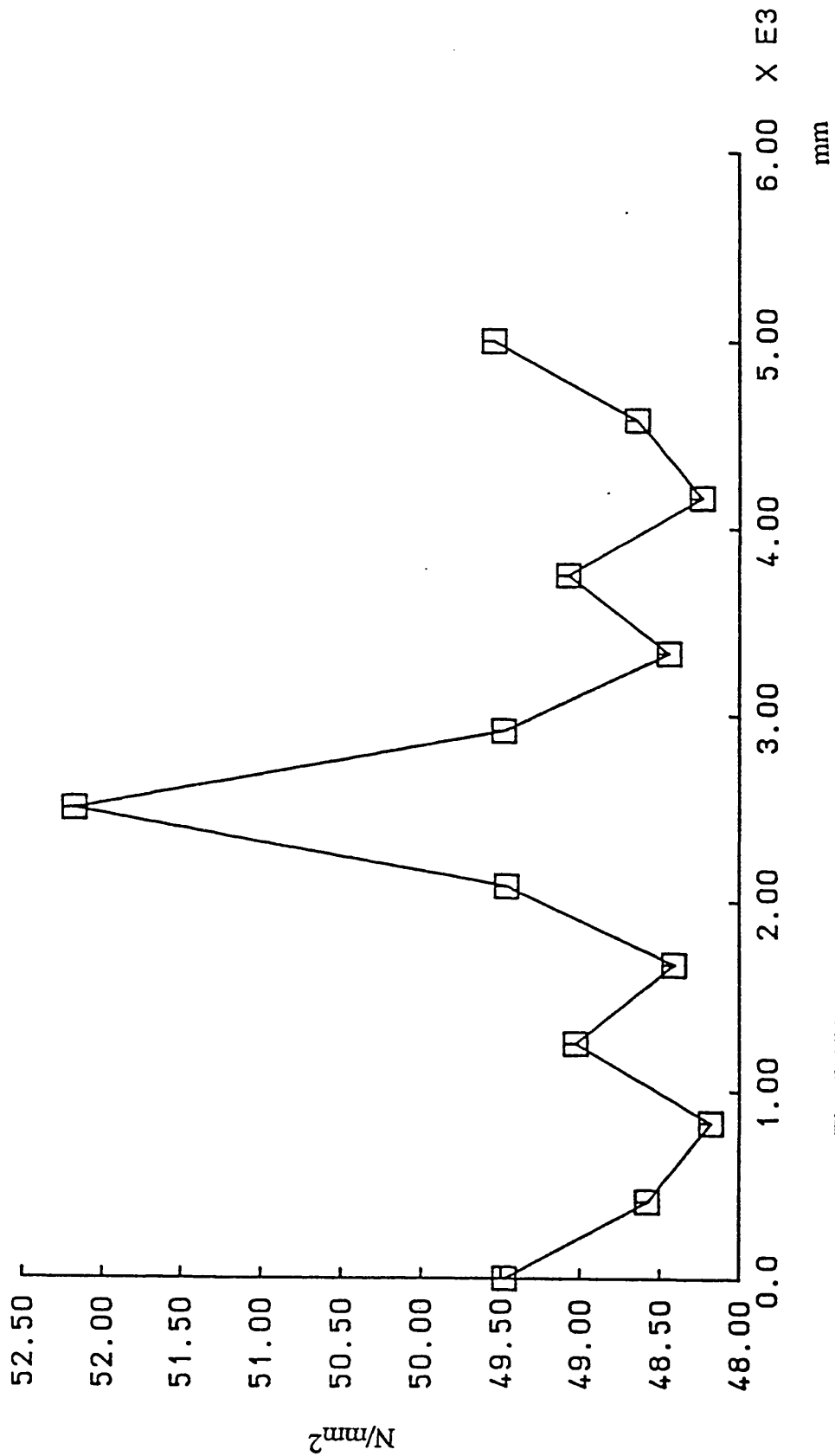


Fig. 5.7(b) Transverse stress distribution at x=-2600 mm on upper deck

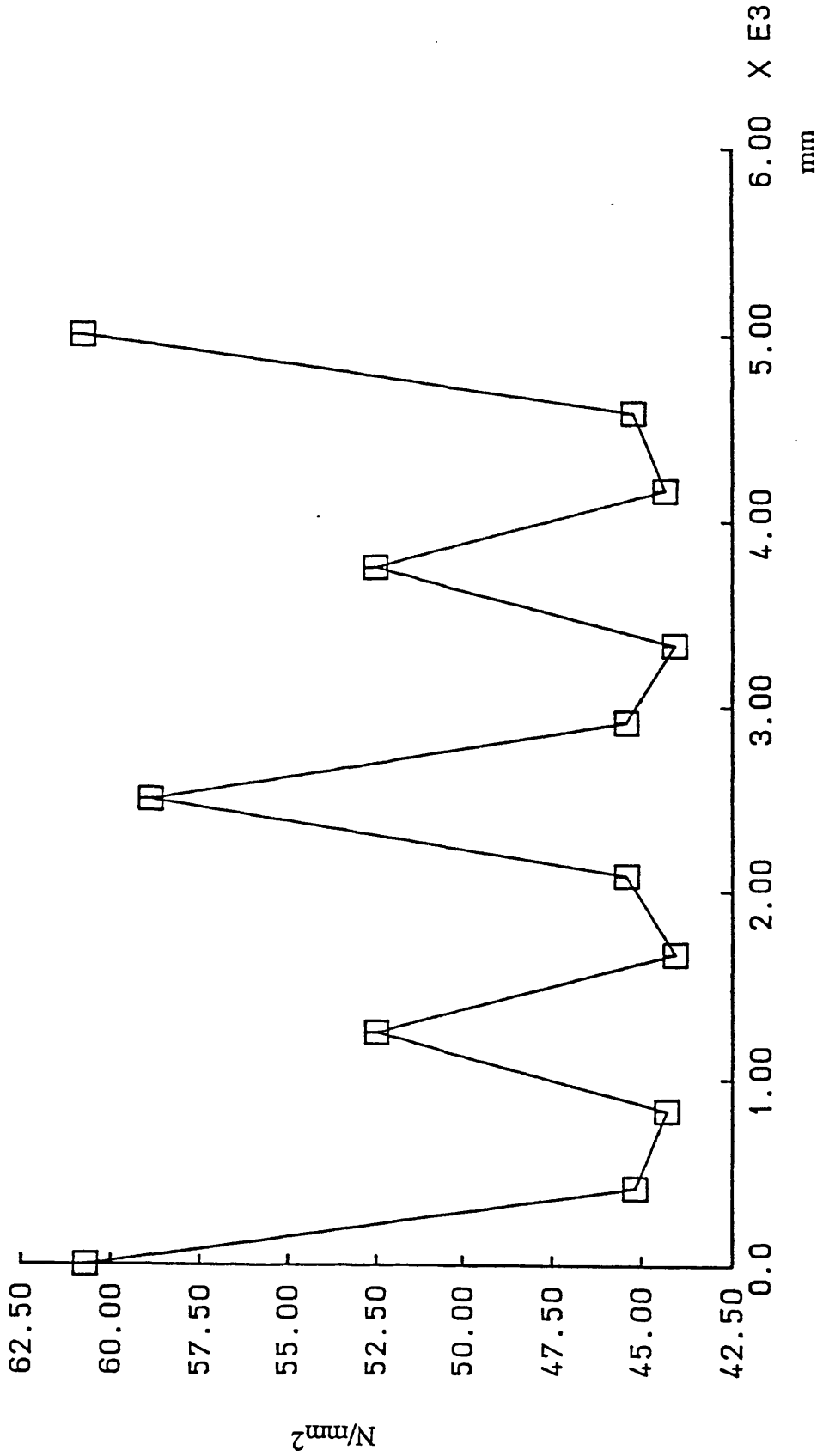


Fig. 5.7(c) Transverse stress distribution at x=-3400 mm on upper deck

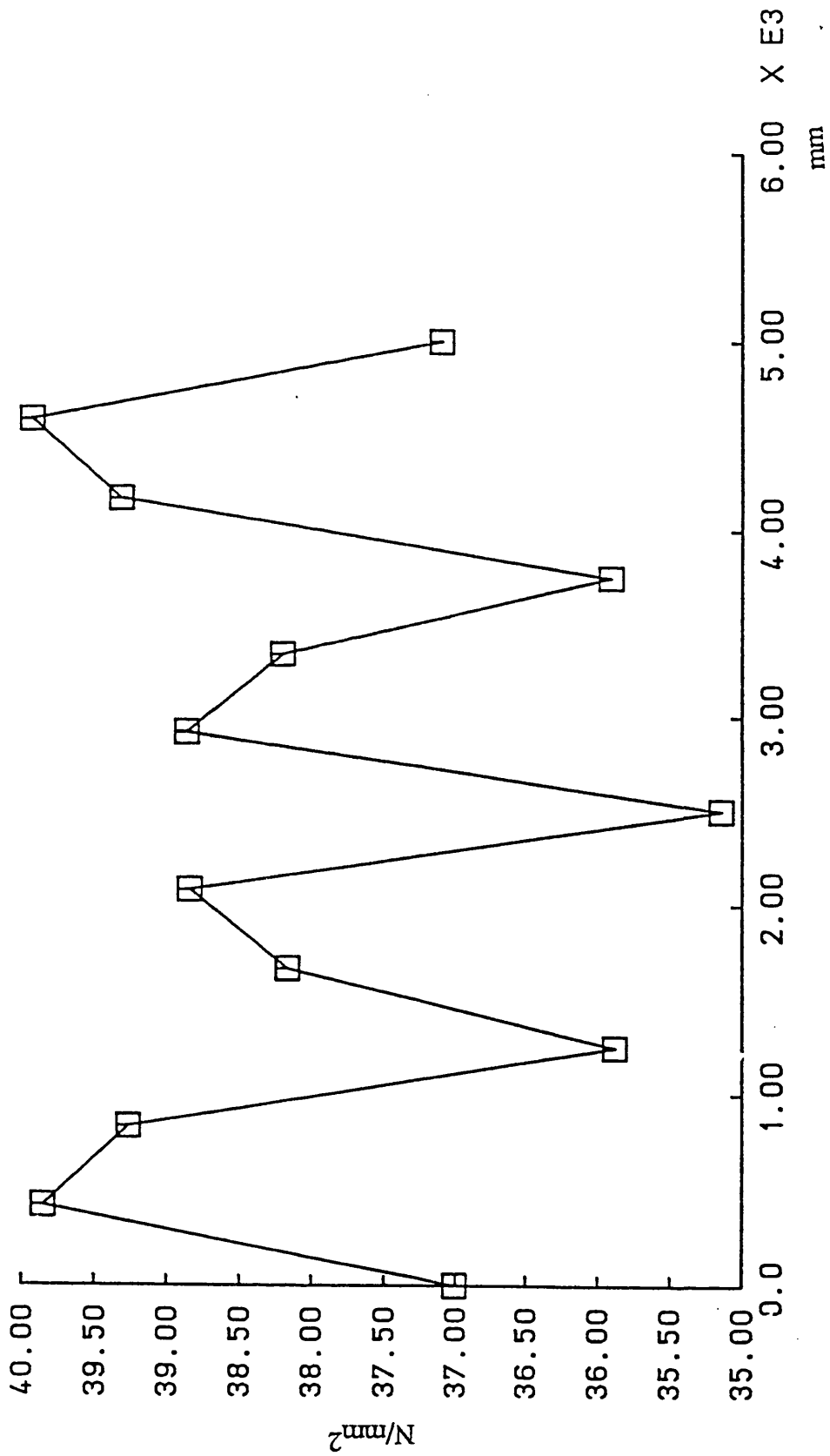


Fig. 5.7(d) Transverse stress distribution at x=-4390 mm on upper deck

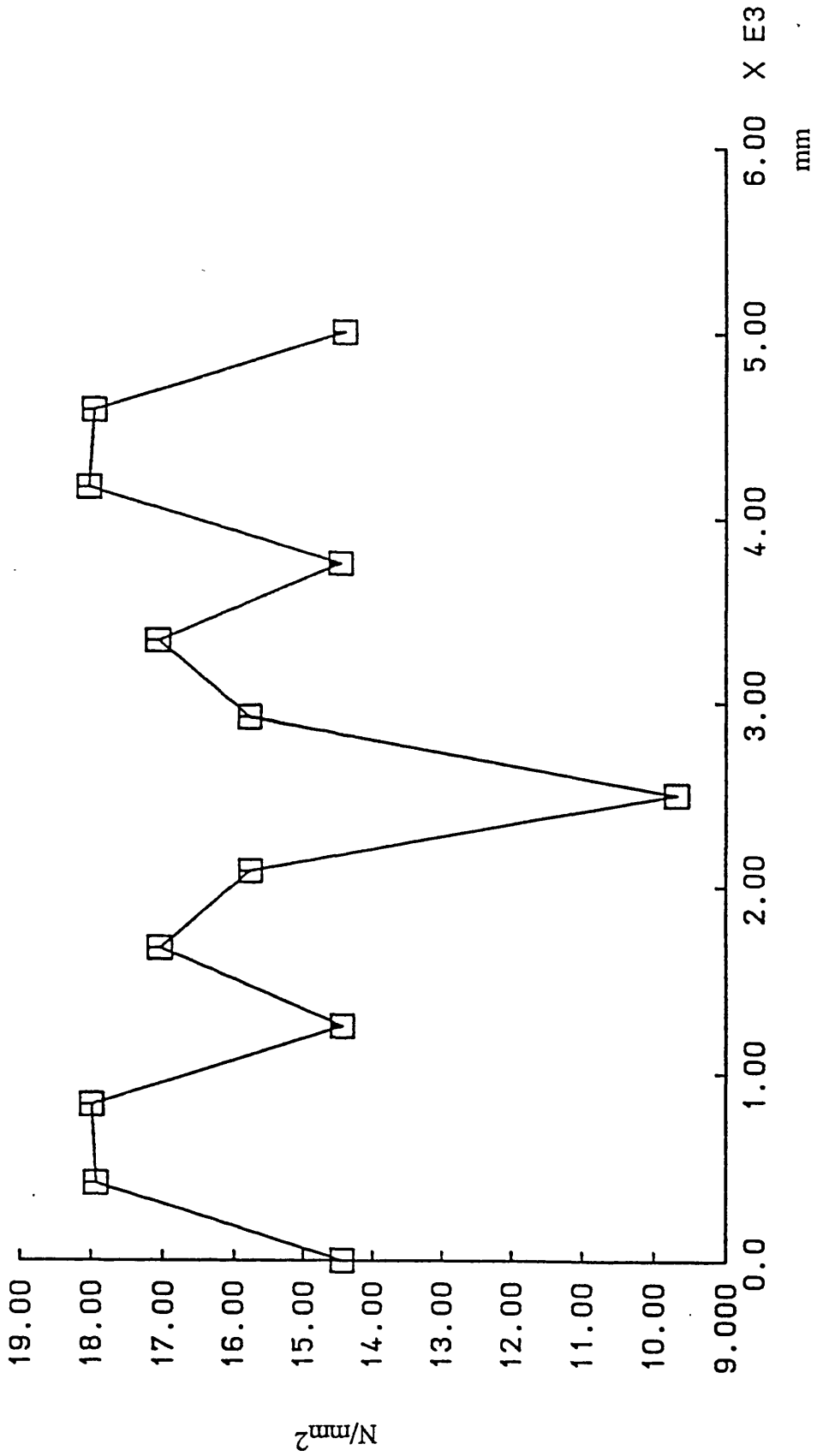


Fig. 5.7(e) Transverse stress distribution at x=-5400 mm on upper deck

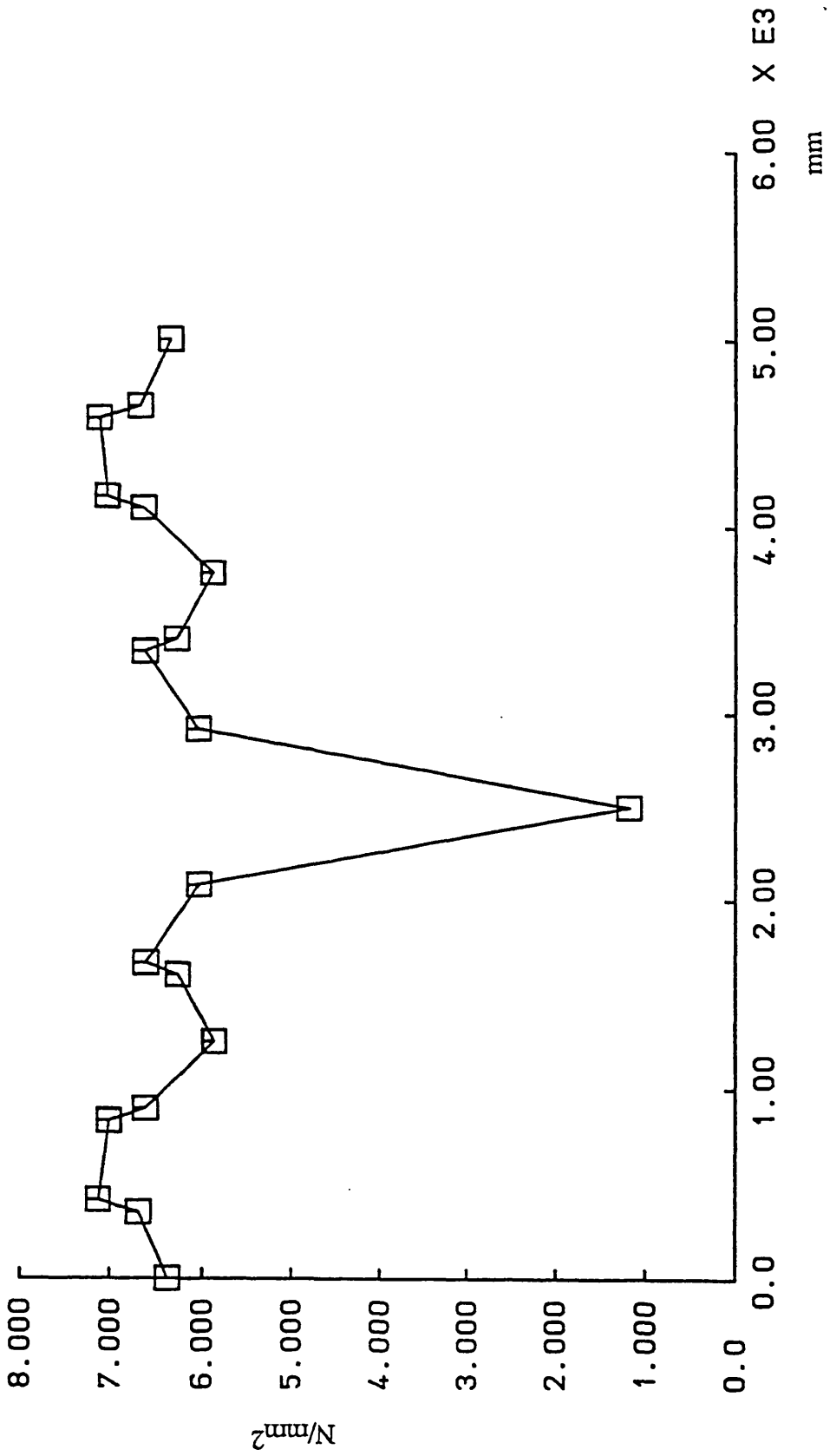


Fig. 5.7(f) Transverse stress distribution at x=6000 mm on upper deck

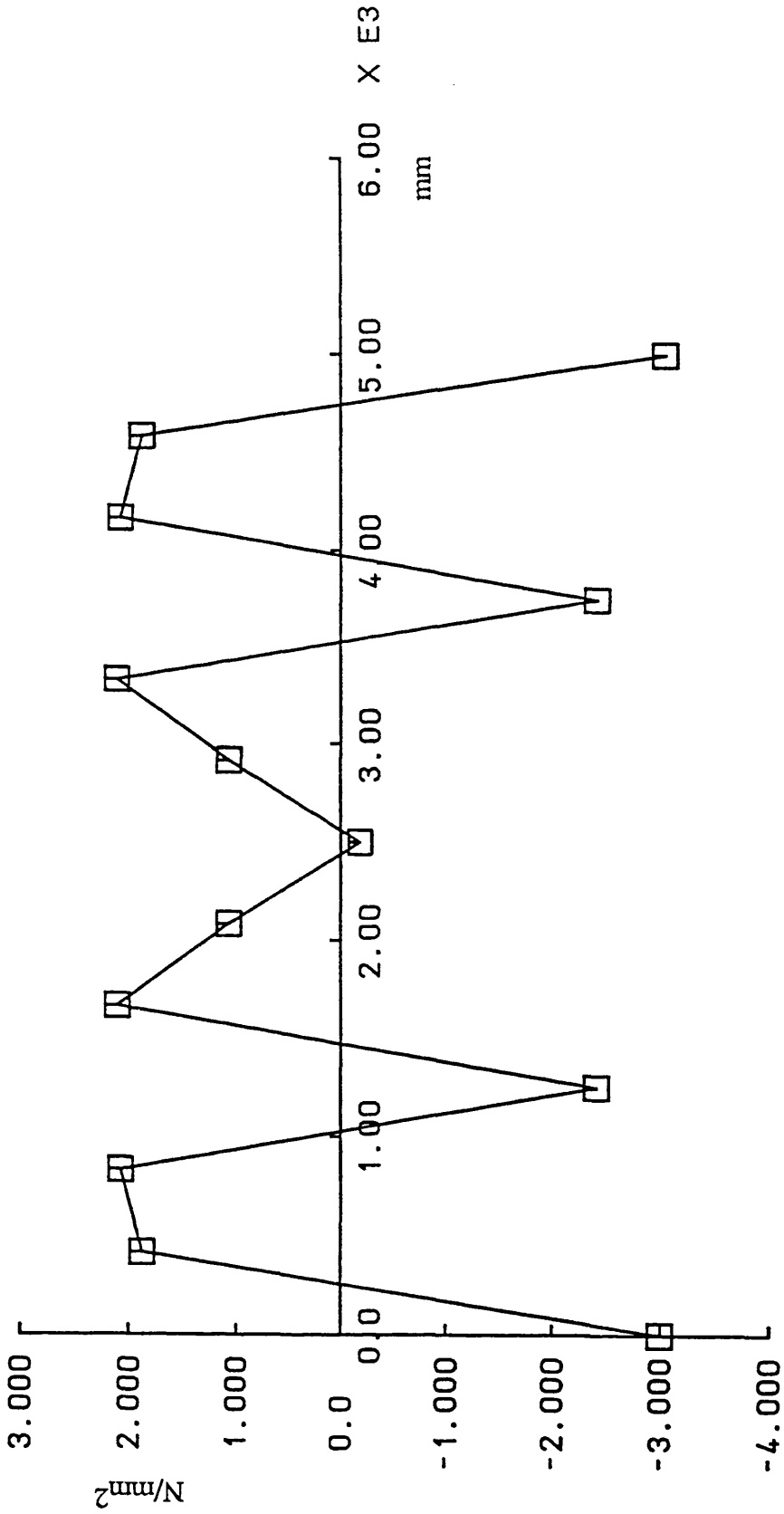


Fig. 5.7(g) Transverse stress distribution at x=-6480 mm on upper deck

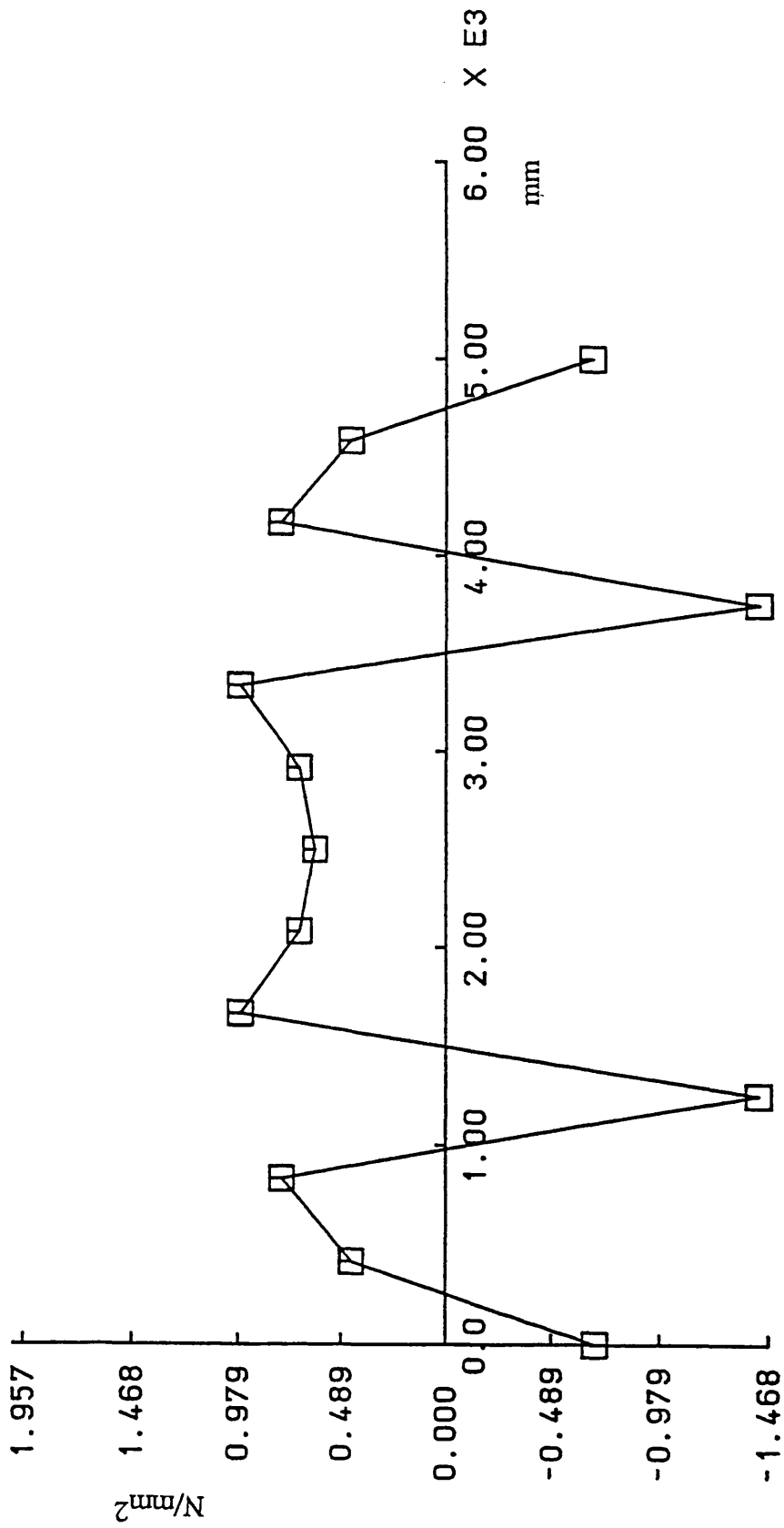


Fig. 5.7(h) Transverse stress distribution at Y=-10 mm on side shell

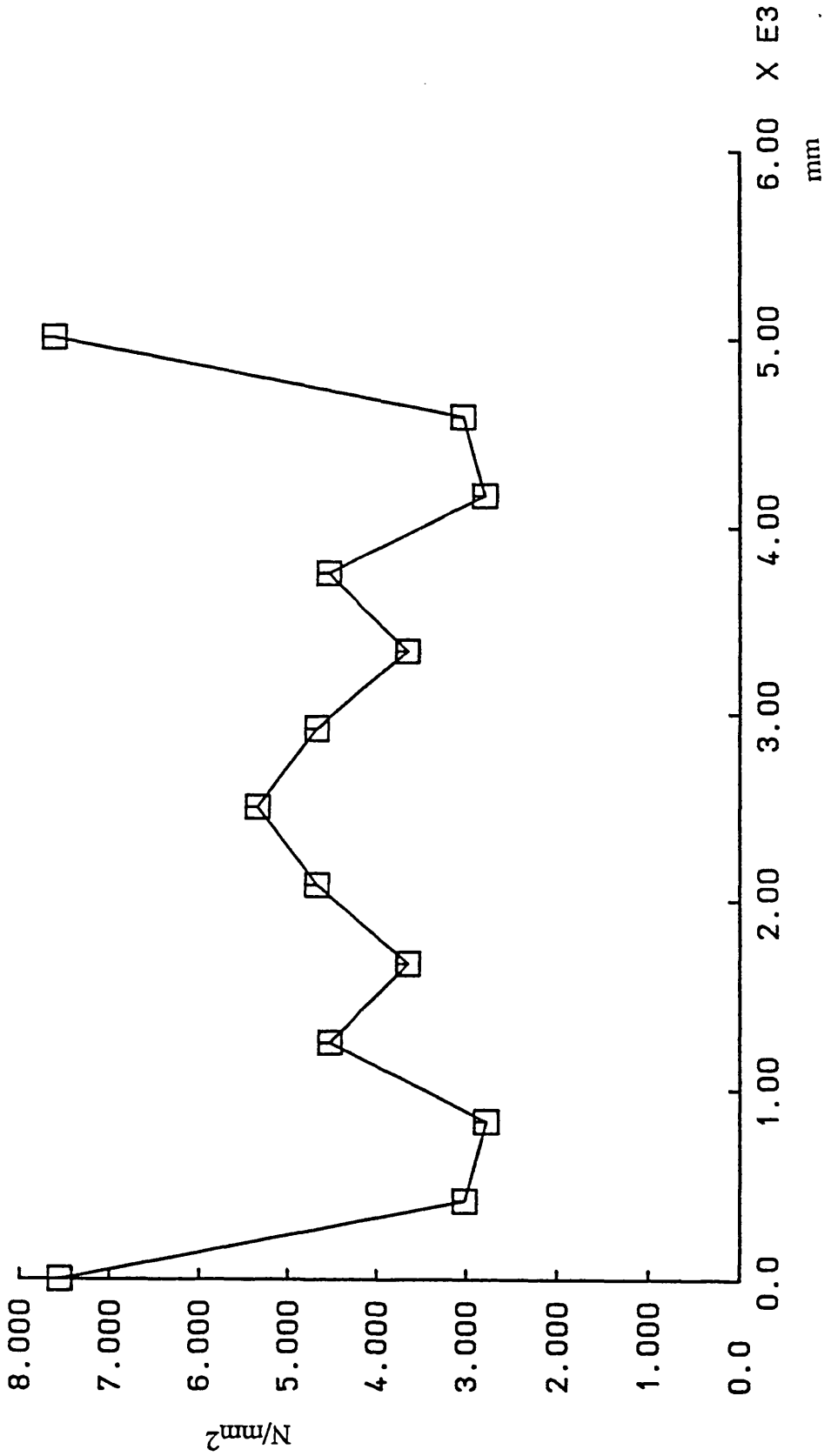


Fig. 5.7(i) Transverse stress distribution at Y=-500 mm on side shell

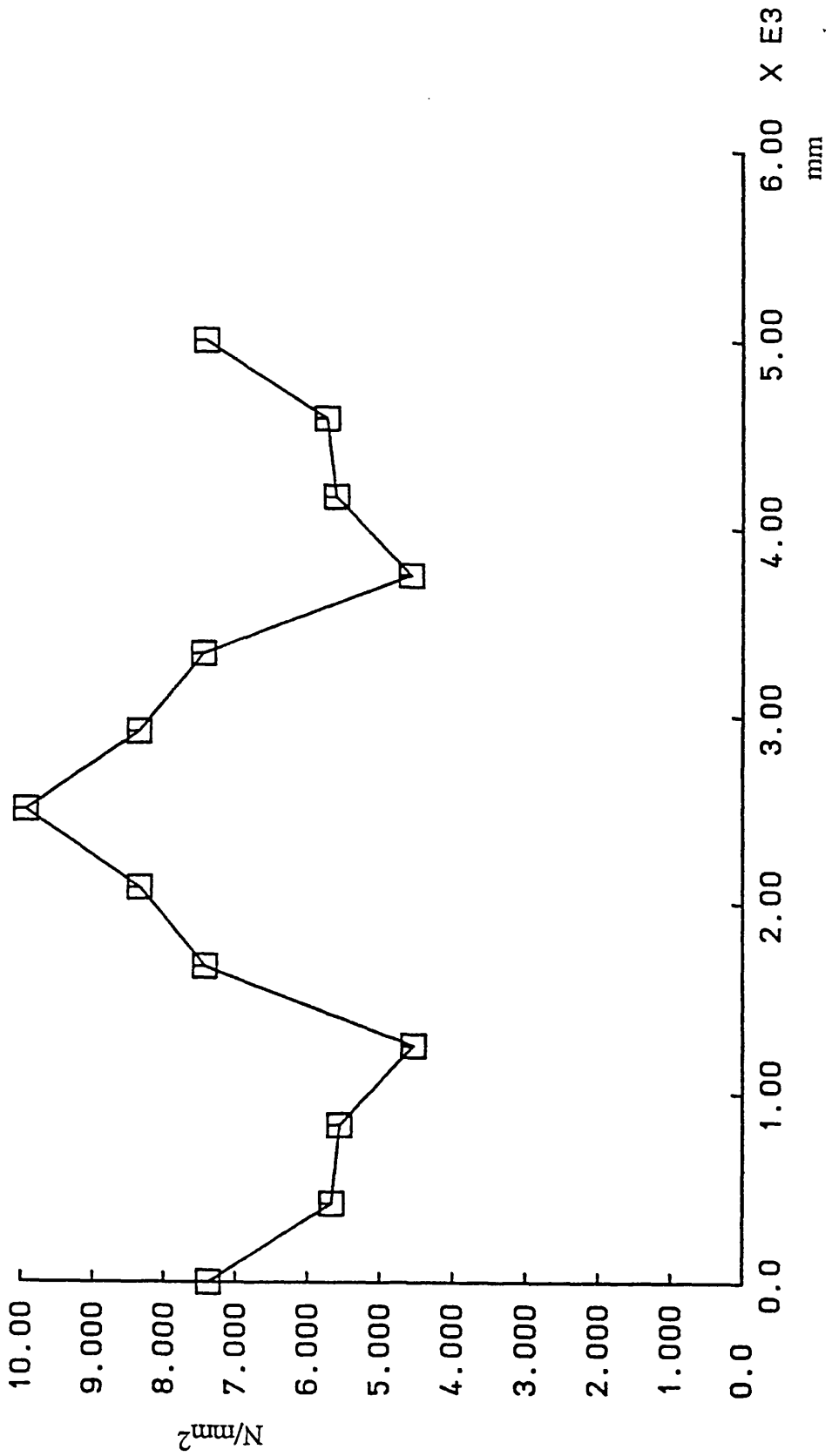


Fig. 5.7(j) Transverse stress distribution at Y=-990 mm on side shell

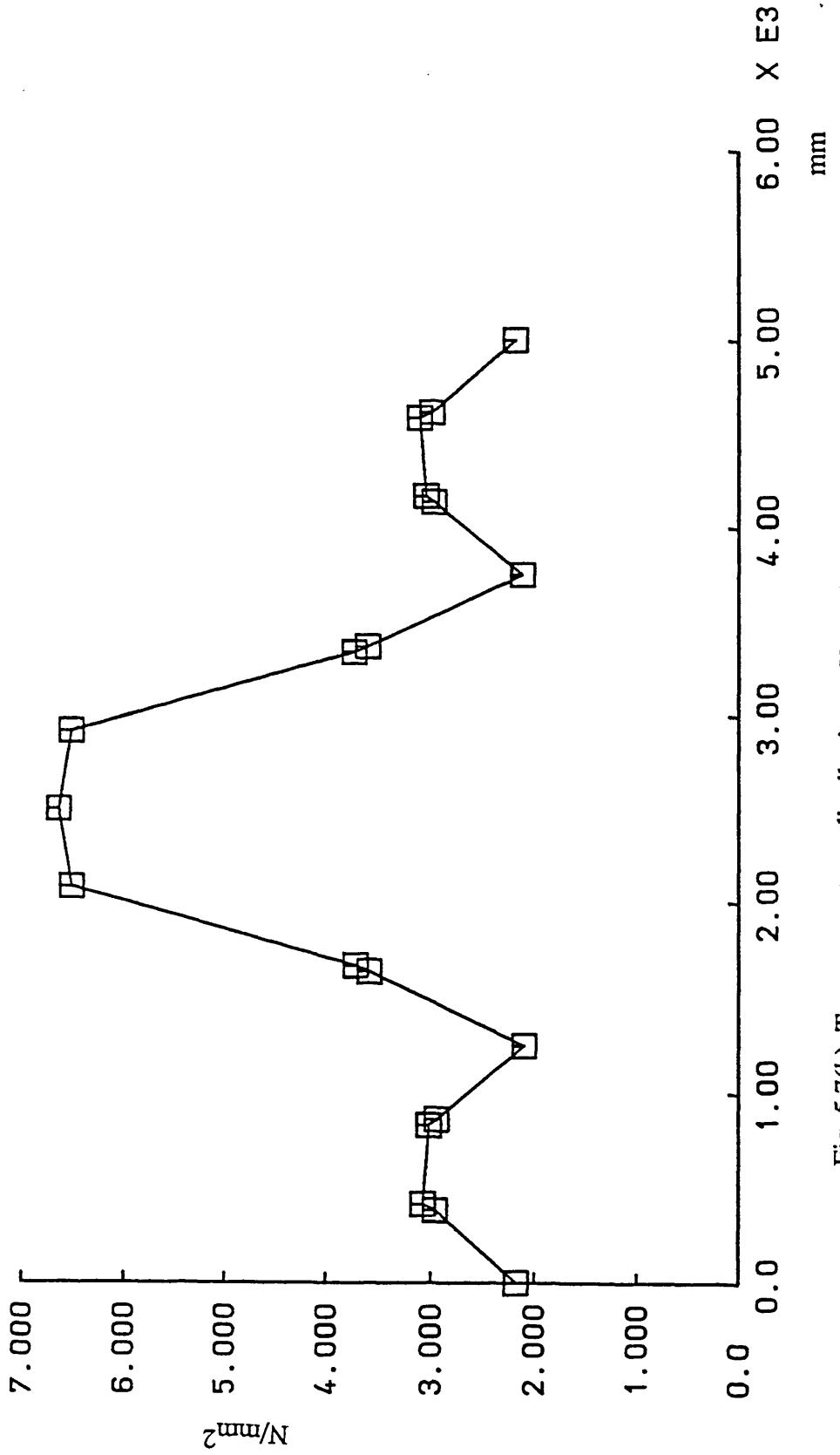


Fig. 5.7(k) Transverse stress distribution at Y=-1010 mm on out haunch

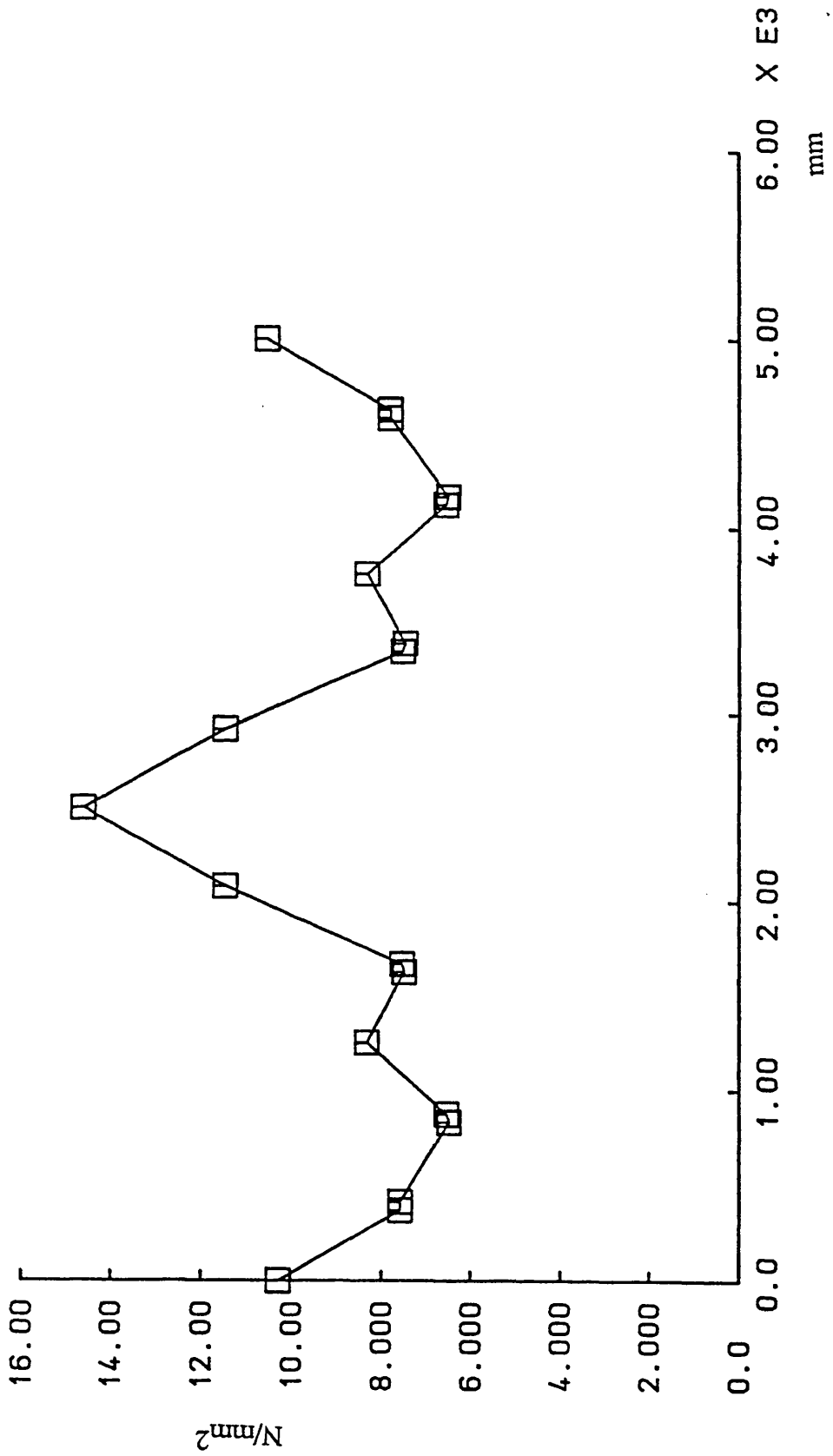


Fig. 5.7(1) Transverse stress distribution at Y=-1800 mm on out haunch

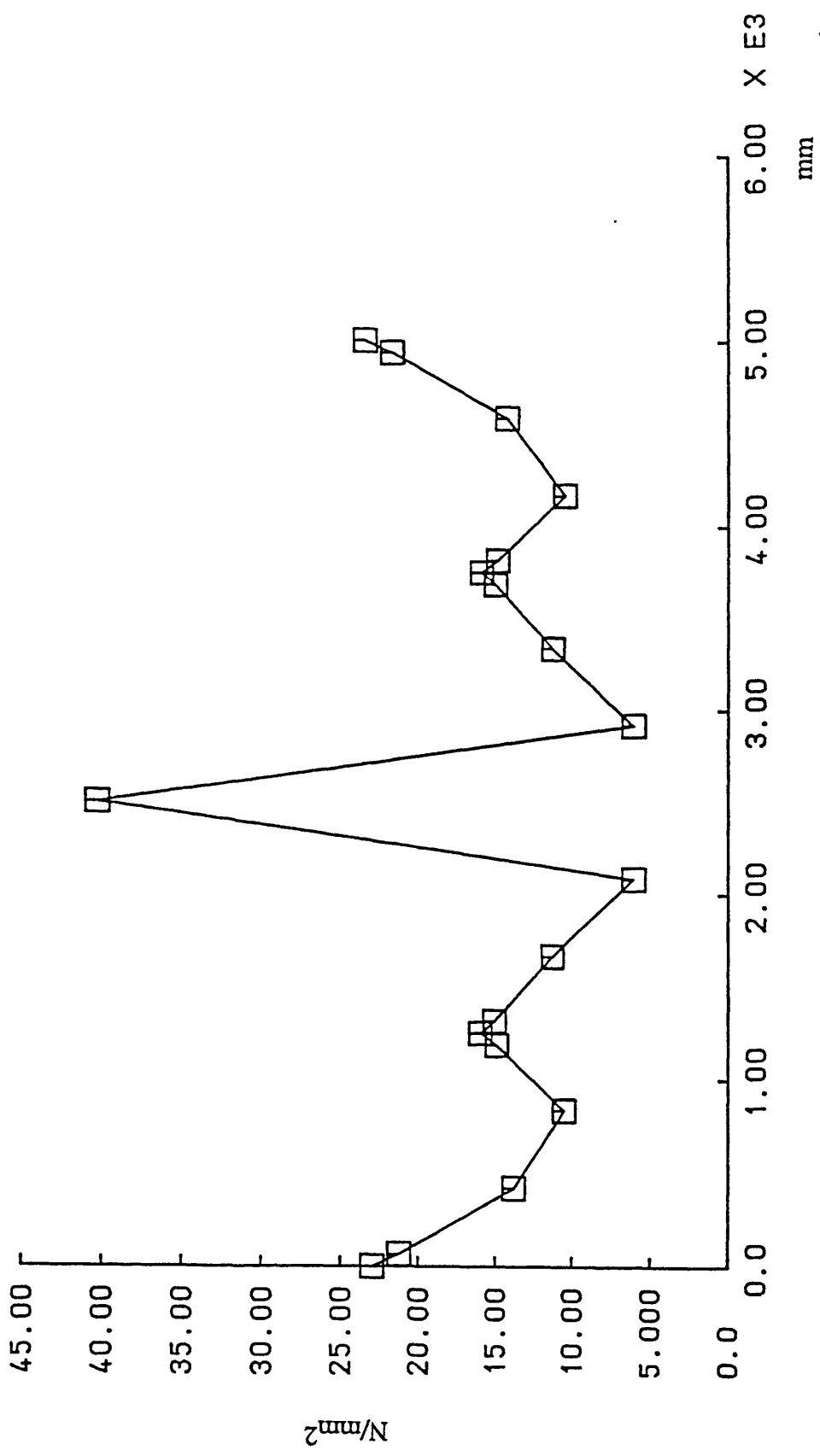


Fig. 5.7(m) Transverse stress distribution at Y=-2200 mm on out haunch

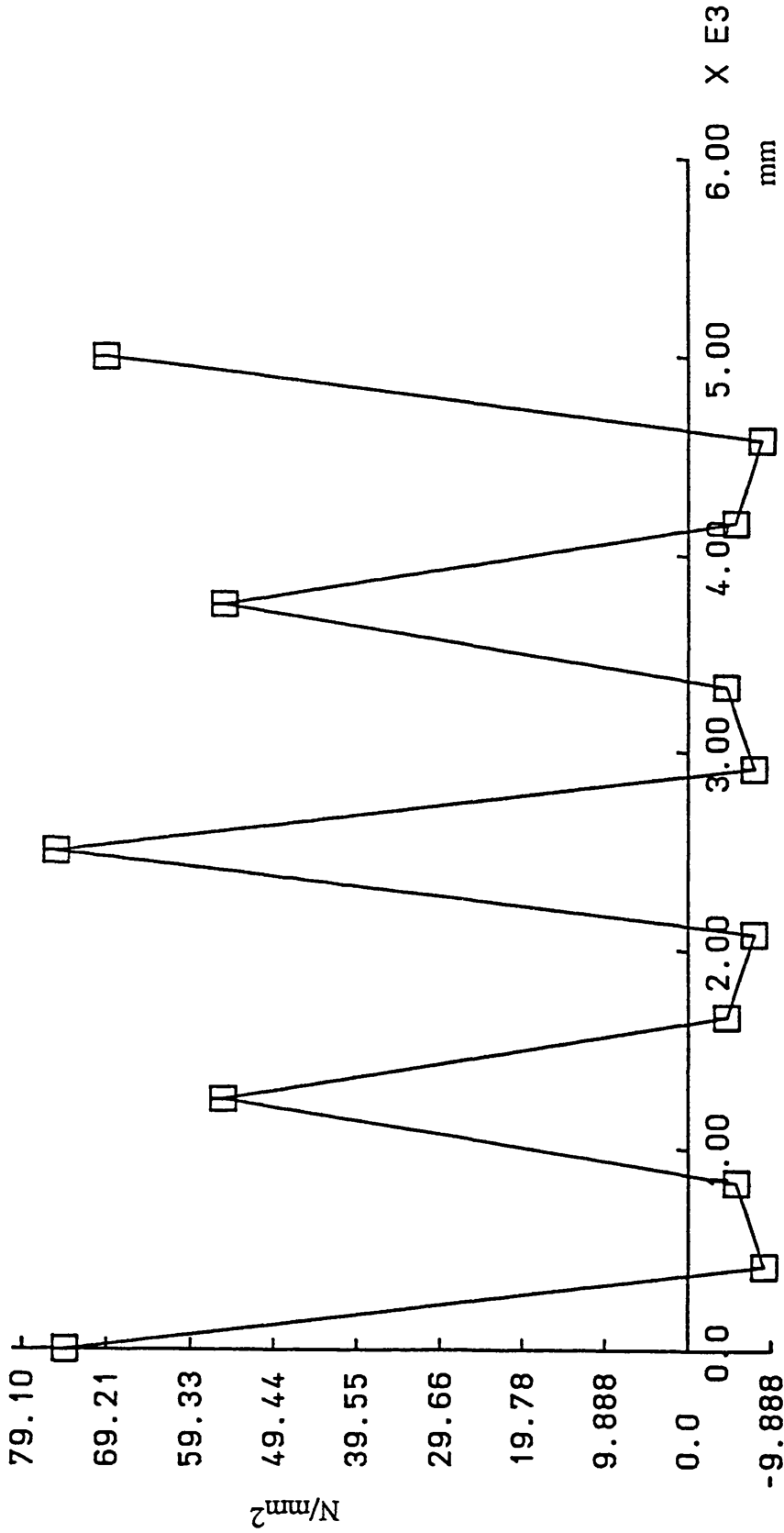


Fig. 5.7(n) Transverse stress distribution at Y=-2580 mm on out strut

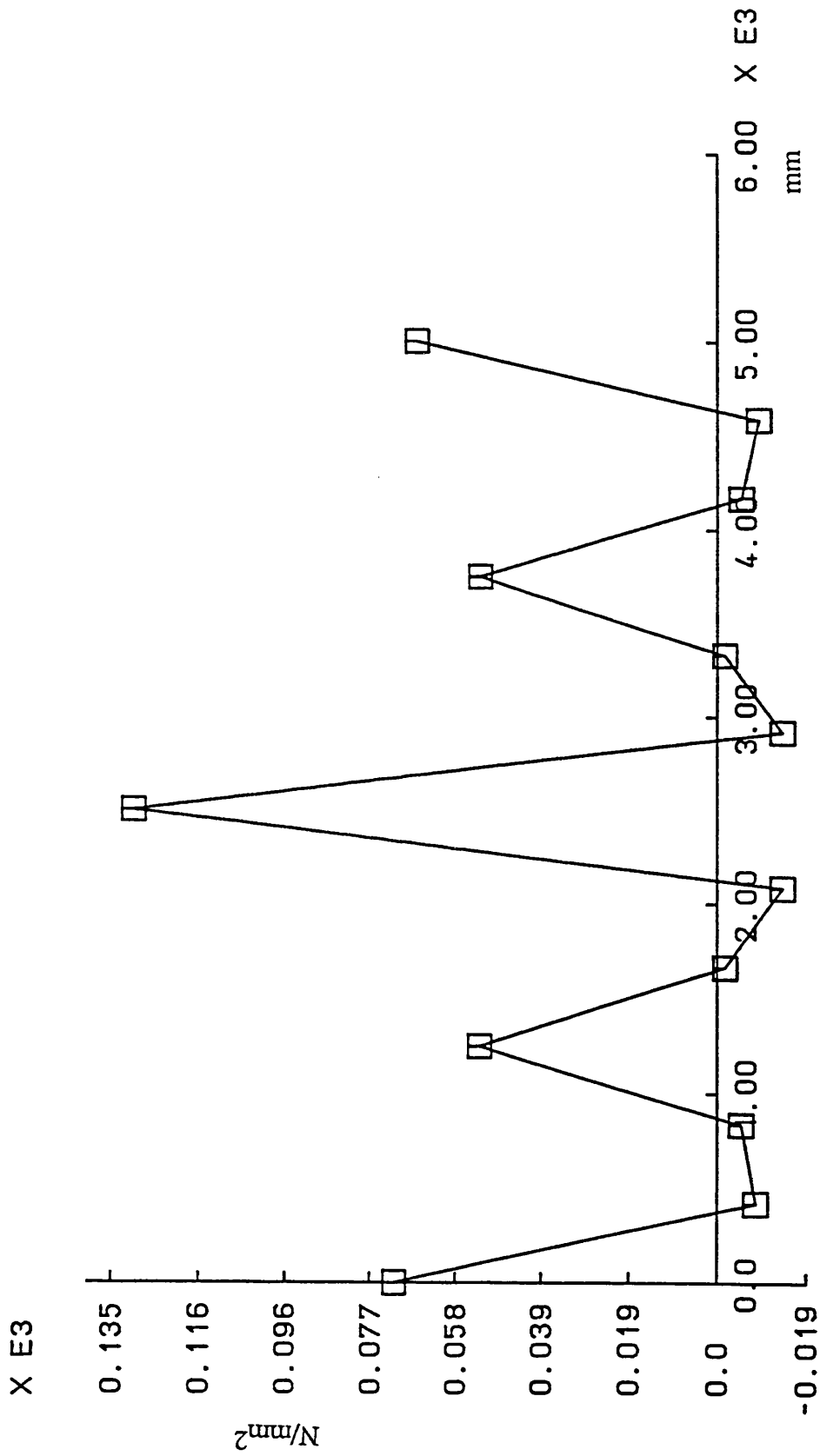


Fig. 5.7(p) Transverse stress distribution at Y=-2620 mm on out strut

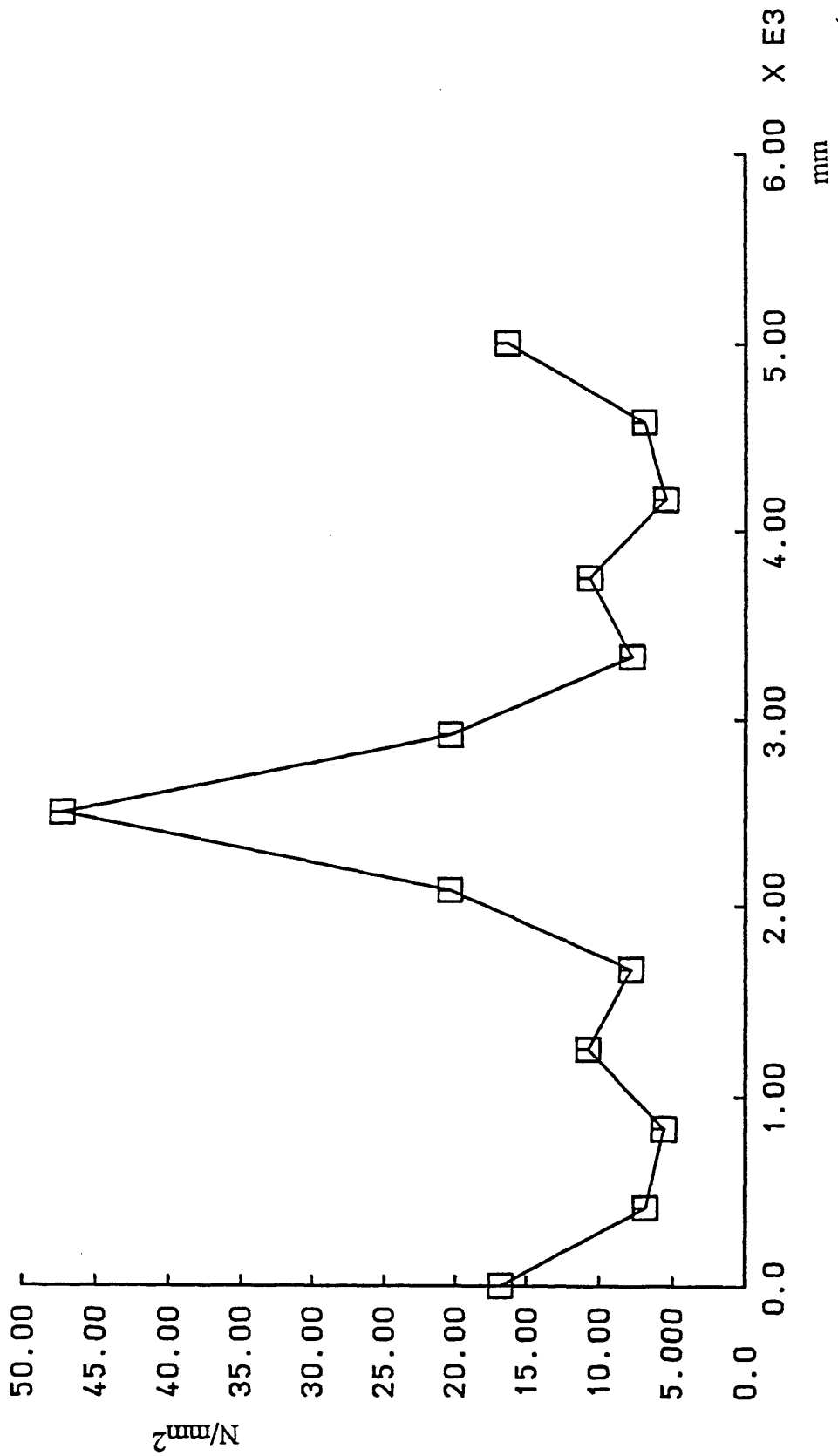


Fig. 5.7(q) Transverse stress distribution at Y=-3400 mm on out strut

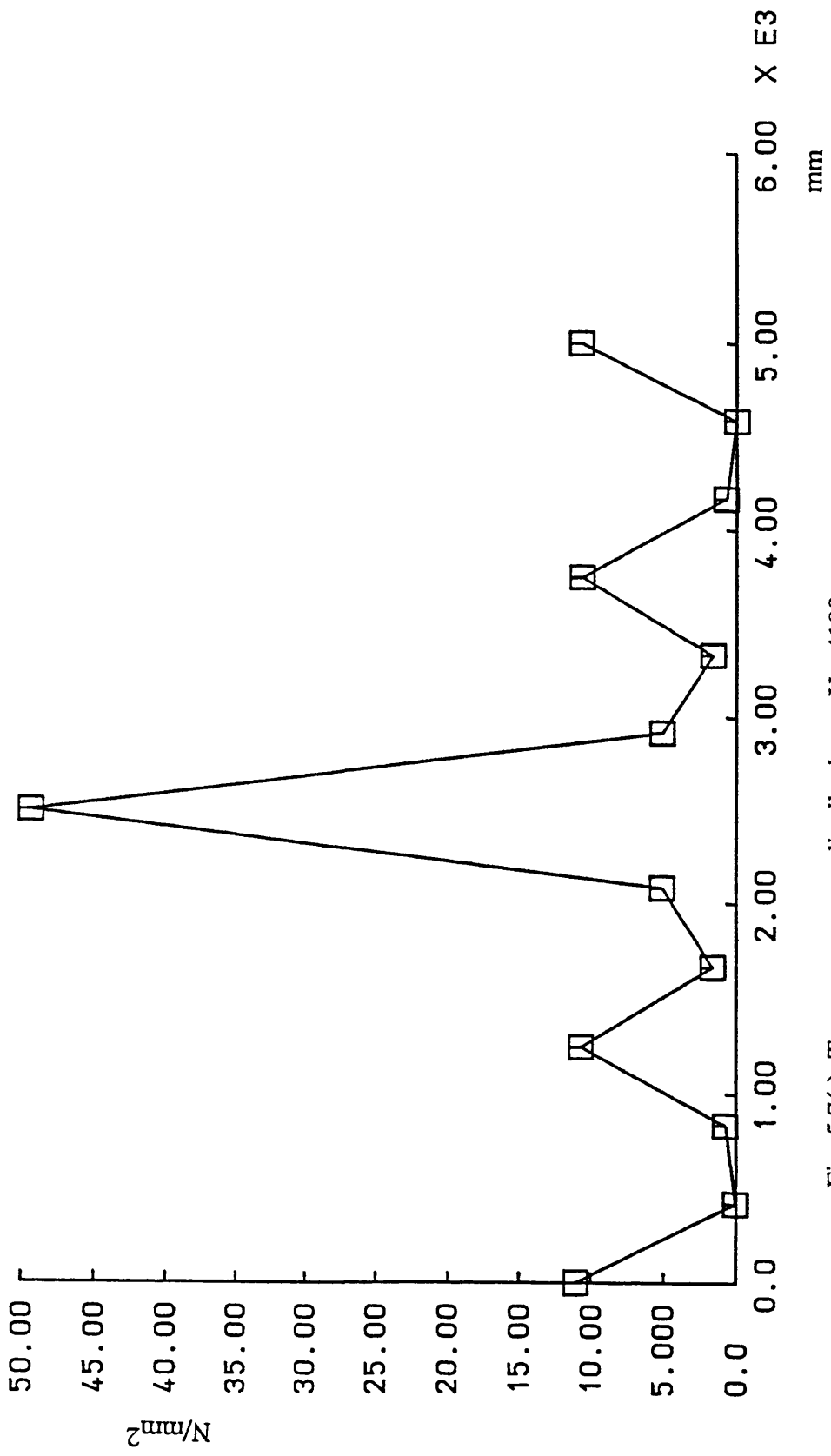


Fig. 5.7(r) Transverse stress distribution at Y=-4100 mm on out strut

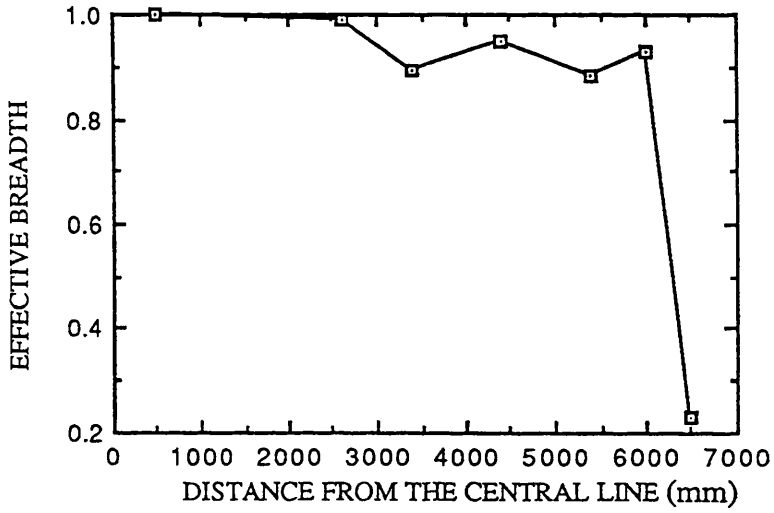


Fig. 5.8(a) Effective breadth in the decks

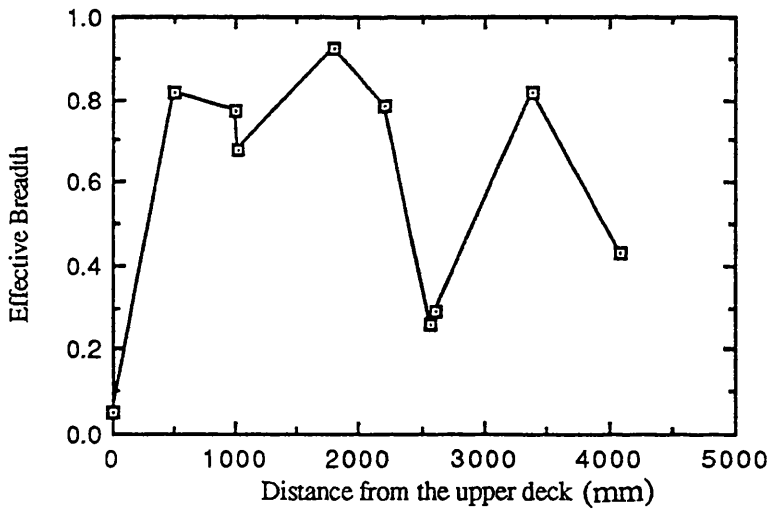


Fig. 5.8(b) Effective breadth in the haunch and strut

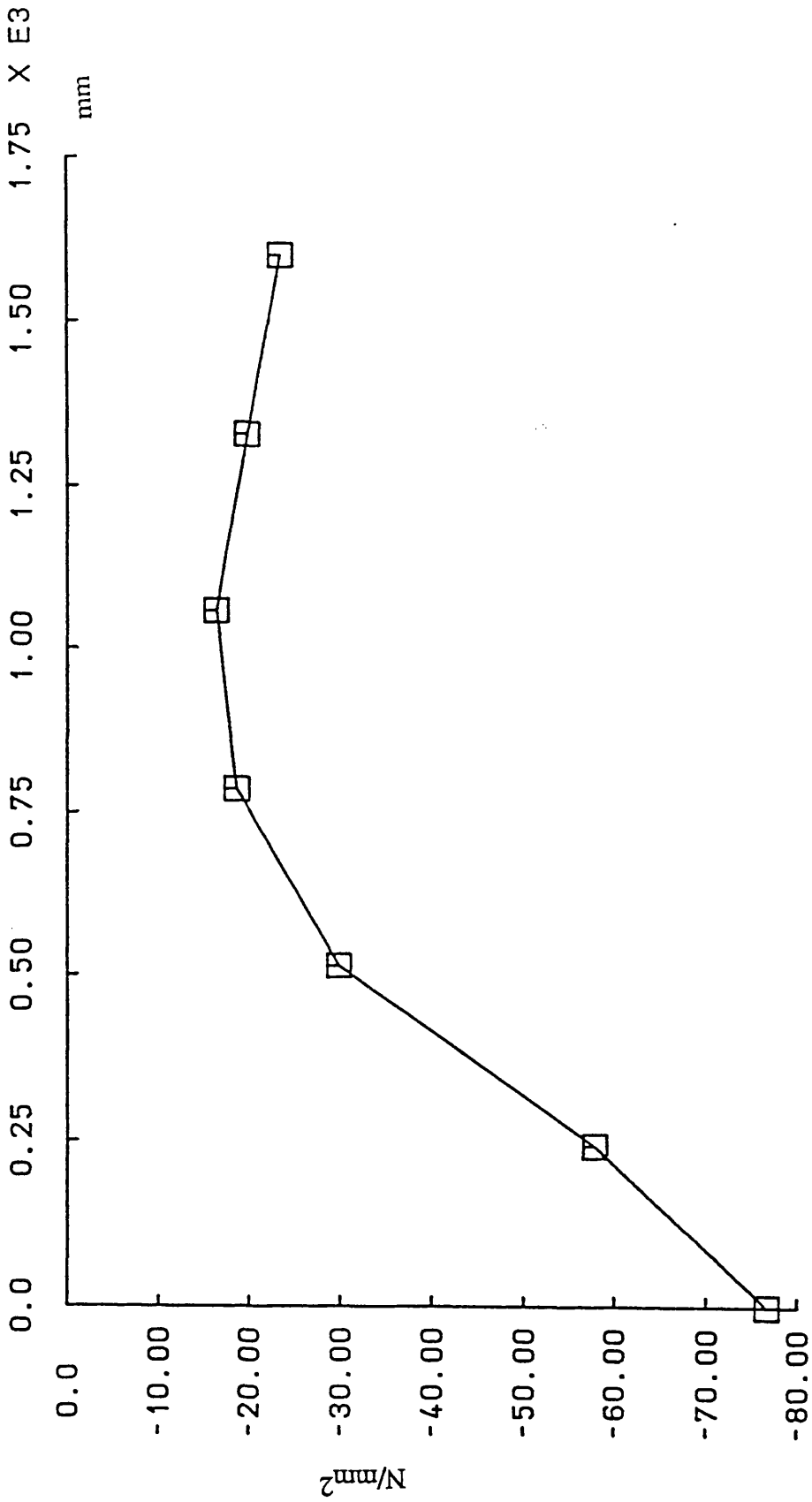


Fig. 5.9(a) Transverse stress distribution at $z=-2500$ mm on inner haunch

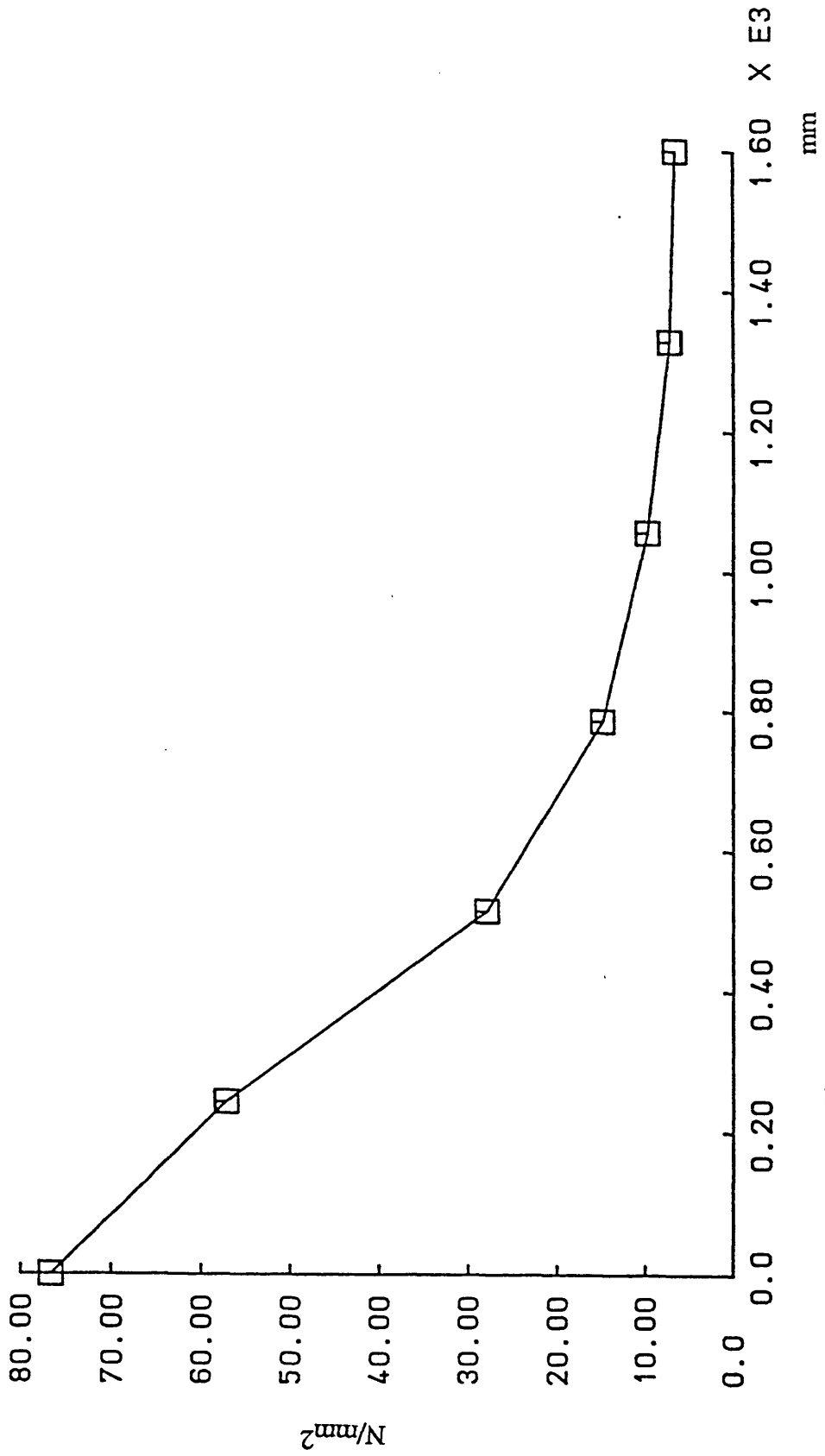
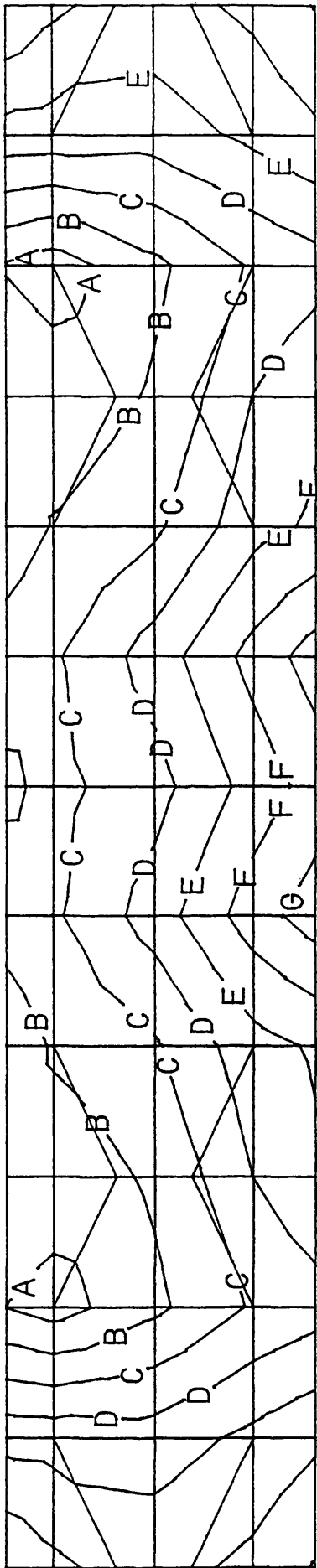


Fig. 5.9(b) Transverse stress distribution at z=-2500 mm on out haunch



CONTOUR VALUE

A	4.323
B	6.841
C	9.360
D	11.88
E	14.40
F	16.92
G	19.43

Fig. 5.10 Equivalent stress contour in the longitudinal bulkhead

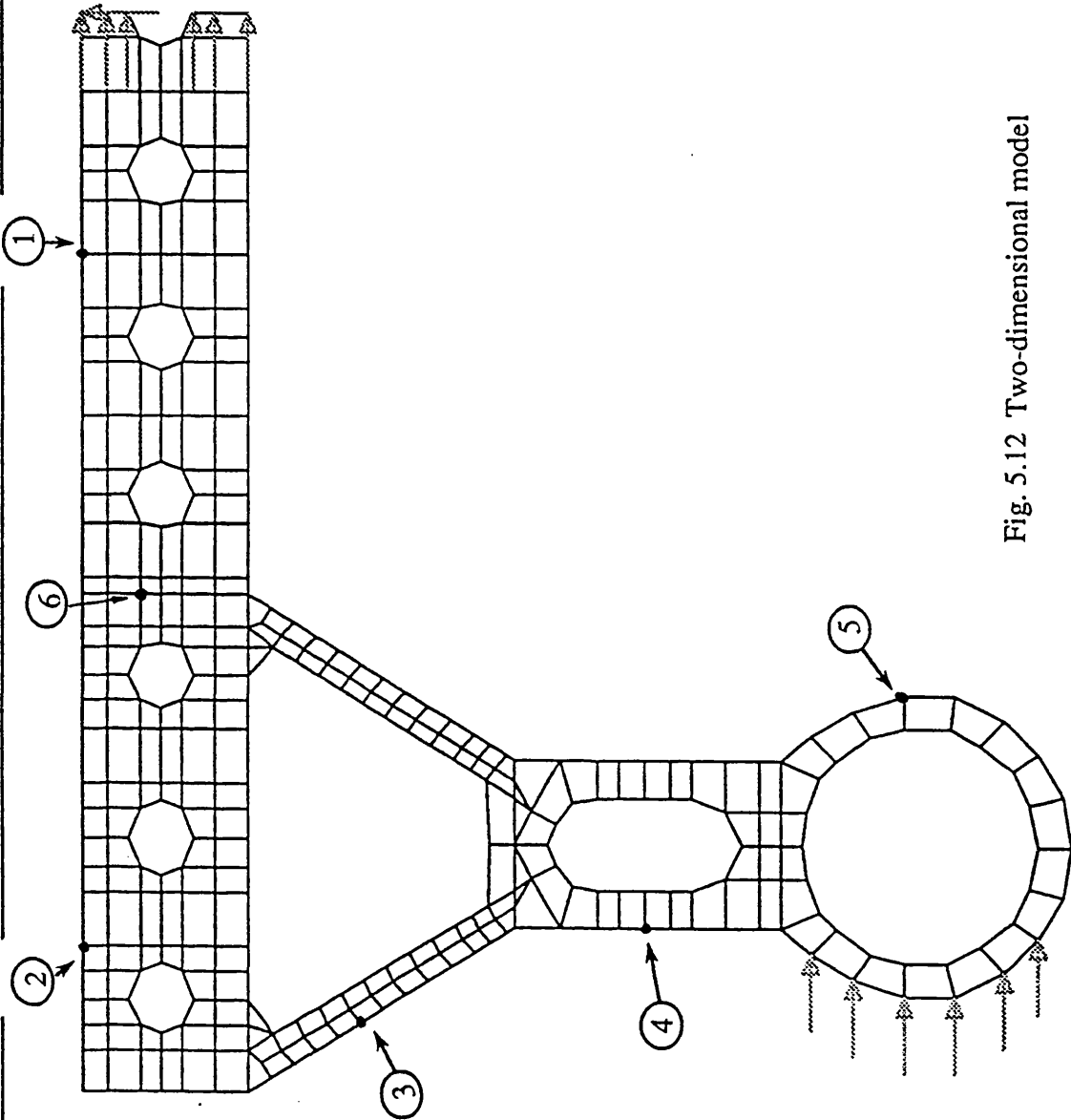


Fig. 5.12 Two-dimensional model

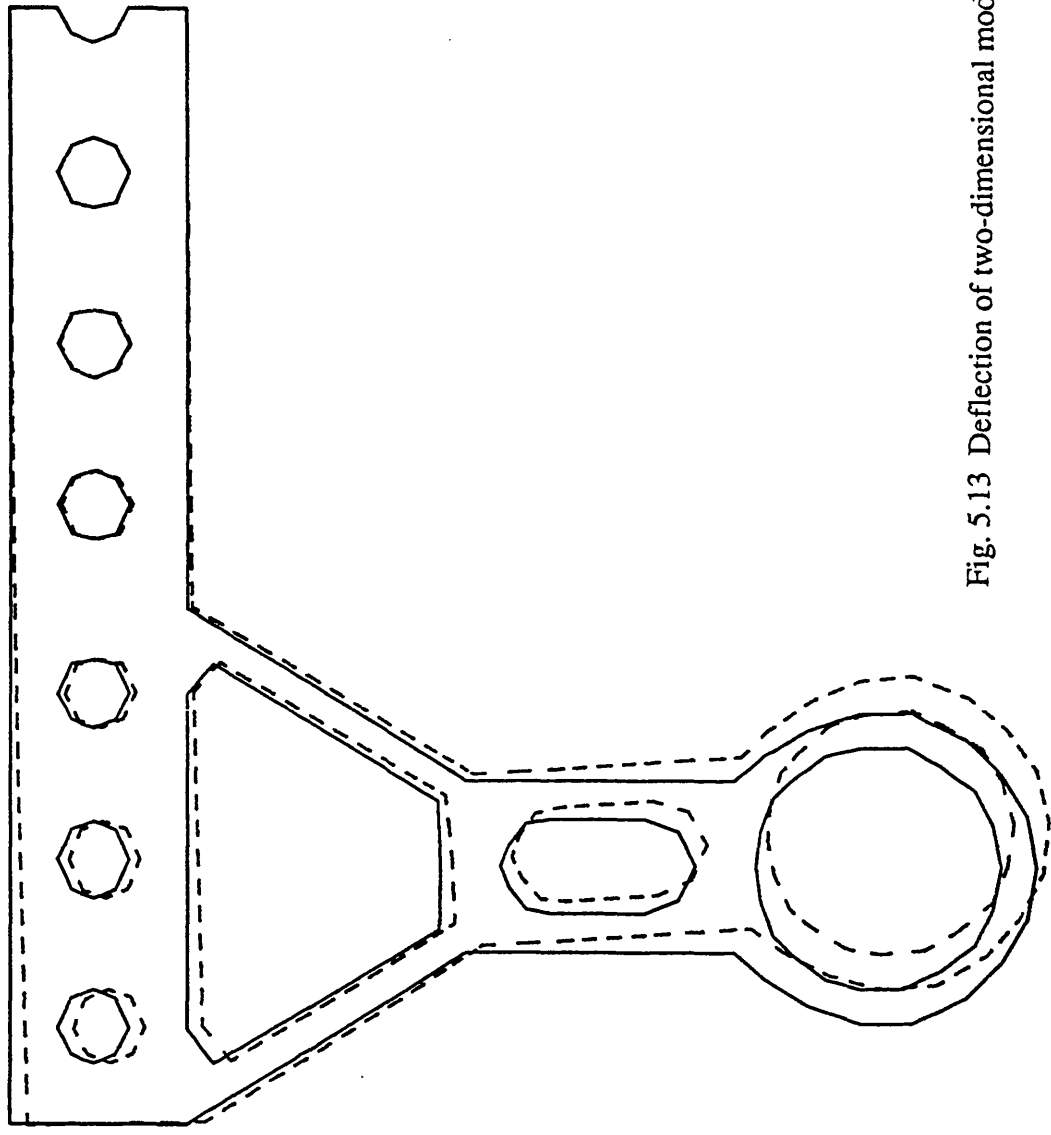


Fig. 5.13 Deflection of two-dimensional model

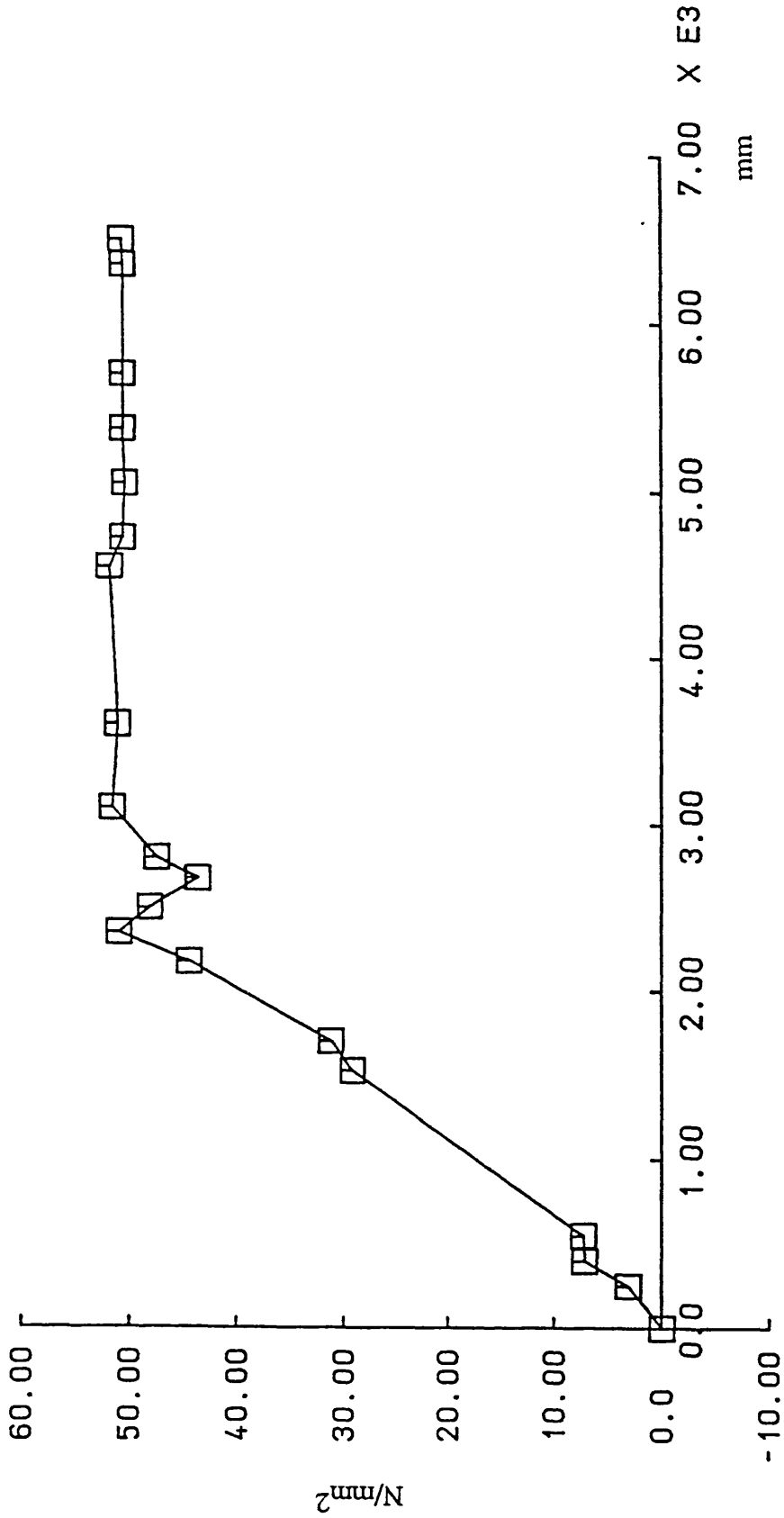


Fig. 5.14(a) Transverse stress distribution in the upper deck

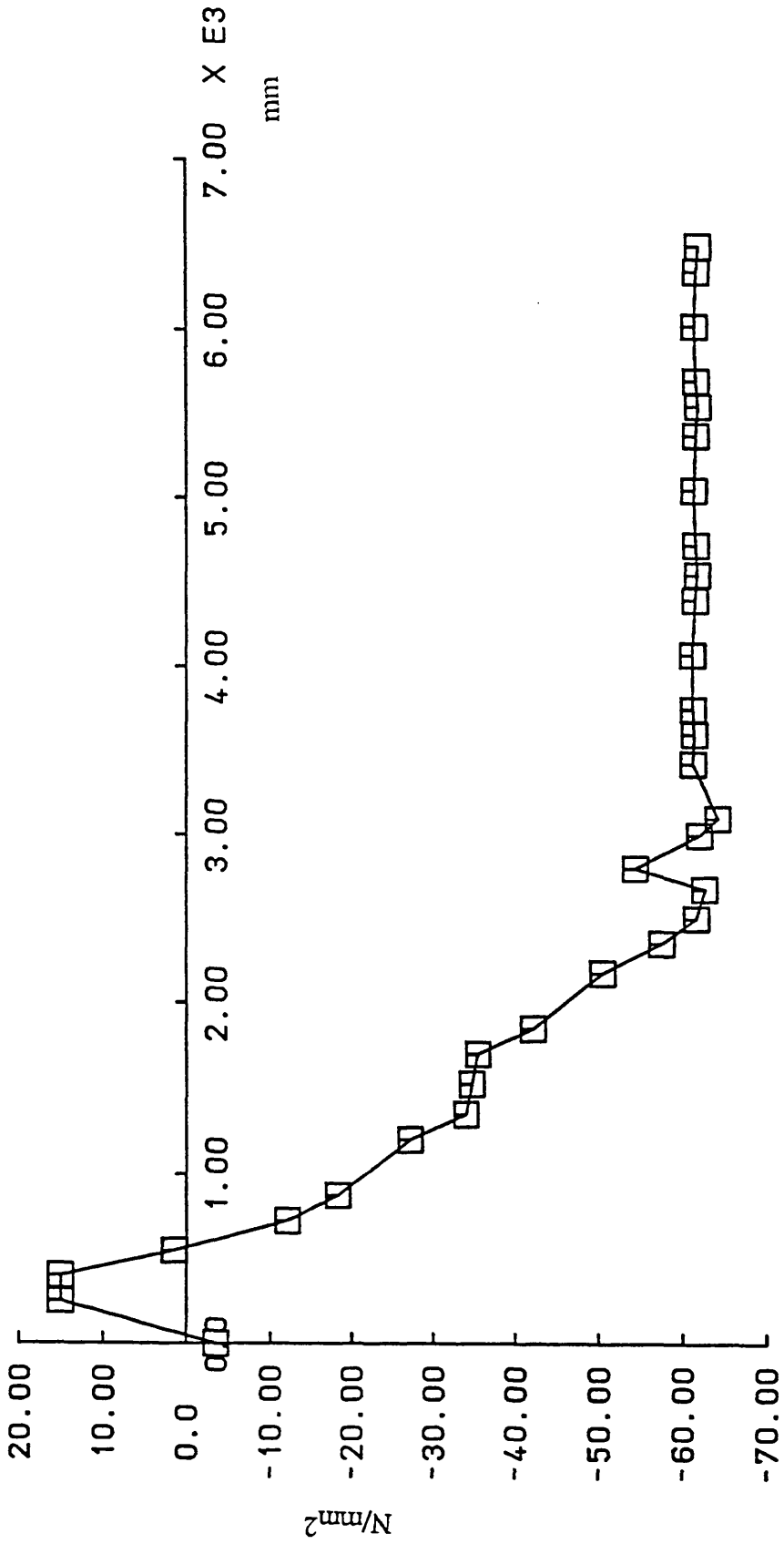


Fig. 5.14(b) Transverse stress distribution in the lower deck

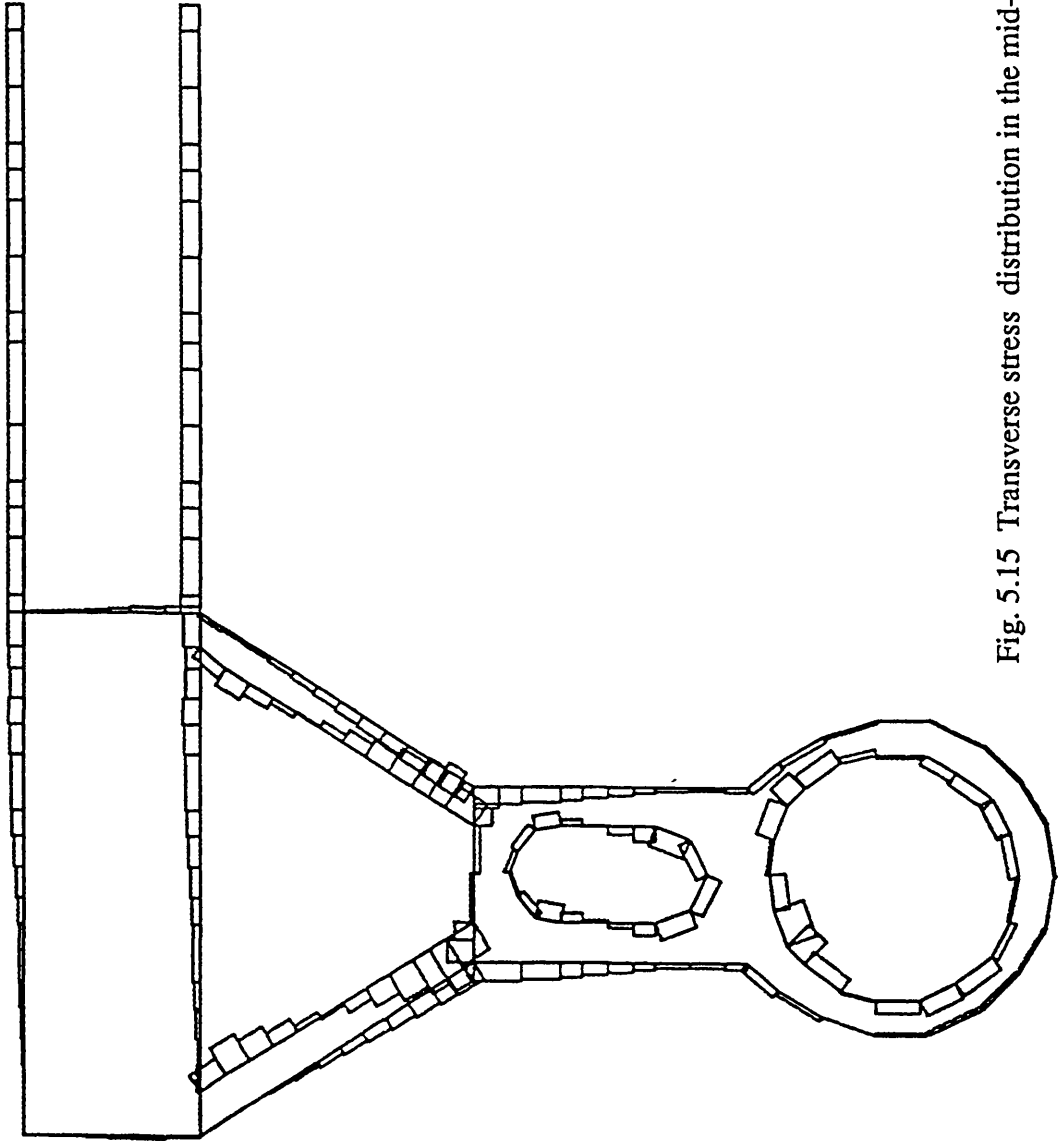
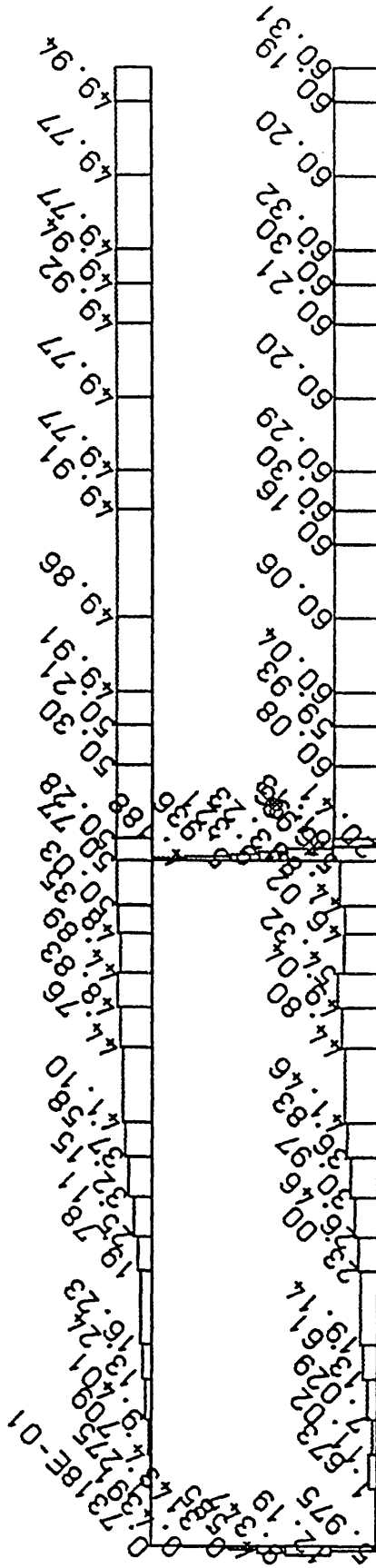


Fig. 5.15 Transverse stress distribution in the mid-frame



MYSTRO: 10.2-3

DATE: 17-12-92

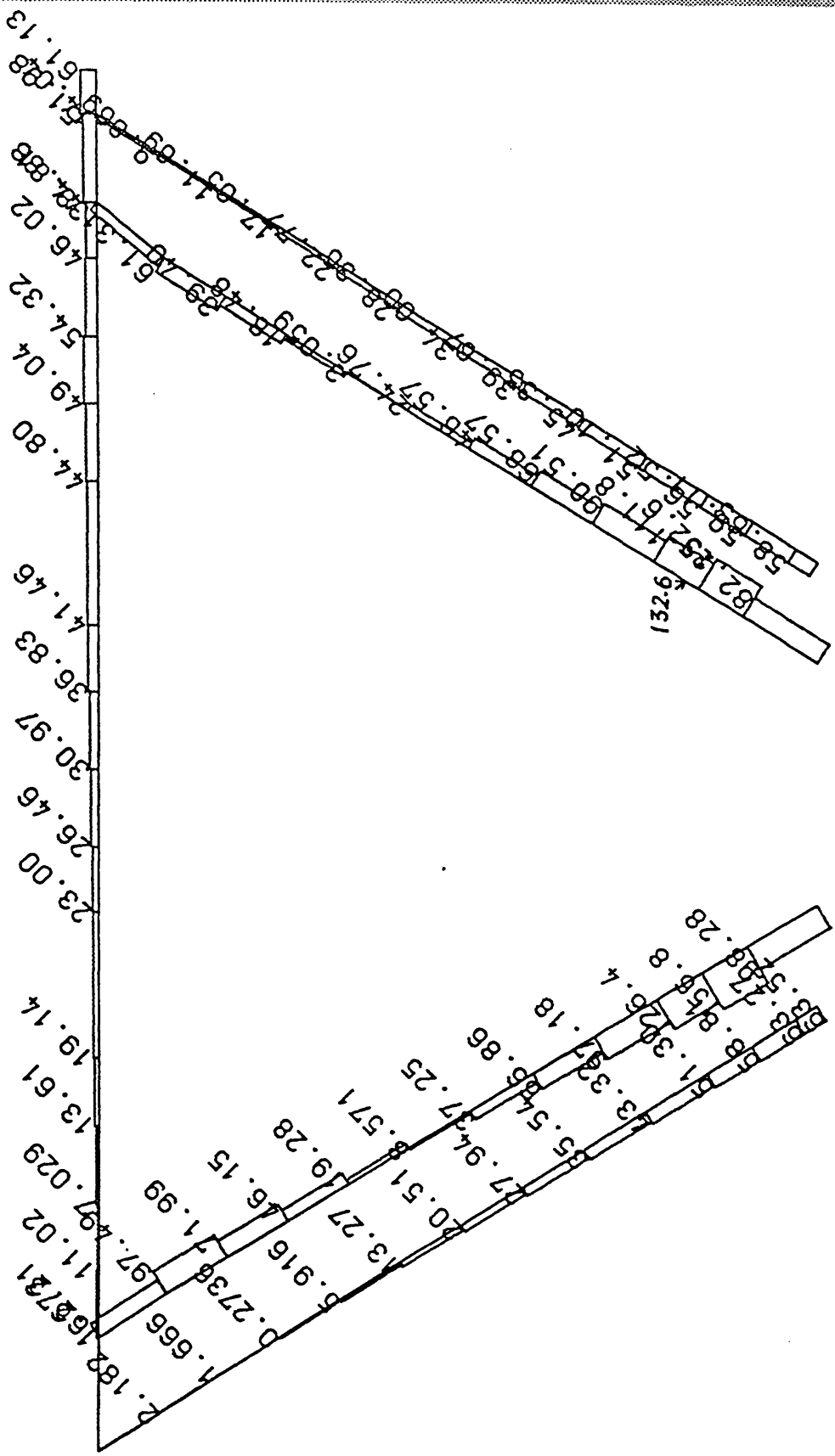


Fig. 5.15(b) Stress at the haunch

TITLE: TWO-DIMENSIONAL ANALYSIS OF PATRIA(SIXTH VERSION)

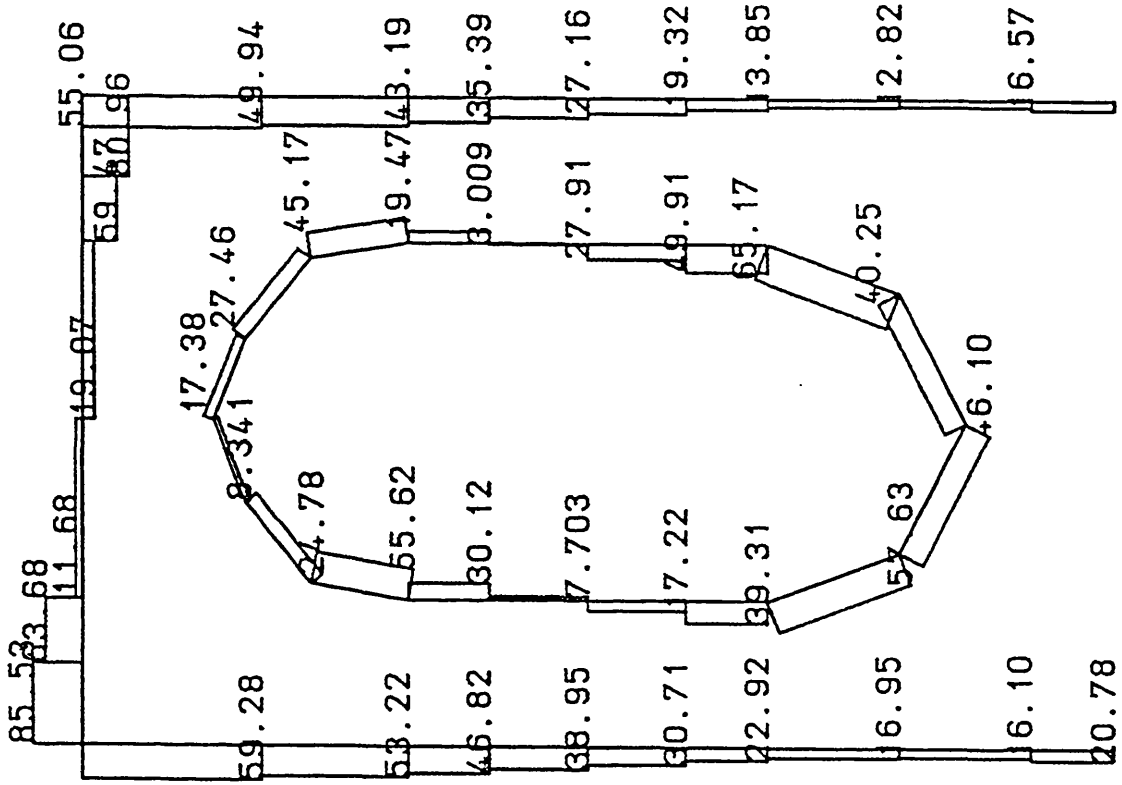


Fig. 5.15(c) Stress at strut

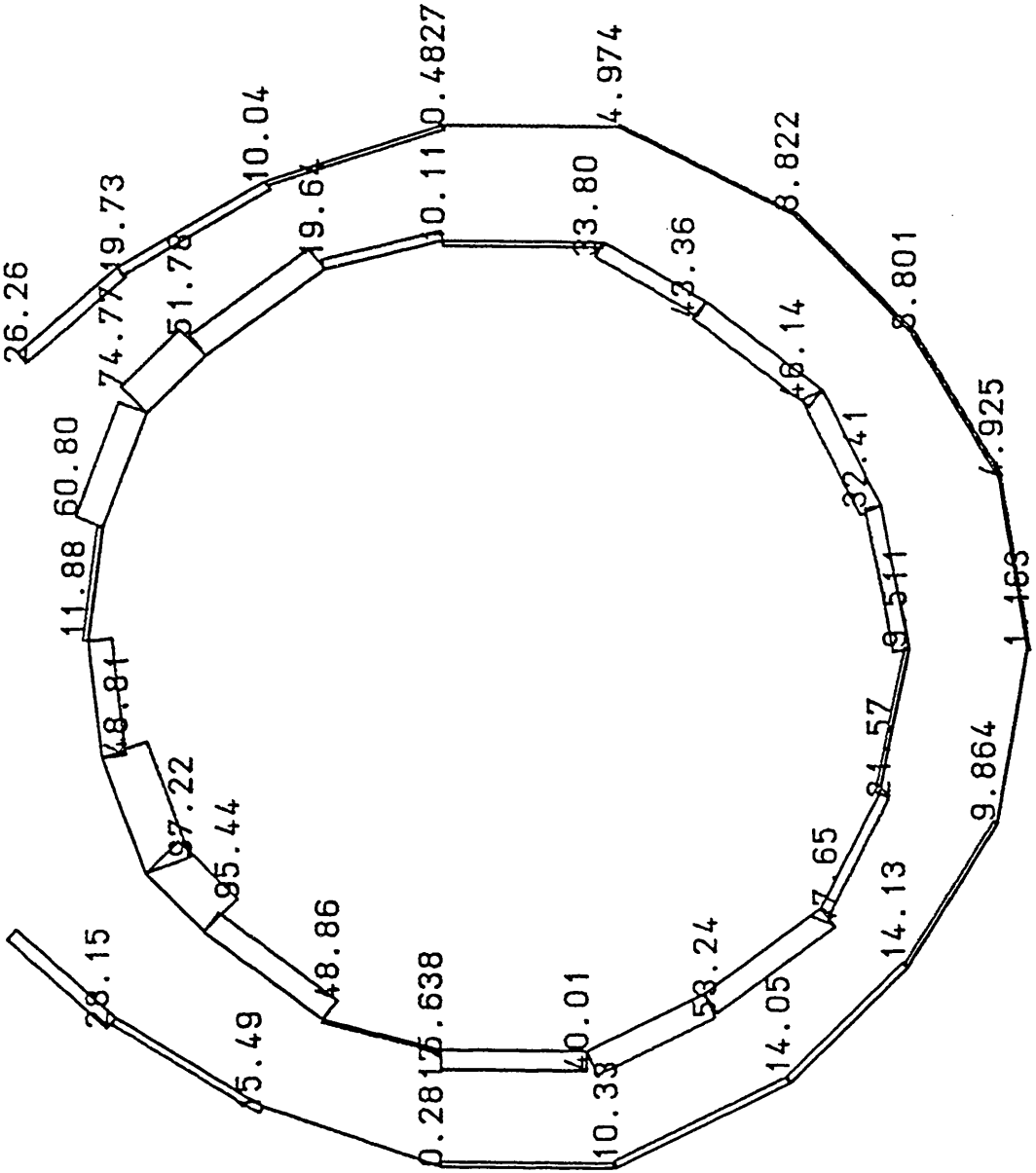


Fig. 5.15(d) Stress at lower hull

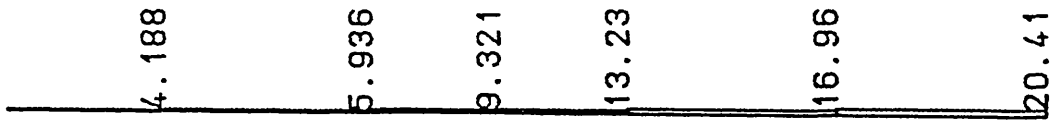


Fig. 5.15(e) Stress at the bar between the decks

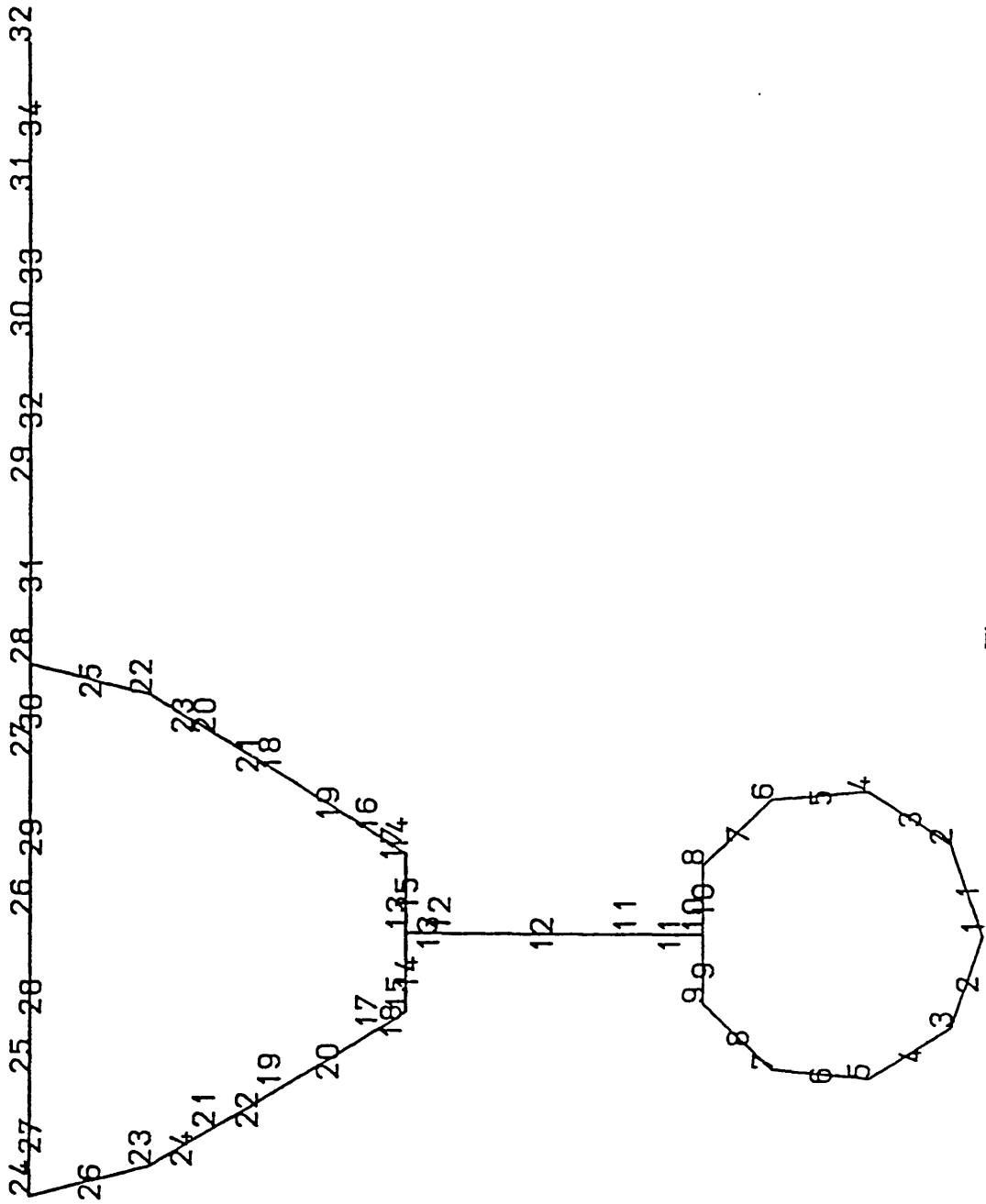


Fig. 5.16 One-dimensional model

MYSTRO: 10.2-3

DATE: 8-02-93

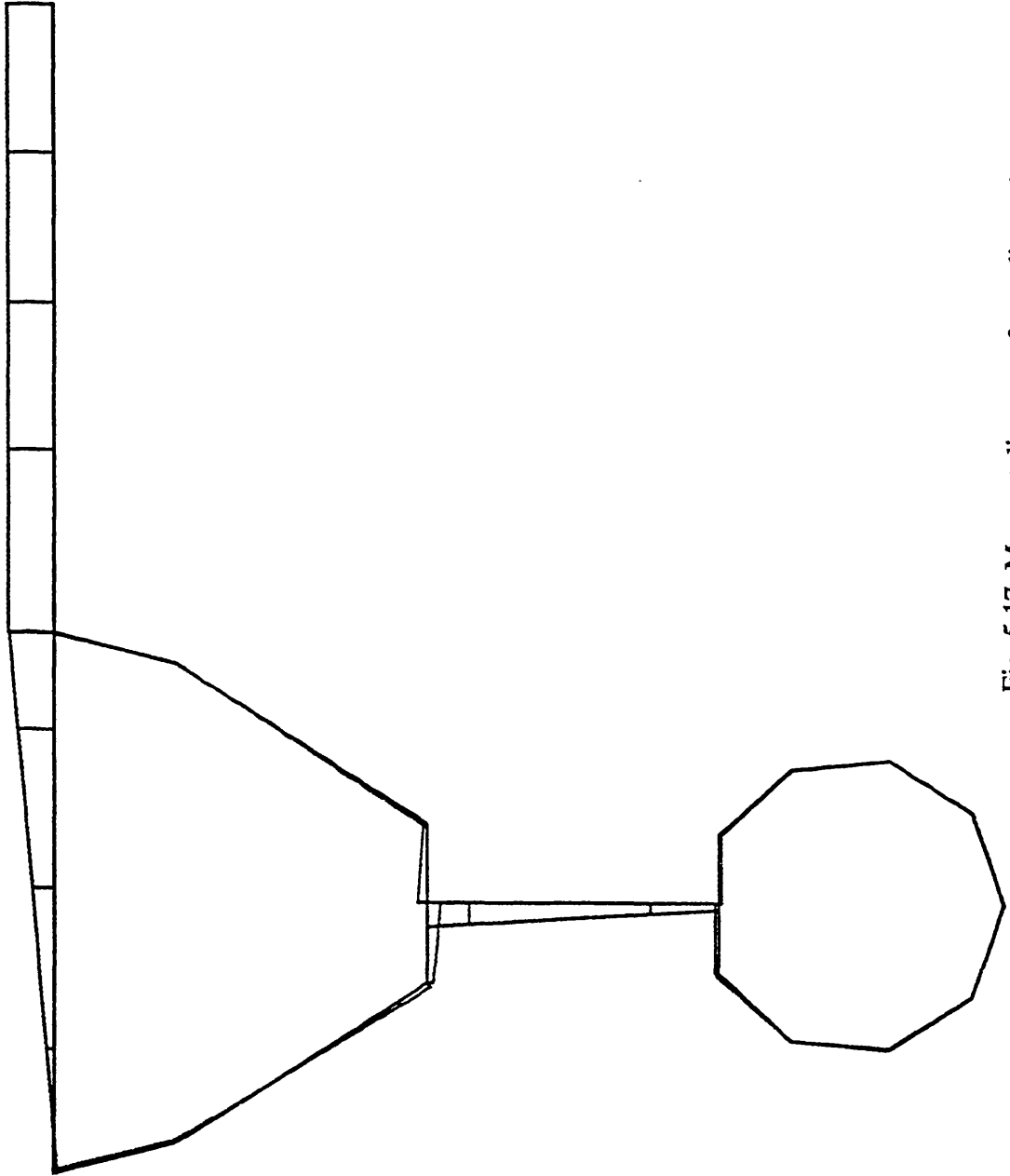


Fig. 5.17 Moment diagram of one-dimensional model

TITLE: ONE DIMENSIONAL ANALYSIS OF PATRIA (FORTH VERSION)

DATE: 8-02-93

MYSTRO: 10.2-3

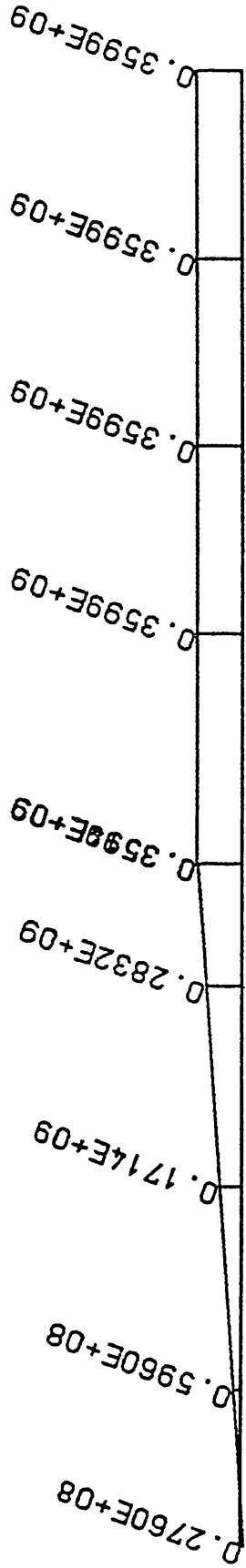


Fig. 5.17(a)

TITLE: ONE DIMENSIONAL ANALYSIS OF PATRIA (FORTH VERSION)

MYSTRO: 10.2-3

DATE: 8-02-93

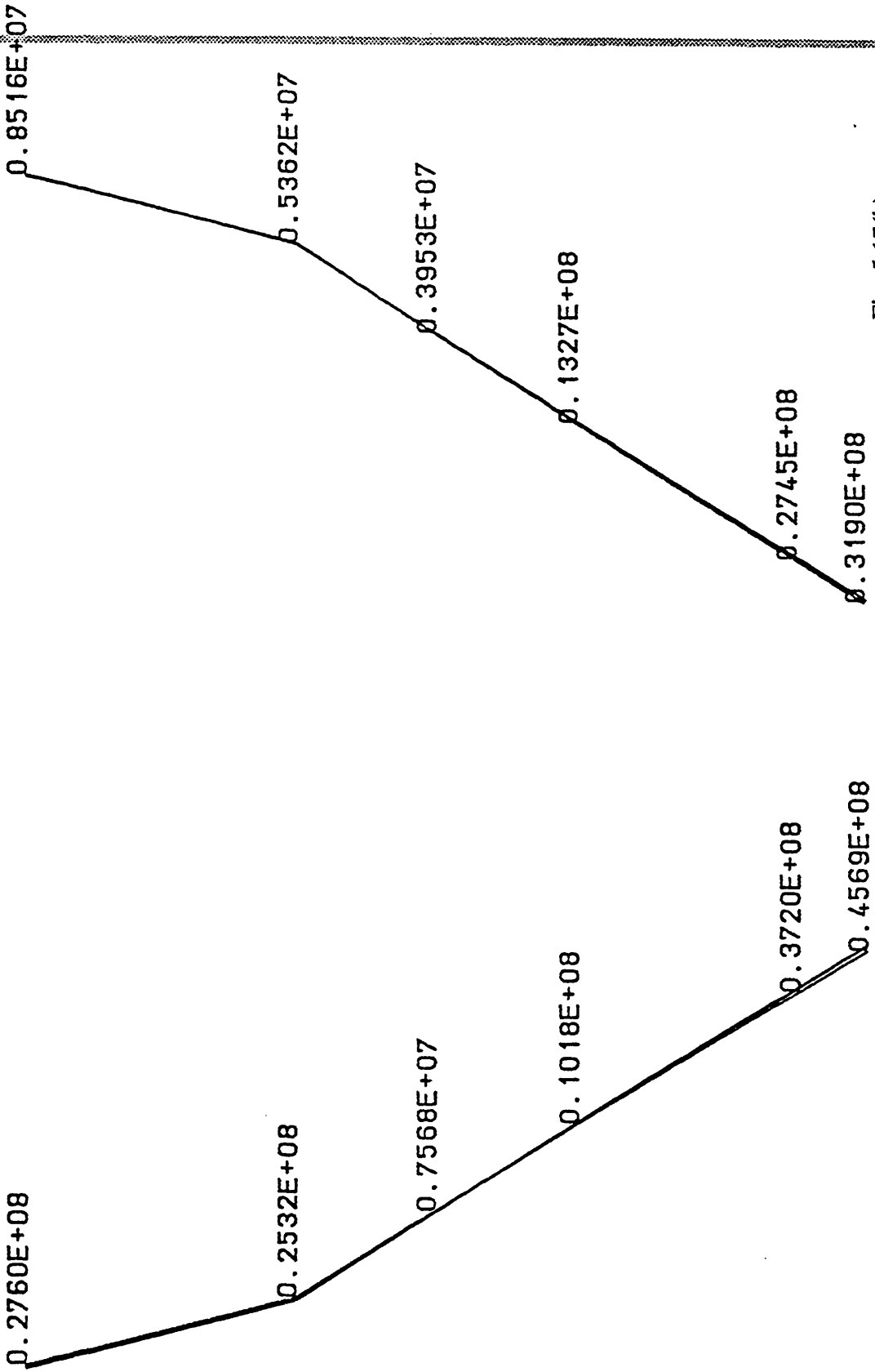


Fig. 5.17(b)

TITLE: ONE DIMENSIONAL ANALYSIS OF PATRIA (FORTH VERSION)



Fig. 5.17(c)

MYSTRO: 10.2-3

DATE: 8-02-93

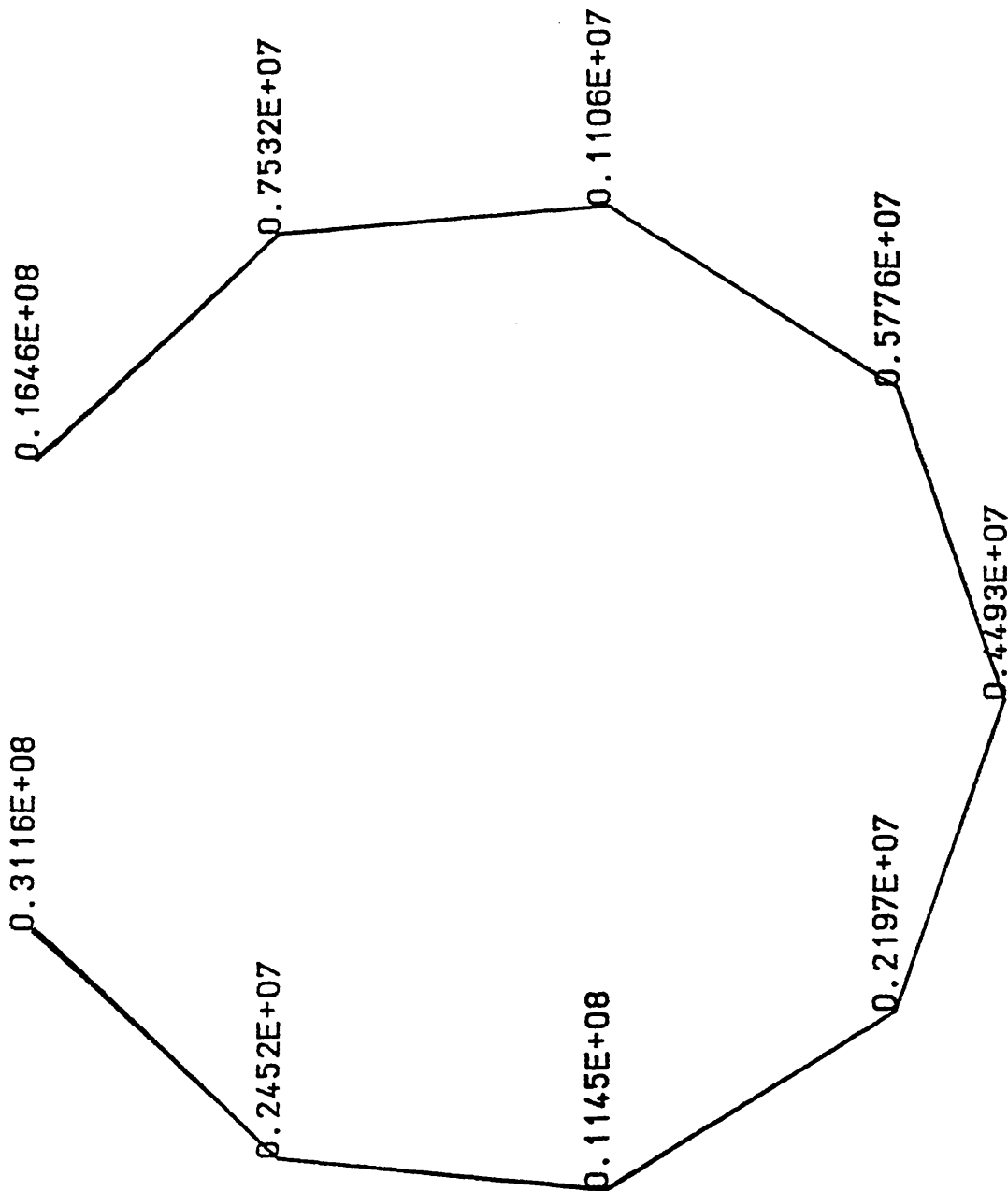


Fig. 5.17(d)

TITLE: ONE DIMENSIONAL ANALYSIS OF PATRIA (FORTH VERSION)

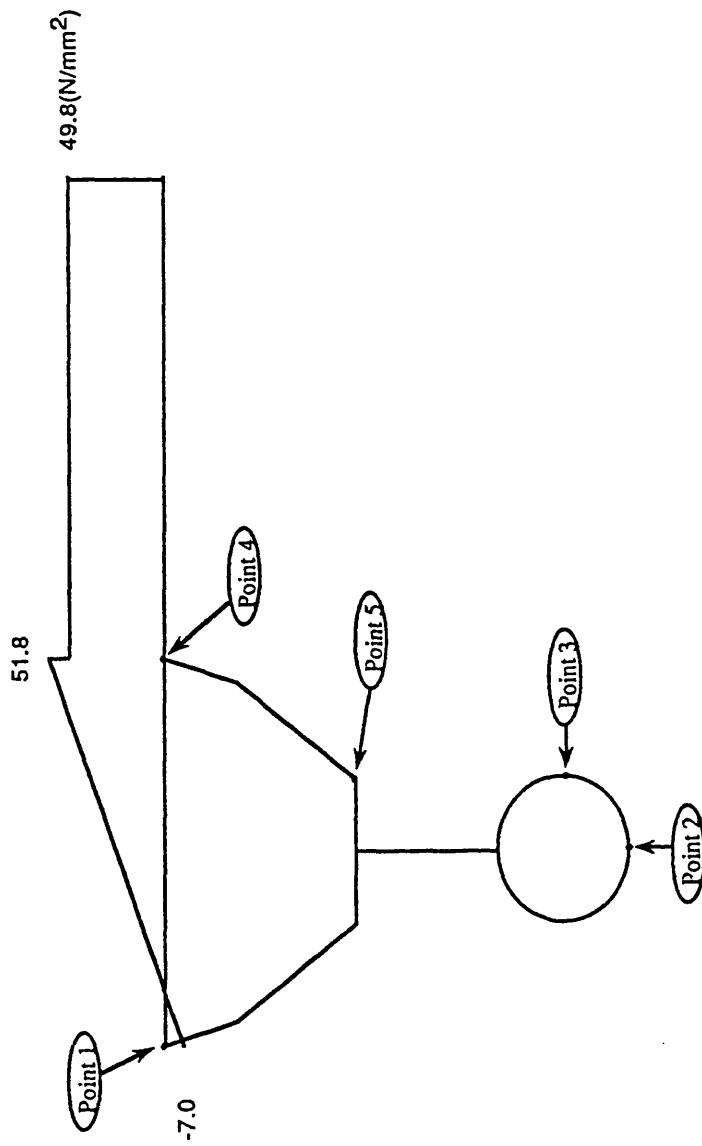


Fig. 5.18 Transverse stress distribution at upper deck of one-dimensional model

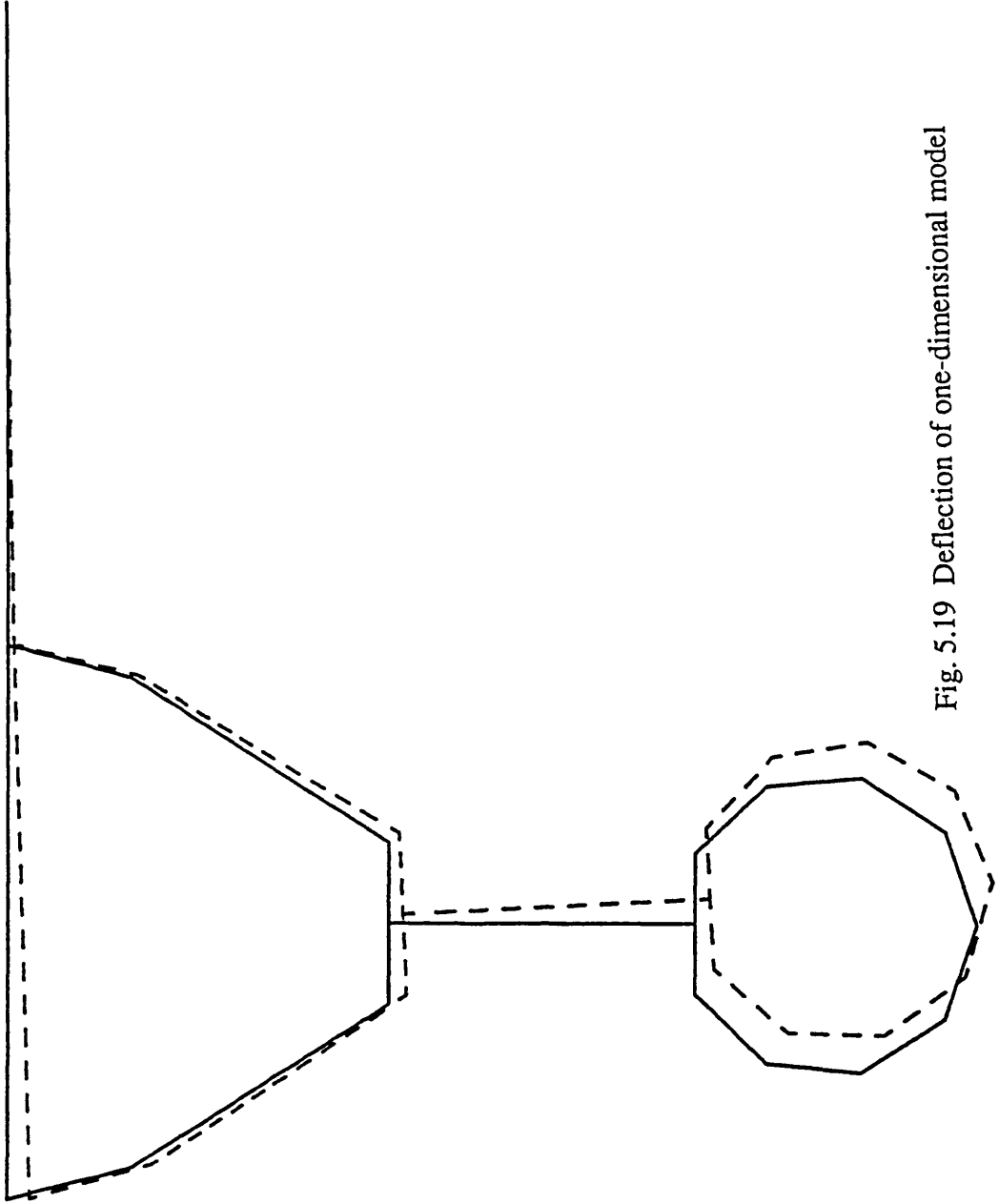
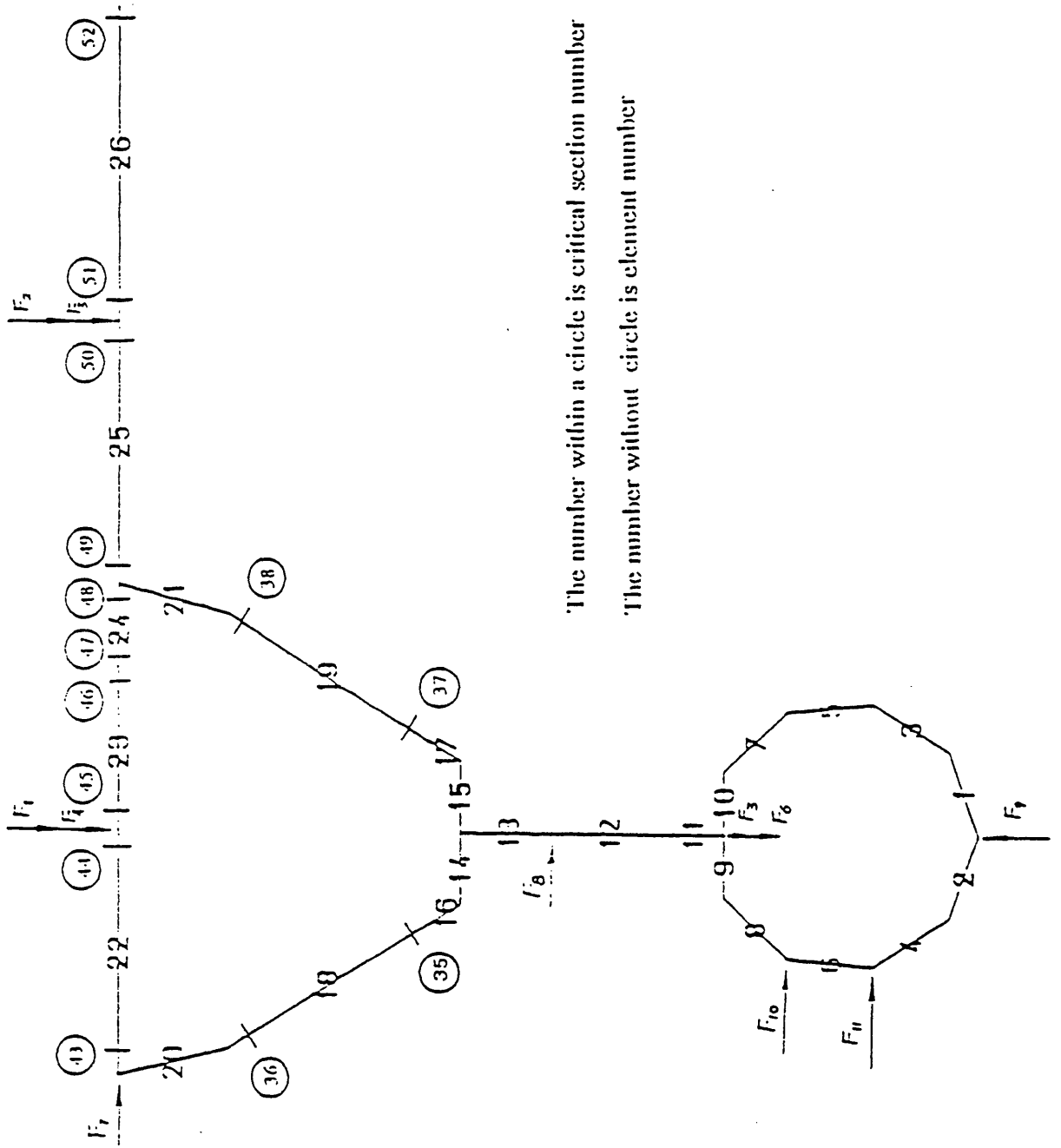


Fig. 5.19 Deflection of one-dimensional model



The number within a circle is critical section number

The number without circle is element number

Fig. 5.20 One-dimensional model of SWATH

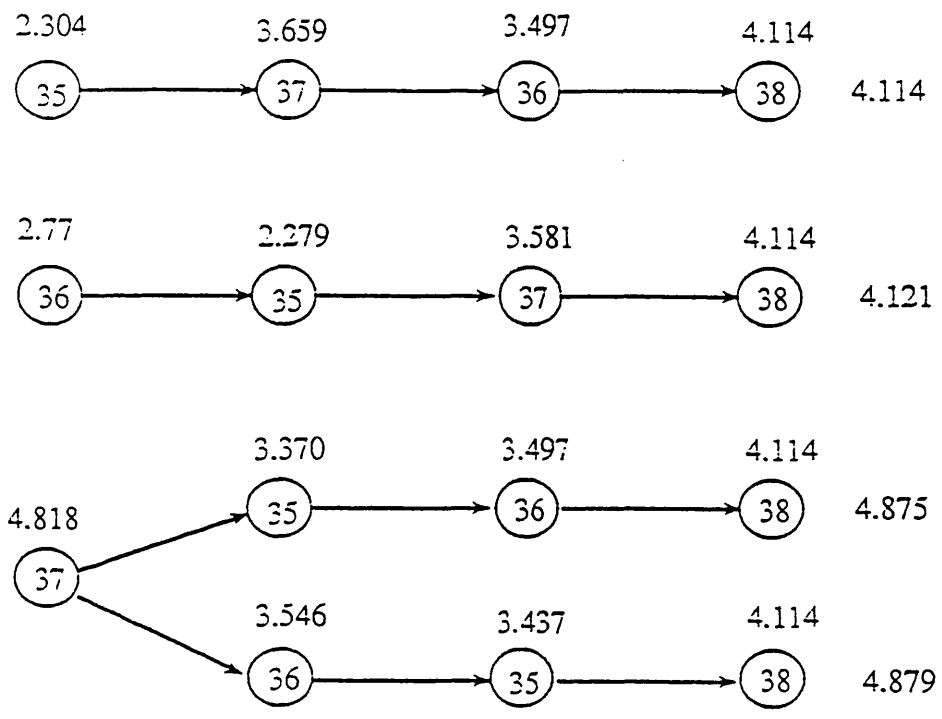


Fig. 5.21 Identified failure tree of PATRIA

CHAPTER 6 STRUCTURAL SYSTEM RELIABILITY INDEX-BASED OPTIMISATION OF SWATH SHIPS

6.1 INTRODUCTION

There are usually many design parameters to be calculated in a structural design process. The aim of a design is to achieve maximum safety with minimum cost. Conventional optimisation, which is generally used in practice, is a deterministic process (Arora, 1990; Olhoff, 1983 and Venkayya, 1978). It has been observed that the optimum structures obtained through deterministic optimisation do not necessarily have high reliability (Das and Frieze, 1982; Feng and Moses, 1986b). Hence it is likely that the failure probability of the optimum structure does not satisfy the reliability criteria. The optimisation based on reliability concepts will have more consistent safety in the structure system.

The object of reliability-based design is to achieve a uniform and consistent reliability within a structural system. The advantages of reliability-based design could be summarised as follows (Thoft-Christensen and Baker, 1982):

- * it can treat the uncertainties or errors of all variabilities in strength and loading in a more rational way, and thus provide a better framework for safety evaluation of a structure
- * it tends to lead to a balanced design and allows the engineer to check the design (or the code) against the influence of the stochastic parameters of resistance, loading variables, etc
- * it provides a logical framework for the choice between alternative solutions with a subjective acceptance of the estimated probabilities as degree of belief in the reliability of the structure.

There are two types of reliability-based optimisation formulations, one is the component reliability index-based optimisation, another is the system reliability index-based optimisation. Most work in reliability-based optimisation in the last decades is based on the elemental reliability, such as Murotsu et al, 1983; Enevoldsen, 1994; Madson and Hansen, 1991; Nikolaidis and Burdisso, 1988; and others. In the analysis the reliability indices, which are usually evaluated by AFOSM method, for all the critical elements are restricted to an acceptable range, eg. greater or equal to

3.0. It may be said that this method could be applied to practical cases without many problems.

The progress in system reliability index-based optimisation is relatively slow, because the computational time is then a big problem. As mentioned in Chapter 2, the structural system reliability analysis itself is time-consuming, and much time is spent on searching for significant failure modes and on multi-normal integration (if it is necessary). During the process of optimisation, the design variables are changed in each iteration, and the system reliability index of the structure needs to be re-evaluated. Because of the amount of calculation the method is only applied to relatively simple cases, although much effort has been made by researchers, such as Thoft-Christensen and Murotsu, 1986; Enevoldsen and Sorensen, 1993; Feng and Moses, 1986a and 1986b; Frangopol and Fu, 1989; etc.

In this chapter, various formulations for reliability-based optimisation and the possible problems associated with these formulations are discussed. A new algorithm, in which the component and system reliability requirements can be balanced, is proposed, and the typical frame of a built SWATH ship is optimised by the proposed method.

6.2 OPTIMISATION BASED ON ELEMENTARY RELIABILITY INDEX

The formulation for elemental reliability-based optimisation is expressed as:

$$\min \quad C(\mathbf{d}, \mathbf{X}) \quad (6.1)$$

$$\text{subject to} \quad \beta_{ci} \geq \beta_{cia} \quad (i=1, \dots, nc) \quad (6.2)$$

$$d_i^L \leq d_i \leq d_i^u \quad i=1, \dots, n \quad (6.3)$$

where $C(\mathbf{d}, \mathbf{X})$ is the objective function referring to cost or weight, \mathbf{d} is design variable vector, \mathbf{X} is random variable vector, β_{ci} is the reliability index of i th critical section, β_{cia} is the allowable reliability index for the i th critical section. d_i^L and d_i^u are the lower and upper bounds of the i th design variable.

The safety margins of constraints in Eq.(6.2) could be transformed from the deterministic requirements (Nikolaidis and Burdisso, 1988; Thanedar and Kodiyalam, 1992; etc) or established using a plasticity condition by a finite element method (Murotsu, et al, 1983). The reliability indices of the constraints could be evaluated by AFOSM method. Nikolaidis and Burdisso (1988) found that if the Mean Value First Order Second Moment is used the results might be wrong in some cases. The method developed in Chapter 2 is used in this case.

The optimisation problem in (6.1)-(6.3) can, in principle, be solved by any general non-linear optimisation method. But its efficiency and robustness are very important because in practice safety margins of constraints for a large structure are usually generated by the finite element method. It has been shown that the Sequential Quadratic Programming method has many advantages over the others (Arora, 1990; Tseng and Arora, 1988a and 1988b). The method developed by Schittkowski (1985) is a very efficient and robust algorithm, which is used in the present study. The first-order derivatives of reliability index of constraints can be calculated by the method suggested by Bjerager and Krenk (1989).

$$\frac{d\beta}{d\theta} = \frac{1}{|\nabla_M(u^*)|} \frac{\partial M}{\partial \theta}$$

where M is the failure surface equation, θ is a deterministic parameter and u^* is the design point in standard normalised space.

$|\nabla_M(u^*)|$ is already calculated in the AFOSM. The $\frac{\partial M}{\partial \theta}$ could be evaluated by a semi-analytical method, or a numerical method, or the techniques suggested by Santos (1991) and Zotemantel(1991).

6.3 OPTIMISATION BASED ON THE SYSTEM RELIABILITY INDEX

The formulation for this problem is expressed as:

$$\min \quad C(d, X) \quad (6.4)$$

$$\text{subject to} \quad \beta_s(d, X) \geq \beta_{sa} \quad (6.5)$$

$$d_i^L \leq d_i \leq d_i^u \quad i=1,\dots,n \quad (6.6)$$

Most of the early works in this aspect have a common limitation that the significant failure modes of the structure system are known a priori. In practice this is hardly the case for a complex structure. So it may be said that all these methods have only academic value. Various formulations are fully discussed by Thoft-Christensen and Murotsu (1986).

If the significant failure modes are generated during the optimisation, the calculation of system reliability is time consuming. Hence, if the formulations (6.4)-(6.6) are directly used in the optimisation, at each iteration the system reliability index needs to be evaluated again. Furthermore, the computation of first-order derivatives of the constraint is also repeated in each iteration. If they are computed by numerical differences, it is not only very computationally expensive but also inaccurate in many cases because of approximations during the process. Sometimes it could also cause convergence problems.

Another possible problem is that actually in the process of calculating system reliability, only significant failure modes are included in the evaluation. So at different iteration, the significant failure modes are, generally speaking, not the same. This does not meet the convergence requirement for optimisation. So the optimisation may not converge. Fortunately, in practice, the significant failure modes identified in system reliability analysis tend to be stable after a few iterations.

In the past decade, much effort has been made by some researchers to solve these problems. Murotsu et al (1994) established an alternative to the original formulation and is expressed as:

$$\min \quad C(\mathbf{d}, \mathbf{X}) \quad (6.7)$$

$$\text{subject to} \quad \beta_{ip}(\mathbf{d}, \mathbf{X}) \geq \beta_{ipa} \quad i=1,\dots,M_p \quad (6.8)$$

$$d_i^L \leq d_i \leq d_i^u \quad i=1,\dots,n \quad (6.9)$$

where

β_{ip} are the reliability indices of the i th failure mode

β_{ipa} are the allowable values for the i th failure mode

M_p is the number of the failure modes.

This formulation is based on the fact that the system reliability index depends on the reliability indices of all significant failure modes and the correlation between them. It is observed that the ratio of the system reliability index to the minimum reliability index of significant failure modes varies within a very small range for a specific structure.

A failure mode is introduced in the analysis only when it is active. Such a technique could save computational time. Because only bending moment is considered in the analysis, the safety margin of a failure mode can be expressed by the safety margin of the last failed hinge. In this case, the safety margin is a linear combination of resistances and external loads, so the failure probability of a failure mode could be evaluated by AFOSM (see Eqs. 12&13 in Murotsu et al, 1994). In Eq. 12, the coefficient a_{irk}, b_{ij} do not vary when the design variables are changed during the optimisation. That means the coefficients for the safety margins of failure modes only need to be generated once during the analysis. It should be pointed out that the above mentioned good features do not exist when the interaction of bending moment and axial force including buckling effect is taken into consideration. In this case each failure mode should be modelled as a parallel system which consists of all the failed elements in that failure path.

A similar formulation is derived by Enevoldsen and Sorensen (1993) for more general cases. The original formulation was also transformed to the same form as above. The differences are: (1) the failure modes in the constraints are actually parallel systems. (2) The allowable values for constraints can be adjusted by the Constant Objective Function Method or the Bounds Iteration Method in such a way that the system reliability index meets the original requirement. This guarantees that the original system reliability index is within the feasible region at the price of more computation. In addition, a semi-analytical method was derived to calculate the first-order derivatives of the constraints in the analysis which is very attractive.

Takada et al (1993) presented a method which could be applied to space truss structures. The constraints are first linearized by the Taylor expansion, then the optimisation formulation is transformed to a linear programming problem, which can be solved easily by a general package.

Liu and Moses (1991) advocated that, not only the system reliability index, but also the redundancy (e.g. system reliability of damaged structure) should be included in the formulation because the system reliability level could be very low after the failure of a member if the redundancy is not considered. A bridge was optimised by this formulation. Similar formulations were also used by other researchers such as Feng and Moses (1986a and 1986b); Frangopol and Fu (1989), but these formulations were only applied to relatively simple cases.

It may be said that a complete reliability-based optimisation formulation should be expressed as:

$$\min \quad C(d, X) \quad (6.10)$$

$$\text{subject to} \quad \beta_{ci} \geq \beta_{cia} \quad (6.11)$$

$$\beta_s \geq \beta_{sa} \quad (6.12)$$

$$\beta_{R,s} \geq \beta_{R,sa} \quad (6.13)$$

$$d_i^L \leq d_i \leq d_i^u \quad i=1, \dots, n \quad (6.14)$$

where $\beta_{R,s}$ and $\beta_{R,sa}$ are residual system reliability and its allowable value respectively. The reliability of some important components, system reliability, and residual system reliability are included in this formulation.

6.4 PROPOSED ALGORITHM FOR SYSTEM RELIABILITY-BASED OPTIMISATION

As mentioned before, a complex structure usually possesses reserve strength. This means that the failure of a component does not result in the collapse of the structure. So it is widely recognised that the structural system reliability index should be considered in optimisation. But the application of this is limited in some simple structures.

On the other hand, if only the system reliability index is used in optimisation, it is likely that the reliability indices of some components are too small, say less than 2.0 or

even lower. Leaving the component reliability indices in such small values might not be a good idea, and may in practice increase the need for repair costs. In addition, some components in a structure may be so important that the failure of these components could render the structure unserviceable - possibly even leading to progressive collapse associated with cracking, etc. Furthermore, directly solving formulations (6.4)-(6.6) is very time-consuming. Therefore it is necessary to find an alternative in which the component and system reliability could be balanced.

An algorithm in which both component and system reliability are considered is proposed. The possibility of using such an idea was first pointed out by Thoft-Christensen and Murotsu (1986), but it was not there fully developed.

The proposed procedure is as follows:

- Step 1 Set initial allowable reliability indices in Eq.(6.2). Solve the problem (6.1)-(6.3)
- Step 2 Calculate the structural system reliability of the optimum structure in Step 1
- Step 3 Check if the system reliability meets the requirement. If yes, stop the calculation; if no, adjust the allowable reliability indices in Eq.(6.2), then repeat Steps 1-3 until the system reliability requirement is met.

Adjusting the allowable reliability

The efficiency of the proposed algorithm depends on the way the allowable reliability is adjusted. A heuristic procedure is established. It is observed that the structural weight (or cost) is only affected by the active allowable reliability indices in Step 1 and the structural system reliability strongly depends on the reliability of the failure paths with the highest failure probability, which in turn rely on the components with the smallest reliability index. Based on the above facts, the procedure to adjust the allowable reliability indices is:

- 1) Select the sections which are in the active constraints in Step 1
- 2) Select the sections which are included in the failure paths with the highest failure

probability

- 3) The sections, whose allowable reliability indices will be adjusted, are those appearing in both 1) and 2)
- 4) Put the selected sections into nine groups according to their current allowable reliability indices, then adjust the allowable reliability indices according to the desired direction.

Group No.	β_{ja}
1	2.0
2	2.25
3	2.5
4	2.75
5	3.0
6	3.25
7	3.5
8	3.75
9	4.0

In the program, the allowable reliability indices are adjusted in an interactive way so that designer's experience and preference could be applied. The flow chart of the program is shown in Fig. 6.1.

6.5 TARGET RELIABILITY IN THE OPTIMISATION

Determination of target reliability is a very important and difficult step in reliability-based optimisation. In the current rules only component reliability is considered and the system effect factor is set to one. The target reliability is determined by social and economic considerations. The social considerations are dominant for assessing the acceptable risks of collapse of primary structural components, which could have serious consequences to lives or the environment (i.e. with reference to the ultimate limit states). The economic considerations are dominant for assessing the acceptable risks of loss of quality of the structure, increased maintenance and repair

costs, permanent or temporary interruption of normal service operations (i.e. with reference to the serviceability limit states).

Faulkner (1984) has studied the target reliability for various steel structures, which are shown in Fig.6.2. It is observed that the reliability for merchant ships and British frigates vary in a very large range. A value of $\beta=3.0$ for frigates and 3.0 to 4.0 for merchant ships was recommended.

It should be mentioned that the above target values were determined neglecting the redundancy effect. It is found that a non-redundant structure would need a higher safety margin than a redundant one to achieve the same acceptable level of damage tolerance. So if the system reliability index is considered in optimisation, the requirements for component target reliability could be relaxed to some extent. As can be seen in Fig. 6.2, in rare cases the reliability index of a ship is below 2.0. Therefore a value of $\beta=2.0$ might be a reasonable lower limit for the proposed optimisation.

Unfortunately, so far there is not a general rule to select the allowable system reliability index. Designer's experience and preference still play an important role in the process. Liu and Moses (1991) used 4.5 as the target system reliability index to optimise a bridge. From the results in Lee (1989) and Lee and Faulkner (1989), it is seen that when component reliability index is equal to 3.0 and $n=1.5$ (n is defined as the ratio of the mean system collapse load to the mean component collapse load), the corresponding system reliability index is 4.64, assuming the resistance and load effect are log-normally distributed. It seems that 4.5 is an acceptable value.

6.6 APPLICATION TO A SWATH SHIP

A typical frame of a built SWATH ship is optimised by the proposed algorithm. Its particulars and loading applied on it were shown in Chapter 5. The weight of the structure is used as the objective function, and the fourteen constraints are that the reliability indices at fourteen critical sections, which are marked in Fig. 6.3, are greater than or equal to their allowable values. Also shown in Fig. 6.3 are the eight design variables d_1, \dots, d_8 , whose lower and upper bounds in optimisation are listed in Table 6.1.

Table 6.1: Design variables and their ranges (mm)

Variables	Low Bound	Upper Bound
d1	3.5	6.0
d2	3.5	6.0
d3	800	1200
d4	3.5	6.0
d5	150	300
d6	4.0	8.0
d7	150	300
d8	4.0	8.0

The objective function in Eq.(6.1) is expressed as:

$$\begin{aligned}
 c(\mathbf{d}, \mathbf{X}) = & \rho \{ [1250 \times (d_1 + d_2) + d_3 \times d_4] \times 6500 \\
 & + [200 \times d_5 + d_6 \times 758.3 + 750] \times 836.9 \\
 & + [200 \times d_7 + d_8 \times 758.3 + 750] \times 836.9 \} \quad (6.15)
 \end{aligned}$$

The safety margins for the fourteen constraints are automatically generated by computer in the similar way in Chapter 5. The value of 750 in Eq. (6.15) is the area of flange in the haunch part. At present the plasticity condition is used as the failure criteria of critical sections, and the interaction of bending moment and axial force including the buckling effect is considered in the analysis. Only the loads and material strength are treated as random variables, the others are deterministic. So the safety margins are expressed as:

$$M_i = \sigma_{yi} w_i(\mathbf{d}) - \mathbf{C}_i^T \mathbf{x}_t \quad (i=1, \dots, 14) \quad (6.16)$$

where:

$$\mathbf{C}_i^T = \left(\gamma \frac{w_i(\mathbf{d})}{A_i(\mathbf{d})} \text{sign}(F_{xi}) \quad 0 \quad \text{sign}(M_{zi}) \right) \quad (6.17)$$

γ is the factor to consider the effect of buckling.

$$\gamma = \begin{cases} 1 & \text{for tension} \\ \sigma_{yi} / \sigma_{ei} & \text{for compression} \end{cases} \quad (6.18)$$

σ_{ei} is the buckling stress of the member

$$\mathbf{x}_t = \begin{pmatrix} F_{xi} & F_{yi} & M_{zi} \end{pmatrix} \text{ is the nodal forces in the member.} \quad (6.19)$$

The nodal forces can be expressed by external loads as follows:

$$F_{xi} = \sum_{j=1}^{ml} a_{ij}(\mathbf{d})L_j \quad (6.20)$$

$$F_{yi} = \sum_{j=1}^{ml} c_{ij}(\mathbf{d})L_j \quad (6.21)$$

$$M_{zi} = \sum_{j=1}^{ml} b_{ij}(\mathbf{d})L_j \quad (6.22)$$

where ml is the number of external loads.

so the safety margin in Eq.(6.16) is re-arranged as:

$$M_i = \sigma_{yi} w_i(\mathbf{d}) - \sum_{j=1}^{ml} \left\{ \gamma \frac{w_i(\mathbf{d})}{A_i(\mathbf{d})} \text{sign}(F_{xi}) a_{ij}(\mathbf{d}) + \text{sign}(M_{zi}) b_{ij}(\mathbf{d}) \right\} L_j \quad (6.23)$$

Then the reliability indices are calculated by AFSOM method. Because the first derivatives of the constraints are needed in the optimisation they are evaluated by the method suggested by Bjerager and Krenk (1989).

$$\frac{d\beta}{d\theta} = \frac{1}{|\nabla M(\mathbf{u}^*)|} \frac{\partial M}{\partial \theta} \quad (6.24)$$

where θ is a deterministic parameter, at present it is a design variable d_k , $k=1,8$. u^* is the design point in standard normalised space.

$|\nabla M(u^*)|$ is already calculated in AFOSM. From Eq.(6.16), the $\frac{\partial M}{\partial \theta}$ is equal to

$$\frac{\partial M}{\partial \theta} = \sigma_{yi} \frac{\partial w_i(\mathbf{d})}{\partial \theta} - \left\{ \frac{\partial \mathbf{C}_i^T}{\partial \theta} \mathbf{x}_t + \mathbf{C}_i^T \frac{\partial \mathbf{x}_t}{\partial \theta} \right\} \quad (6.25)$$

where:

$$\frac{\partial \mathbf{C}_i^T}{\partial \theta} = \left\{ \gamma \text{sign}(F_{xi}) \left[\frac{\partial w_i(\mathbf{d})}{\partial \theta} A_i(\mathbf{d}) - w_i(\mathbf{d}) \frac{\partial A_i(\mathbf{d})}{\partial \theta} \right] / A_i^2(\mathbf{d}) \quad 0 \quad 0 \right\} \quad (6.26)$$

$$\frac{\partial \mathbf{x}_t}{\partial \theta} = \left\{ \frac{\partial F_{xi}}{\partial \theta} \quad \frac{\partial F_{yi}}{\partial \theta} \quad \frac{\partial M_{zi}}{\partial \theta} \right\} \quad (6.27)$$

The derivatives $\frac{\partial w_i(\mathbf{d})}{\partial \theta}$, $\frac{\partial A_i(\mathbf{d})}{\partial \theta}$, $\frac{\partial F_{xi}}{\partial \theta}$, $\frac{\partial F_{yi}}{\partial \theta}$, and $\frac{\partial M_{zi}}{\partial \theta}$ in Eqs.(6.25)-(6.27) are evaluated by the numerical difference method. It is worth mentioning that, in calculating the last three derivatives, the finite element method needs to be called again, therefore much computational time will be spent on this operation.

In Step 1 the initial allowable reliability indices are assigned as 3.0, then the problem (6.1)-(6.3) is solved. The flow chart of the program is shown in Fig. 6.4 where:

NLPQL a general non-linear mathematical programming program by a sequential quadratic algorithm developed by Schittkowski (1985)

NLFUNC a user supplied subroutine for calculating the objective and constraint functions at the given design variables

NLGRAD a user supplied subroutine for evaluating the gradients of objective and constraints at the given design variables

MOMENT for calculating the geometrical properties of a I section

FEM the general finite element program, which is used to generate the safety margins of constraints

AFOSM advanced first order second moment method, which is used to evaluate the reliability indices of constraints.

The optimum values for eight design variables are shown in Table 6.2. The convergence history is shown in Fig. 6.5. It is observed that only constraint 14, which is shown in Fig. 6.3, is active, constraint 13 is close to zero (0.21), the other constraints are much greater than zero.

Table 6.2: The optimum structure in Step 1

	Design Variable								Weight
	d ₁	d ₂	d ₃	d ₄	d ₅	d ₆	d ₇	d ₈	
Original	4.85	4.85	1000	4	200	6	200	6	487.7
Optimal	3.5	3.5	1000.5	3.5	213.9	7.53	202.8	5.83	429.6

In Step 2 the system reliability of the optimum structure in Step 1 is evaluated by the method in Pu and Das (1994). The system reliability index of the optimum structure is 4.712, which is higher than that (3.756) of the original structure.

Other important information obtained from the analysis is the sensitivity factors, which clearly show how the reliability index of each critical section varies with the change of each design variable. The sensitivity factors of the optimum structure are listed in Table 6.3, and are defined as the first derivatives of constraints to design variables $\left(\frac{d\beta_j}{dd_k}, j = 1, \dots, 14, k = 1, \dots, 8 \right)$.

Table 6.3: The sensitivity factors of the optimum structure

Constn No.	Design				Variables			
	d ₁	d ₂	d ₃	d ₄	d ₅	d ₆	d ₇	d ₈
1	0.9856	0.9856	0.0124	0.4054	<10 ⁻¹⁰	<10 ⁻¹⁰	<10 ⁻¹⁰	<10 ⁻¹⁰
2	0.9856	0.9856	0.0124	0.4054	<10 ⁻¹⁰	<10 ⁻¹⁰	<10 ⁻¹⁰	<10 ⁻¹⁰
3	0.9856	0.9856	0.0124	0.4054	<10 ⁻¹⁰	<10 ⁻¹⁰	<10 ⁻¹⁰	<10 ⁻¹⁰
4	0.9856	0.9856	0.0124	0.4054	<10 ⁻¹⁰	<10 ⁻¹⁰	<10 ⁻¹⁰	<10 ⁻¹⁰
5	0.9900	0.9900	0.0125	0.4002	0.0026	0.0086	-0.0008	0.0018
6	1.0199	1.0199	0.0129	0.4122	0.0027	0.0092	-0.0010	0.0021
7	1.0199	1.0199	0.0129	0.4122	0.0027	0.0092	-0.0010	-0.0021
8	1.0615	1.0615	0.0134	0.4289	0.0029	0.0103	-0.0011	-0.0024
9	1.0615	1.0615	0.0134	0.4289	0.0029	0.0103	-0.0011	-0.0024
10	1.1073	1.1073	0.0143	0.4440	-0.0013	-0.0049	0.0005	0.0007
11	-0.1795	-0.1795	-0.0039	-0.0483	0.0159	0.0463	0.065	0.320
12	-0.0618	-0.0618	-0.0013	-0.017	0.0177	0.066	0.0408	0.225
13	0.0987	0.0987	0.0022	0.0268	0.0351	0.0892	0.0073	0.009
14	0.0695	0.0695	0.0015	0.0189	0.0379	0.1084	0.0091	0.029

From Table 6.3, it is seen that:

- * The design variables d_k , $k=5, \dots, 8$, have hardly influenced the reliability index of the upper box part, so the optimisation of this part could be carried out separately.
- * The design variables d_k , $k=1, \dots, 4$, have relatively small effect on the haunch area, so the optimisation of the haunch part can also be carried out separately without much loss of accuracy.
- * The most efficient way to increase the safety in the haunch area is to increase the thickness of the side shell in this part.

If the target system reliability index is set to be 4.5, the optimum structure could be accepted as the final optimum structure, because the present system reliability index is 4.712, which is very close to the target. Of course, a closer value of system reliability index can be achieved by adjusting the allowable reliability index at section 14. Nevertheless in practice, it is not really worth carrying out more calculations to level out such small differences.

6.7 CONCLUSIONS

Various reliability-based optimisation formulations are discussed in this chapter. Although it is recognised that the formulation (6.10)-(6.14) might be the most rational one in the sense that the safety levels of important components, system reliability and residual system reliability are considered, nevertheless the application of these formulations is still at its early stage, computational time being the main problem. For this reason a new algorithm in which the component and system reliability indices could be balanced is proposed, and it is applied to the optimisation of a typical frame structure in a built SWATH ship. It is found that:

- * The algorithm works very well. Computational time in the analysis is not a problem because the system reliability calculation is only applied to the optimum structure in Step 1.
- * The original design is quite close to the optimal one, so the margin for optimisation is small. It is interesting to note that the system reliability index for the original structure is only 3.756, while it is 4.712 for the optimum structure, at the same time the optimum one is 13% lighter than the original one.
- * The haunch area is confirmed as the critical part. From the values of design variables of the optimum structure, it is observed that increasing the thickness of the side shell is the most efficient way to improve the safety in this area. Because the dimensions of the flange were fixed during optimisation, their effect on the safety is not investigated in this study. The dimensions of the flange might be an important factor influencing the safety because increasing of the area of the flange would shift the neutral axis toward the flange so that the maximum stress in the flange would decrease.

On the whole, reliability-based optimisation is a powerful tool to achieve efficient designs.

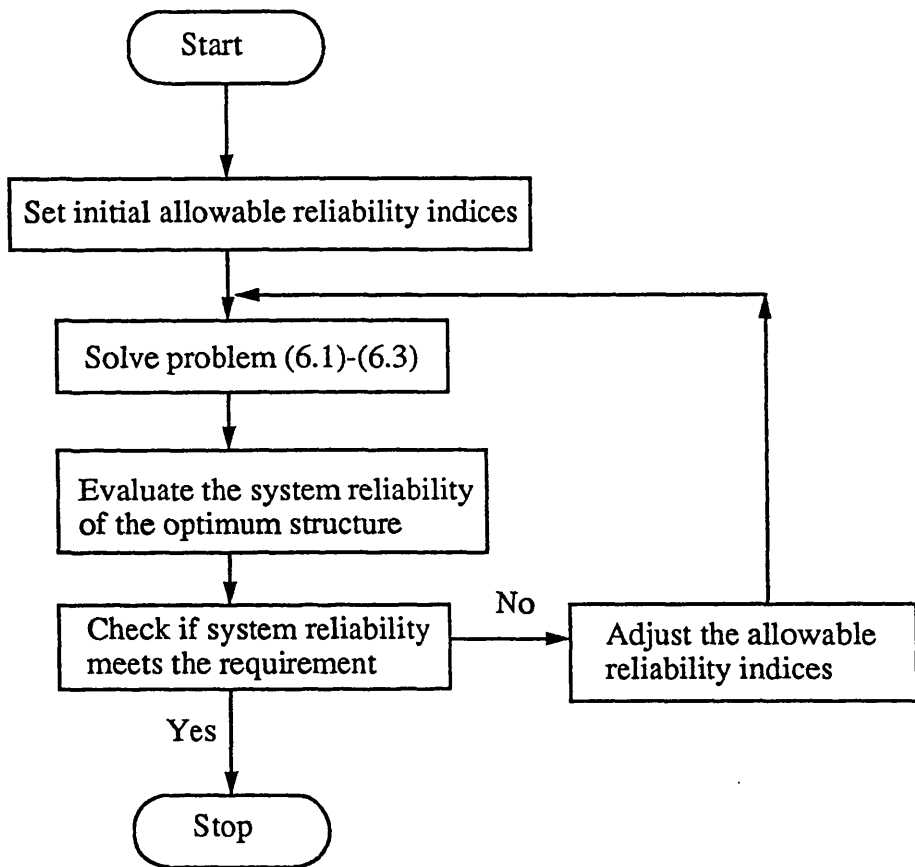


Fig. 6.1 The Flow chart of the proposed algorithm

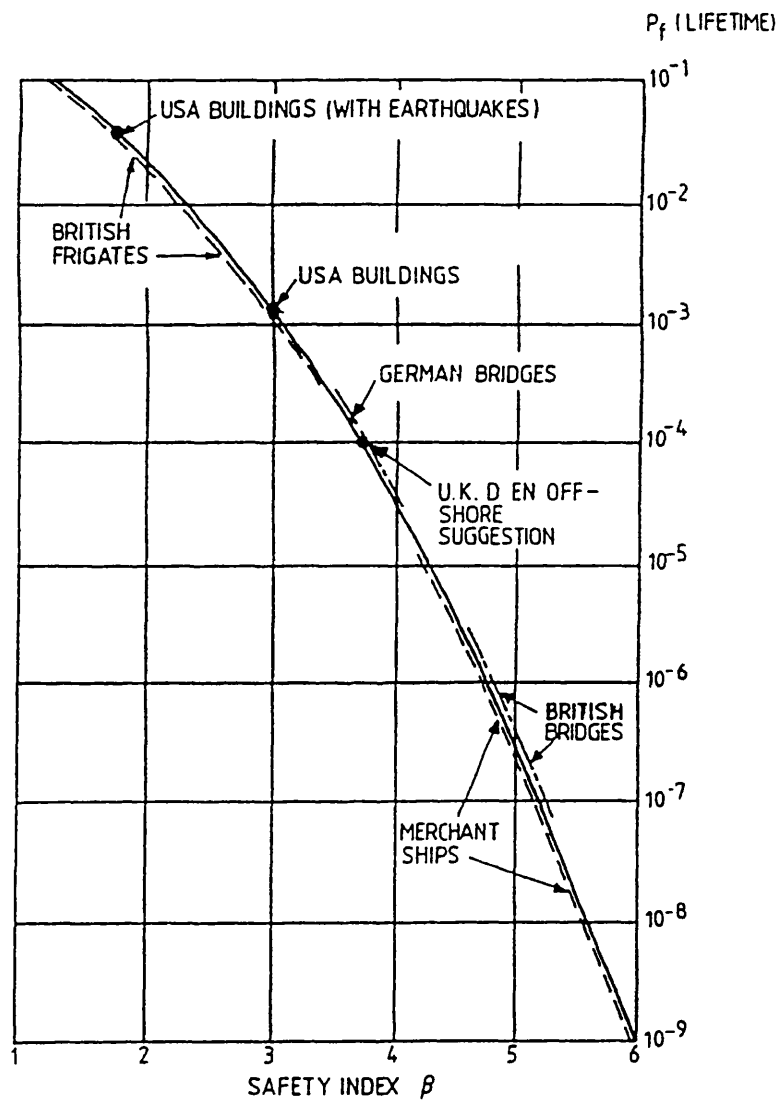


Fig. 6.2 Safety index vs probability of failure (Faulkner, 1984)

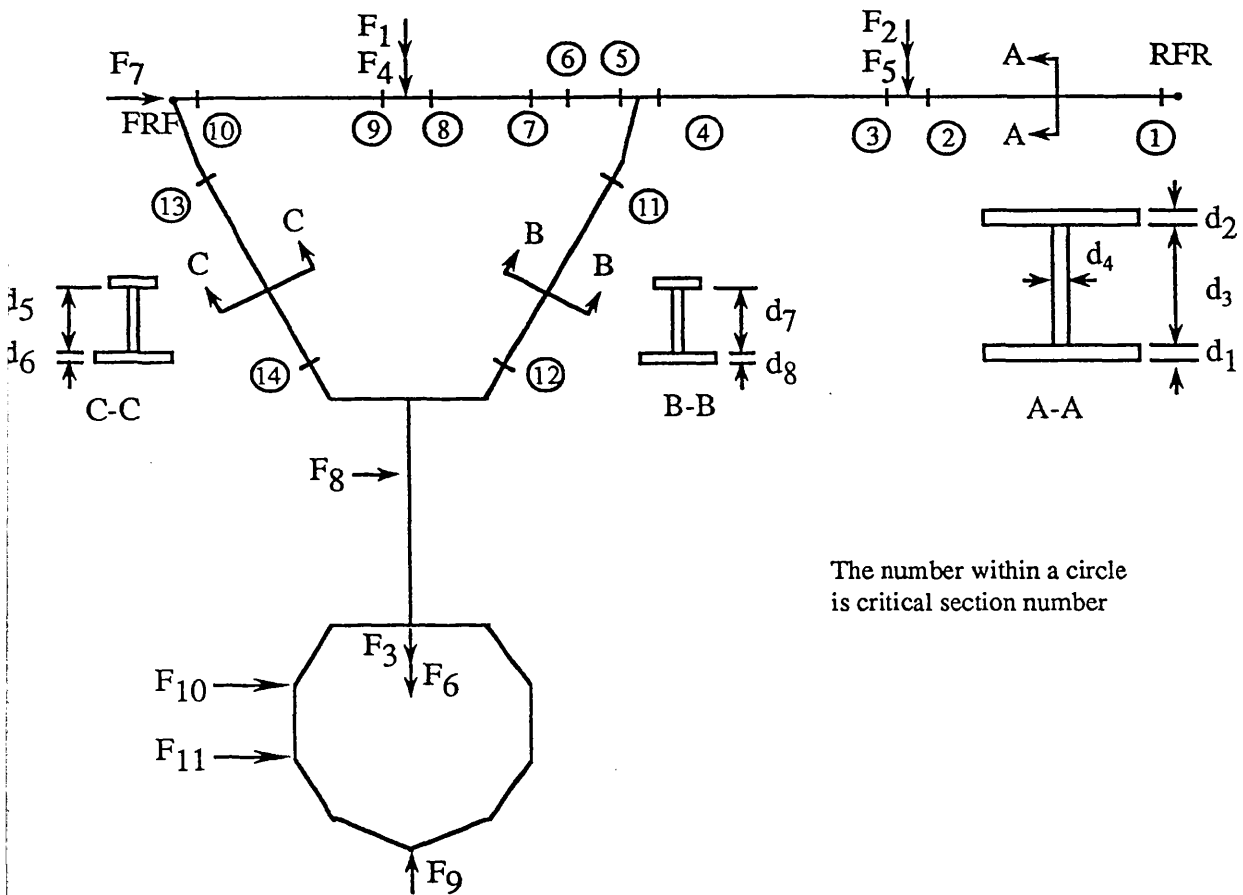


Fig. 6.3 The typical frame in a built SWATH

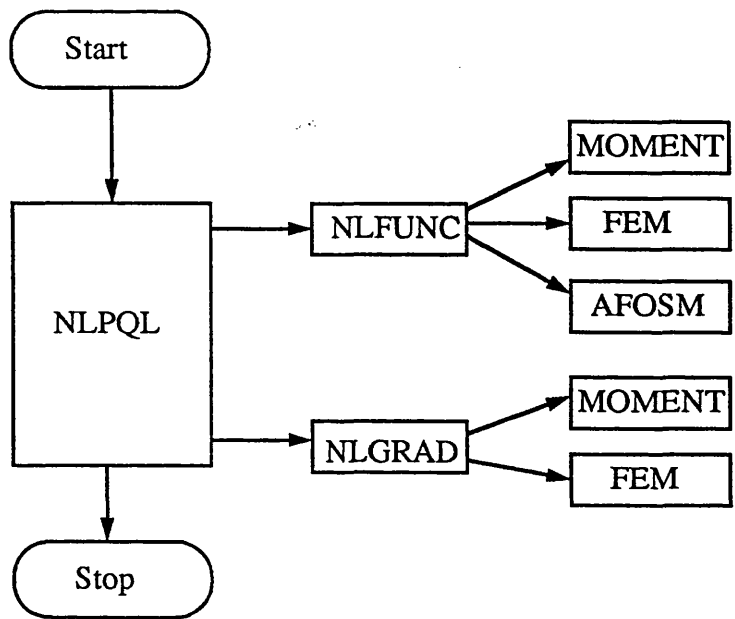


Fig. 6.4 The flow chart for solving problem (6.1)-(6.3)

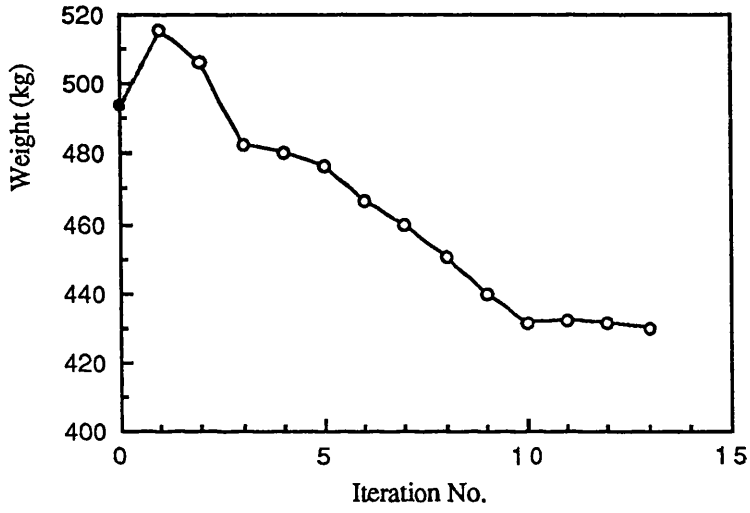


Fig. 6.5 Convergence history

CHAPTER 7 CONCLUSIONS AND RECOMMENDATIONS

7.1 GENERAL

The primary objective of the current research presented in this thesis was to develop a rationally-based structural design procedure for SWATH type vessels by applying reliability analysis and reliability-based optimisation techniques. Due to the limited availability of documents about existing SWATH ships, the analyses were only applied to one built SWATH, the M.V. PATRIA.

Firstly, the primary loads for PATRIA were calculated by a theoretical method. The response amplitude operators of loads in regular waves were calculated by a three-dimensional oscillating source distribution method in association with linearised potential theory. The various extreme design values were then evaluated by spectral analysis.

Having determined the primary loads acting on PATRIA, a series of finite element analyses was carried out aimed at increasing the understanding of the structural behaviour of the ship, and establishing a simplified model for system reliability analysis and multiple criteria optimisation.

At the component level the existing ultimate strength formulations for plate panels and stiffened plates were discussed and calibrated by using a considerable amount of experimental and numerical data. A new algorithm for stiffened plates was proposed. The reliability of plating and stiffened plates was then evaluated by using AFOSM, SORM and Monte Carlo simulation methods to investigate the accuracy of these methods for these types of limit states equations.

At the system level the conventional β -unzipping method was extended by introducing a discarding process in searching for significant failure modes of the structural system. The extension could save computational time when the combined load effects are considered in the analysis. The method was then used to analyse a typical frame in PATRIA, the critical parts and possible failure paths were identified through the analysis.

Finally, the reliability-based optimisation techniques were used to achieve an efficient design. Various reliability-based optimisation formulations and their associated problems were first discussed. An algorithm, in which the component and system reliability indices could be balanced, was proposed. The proposed strategy was then applied to optimise the one-dimensional model for the transverse cross-deck frame in PATRIA.

The function of this final chapter is to summarise the principal conclusions in the present study and to identify the possible promising research areas.

7.2 PREDICTION OF PRIMARY LOADS

Prediction of primary loads is a very crucial step in the structural design process. To bridge the gap between hydrodynamicists and structural engineers, several important issues related to primary loads were discussed. Having calculated the response amplitude operators in regular waves by using MARCHS (Chan, 1990), a spectral analysis program was developed to evaluate the various design extreme values, and an 'equivalent wave system' was adopted to generate the instantaneous hydrodynamic pressure distributions, which could be directly used in finite element analysis. This was demonstrated in Zanic et al (1993). Based on this analysis, the following conclusions may be drawn:

- * Although no experimental data is available to verify the analytical results, good agreement exists between the calculated side force and that used by the FBM Marine Company when designing PATRIA.
- * The largest side force occurs in beam seas at zero forward speed. The wave length, at which the largest RAO of side force occurs, is about four times the width of the ship. This is the dominant load component in structural design.
- * Although the side force in this beam sea is 2.76 times of that in the equivalent bow quartering sea, nevertheless the yaw splitting moment in the bow quartering sea is 6.9 times of that in the beam sea. So it is possible that the combination of the loads in bow quartering seas is also as critical as in beam seas.

- * The largest pitch torsional moment, which is relatively small, also occurs in beam seas. So it is not so important as the side force and yaw splitting moment.
- * The longitudinal distribution of the hydrodynamic forces shows that the interaction between the two hulls is strong, and the uniform distribution of side forces suggested by Sikora and Dinsenbacher (1990) is not suitable to this case. A sinusoidal distribution is preferred based on the results.
- * Load combinations suggested by Chalmers (1989) seem to be too conservative in this case. More cases need to be evaluated to establish a simple and accurate combination approach for design loads.

7.3 ULTIMATE STRENGTH AND RELIABILITY ANALYSIS OF PLATE PANELS AND STIFFENED PLATES

Plate panels and stiffened plates are also common structural elements in SWATH ships as in mono-hull ships. To efficiently design these components is a prerequisite for achieving rational design of the whole ship. The model uncertainty factor is always one of the important factors which affect the reliability level of structures (Frieze, 1986; Faulkner, 1991). To select the best ultimate strength formulae (in the sense of small bias and coefficient of variation of the model uncertainty factor) for panels and stiffened plates, the existing strength formulae were calibrated by using a considerable amount of experimental and numerical data. A new approach for stiffened plates was proposed by incorporating Guedes Soares' formula for plate panels into Faulkner's formula for stiffened plates. Furthermore reliability analysis of panels and stiffened plates were carried out by AFOSM, SORM and Monte Carlo simulation methods. It was found that:

- * Guedes Soares' formulae and Faulkner's method are the best for plate panels and stiffened plates respectively. The proposed formulae have only more or less the same accuracy as Faulkner's original approach.
- * The results for failure probability from SORM are much better than those from AFOSM. In these cases the AFOSM always underestimates the failure probability, and the largest relative errors of failure probability and reliability index reach -45.1% and 7.4% respectively. Considering the nominal nature of

the reliability index the difference between the two methods is so small that the values obtained from AFOSM are acceptable in practice.

7.4 STRUCTURAL ANALYSIS AND SYSTEM RELIABILITY ANALYSIS OF PATRIA

The finite element analyses of PATRIA were carried out to increase the understanding of the structural behaviour and establish a simplified model for system reliability analysis. Various models at different level were generated.

In structural system reliability analysis the combined load effect was considered. Because buckling is a common failure mode in SWATH ships the interaction of bending moment and axial force including buckling effects is considered in the analysis. In this case the safety margin equation of the last formed plastic hinge can no more be used as the safety margin equation of the failure path. So an efficient multi-normal integration method must be used to establish the 'equivalent safety margin equation' for a failure path (parallel system). In the study, Tang and Melcher's algorithm (1987) was adopted because of its accuracy and efficiency, and its intermediate results can be fully used in the discarding process in the extended β -unzipping method. The developed method was then applied to a typical frame which is idealised by a one-dimensional model of PATRIA.

Through these calculations it was found that:

- * The two-dimensional model is less time-consuming compared to the three-dimensional model, and has good results when the effective breadth can be accurately obtained from the empirical formula. So, for a conceptual study of a new type of design, it is suggested that a three-dimensional model between critical parts of the structure should be carried out first to establish the effect of shear lag for eventual feedback to a two-dimensional model. Thus a rational design procedure, both for the frame and bulkheads, can be established which is less time consuming and more cost effective.
- * The most critical part in the typical frame is the section in the haunch area. This finding is the same as that by conventional deterministic methods.

- * The buckling has a moderate effect on the system reliability index in this particular case, and should be considered in the analysis.
- * All the critical sections included in the significant failure paths are in the haunch area. Hence it may be said that more attention should be paid to design in this area.

It should be pointed out that the bulkheads and their associated plating are the main structures to resist the side forces. Evaluating the system reliability of bulkheads and optimising them would be even more significant than that of frames. Unfortunately, these present techniques can not do this so far.

7.5 RELIABILITY-BASED OPTIMISATION

Having assessed various reliability-based optimisation formulations, a new algorithm was proposed. In this method the reliability requirements of critical components and the structural system are dealt with separately. This avoids repeated calculations of system reliability in conventional methods.

The method was used to optimise the typical cross-deck frame in PATRIA. It may be said that:

- * The algorithm works very well. Computational time in the analysis is not a problem because the system reliability calculation is only applied to the optimum structure in step 1.
- * The original design is quite close to the optimal one, so the margin for optimisation is small. It is interesting to note that the system reliability index for the original structure is only 3.76, while it is 4.71 for the optimum structure, at the same time the optimum one is 13% lighter than the original one.
- * The haunch area is confirmed as the critical part. From the values of design variables of the optimum structure, it is observed that increasing the thickness of the side shell is the most efficient way to improve the safety in this area. Because the dimensions of the flange were fixed during the optimisation, their effect on the safety is not investigated in this study. The dimensions of the flange might be an important factor influencing safety because increasing the

area of the flange shifts the neutral axis toward the flange so that the maximum stress in the flange would decrease.

7.6 RECOMMENDATIONS FOR FUTURE STUDY

The Department in the University of Glasgow has been actively involved in research of SWATH ships since the early 80's. Much experience in both prediction of primary hydrodynamic loads and preliminary structural design has been acquired. It is significant to integrate all the existing programs within the department as a comprehensive and sophisticated program, which can be used to analyse a structure in the detail design stage. This could greatly increase the synthesis capacity of the Department. The organisation of the program is shown in Fig. 7.1. Most of the modules in the proposed program are ready for integration (only interfaces are expected). With the completion of an ongoing research project, Hydro-Structural Design of SWATH Ships, it is likely that the slamming force module will be ready for use soon.

In all the existing structural system reliability methods many assumptions are introduced in the analysis. It is necessary to investigate the errors which result from these assumptions and the applicable ranges of these methods. Karamchandani (1990) has made a good start, but further work needs to be done on this aspect.

Most practical structures experience cyclic loads in their life span. It is important that dynamic effects are considered in the analyses. The response surface method combined with importance sampling techniques might be a promising method to carry this out. In addition, this method can be used to analyse structures with plate elements.

As mentioned before, computational time for reliability-based optimisation is still a problem when the structure is complicated. How to increase the efficiency of the algorithm needs to be further explored. It is observed that much computation is spent on the calculation of the objective function and constraints as well as their derivatives. Deriving some analytical or semi-analytical methods to evaluate the derivatives of the constraints is obviously a promising research area. On the other hand, fuller use of the rapidly developing computer techniques is another way to improve the efficiency.

It is noted that the calculation of the objective function and constraints are independent operations, so parallel processing techniques could easily be applied to this case. Assuming that the objective function and M constraints are sent to $M+1$ processors during the analysis, at least $(M+1)*70\%$ 'speed-up' could be achieved.

There are $(M+1)*N$ derivatives to be calculated where N is the number of design variables. If numerical difference is used to evaluate the derivatives, $(M+1)*N$ function calls are needed. Hence a total of $(M+1)*N*70\%$ 'speed-up' is expected in these calculations. This represents a huge saving in computational time.

In addition, during the calculation of derivatives, the finite element package is called once for each of the N design variable. So the method suggested by Santos (1991) and Zotemantel (1991) can be used to save computational time in this case.

7.7 CLOSING REMARKS

The study presented in this thesis aims at developing a rationally-based structural design procedure for SWATH type vessels by applying reliability methods and reliability-based optimisation techniques. The structural system reliability analyses and reliability-based optimisation of a typical frame of a built SWATH were successfully conducted, and some useful information was obtained through the work. Due to the limitation of the present techniques, the bulkheads, which are the main components resisting the side force in SWATH, can not be analysed. Hence the results presented here are far from complete. Further work needs to be done. It is hoped that the work presented within this thesis will be useful in pursuing further research and in the development of SWATH technology.

REFERENCES

- American Bureau of Shipping (1990), 'Preliminary Guide for Building and Classing Small Waterplane Area Twin Hull (SWATH) Vessels', USA, Sept.
- Ang, G.L., Ang, A.H.-S. and Tng, W.H. (1991): 'Multi-dimensional Kernel Method in Importance Sampling', Proc. of 6th Int. Conf. on Applications of Statistics and Probability in Civil Engineering, Mexico, 1, pp289-296.
- Aronne, E.L., Lev, F.M. and Nappi, N.S. (1974): 'Structural Weight Determination for SWATH Ships', Proc. of the AIAA/SNAME Advanced Marine Vehicles Conf., Paper No. AIAA 74-326, San Diego, USA, Feb.
- Arora, J.S. (1990): 'Computational Design Optimization: A Review and Future Directions', Structural Safety, 7(1990), pp 131-148.
- Ayyub, B.M. and White, G.J. (1987): 'Reliability-Conditioned Partial Safety Factors', J. of Struct. Engng., Vol. 113, No. 2, Feb., pp279-294.
- Baker, M.J. and Vrouwenvelder, A.C.W.M.(1992): 'Reliability Methods for the Design and Operation of Offshore Structures', Vol II, OMAE, pp 123-132.
- Baker, M.J. (1985): 'The Reliability Concept as an Aid to Decision Making in Offshore Engineering', Proc. 4th Intl. Conf. on Behaviour of Offshore Structures, Delft, The Netherlands July 1-5, pp 75-94.
- Bathe, K.J.: 'Finite Element Procedures in Engineering Analysis', Prentice-Hall, 1982.
- Becker, H., Goldman, R. and Pazerycki, J. (1970): 'Compressive Strength of Ship Hull Girders, Part 1, Unstiffened Plates', Ship Structures Committee Report SSC-217, Washington, DC.
- Becker, H. and Colao, A. (1977): 'Compressive Strength of Ship Hull Girders. Part 3, Theory and Additional Experiments', Ship Structures Committee Report SSC-267, Washington, DC.

- Beghin, D., Huther, M. and Parmentier, G. (1992): 'The Probabilistic Approach : A Tool for Ship Rules Improvement' Proc. Int. Conf. on Practical Design of Ships and Mobile Units, PRADS 92, Vol. 2, pp. 2.847-2.859, Univ. of Newcastle upon Tyne, May.
- Bennett, R.M.(1987): 'Comments On "First Order vs Second Order Reliability Analysis of Series Structures"', Structural Safety, 4, pp 241-242.
- Betts, C.V. (1988): 'A Review of Developments in SWATH Technology', Proc.Int. Conf. on SWATH Ships and Advanced Multi Hulled Vessels II, RINA, Paper No. 1, London, Nov.
- Bjerager, P. (1988): 'Probability Integration by Directional Simulation', J. of Eng. Mech., ASCE, 114, PP 1285-1302.
- Bjerager, P. and Krenk, S. (1989): 'Parametric Sensitivity in First Order Reliability Theory', Journal of Engineering Mechanics, ASCE, Vol. 115, No. 7, July, pp 1577-1582.
- Bjerager, P.(1990): 'On Computation Methods for Structural Reliability Analysis', Structural Safety, 9, pp 79-96.
- Bonello, M.A., Chryssabthopoulos, M.K. and Dowling, P.J. (1991): 'Probabilistic Strength Modelling of Unstiffened Plates under Axial Compression' Proc. Safety and Reliability Symposium, 10th International Conference on Offshore Mechanics and Arctic Engineering (OMAE), Stavanger, Norway, June.
- Bonello, M.A., Chryssanthopoulos, M.K. and Dowling, P.J. (1992): 'Ultimate Strength Design of Stiffened Plates under Axial Compression and Bending', Charles Smith Memorial Conference "Recent Developments in Structural Research", DRA, Dunfermline, Scotland, July.
- Bonello, M.A., Chryssanthopoulos, M.K. and Dowling, P.J. (1993a): 'Ultimate Strength Design of Stiffened Plates under Axial Compression and Bending', Marine Structures, 6.
- Bonello, M.A. and Chryssanthopoulos, M.K. (1993b): 'Buckling Analysis of Plated Structures Using System Reliability Concepts', OMAE, Vol II, pp 313-321.

- Bradfield, C.D. (1979): 'Tests on Single Plates Under In-plane Compression with Controlled Residual Stress and Initial Out-of-flatness', Dept. of Engineering, University of Cambridge, Report CUED/C-Struct/TR78.
- Bradfield, C.D. (1980): 'Tests in Plates Loaded in In-Plane Compression', J Constructional Steel Research, No. 1, pp 27-37.
- Bradfield, C.D., Stonor, R.W.P. and Moxham, K.E. (1993): 'Tests of Long Plates under Biaxial Compression', J of Construt. Steel Res., Vol. 24, No. 1.
- Breitung, K.(1984): 'Asymptotic Approximations for Multi-normal Integrals', Journal of Engineering Mechanics, ASCE, Vol.110, No.3, March, pp 357-366.
- Bucher, C.G.(1988): 'Adaptive Sampling - an Iterative Fast Monte Carlo Procedure', Structural Safety, 5(2), pp 119-126.
- Cai, G.Q. and Elishakoff, I. (1994): 'Refined Second-Order Reliability Analysis', Structural Safety, 14, pp 267-276.
- Carlsen, C.A. (1977): 'Simplified Collapse Analysis of Stiffened Plates', Norwegian Maritime Research, No. 4.
- Carlsen, C.A. and Czujko, J. (1978): 'The Specification of Post-Welding Distortion Tolerances for Stiffened Plates in Compression', The Structural Engineer, Vol. 56A, No. 5, May.
- Carlsen, C.A. (1980): 'A Parametric Study of Collapse of Stiffened Plates in Compression', The Structural Engineer, Vol. 58B, No. 2, June.
- Chalmers, D.W. and Smith, C.S. (1977): 'The Ultimate Longitudinal Strength of a Ship's Hull', Proc. Int. Conf. on Practical Design of Ships and Mobile Units, PRADS 92, Vol. 2, pp 2.745-2.763, Univ. of Newcastle upon Tyne, May.
- Chalmers, D.W. (1989): 'Structural Design Aspects of SWATH Ships', 10th WEGEMT on High-Speed and Pleasure Craft, University of Genoa, Italy, Oct.
- Chalmers, D.W. and Smith, C.S. (1992): 'The Ultimate Longitudinal Strength of a Ship's Hull', PRADS'92.

- Chan, H.S. (1990): 'User Manual for MARCHS', Report NAOE-90-28, Department of Naval Architecture and Ocean Engineering, University of Glasgow.
- Chan, H.S. (1991): 'Prediction of Motion and Structural Responses of Mono- and Twin-Hull Ships Advancing in Waves', Report NAOE-91-16, Department of Naval Architecture and Ocean Engineering, University of Glasgow.
- Chan, H.S., Djatmiko, E.B., Miller, A.F. and Caldwell, L.B. (1992): 'Structural Loading Aspects in the Design of SWATH Ships', PRADS'92, pp 1.346-1.359.
- Chapman, J.C., Smith, C.S., Davidson, P.C. and Dowling, P.J. (1991a): 'Recent Developments in the Design of Stiffened Plate Structures', Advances in Marine Structures, edited by Smith, C.S. and Clark, J.D., Vol. 2.
- Chapman and Dowling Associates (1991b): 'Model Code Study, Design of Flat Stiffened Plating, Phase I Report', CESLIC Report SP9, Imperial College, London, Dec.
- Chen, X. and Lind, N.C. (1983) : 'Fast Probability Integration by Three-Parameter Normal Tail Approximation', Structural Safety, Vol. 1, No. 4, pp 269-276.
- Covich, P.M. (1986): 'SWATH T-AGOS : a Producible Design', Proc. AIAA 8th Advanced Marine System Conf., Paper AIAA 86-2384, San Diego, USA, Sept.
- Conoco-ABS Rule Case Committee, (1984): 'Model Code for Structural Design of Tension Leg Platforms', Final Report, ABS, Newton, February.
- Das, P.K. and Frieze, P.A. (1982): 'Application of an Advanced Level-II Reliability Analysis Procedure to the Safety Assessment of Stiffened Cylinders', Dept. of Naval Architecture and Ocean Eng., the University of Glasgow, Report No. NAOE-82-08, March.
- Das, P.K. and Pu, Y. (1993): 'Finite Element Based Structural Analysis of SWATH', Report NAOE-93-20, The University of Glasgow, Department of Naval Architecture and Ocean Engineering.
- Davidson, P.C., Chapman, J.C., Smith, C.S. and Dowling, P.J. (1989): 'The Design of Plates Subject to In-Plane Shear and Biaxial Compression', RINA, Vol. 132.

- Davidson, P.C., Chapman, J.C., Smith, C.S. and Dowling, P.J. (1991): 'The Design of Plate Panels Subject to Biaxial Compression and Lateral Pressure', RINA, W3(1991).
- Dean, J.A. and Dowling, P.J. (1976): 'Ultimate Load Tests on Three Stiffened Plates under Combined In-Plane and Lateral Loading', Conference on "Steel Plated Structures" edited by P.J. Dowling, J.E. Harding and P. Frieze, Paper 31, London.
- DeVries, R.L. (1991): 'Producibility Benefits of the SWATH Configuration', Marine Technology, SNAME, Vol. 28, No. 1, pp. 23-29, Jan.
- Dibley, J.E. and Manoharan, A. (1973): 'Experimental Behaviour of a Two-Span Continuous Box Girder', Conference on "Steel Box Girder Bridges", London.
- Ditlevsen, O.(1979): 'Narrow Reliability Bounds for Structural Systems', J. Struct. Mech., 7, pp 453-472.
- Ditlevsen, O. and Bjerager, P.(1986): 'Methods of Structural System Reliability', Structural Safety, Vol. 3, pp 195-229.
- Ditlevsen, O., Melchers, R.E. and Gluwer, H. (1990): 'General Multi-dimensional Probability Integration by Directional Simulation', Computers and Structures, 36, pp355-368.
- Djatkiko, E.B. (1992): 'Hydro-Structural Studies on SWATH Type Vessels', PhD Thesis, Department of Naval Architecture and Ocean Engineering of University of Glasgow.
- Dolinski, K.(1983): 'First-Order Second-Moment Approximation in Reliability of Structural Systems: Critical Review and Alternative Approach', Structural Safety, 1, pp 211-231.
- Dorman, A.P. and Dwight, J.B. (1973): 'Tests on Stiffened Compression Plates and Plate Panels', Conference on "Steel Box Girder Bridges", London.
- Dow, R.S. and Smith, C.S. (1984): 'Effects of Localised Imperfections on Compressive Strength of Long Rectangular Plates', J. Constructional Steel Research, No. 4.

- Dowling, P.J., Chatterjee, S., Frieze, P.A. and Moolani, F.M. (1973): 'Experimental and Predicted Collapse Behaviour of Rectangular Steel Box Girders', Conference on "Steel Box Girder Bridges", London.
- Dwight, J.B. and Moxham, K.E. (1969): 'Welded Steel Plates in Compression', *Structural Engineer*, Vol. 47, No. 2, pp54.
- Dwight, J.B. and Ratcliffe, A.T. (1969): 'The Strength of Thin Plates in Compression', in *Thin Walled Steel Structures*, edited by Rucker, K.C. and Hill, H.V., London, Crosby Lockwood.
- Dwight, J.B. and Little, G.H. (1972): 'Tests in Transverse Welded Box Columns', Report CUED/C-Struct/TR24, Dept. of Engineering, University of Cambridge.
- Edwards, G.E., Heidweiller, A., Kerstens, J. and Vrouwenvelder, A. (1985): 'Methodologies for Limit State Reliability Analysis of Offshore Jacket Platforms', Proc. of 4th Intl. Conf. on Behaviour of Offshore Structures, Delft, The Netherlands, July 1-5, pp 315-324.
- Enevoldsen, I. and Sorensen, J.D. (1992): 'Optimisation Algorithms for Calculation of the Joint Design Point in Parallel Systems', *Structural Optimisation*, **4**, pp121-127.
- Enevoldsen, I. and Sorensen, J.D. (1993): 'Reliability-Based Optimization of Series Systems of Parallel Systems', *J. of Structural Engineering*, ASCE, Vol. 119, No. 4, April, pp 1069-1084.
- Enevoldsen, I. and Sorensen, J.D. (1994): 'Reliability-Based Optimization in Structural Engineering', *Structural Safety*, **15**(1994), pp 169-196.
- Enevoldsen, I. (1994): 'Sensitivity Analysis of Reliability-Based Optimal Solution', *J. of Engineering Mechanics*, ASCE, Vol.120, No. 1, Jan., PP 198-205.
- Engelund, S. and Rackwitz, R. (1993): 'A Benchmark Study on Importance Sampling Techniques in Structural Reliability', *Structural Safety*, **12**(1993), pp255-276.

- Faulkner, D., Adamchak, J.C., Snyder, J.G. and Vetter, F.M. (1973): 'Synthesis of Welded Grillages to Withstand Compression and Normal Loads', *Computers & Structures*, Vol. 3, pp 221-246.
- Faulkner, D. (1975a): 'Compression Strength of Welded Grillages', chapter 21 in 'Ship Structural Design Concept' Edited by Evans, J.M., Cornell Maritime Press.
- Faulkner, D. (1975b): 'A Review of Effective Steel Plating for Use in the Analysis of Stiffened Plating', *J. Ship Res.*, Vol 19, pp 1-17.
- Faulkner, D. (1976): 'Compression Tests on Welded Eccentrically Stiffened Plate Panels', Conference on "Steel Plated Structures" edited by P.J. Dowling, J.E. Harding and P. Frieze, Paper 25, London.
- Faulkner, D. (1977): 'Effects of Residual Stresses on the Ductile Strength of Plane Welded Grillages and of Ring Stiffened Cylinders', *J. Strain Analysis*, Vol. 12, No. 2, pp 130-139.
- Faulkner, D. (1984): 'On Selecting a Target Reliability for Deep Water Tension Leg Platforms', Proc. 11th IFIP Conference on System Modelling and Optimisation, Copenhagen, Denmark, July 25-29, pp 490-513.
- Faulkner, D., Guedes Soares, C. and Warwick, D.M. (1987): 'Modelling Requirements for Structural Design and Assessment', *Integrity of Offshore Structures-3*, September.
- Faulkner, D. (1991): 'Criteria and Guidance for Good Strength Models', Report NAOE-91-15, University of Glasgow, July.
- Feng, Y.S. and Moses, F. (1986a): 'A Method of Structural Optimisation Based on Structural System Reliability', *J. Struct. Mech.* **14**(4), pp 437-453.
- Feng, Y.S. and Moses, F.(1986b): 'Optimum Design, Redundancy and Reliability of Structural Systems', *Computers and Structures*, Vol. 24, No. 2, pp 239-251.
- Feng, Y.S.(1989): 'A Method for Computing Structural System Reliability with High Accuracy', *Computer and Structures*, **33**, pp 1-5.

- Fiessler, B., Neumann, H.J. and Rackwitz, R. (1979): 'Quadratic Limit States in Structural Reliability', Journal of the Engineering Mechanics Division, ASCE, Vol.105, No. 4, August, pp 661-676.
- Fjeld, S. (1977): 'Reliability of Offshore Structures', Proc. 9th OTC, Vol. 4, OTC 3027, PP 459-472.
- Fletcher, R. (1970): 'A FORTRAN Subroutine for General Quadratic Programming', Report No. R6370, AERE, Harwell, Berkshire.
- Frangopol, D.M. (1985): 'Multi-criteria Reliability-Based Structural Optimisation', Structural Safety, 3(1985), pp 23-28.
- Frangopol, D.M. and Fu, G. (1989): 'Limit States Reliability Interaction in Optimum Design of Structural Systems', ICOSSAR'89, PP 1879-1886.
- Frieze, P.A., Dowling, P.J. and Hobbs, R.E. (1976): 'Ultimate Load Behaviour of Plates in Compression', Conference on "Steel Plated Structures", Edited by P.J. Dowling et al, Crosby Lockwood Staples, London.
- Frieze, P.A. (1986): 'Lessons Learnt from Reliability Analysis Studies of Offshore Platforms', Wimpey Offshore Engineers and Constructors Report (unpublished).
- Fu, G. and Moses, F. (1987): 'A Sampling Distribution for System Reliability Application', Proc. of 1st IFIP WG 7.5 Working Conf. on Reliability and Optimisation of Structural Systems, Aalborg, May 6-8, Springer-Verlag, Berlin.
- Galambos, T.V.(1990): 'Systems Reliability and Structural Design', Structural Safety, 7, pp 101-108.
- Gill, E.P., Murray, W., Saunders, M.A. and Wright, M.H. (1985): 'Model Building and Practical Aspects of Nonlinear Programming', in 'Computational Mathematical Programming', ed by K. Schittkowski, NATO ASI Series, Bil. F15, Springer-Verlag Berlin Heidelberg, pp 209-247.
- Gollwitzer, S. and Rackwitz, R. (1983): 'Equivalent Components in First-Order System Reliability', Reliability Engineering, Vol. 5, pp 99-115.

- Gollwitzer, S. and Rackwitz, R. (1988): 'An Efficient Numerical Solution to the Multi-normal Integral', Probabilistic Engineering Mechanics, Vol. 3, No. 2, pp 98-101.
- Gordo, J.M. and Guedes Soares, C. (1993): 'Approximate Load Shortening Curves for Stiffened Plates under Uniaxial Compression', IOS'93, pp189-211.
- Gore, J.L. (1985): 'SWATH Ships', Naval Engineers Journal, Vol. 97, No. 2, ASNE, February, pp 83-112.
- Greig, G. (1992): 'An Assessment of High-Order Bounds for Structural Reliability', Structural Safety, **11**, pp 213-225.
- Guedes Soares, C. and Soreide, T.H. (1983): 'Behaviour and Design of Stiffened Plates under Predominantly Compressive Loads', International Shipbuilding Progress, Vol. 30.
- Guedes Soares, C. (1988a): 'Uncertainty Modelling in Plate Buckling', Structural Safety, No. 5.
- Guedes Soares, C. (1988b): 'Design Equation for the Compressive Strength of Unstiffened Plate Elements with Initial Imperfections', J. Constr. Steel Res., Vol. 9, No. 4, pp 287-310.
- Gupta, S.K. and Schmidt, T.W. (1986): 'Developments in SWATH Technology', Naval Engineers Journal, ASNE, Vol. 98, No. 3, pp 171-178, May.
- Harbitz, A.(1985): 'An Efficient Sampling Method for Probability of Failure Calculation', Structural Safety, **3**, No. 2.
- Harding, J.E., Hobbs, R.E. and Neal, B.G. (1976): 'Ultimate Load Behaviour of Plates Under Combined Direct and Shear In-Plane Loading', Conference on "Steel Plated Structures", Edited by P.J. Dowling et al, Crosby Lockwood Staples, London.
- Hendawi, S. and Frangopol, D.M. (1993): 'Reliability-Based Optimization of Composite-Hybrid Plate Girders', ICOSSAR'93, pp 661-668.

- Hohenbichler, M. (1981): 'Approximate Evaluation of the Multi-normal Distribution Function' in 'Studies in the Reliability of Redundant Structural Systems', Technical University of Munich, Heft 58, pp 55-66.
- Hohenbichler, M. and Rackwitz, R. (1983): 'First Order Concepts in System Reliability', *Structural Safety*, 1(3), pp 177-188.
- Hohenbichler, M., Gollwitzer, S., Kruse, W. and Rackwitz, R. (1986): 'New Light On First- and Second-Order Reliability Methods', *Structural Safety*, 4, pp 267-284.
- Hohenbichler, M. and Rackwitz, R. (1988): 'Improvement of Second-Order Reliability Estimates by Importance Sampling', *Journal of Engineering Mechanics*, Vol. 114, No.12, December, pp 2195-2199.
- Holcomb, R.S. and Allen, R.G. (1983): 'Investigation of the Characteristics of the Small SWATH Ships Configured for the United States Coast Guard Missions', DTNSRDC, Report No. SDD-83-3, June.
- Horne, M.R. and Narayanan, R. (1976): 'Ultimate Capacity of Longitudinally Stiffened Plates Used in Box Girders', *Proc. Instn Civil Engineers, Part 2*, Vol. 61, June.
- Horne, M.R. and Narayanan, R. (1977): 'Influence on Strength of Compression Panels of Stiffener Section, Spacing and Welded Connection', *Proc. Instn Civil Engineers, Part 2*, Vol. 63, March.
- Hughes, O.F. (1983): 'Ship Structural Design: a Rationally-based, Computer-aided, Optimisation Approach', New York.
- Ibrahim, Y. (1991): 'Observations on Applications of Importance Sampling in Structural Reliability Analysis', *Structural Safety*, 9(4), pp 269-282.
- Jendo, S. and Putresza, J. (1993): 'Multicriterion Reliability-Based Optimization of Structural Systems', *ICOSSAR'93*, pp 727-730.
- Kam, J.C.P., Birkinshaw, M. and Sharp, J.V. (1993): 'Review of the Applications of Structural Reliability Technologies in Offshore Structural Safety', Vol II, *OMAE*, pp 289-296.

- Kanda, J. and Inoue, T. (1993): 'Effects of Probability Distribution Model of Loads on Optimum Reliability', ICOSSAR'93, pp 1433-1437.
- Karamchandani, A. (1987): 'Structural System Reliability Analysis Methods', Report No. 83, Department of Civil Engineering, Stanford University, U.S.A., July.
- Karamchandani, A., Bjerager, P. and Cornell, C.A. (1989): 'Adaptive Importance Sampling', Proc. ICOSSAR'89, pp 855-862.
- Karamchandani, A. (1990a): 'Limitations of Some of the Approximate Structural Analysis Methods that are Used in Structural System Reliability', Structural Safety, 7, pp 115-127.
- Karamchandani, A. (1990b): 'New Methods in Systems Reliability', PhD Thesis, Report No. RMS-7, Department of Civil Engineering, Stanford University, May.
- Karamchandani, A. and Cornell, C.A. (1991): 'Adaptive Hybrid Conditional Expectation Approach for Reliability Estimation', Structural Safety, 11, pp 59-74.
- Kiureghian, A.D., Lin, H.Z. and Hwang Shyh-Jiann (1987): 'Second-Order Reliability Approximations', Journal of Engineering Mechanics, ASCE, Vol, 113, No. 8, August, pp 1208-1225.
- Kiureghian, A.D., Stefano, M.O. and Trombetti, T. (1991): 'An Efficient Second-Order Reliability Method', OMAE, Vol. II, pp 151-156.
- Kobayashi, M. and Shimada, K. (1990): 'Wave Loads on a Small-Waterplane-Area Twin-Hull (SWATH) Ship with Forward Speed', 19th ITTC, Vol.2, 16-22 September.
- Lee, C.M. and Curphey, R.M. (1977): 'Prediction of Motion, Stability and Wave Load of Small Waterplane-Area, Twin-Hull Ships', Transactions SNAME, Vol 85.
- Lee, J.S. and Faulkner, D. (1988): 'System Reliability Analysis of Structural Systems', Report NAOE-88-33, Department of Naval Architecture and Ocean Engineering, University of Glasgow.

- Lee, J.S. (1989): 'Reliability Analysis of Continuous Structural Systems', PhD Thesis, Department of Naval Architecture and Ocean Engineering, The University of Glasgow.
- Lee, J.S. and Faulkner, D. (1989): 'System Design of Floating Offshore Structures', RINA Spring Meeting.
- Lee, K.Y., Lee, D.K. et al (1988): 'On the Design Technology of a SWATH Ship for High Speed Coastal Passenger Vessels', International High Speed Surface Craft Conference (6th), held London, 14-15 January.
- Lewis, E.V. (1967): 'The Motion of Ships in Waves', chapter IX in 'Principles of Naval Architecture', edited by J.P. Comstock.
- Little, G.H. (1976): 'Stiffened Steel Compression Panels-Theoretical Failure Analysis', *The Structural Engineer*, Vol. 54, No. 12, December.
- Liu, N. (1989): 'Development and Analysis of SWATH Ships', lecture presented at The Hellenic Institute of Marine Technology, Piraeus, Greece.
- Liu, P.-L. and Kiureghian, A.D. (1991): 'Optimisation Algorithms for Structural Reliability', *Structural Safety*, **9**, pp 161-178.
- Liu, Y. and Moses, F. (1991): 'Bridge Design with Reserve and Residual Reliability Constraints', *Structural Safety*, **11**(1991), pp 29-42.
- Loscombe, R. (1987): 'An Exploratory Study of Alternative Structural Materials for Small SWATH Craft', Ship Science Report, No. 34, Dept. of Ship Science, Univ. of Southampton, May.
- Loscombe, R. (1988): 'An Exploratory Study of Alternative Structural Materials for Small SWATH Ships', *Int. Shipbuilding Progress*, Vol. 35, No. 404, pp. 331-347, Dec.
- Loscombe, R. (1989): 'Key Aspects of the Structural Design of Small SWATH Ships', PhD Thesis, Dept. of Ship Science, Univ. of Southampton, Dec.

Luedeke, G.Jr., Montague, J., Posnansky, H. and Lewis, Q. (1985): 'The RMI SD 60 SWATH Demonstration Project', Proc. Int. Conf. on SWATH Ships and Advanced Multi Hulled Vessels, RINA, Paper No. 10, London, April.

LUSAS Finite element Program, FEA Limited, Kingston upon Thames.

MacGregor, J.R. (1989): 'A Computer Aided Method for Preliminary Design of SWATH Ships', PhD Thesis, Dept. of NA&OE, Univ. of Glasgow, May.

Machida, S., Itagaki, H. Oishi, T. and Ishikawa, K. (1992): 'Recent Japanese Research Activities on Structural Reliability of Ships and Offshore Structures', BOSS'92, Vol.1, pp 67-77.

Madsen, H.O. (1985): 'First Order vs Second Order Reliability Analysis of Series Structures', Structural Safety, 2, pp 207-214.

Madsen, H.O. and Hansen, P.F. (1991): 'A Comparison of Some Algorithms for Reliability Based Structural Optimization and Sensitivity Analysis', Proc. of the 4th IFIP WG7.5 Conference, 'Reliability and Optimization of Structural Systems', ed by R. Rackwitz and P. Thoft-Christensen, Munich Germany, Sept. 11-13, pp 443-451.

Mahadevan, S. and Haldar, A. (1989): 'Structural Optimization Based on Component-Level Reliabilities', ICOSSAR'89, pp 1887-1894.

Marti, K.(1993): 'Approximations and Derivatives of Probabilities in Structural Reliability and Design', ICOSSAR'93, pp 1295-1299.

Matsuho, S. and Shiraki, W. (1993): 'Reliability-Based Optimization Method of Structural System Using Information Integration Method', ICOSSAR'93, pp 669-675.

Mebarki, A., Lorrain, M. and Bertine, J. (1990) : 'Structural Reliability Analysis by a New Level-2 Method: the Hypercone Method', Structural Safety, 9 (1), pp 31-40.

Massonnet, C. and Maquoi, R. (1973): 'New Theory and Tests On the Ultimate Strength of Stiffened Box Girders', Conference on "Steel Box Girder Bridges", London.

- Melchers, R.E. and Tang, L.K. (1984): 'Dominant Failure Modes in Stochastic Structural Systems', *Structural Safety*, **2**, pp 127-143.
- Melchers, R.E. (1989): 'Importance Sampling in Structural Systems', *Structural Safety*, **6**, pp 3-10.
- Melchers, R.E. (1990): 'Search-Based Importance Sampling', *Structural Safety*, **9**, pp 117-128.
- Meyerhoff, W.K. et al (1988): 'Novel Design Concepts - SWATH' Report of Committee V.4, Proc. of 10th International Ship and Offshore Structures Congress, vol. 2, Denmark.
- Miller, A.F. (1991): 'A Review of Techniques Employed to Predict Wave Induced Global Loadings on SWATH Ships', Report No. NAOE-91-29, Department of Naval Architecture and Ocean Engineering, University of Glasgow.
- Moan, T. (1994): 'Reliability and Risk Analysis for Design and Operations Planning of Offshore Structures', ICOSAR'93, PP 21-43.
- Moolani, F.M. and Dowling, P.J. (1976): 'Ultimate Load Behaviour of Stiffened Plates in Compression', Conference on "Steel Plated Structures" edited by P.J. Dowling, J.E. Harding and P. Frieze, Paper 3, London.
- Moses, F. (1977): 'Structural System Reliability and Optimization', *Computers and Structures*, Vol.7, pp 283-290.
- Moses, F. (1981): 'Guidelines for Calibrating API RP2A for Reliability-Based Design', Final Report, APIPRAC 80-22, American Petroleum Institute, October.
- Moses, F. (1982): 'System Reliability Developments in Structural Engineering', *Structural Safety*, Vol. I, pp 3-13.
- Moses, F. (1986): 'Development of Preliminary Load and Resistance Design Document for Fixed Offshore Platforms', API PRAC PROJECT 85-22, Final Report, Prepared for American Petroleum Institute, 211 N. Ervay, Suite 1700, Dallas, Texas 75201, January.

- Moses, F. (1990): 'New Directions and Research Needs in System Reliability Research', *Structural Safety*, 7, pp 93-100.
- Moses, F. and Liu, Y.W. (1992): 'Methods of Redundancy Analysis for Offshore Platforms', *Proc. of 11th OMAE*, Vol II, pp 411-416.
- Moxham, K.E. (1971): 'Buckling Tests on Individual Welded Steel Plates in Compression', *Cambridge University Report CUED/C-Struct/TR.3*.
- Murotsu, Y., Yonezawa, M., Oba, F. and Niwa, K. (1977): 'A Method for Reliability Analysis and Optimum Design of Structural Systems', *Proc. of 12th Int. Symposium of Space Technology and Science*, Tokyo, pp 1047-1054.
- Murotsu, Y., Kishi, M., Okada, H., Yonezawa, M. and Taguchi, K. (1983): 'Probabilistically Optimum Design of Frame Structure', *Proc. of 11th IFIP Conference on System Modelling and Optimization*, Copenhagen, Denmark, July 25-29, pp 545-554.
- Murotsu, Y. (1986): 'Development in Structural Systems Reliability Theory', *Nuclear Engineering and Design*, Vol. 94, pp 101-114.
- Murotsu, Y. et al (1987): 'On System Reliability of Semi-Submersible Platform', *Proc. of PRADS'87*, pp 752-764.
- Murotsu, Y. and Okada, H. (1989): 'System Reliability of Semi-Submersible Platforms', *ICOSSAR'89*, *Proc. of 5th International Conference on Structural Safety and Reliability*, pp 879-886.
- Murotsu, Y. et al (1990): 'Structural System Reliability Assessment of Semi-Submerged Catamaran', *J. SNAJ*, Vol.167, May, pp 205-213.
- Murotsu, Y. et al (1991): 'Reliability Assessment Techniques Applied to the Design of Marine Structures', Vol II, *OMAE*, pp 229-235.
- Murotsu, Y. et al (1992): 'Application of the Structural Reliability Analysis System (STRELAS) to a Semi-submersible Platform', Vol II, *OMAE*, pp 209-217.

- Murotsu, Y., Okada, H., Hibi, S. and Niho, O. (1993): 'A System for Collapse and Reliability Analysis of Ship Structures Using Spatial Plate Element Model', OMAE, Vol. 2, pp 305-312.
- Murotsu, Y., Shao, S. and Watanabe, A. (1994a): 'An Approach to Reliability-Based Optimization of Redundant Structures', Structural Safety, 16(1994), pp 133-143.
- Murotsu, Y., Okada, H., Hibi, S., Niho, O. and Kaminaga, H. (1994b): 'A System for Collapse and Reliability Analysis of Ship Structures Using a Spatial Element Model', Marine Structures, 8, pp 1-17.
- Mulligan, R.D. and Edkins, J.N. (1985): 'ASSET/SWATH - A Computer Based Model for SWATH Ships", Proc. Int. Conf. on SWATH Ships and Advanced Multi Hulled Vessels, RINA, London, April.
- Nethercote, W.C.E. and Schmitke, R.T. (1982): 'A Concept Exploration Model for SWATH Ships', Trans. RINA, Vol. 124, pp. 113-130.
- Nikolaidis, E. and Burdisso, R. (1988): 'Reliability Based Optimization: A Safety Index Approach', Computers and Structures, Vol. 28, No. 6, pp 781-788.
- Nikolaidis, E. and Kapania, K. (1990): 'System Reliability and Redundancy of Marine Structures: A Review of the State-of-the-Art', Journal of Ship Research , Vol. 34, No. 1, March, pp 48-59.
- NPD (1977): 'Regulation for the Design of Fixed Structures on the Norwegian Continental Shelf', Stavanger, Norwegian Petroleum Directorate.
- Ochi, M.K. (1973): 'On Prediction of Extreme Values', Journal of Ship Research, March, pp 29-37.
- Ochi, M.K. and Wang, S. (1976): 'Prediction of Extreme Wave-Induced Loads in Ocean Structures', Proc., Symposium on the Behaviour of Offshore Structures.
- Ochi, M.K. (1978): 'Wave Statistics for the Design of Ships and Ocean Structures', Trans. SNAME, Vol. 86, pp 47-76.

- Ochi, M.K. (1981): 'Principles of Extreme Value Statistics and their Application', Proc., Symposium of Extreme Loads Response, Arlington, VA.
- Okada, H. et al (1991): 'A Method for Reliability Assessment of Spatial Plate Structures through Automatic Generation of Ultimate Collapse Modes', J. SNAJ, Vol. 170, November.
- Olhoff, N. and Taylor, J.E. (1983): 'On Structural Optimization', J. of Applied Mechanics, Vol. 50, Dec. , pp 1139-1151.
- Papanikolaou, A., Zaraphonitis, G. and Androulakis, M. (1991): 'Preliminary Design of a High-speed SWATH Passenger/Car Ferry', Marine Technology, Vol. 28, No. 3, May.
- Powell, M.J.D. (1978): 'A Fast Algorithm for Nonlinearly Constrained Optimization Calculations', in Numerical Analysis, ed. G.A.Watson, Lecture Notes in Mathematics, Vol. 630 (Springer-Verlag, Berlin-Heidelberg-New York).
- Prasad, B. and Emerson, J.F. (1984): 'Optimal Structural Remodeling of Multi-Objective Systems', Computers and Structures, Vol.18, No. 4, pp 619-628.
- Pu, Y. (1993): 'On Prediction of Primary Loads on SWATH Ships', Report NAOE-93-21, The University of Glasgow, Department of Naval Architecture and Ocean Engineering.
- Pu, Y. and Das, P.K. (1993): 'Evaluation of Multinormal Distribution Function for Use in Structural Reliability Analysis', Report NAOE-94-32, The University of Glasgow, Department of Naval Architecture and Ocean Engineering.
- Pu, Y. and Das, P.K. (1994): 'Structural System Reliability Analysis of Frame Structures and SWATH Ships', Report NAOE-94-33, Department of Naval Architecture and Ocean Engineering, The University of Glasgow.
- Rackwitz, R. (1986): 'Discussion to Ref. of Harbitz, 1985', Structural Safety, Vol.4, No.4.
- Ramachandran, K. (1984): 'System Bounds : A Critical Study', Civil Engineering Systems, 1, pp 123-128.

- Ranganathan, R. and Deshpande, A.G. (1987): 'Generation of Dominant Modes and Reliability Analysis of Frames', *Structural Safety*, 4, pp 217-228.
- Rashedi, R. and Moses, F. (1986): 'Application of Linear Programming to Structural System Reliability', *Computers and Structures*, Vol. 24, No. 3, pp 375-384.
- Rashedi, R. and Moses, F. (1988): 'Identification of Failure Modes in System Reliability', *J. of Structural Engineering*, ASCE, Vol.114, No. 2.
- Reilly, E.T., Shin, Y.S. and Kotte, E.H. (1988): 'A Prediction of Structural Load and Response of a SWATH Ship in Waves', *Naval Engineers Journal*, ASNE, pp 251-264.
- Rhodes, J. (1981): 'On the Approximate Prediction of Elasto-Plastic Plate Behaviour', *Proc. Instn. Civ, Eng.*, Vol. 71, pp 165-183.
- Rosyid, D.M. (1992): 'Elemental Reliability Index-Based System Design for Skeletal Structures', *Structural Optimization*, Vol. 4, pp 1-16.
- Sadden, J.A. (1976): 'Primary Strength Design for Destroyers and Frigates', *Conference on "Steel Plated Structures"*, Edited by P.J. Dowling et al, Crosby Lockwood Staples, London.
- Santos, J.L.T. (1991): 'Numerical Techniques for Design Sensitivity Analysis of Structural Systems', *Proc. of the 4th IFIP WG7.5 Conference, 'Reliability and Optimization of Structural Systems'91*, ed by R. Rackwitz and P. Thoft-Christensen, Munich Germany, Sept. 11-13 , pp 83-98.
- Schall, G., Gollwitzer, Z. and Rackwitz, R. (1988): 'Integration of Multinormal Densities on Surfaces', *Proc. of the 2nd IFIP WG7.5 Conf. on Reliability and Optimisation of Structural Systems*, London, UK, Springer Verlag, pp 235-248.
- Schittkowski, K. (1985): 'NLPQL: A FORTRAN Subroutine Solving Constrained Nonlinear Programming Problems', *Annals of Operations Research* 5(1985), pp 485-500.
- Schueller, G.I. and Stix, R. (1987): 'A Critical Appraisal of Methods to Determine Failure Probabilities', *Structural Safety*, 4, pp 293-309.

- Schueller, G.I., Bucher, C.G, Bourgurd, U. and Ouypornprasert, W. (1989): 'On Efficient Computation Schemes to Calculate Structural Failure Probabilities', *Journal of Probabilistic Engineering Mechanics*, 4(1), pp 10-18.
- Shinozuka, M. (1983): 'Basic Analysis of Structural Safety', *Journal of Structural Engineering*, ASCE, 109(3), pp 721-740.
- Sikora, J.P., Dinsenhacher, A.L. and Beach, J.E. (1983): 'A Method for Estimating Lifetime Loads and Fatigue Lives for SWATH and Conventional Monohull Ships', *Naval Engineers Journal*, pp 63-85.
- Sikora, J.P. (1986): 'Automated Method for Predicting Maximum Lifetime Loads and Fatigue Lives of Ships', *Proc. 9th Annual Energy Source Technology Conference and Exhibition*, ASME, "Current Practices and New Technology in Ocean Engineering", New Orleans, USA, February.
- Sikora, J.P. (1988): 'Some Design Approaches for Reducing the Structural Weight of SWATH Ships', *Proc. of 2nd International Conference on SWATH Ships and Advanced Multi-Hulled Vessels*, RINA, Paper No. 18, London, Nov.
- Sikora, J.P. and Dinsenhacher, A.L. (1990): 'SWATH Structure: Navy Research and Development Applications', *Marine Technology*, Vol. 27, No. 4, pp. 211-220.
- Smith, C.S. (1975): 'Compressive Strength of Welded Steel Ship Grillages', RINA, LONDON.
- Smith, C.S. (1981): 'Imperfection Effects and Design Tolerances in Ships and Offshore Structures', *Trans. Instn. Engineers and Shipbuilders in Scotland*, Vol. 124.
- Smith, C.S., Davidson, P.C., Chapman, J.C. and Dowling, P.J. (1987): 'Strength and Stiffness of Ships' Plating under in-Plane Compression and Tension', RINA.
- Smith, C.S., Anderson, N., Chapman, J.C., Davidson, P.C. and Dowling, P.J. (1991): 'Strength of Stiffened Plating under Combined Compression and Lateral Pressure', RINA, Spring Meeting, Paper No. 4.
- Soreide, T.H., Bergan, P.G. and Moan, T. (1976): 'Ultimate Collapse Behaviour of Stiffened Plates Using Alternative Finite Element Formulations', *Conference on*

"Steel Plated Structures" edited by P.J. Dowling, J.E. Harding and P. Frieze, Paper 26, London.

Soreide, T.H., Moan, T. and Nordsve, N.T. (1978): 'On the Behaviour and Design of Stiffened Plates in Ultimate Limit State', Journal of Ship Research, Vol. 22, No. 4, December.

Sorensen, J. (1987): 'PRADS - Program for Reliability and Design of Structural Systems', Structural Reliability Theory Paper No. 36, Institute of Building Technology and Structural Engineering, Aalborg University, Denmark.

Stirling, A.G., Jones, G.L. and Clarke, J.D. (1988): 'Development of a SWATH Structural Design Procedure for Royal Navy Vessels', Proc. of the RINA 2nd International Conference in SWATH Ships and Advanced Multi-Hulled Vessels, London.

Takada, T., Kohama, Y. and Miyamura, A. (1993): 'Reliability-Based Minimum Weight Design of Space Truss: A Case Under Constraint of System Reliability', ICOSSAR'93, pp 677-683.

Takeuchi, M., Takagawa, S., Miyanabe, R. and Watanabe, T. (1985): 'Structural Design of the Semi-Submerged Catamaran-Type Underwater Work Test Vessel', JAMSTEC, Technical Report No. 15.

Tang, L.K. and Melcher, R.E. (1987): 'Improved Approximation for Multi-normal Integral', Structural Safety, 4, pp 81-93.

Thanedar, P.B. and Kodiyalam, S. (1992): 'Structural Optimization Using Probabilistic Constraints', Structural Optimization, Vol. 4, pp 236-240.

Thoft-Christensen, P. and Baker, M.J. (1982): 'Structural Reliability Theory and its Applications', Springer-Verlag.

Thoft-Christensen, P. and Murotsu, Y.(1986): 'Application of Structural Systems Reliability Theory', Berlin, Heidelberg, New York, Springer-Verlag, West Germany.

Tolikas, C., Morandi, A.C., Das, P.K. and Faulkner, D.(1994): 'Reliability-Based Multiple Criteria Optimization of a Fast SWATH Ship', Proc. of 2nd Int.

Conference on Computational Stochastic Mechanics, held in Athens, Greece, 13-15 June.

Tseng, C.H. and Arora, J.S.(1988a): 'On Implementation of Computational Algorithms for Optimal Design 1: Preliminary Investigation', Int. J. for Numer. Methods in Engineering, Vol.26, pp 1365-1382.

Tseng, C.H. and Arora, J.S.(1988b): 'On Implementation of Computational Algorithms for Optimal Design 2: Extensive Numerical Investigation', Int. J. for Numer. Methods in Engineering, Vol.26, pp 1383-1402.

Tvedt, L. (1984): 'Two Second-Order Approximations to the Failure Probability', Section on Structural Reliability, A/S Veritas Research, Hovik, Norway.

Tvedt, L. (1985): 'On the Probability Content of a Parabolic Failure Set in a Space of Independent Standard Normally Distributed Random Variables', Section on Structural Reliability, A/S, Veritas Research, Hovik, Norway.

Tvedt, L. (1988): 'Second Order Reliability by an Exact Integral', Proc. of 2nd IFIP Working Conference on Reliability and Optimisation on Structural Systems, edited by P.Thoft-Christensen, Springer, pp 377-384.

Ueda, U. et al (1975): 'Ultimate Strength of Square Plates Subject to Compression (1st report) - Effects of Initial Deflection and Welding Residual Stresses', J. Soc. Naval Architects of Japan, Vol. 137, pp 210-221.

Valsgard, S. (1980): 'Numerical Design Predictions of Plates in Biaxial In-Plane Compression', Computers and Structures, Vol. 12, pp 729-739.

Venkayya, V.B. (1978): 'Structural Optimization: A Review and Some Recommendations', Int. J. for Numer. Methods in Engng, Vol.13, pp 203-228.

Verma, D., Fu, G. and Moses, F. (1989): 'Efficient Structural System Reliability Assessment by Monte Carlo Methods', Proc. ICOSSAR'89, pp 895-901.

Vilnay, O. and Rockey, K.C. (1981): 'A Generalised Effective Width Method for Plates Loaded in Compression', J. Const. Steel Res., Vol. 1, No. 3, pp 3-12.

Walker, M.A. (1984): 'SWATH vs Monohull Initial Design', MSc Dissertation, Univ. College London, Oct.

- Wen, Y.K. (1993): 'Reliability-Based Design under Multiple Loads', *Structural Safety*, **13**(1993), 1993, pp 3-19.
- White, G.J. and Ayyub, B.M. (1987): 'Reliability-Based Design for Marine Structures', *J. of Ship Research*, Vol. 31, No. 1, March, pp 60-69.
- Wiernicki, C.J., Gooding, T.G. and Nappi, N.S. (1983): 'The Structural Synthesis Design Program - Its Impact on the Fleet', *Naval Engineers Journal*, ASNE, Vol. 95, No. 3, pp 87-99, May.
- Wu, Y.L. and Moan, T. (1989): 'A Structural System Reliability Analysis of Jacket Using an Improved Truss Model', *ICOSSAR'89*, pp 887-894.
- Wu, Y.L. and Moan, T. (1991): 'An Incremental Load Formulation for Limit States in the Reliability Analysis of Nonlinear Systems', *Structural Safety*, **10**, pp 307-325.
- Wu, Y.-T. and Wirsching, P.H. (1987) : 'New Algorithm for Structural Reliability Estimation', *J. of Engng. Mech.*, Vol. 113, No. 9, Sept., pp 1319-1336.
- Wu, Y.-T. (1992): 'An Adaptive Importance Sampling Method for Structural System Reliability Analysis', presented at the ASME 1992 Annual Meeting, Symposium on Reliability Technology.
- Xiao, Q. and Mahadevan, S. (1994): 'Fast Failure Mode Identification for Ductile Structural System Reliability', *Structural Safety*, **13**, pp 207-226.
- Yasuhiro Mori and Ellingwood, B.R. (1993): 'Time-Dependant System Reliability Analysis by Adaptive Importance Sampling', *Structural Safety*, **12**, pp 59-73.
- Yang, T.C. and Tseng, C.H. (1993): 'Integrating and Automating Analysis and Optimization', *Computers and Structures*, Vol.48, No.6, pp 1083-1106.
- Zanic, V., Das, P.K., Pu, Y. and Faulkner, D. (1993): 'Multiple Criteria Synthesis Techniques Applied to Reliability-Based Design of SWATH Ship Structure', *Integrity of Offshore Structures-5*, edited by D. Faulkner, M.J. Cowling et al, pp 355-386.

Zhu, T.-L. (1993): 'Numerical Integration in Affine Space to Compute Structural System Reliability', *Computers & Structures*, Vol 48, No. 4, pp 749-753.

Zotemantel, R. (1991): 'MBB-Lagrange: A General Structural Reliability and Optimization Structural System', *Proc. of the 4th IFIP WG7.5 Conference, 'Reliability and Optimization of Structural Systems'*, ed by R. Rackwitz and P. Thoft-Christensen, Munich Germany, Sept. 11-13 , pp 427-442.